

THE UNIVERSITY OF HULL

**Paper Microfluidics for
Clinical Diagnostics
using
Colourimetric Detection Methods**

being a Thesis submitted for the Degree of

Doctor of Philosophy

in the University of Hull

by

Amy Dawson
MSc, BSc

January 2014

Acknowledgements

I would like to thank my three supervisors, Dr. Tom McCreedy for his support and advice throughout this PhD, Dr. Sandra Jones for her guidance and help in writing this thesis and her support over the years. Finally, I thank Prof. John Cleland for his advice in the clinical aspect of the thesis and assistance in ethical approval with collecting samples.

I would like to thank the nurses Julie Davies and Stella Rimmer for supplying serum and plasma samples, plus the results from the hospital pathology laboratory. I would also like to thank Tony Sinclair for the SEM images of the filter paper.

I would like to thank the analytical group for their kind words and constant help with ideas in times of need, especially Dr. Nicole Pamme, Prof. Stephen Haswell, Dr. Giuseppe Benazzi and Dr. Mark Tarn.

My family have been my rock for the last three years, without their help and support this thesis would not have been possible, so thank you, I love you all! Mum, for pushing me through these last few steps, for the hugs and “pick me ups”.

Dad, for offering all the time to “help” write this for me.

Sam, for always cheering me up and wanting to go to the pub!

Christine and John Pearcey, for your all your encouragement, I always knew you were a phone call away ready to offer any help or advice I needed.

Abstract

Microfluidics is a technology currently aiming to advance the medical devices currently available in the developing and developed world through simultaneously creating point-of-care devices which are “as good” or better than current methods at a cheaper production cost. To be able to diagnose diseases and infections quickly and affordably remains the aim of many researchers and the use microfluidics has advantages which plug this difficulty. However, one main gap in the research is to train users for these devices which give accurate results when compared to current methods. Described herein are three point-of-care devices which would not require specialist users and give no significantly different results from hospital methods.

The aim of this project was to design, fabricate and use a microfluidic device made from filter paper as a cheaper alternative to current microfluidic devices already available. The creation of channels to direct the movement of fluid within the paper matrix was established by modifying a photolithography method, thereby providing hydrophilic channels surrounded by a hydrophobic barrier.

A three dimensional device was constructed entirely from filter paper to incorporate the simultaneous removal, reduction and detection of iron(II) via bathophenanthroline detection for the determination of iron(II) levels in a patient, indicative of the nutritional state of the patient e.g. does the patient suffer from anaemia. This method was deemed accurate by comparing the results to a conventional laboratory method (spectrophotometer analysis) completed in a hospital pathology laboratory. No significant difference was observed between results received from the hospital and results found using the paper microfluidic device, $15 \mu\text{M} \pm 0.6\% \text{ SEM}$ versus $15.5 \mu\text{M} \pm 0.8\% \text{ SEM}$ respectively.

Two paper devices were developed to allow a quick and reliable measurement assessment of a patient's renal function. The first for urea, as a simple colour change for a high or low readout of urea levels in serum samples, e.g. $\geq 150 \mu\text{g/mL}$ then an orange/red colour would be seen on the paper device, indicative of renal failure $\leq 150 \mu\text{g mL}^{-1}$. The second device used the Jaffe reaction on filter paper as a dipstick assay. No significant difference was observed between results received from the hospital and results found using the paper device $3.92 \pm 1.2\%$ *versus* $3.88 \text{ mg mL}^{-1} \pm 0.6\%$ respectively.

These three devices fulfil the aims of the project outline by remaining simplistic to use and are cost effective in both the developing and developed world, whilst maintaining accuracy as seen in the results received from hospital pathology laboratories.

Contents

Acknowledgements	<i>i</i>
Abstract	<i>ii</i>
List of Figures.	<i>viii</i>
Equations	<i>xii</i>
List of Tables.	<i>xiii</i>
Abbreviations	<i>xv</i>
Chapter 1: Introduction	<i>1</i>
1.1 Microfluidics	<i>1</i>
1.2 Point of Care	<i>4</i>
1.2.1 Telehealth	<i>7</i>
1.3 Paper Microfluidics	<i>9</i>
1.3.1 Fabrication Methods	<i>12</i>
1.3.2 Types of Paper	<i>14</i>
1.3.3 Physical Properties of Paper	<i>17</i>
1.3.4 Analysis with Paper	<i>21</i>
1.3.5 Three Dimensional Paper Devices	<i>23</i>
1.3.6 Advantages of Paper Microfluidics	<i>24</i>
1.4 Photolithography	<i>25</i>
1.4.1 Negative Photoresist	<i>28</i>
1.4.2 Positive Photoresists	<i>30</i>
1.5 Colourimetric Assays	<i>34</i>
1.5.1 Transition Metals in Coloured Complexes	<i>38</i>
1.5.2 Condensation Reactions	<i>39</i>
1.5.3 The Jaffe Reaction	<i>40</i>
1.6 Iron and Anaemia	<i>42</i>
1.6.1 Transferrin	<i>43</i>
1.6.2 Haemoglobin	<i>45</i>
1.6.3 Anaemia	<i>46</i>
1.6.4 1,10-Phenanthroline	<i>50</i>
1.6.5 Bathophenanthroline	<i>52</i>
1.7 The Kidneys and Renal Failure	<i>53</i>
1.7.1 Renal Failure	<i>54</i>
1.7.2 Urea	<i>58</i>
1.7.2.1 The Jung Method	<i>59</i>
1.7.3 Human Metabolism of Creatinine	<i>60</i>
1.7.3.1 The Jaffe Reaction	<i>61</i>
1.8 Aims and Hypothesis	<i>62</i>
Chapter 2: Experimental	<i>64</i>

2.1 Fabrication of the Paper Device for Iron Analysis	64
2.1.1 Summary	64
2.1.1 Materials	65
2.1.1 Method	65
2.2 Contact Angles	68
2.2.1 Summary	68
2.2.1 Materials	70
2.2.1 Method	70
2.3 Colourimetric Detection of Iron Spectrophotometrically	70
2.3.1 Summary	70
2.3.1 Materials	71
2.3.1 Method	71
2.4 Colourimetric Detection of Iron on a Paper Device	72
2.4.1 1,10-Phenanthroline Detection	73
2.4.1 Summary	73
2.4.1 Materials	73
2.4.1 Method	73
2.4.2 Bathophenanthroline Detection	74
2.4.2 Summary	74
2.4.2 Materials	74
2.4.2 Method	75
2.4.3 Reduction of Iron in Human Serum Samples on Paper	76
2.5.3 Summary	76
2.4.3 Materials	77
2.4.3 Method	77
2.4.4 Iron(II) Detection via a Hospital Pathology Laboratory	78
2.5 Colourimetric Detection of Urea using a Spectrophotometer.	79
6.5.1 Summary	79
2.5.1 Materials	79
2.5.1 Method	80
2.5.2 Colourimetric Detection of Urea on Paper	81
2.5.2 Summary	81
2.5.2 Materials	81
2.5.2 Method	81
2.5.3 Urea Detection via a Hospital Pathology Laboratory	82
2.6 Colourimetric Detection of Creatinine using a Spectrophotometer	83
2.6.1 Summary	83
2.7.1 Materials	83
2.6.1 Method	84
2.6.2 Colourimetric Detection of Creatinine using Paper	84
2.6.2 Materials	84
2.6.2 Method	85

2.6.3 Creatinine Detection via a Hospital Pathology Laboratory _____	86
2.7 Analysis of Paper Device Images _____	86
2.7.1 Summary _____	86
2.7.1 Materials _____	87
2.7.1 Method _____	87
2.8 Mask Designs _____	90
2.9 Statistical Analysis of Data _____	91
Chapter 3: Fabrication _____	92
3.1 Optimisation Results _____	94
3.1.1 Temperature _____	94
3.1.2 Exposure _____	95
3.1.3 Development _____	100
3.2 Determination of Development by Contact Angle Analysis _____	102
3.3. Cost of Fabrication _____	107
3.4 Discussion _____	108
Chapter 4: Colourimetric Detection of Iron _____	113
4.1: 1-10,Phenanthroline Results on Paper _____	114
4.2: Bathophenanthroline Detection _____	121
4.3 Human Samples _____	128
4.3.1 Whole Blood Samples _____	128
4.3.2 Serum and Plasma Samples _____	128
4.3.3 Clinical Samples of Human Serum _____	131
4.4 Validation of Iron(II) Measurements using the Paper Device _____	137
4.3: Smartphone Analysis _____	142
4.4: Whole Blood Analysis Revisited _____	146
4.5: Discussion _____	150
Chapter 5: Colourimetric Detection of Urea _____	156
5.1 Conventional Measurement of Urea _____	157
5.1.1 Optimisation _____	157
5.2 Measuring Urea using a paper device _____	163
5.2.1 Optimisation _____	163
5.3 Discussion _____	171
Chapter 6: Colourimetric Detection of Creatinine _____	175
6.1 Conventional Measurement of Creatinine _____	176
6.2 Creatinine Detection using a Paper Based Method _____	177
6.3 Discussion _____	193

Chapter 7: Discussion and Conclusion	197
Conclusion	202
7.1 Further Work	202
Iron	202
Urea	203
Creatinine	204
References	205
Appendix	223
1) Posters and Presentations	224
2) Planned Publications	224
3) Ethical Approval	225

List of Figures.

Figure 1. 1: Potential LOC device fabricated from glass.....	2
Figure 1. 2: Point of care requirements for a medical device to be used at home. ...	7
Figure 1. 3:Telehealth requirements for patient to “self test” at home and send results to the doctor or specialist.....	9
Figure 1. 4: Scanning electron microscope image of filter paper. ⁴⁵	11
Figure 1. 5:Advantages of using paper microfluidics as opposed to conventional microfluidic devices already available.	25
Figure 1. 6: Traditional photolithography method for both a negative and positive photoresists.	28
Figure 1. 7:Cyclised poly(cis-isoprene) polymer used in negative photoresists.	29
Figure 1. 8: The polymer of the Novolac resin.....	31
Figure 1. 9: The diazonaphthaquione structure.....	32
Figure 1. 10: The Wolff rearrangement	33
Figure 1. 11: A comparison between the two methods of using a positive or negative photoresist.	34
Figure 1. 12:Colour wheel of absorption within the visible region of light.....	36
Figure 1. 13:Schematic illustration of a typical colourimetric assay performed using a conventional microfluidic device.....	38
Figure 1. 14: Condensation reaction for a colourimetric assay for the detection of urea.	40
Figure 1. 15: The colourimetric assay of creatinine measurements in human samples.	41
Figure 1. 16: The colourimetric detection using dissociation, reduction and reaction of iron(II) with bathophenanthroline in serum samples.	45
Figure 1. 17:1,10-Phenanthroline Molecule.....	51

Figure 1. 18:1,10-phenanthroline reaction with iron(II).	51
Figure 1. 19: Bathophenanthroline reaction with iron(II).	52
Figure 1. 20:The kidneys and the renal tubule for filtering waste products.	54
Figure 1. 21: The Glomerular filtration rate to measure kidney function.	57
Figure 1. 22: The Urea molecule, produced as a waste product of human metabolism.	59
Figure 1. 23: The urea reaction for colourimetric detection spectrophotometrically.	60
Figure 1. 24: A Creatinine molecule produced as waste from muscle activity.	61
Figure 2.1: Schematic diagram of double-sided photo-mask.....	66
Figure 2.2: An illustration of the exposure of the photoresist-coated paper.	67
Figure 2.3: Contact angle measurements	69
Figure 2.4: Schematic diagram of 2 nd generation paper device design.....	76
Figure 2.5: Pathology Laboratory Method for iron(II) detection.....	79
Figure 2.6: Pathology Laboratory Method for urea detection.....	83
Figure 2.7: Schematic of creatinine dipstick assay	86
Figure 2.8: ImageJ analysis of iron paper devices	89
Figure 2.9: Mask designs created with Microsoft word and used throughout this project to fabricate paper microfluidic devices from photolithography.....	90
Figure 3. 1: Concept of barriers and channels in a piece of filter paper.	92
Figure 3.2: Photolithography in filter paper, highlighting areas requiring optimisation.	93
Figure 3.3: First attempt of fabricating a paper device with a simple photo-mask design for fabricating paper microfluidic devices using photolithography.	96

Figure 3.4: Second attempt of fabricating a paper device with a simple photo-mask design for fabricating paper microfluidic devices using photolithography.	98
Figure 3.5: Schematic diagram illustrating the use of a double sided photo-mask..	99
Figure 3.6: Determining optimum development time.	101
Figure 3.7: Contact angle results using the “initial device” design.	103
Figure 3.8: Complicated designs of channels that can be fabricated into a paper device. ⁴³	104
Figure 3.9: Channel designs used for various measurements of analytes.....	106
Figure 4.1: Coloured reaction of 1,10-phenanthroline with iron(II) on a paper device	116
Figure 4.2: Preliminary results of iron(II) detection on paper microfluidic device using 1,10-phenanthroline.....	119
Figure 4.3: Spectrophotometer analysis of iron concentrations,	121
Figure 4. 4: Analysis of paper device using bathophenanthroline.....	124
Figure 4.5: Bathophenanthroline analysis on paper microfluidic device	125
Figure 4.6: Spectrophotometric results using bathophenanthroline,	127
Figure 4.7: Comparison of methods using standard concentrations of iron(II),.....	131
Figure 4.9: A paper device for iron(II) analysis in human serum.....	133
Figure 4. 10: Iron analysis for human serum samples using paper device versus hospital pathology laboratory method	135
Figure 4. 11: Linear regression of results found using paper device vs. pathology results.....	136
Figure 4.12: Paper device using human serum sample taken with a Smartphone camera (iPhone4s)	143
Figure 4.13: Blood separation using the LF1 membrane on the paper device.....	148

Figure 5.1: Standard concentrations for urea detection.....	158
Figure 5.2: Absorption of urea when incubated at room temperature versus 37°C,	160
Figure 5.3: Standard urea concentrations of adapted method.....	162
Figure 5.4: Schematic diagram illustrating paper device for urea detection.....	164
Figure 5.5: Urea concentrations on filter paper previously soaked in the reagents	167
Figure 5.7: Urea detection on a paper device	168
Figure 6.1: Creatinine concentration within the clinical range,.....	177
Figure 6.2: Jaffe Reaction on filter paper illustrating the chromatographic effect..	178
Figure 6.3: Preliminary creatinine assay using a paper device as a dipstick assay	180
Figure 6.4: Analysis of paper based assay for creatinine standard concentrations,	181
Figure 6.5: Analysis of creatinine standard concentrations using a paper device .	184
Figure 6. 6: Creatinine detection using paper device versus spectrophotometer..	190
Figure 6. 7: Linear regression of results found using paper device vs. spectrophotometer.....	192

Equations

Equation 1. 1: The Reynolds number.....	18
Equation 1. 2 The Washburn Equation. ⁷⁹	19
Equation 1. 3: Darcy's law, describing fluid behaviour in paper networks. ⁸⁶	20
Equation 1. 4: The Youngs Relation Equation to describe the hydrophobic and hydrophilic angle of a platform.	21
Equation 1. 5: The Beer Lambert Law to measure the transmission of light.....	39

List of Tables.

Table 1.1: WHO's threshold to define anaemia.....	48
Table 3. 1: Adjusted development time for contact angles	105
Table 3. 2: Cost of consumables for fabricating 100,000 paper devices using the photolithography method when optimised.....	108
Table 4.1: Comparison between results obtained from the paper device versus the clinical specified method.....	134
Table 4.2: Statistical analysis of results from table 4.1, $P= 0.42$	137
Table 4.3: High levels of iron in serum samples to determine accuracy of method outside the clinical range	139
Table 4.4: Statistical analysis for high levels of iron(II) in serum (Paired T-test) ...	139
Table 4.5: Statistical analysis for high levels of iron(II) in serum (F-test for Variance)	140
Table 4.6: Low levels of Iron in Serum Samples	140
Table 4.7: Statistical analysis for low levels of iron(II) in serum (Paired T-test)	140
Table 4.8: Statistical analysis for low levels of iron(II) in serum (F-test for variance)	141
Table 4.9: Results from patients serum samples when using a Smartphone camera,	144
Table 4.10: Plasma Level of Iron from Whole Blood Samples.....	149
Table 5.1: Reduction of incubation time frame at room temperature,	161
Table 5.2: Varying chemical applications tested for urea detection on the paper device	166
Table 5.3: Comparison of patient results.....	169
Table 5.4: Statistical analysis of results from table 5.3.....	170

Table 6.1: Results of creatinine level when using the paper platform compared to artificial serum samples	185
Table 6.2: Paired Students T-test illustrating no significant difference shown in table 6.1,	187
Table 6.3: F-test illustrating no significant variances in the results shown in table 6.1	188
Table 6.4: Comparison of creatinine results from human serum samples using the paper device to the spectrophotometer method,	189
Table 6.5: Statistical analysis taken from figure 6.6 illustrating no significant differences within results.....	191

Abbreviations

3D	Three Dimensional
4,7-Diphenyl-1,10-phenanthroline	Bathophenanthroline
AFM1	Aflatoxin M1
AKD	Alkyl Ketene Dimers
AKI	Acute Kidney Injury
ARF	Acute Renal Failure
AuNP	Gold Nanoparticles
BP	Blood Pressure
BSA	Bovine Serum Albumin
BUN	Blood Urea Nitrogen
CKD	Chronic Kidney Disease
CL	Chemiluminescence
DNA	Deoxyribonucleic Acid
ELISA	Enzyme-Linked Immunosorbent Assay
ESRD	End Stage Renal Disease
FRTA	Free Radical Theory of Ageing
GFR	Glomerular Filtration Rate
GP	General Practitioner
Hb	Haemoglobin
HbO ₂	Oxyhaemoglobin
hCG	Human Chorionic Gonadotropin
HIV	Human Immunodeficiency Virus
IC	Integrated Circuit
IDA	Iron Deficiency Anaemia
LED	Light Emitting Diode
LOC	Lab on Chip
MI	Myocardial Infarction
NED	N-(1-Naphthyl)ethylenediamine
PDMS	Polydimethylsiloxane
PCR	Polymerase Chain Reaction
POC	Point of Care
RBC	Red Blood Cell

ROS	Reactive Oxygen Species
SEM	Standard Error of the Mean
STI	Sexually Transmitted Infection
TB	Tuberculosis
TNT	Trinitrotoluene
TnT	Troponin T
UK	United Kingdom
USA	United States of America
UV	Ultraviolet Light
UV/Vis	Ultraviolet / Visible Light
WBCs	White Blood Cells
WHO	Worlds Health Organisation

Chapter 1: Introduction

1.1 Microfluidics

Microfluidics or lab-on-a-chip (LOC) is a branch of science in which laboratory functions can be scaled down into a miniaturised system whilst maintaining the accuracy and precision observed in the larger scaled experiments.¹⁻⁵ The development of LOC allows a new technology to be taken outside of the laboratory setting and away from the use of more costly conventional methods, it was time saving, more efficient and integrated several processes into one device.⁶⁻⁸

LOCs first emerged in the mid-1980s as a way to deal with the behaviour, control and manipulation of fluids constrained to a sub-millimeter scale. Fluid flows through channels which can be manufactured/fabricated in polymers, glass or silicon substrates and subsequently detected electrochemically, fluorescently, colourimetrically, enzymatically or optically etc.⁹ The detection system can be integrated into the chip design alongside valves, mixers and pumps which automate the system and allow the user more control over the sample e.g. speed and duration.⁹

One of the first examples of microfluidics and the use of small scale volumes been used was the development of the glucose meter, which through a fingerprick of whole blood (~10 μL required in total) the glucose concentration could be measured.¹⁰⁻¹⁵ Since Anton Clemens (USA) first developed the first blood glucose meter (in which he combined dry chemistry test strips (Dextrostix) with reflectance photometry to measure blood

glucose) many alterations have been made to this device but ultimately the goal has always been to allow diabetic patients to “self-monitor” their condition.¹⁵ Thereby allowing patients to monitor their own glucose levels, reducing the frequency of visits to the doctor, thus saving money and effort for both the patient and the National Health Service (NHS).¹⁰⁻¹⁵ One study showed that from sixty four patients, fifty three of these patients led to a significant improvement in blood-glucose control, ultimately reducing the incidence of long-term diabetic complications.¹⁵

An area for microfluidics under continuously development is in the aspect of medical science. New diseases, infections and viruses are continually been discovered which require constant treatment and production of drugs, with an overall aim to develop a device which is inexpensive to manufacture and produce yet as effective as the methods and techniques currently available, figure 1.1.¹⁻⁵

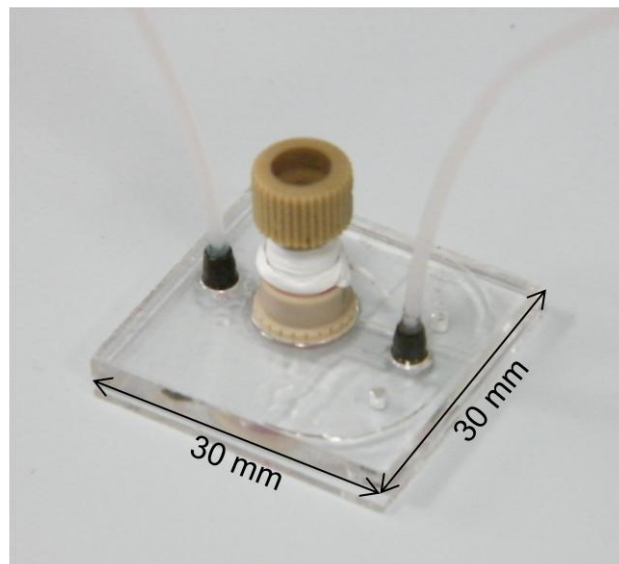


Figure 1. 1: Potential LOC device fabricated from glass.¹⁶

A problem which LOC has helped develop and solve is the ability to study tissue and cells in an environment which mimics the hosts. In many *in vitro* studies the *in vivo* environment has been lost but microfluidics replicates parameters which otherwise would have been absent.¹⁶⁻¹⁸ This includes laminar flow, transport of analytes driven via diffusion and constant waste removal. In comparison with conventional tissue culture methods nutrient supply are in batches, which decrease as metabolism occurs and waste products increase. However, in microfluidics nutrients and growth factors can be continually flowed into the tissue very much as a biomimetic microenvironment.^{16,19}

A microfluidic system should compile of generic components such as the introduction of a sample, movement of a sample, mixing/washing stages and a detection system.⁶ The design and approach for these components can vary greatly within research groups but with each sharing an end goal, to produce a device which can function easier and just as well as the conventional methods currently available.^{5,9,20,21} Once the development process for microfluidics has been completed, microfluidics can then be applied to the problems of scientific research rather than to just demonstrate the principles and what can be achieved on a microfluidic device, as stated by George Whitesides.⁶

Microfluidic technology can have many advantages over conventional laboratory methods such as it uses comparatively small samples and small reagent volumes, most devices can be portable and can be as sensitive as conventional methods allowing for accurate result analysis when in

comparison to the conventional methods available.²² However some drawbacks remain as it may require an external pump to create flow in the chip, an external detection device may be needed and some techniques may require pre-treatment of sample before they are loaded into the device.²⁰

Diagnosis is the first step in the treatment of any disease or but yet there lacks for many diseases and infections a method which is simplistic, quick and easy to do.⁴⁸⁻⁵¹ This is seen mainly in the developing world where poverty stricken areas do not have the facilities or equipment to perform an accurate diagnosis, as outlined in section 1.2. Out dated equipment, a lack of electrical power, contamination and a lack of healthcare workers prevent routine tests from been performed but this could be altered by the infusion of research into the use of developing microfluidic devices which are simple to use and do not need technical or expensive equipment.⁴⁸⁻⁵¹

1.2 Point of Care

Point of care testing is a medical device or system which can be brought to the patient's bedside or home rather than in a hospital or doctor's surgery and the results received by the patient either immediately after the test or a short time afterwards, as opposed to a few days.²³⁻²⁶ A POC device must also be small to allow for portability and in-expensive to manufacture. The features of microfluidics create a perfect platform for POC, the small consumption of reagents and sample allow for a fast turnaround in analysis, and the key idea is that rapid testing will lead to a rapid intervention improving the prognosis for the patient, figure 1.2.²⁷ The reduction in analysis time is due to the increased surface to volume ratio, thereby radically

reducing the diffusion time (mixing process of solutions) in some cases from minutes to seconds.²⁸ As previously mentioned, one of the earliest POC system was used to detect glucose through a tablet, after which came the dipstick assays for pregnancy testing and human immunodeficiency virus (HIV) which only require the addition of a sample.²⁹ Therefore most research has been aimed at producing a device for a POC system that is simple to use which in turn requires minimal equipment and an easy analysis, however this remains mostly an unrealised goal so far.^{3,30}

LOCs suited for POC testing would also allow improvements to be made in global health, especially in developing countries where the requirement for cheap and fast diagnosis of infections is urgently needed.³¹ An early and accurate diagnosis is important for a patient's health in both developed and developing countries alike, it limits the spread of a disease or infection, provides a better diagnosis and minimises the waste of resources.^{31,32} The developing world the diseases, which are most burdensome, include tropical diseases such as *African trypanosomiasis* (sleeping sickness), sexual transmitted infections (STIs) and human immunodeficiency virus (HIV), malaria and tuberculosis (TB).³³

An area recently developed by Chin *et al.* and Zhao *et al.* have both addressed the issues of using LOC in developing countries which could be a possible solution to the limitations in developing countries.³¹ In areas which do not have ready access to a laboratory and necessary equipment such as fridges and freezers for storage, the tropical climate can frequently denature biomolecules (> 45°C) which causes a loss of sensitivity in the traditional

bioassays.³⁴ The use of gold nanoparticles (AuNP) acting as a signal transducer on paper has an intense red colour when in the presence of water.³⁴ If this was coupled with the assay for the endonuclease (DNase I) enzyme the red colour of the AuNP was turned on depending how much was present in the sample.³⁴ This allows for the colourimetric detection of deoxyribonucleic acid (DNA) and at the same time prevents the denaturing of the DNA at high temperatures.³⁴

Alongside this, in the developed world such as in the United Kingdom (UK) and the United States of America (USA), several companies such as iSTAT™ and Biosite™ have started to manufacture disposable microelectronic and microfluidic devices for POC systems used in hospitals.

^{35,35} An example of these tests recently trialled has been patients suffering a myocardial infarction (MI), by measuring troponinT (TnT) levels, whereby an increase in expression strongly indicates a MI event has occurred.^{36,37} This was manufactured by iSTAT™ but no further data has yet been published.³⁶

This work is supported by several studies that have been completed by Apple *et al.* and Cramer *et al.* to conclude that these methods of diagnosis do give a greater prognosis for the patient due their fast result.^{36,38,}

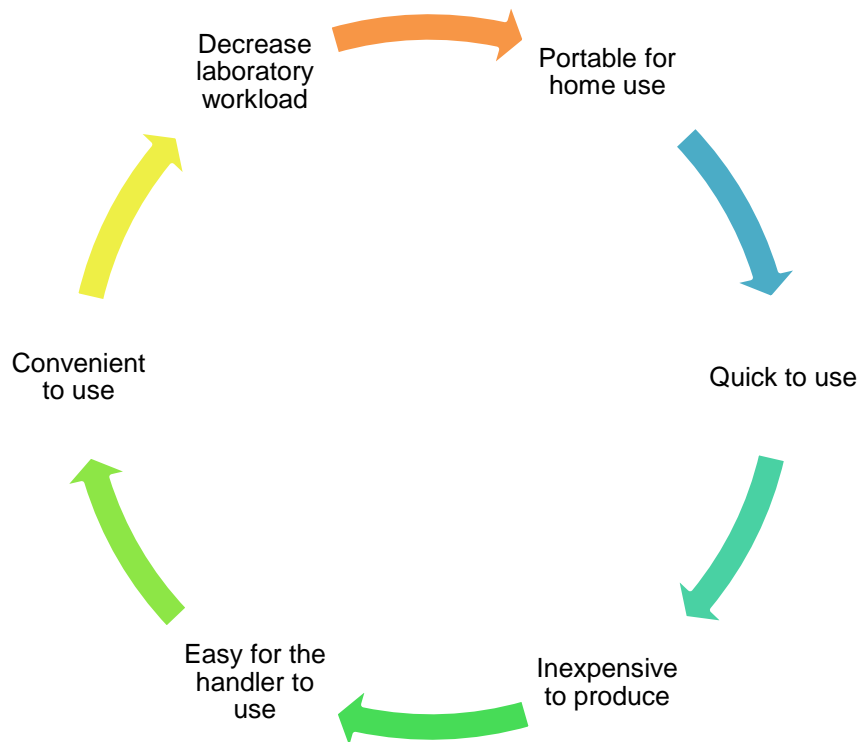


Figure 1. 2: Point of care requirements for a medical device to be used at home.

As microfluidics and LOC have a huge potential for practical devices in POC diagnostics they are slowly and successfully been introduced into the commercial market of today.⁴⁰ However, the initial delay in the development of these devices was due to problems with calibration and quality control in the manufacture of accurate but yet portable POC devices which are easy to use with little or no training.³ Nevertheless, with the emerging literature for new microfluidic platforms on which assays and POC diagnostics can be performed on (such as paper), a new era for microfluidics may allow for the development of more tests to be carried out by POC devices and which could be used by the patients at home as opposed to a clinical setting.³

1.2.1 Telehealth

A new aspect of POC devices currently undergoing development is a scheme referred to as “telehealth”.⁴¹ This is aimed at patients who suffer

from long term conditions such as diabetes or kidney failure or patients who have to continually travel to a hospital or general practitioners (GP) surgery for routine tests.^{41,42} It allows patients to live independently whilst maintaining stable health, a patient would be shown how to perform routine tests at home on a simple POC device and the results be transmitted automatically or emailed or telephoned by the user to their doctor, figure 1.3.^{41,42} The doctor would monitor the results of the patients and only contact the patient to visit the surgery or hospital if there was a change in status or unusual, thus reducing the burden on the NHS.^{41,42}

However, as with any new scheme there are currently some drawbacks with this system and limiting the scheme to particular conditions and age groups.^{41,42} There are still many inaccuracies in this scheme, mostly from either the patient when performing the test, forgetting to send the doctor results, misinterpretation of results by user etc.^{41,42} Desirable tests for the future would have minimal error and be easy to use such as the home pregnancy test and glucose meter for use in diabetes.^{41,42}

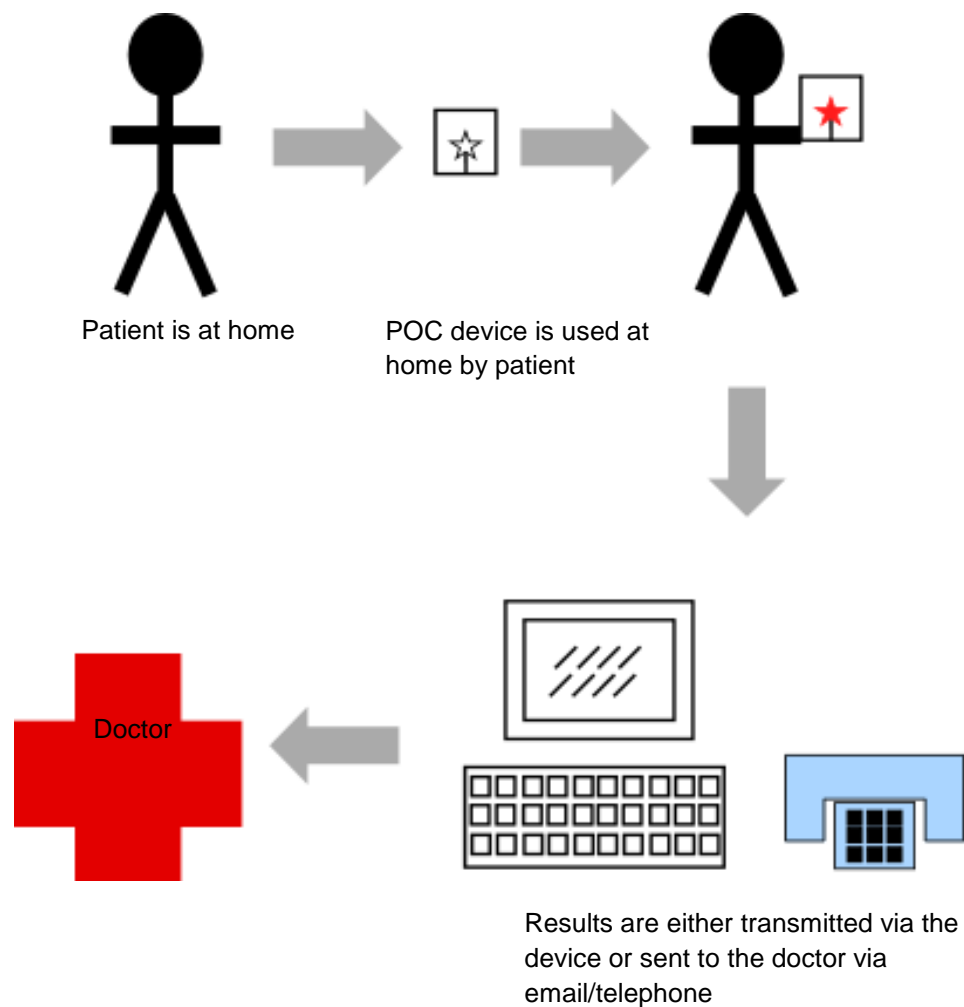


Figure 1. 3: Telehealth requirements for patient to “self test” at home and send results to the doctor or specialist.

1.3 Paper Microfluidics

Microfluidics is continuing to expand by using alternative and less expensive materials e.g. paper. Paper microfluidics is the basis of microfluidics as outlined in section 1.1 however the platform of the device is fabricated either entirely or partially from paper (e.g. filter paper) to allow the movement of liquids for detection.

Paper is a universally available porous material made up of cellulose fibres, a polymer of the simple sugar and glucose can be obtained from wood pulp, figure 1.3.⁴³ The polymer chains have –OH groups attached creating a surface similar to a silica gel, attracting water vapour from the atmosphere.⁴⁴ The cellulose in the paper is naturally hydrophilic, thus allows penetration of aqueous solutions providing a solid foundation to use paper as a microfluidic system to replace the glass and polydimethylsiloxane (PDMS) devices.⁴³

Paper based microfluidics has become a rapidly advancing field, pioneered and led by Whiteside's group at Harvard University.^{6,7} Its use can be for a variety of systems such as health diagnostics, environmental monitoring and food quality testing.⁴⁵ Researchers have begun experiments using paper as a cheaper alternative to the microfluidics devices that are currently in use. They offer a wide variety of advantages, such as price, easy storage and transportation and are easily disposable.⁴⁶ It also offers the advantage that it requires no external pumping as paper naturally wicks fluid.⁴³

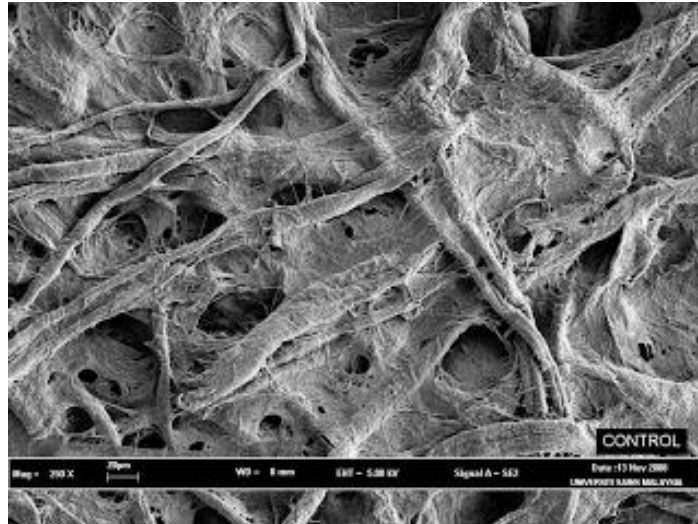


Figure 1. 4: Scanning electron microscope image of filter paper.⁴⁵
The paper matrix of the cellulose fibres in Whatman number 1 filter paper.

As previously mentioned in section 1.1, the first medical device was made from paper in 1956 to detect glucose in urine through a colour change from yellow to green. If the paper turned green, glucose was detected in the urine (positive result), if the paper remained yellow, no glucose was detected in the urine (negative result).⁴⁷ The paper was soaked in glucose oxidase, catalase and horseradish peroxidase and the result read from a colour chart after 1 min of been dipped in the sample and this test is still routinely done in modern day science for the diagnosis of diabetes type I and type II.⁴⁷

Currently, at the forefront of paper devices are the dipstick and lateral flow assays such as the home pregnancy testing kit.⁵² This test uses paper to wick fluid (urine) towards a detection zone driven via capillary force where the antigen (human chorionic gonadotropin (hCG), which is only present in the urine and blood-stream of a pregnant woman) will bind to the antibody (creating an antibody conjugate) and is detected via a colour signal which is

visualised within minutes of the sample been applied.^{32,52} It's limitation is a simple yes or no answer with no quantification needed. Recent advances however allow some devices to “estimate” how many weeks pregnant the user is by the concentration of hCG present.⁴⁵

1.3.1 Fabrication Methods

The idea of using paper as a platform for microfluidic devices takes advantage of the natural ability of the paper to wick fluids.^{45,53,54} However, usually this ability cannot be controlled and fluid will wick in every direction as there are no barrier to restrict the fluid flow. Researchers have shown that barriers can be created in paper by treating the paper and making areas hydrophobic whilst keeping certain areas hydrophilic (as a channel) steering fluid towards a specific area or detection zone.^{45,53,54}

Since the initial idea of creating channels into a paper substrate there have been many variations in the fabrication process of how this could be ideally completed.^{45,53,54} The most commonly used are wax printing, photolithography and screen printing.^{45,53,54} The main priority of each of these methods is to pattern a hydrophilic hydrophobic contrast channel, which defines liquid penetration pathways into the paper either physically or chemically.⁵⁵

However, there are more methods that have been published to date that create channels within in the paper matrix such as: ⁴⁵

Photolithography - Using a negative or positive photoresist to physically block the pores in the paper and selectively pattern channels by entire

hydrophobization followed by selective dehydrophobization.⁵⁶⁻⁵⁸ Devices fabricated from photolithography have been used to detect glucose and proteins in human urine samples.⁵⁸

Analogue Plotter - Uses PDMS to physically block the pores in the paper to create a channel by selective hydrophobization, this has been previously shown to detect albumin in human serum samples.^{59,60}

Ink Jet Etching - Polystyrene is deposited on to the paper surface and by entire hydrophobization followed by selective dehydrophobization channels are created on the papers surface.^{61,62} Devices fabricated in this manner have been use to detect glucose in human urine samples.^{61,62}

Plasma Treatment - The paper is chemically modified by using an alkyl ketene dimer (AKD) which is a cellulose reactive agent commonly used as a paper sizing agent in the paper making industry.⁶³ The chemically modified paper surface is then patterned by entire hydrophobization followed by selective dehydrophobization.⁶³ This device has been used for the detection of sodium hydroxide via phenolphthalein.⁶³

Wax Printing - Wax is deposited on to the paper and its physical deposition on the surface allows for selective hydrophobization.⁶⁴⁻⁶⁷ Devices fabricated via wax printing have been used for the simultaneous detection of glucose and proteins in human urine samples.⁶⁴⁻⁶⁷

Ink Jet Printing - Also uses AKD to chemically modify the paper fibres which can then create channels through selective hydrophobization.^{61,62} Fabrication

using ink jet printing has been shown to be successful for the detection of nitrogen dioxide (NO_2^-).^{61,62}

Flexography Printing - Also uses polystyrene that through selective hydrophobization alters the physical reagent at the fibres surface of paper.⁶⁸ Flexography printing has been shown to successfully detect varying concentrations of glucose dissolved in water.⁶⁸

Screen Printing - Uses wax to change the physical property of the papers fibres and creates channels through selective hydrophobization.^{69,70} Devices have been used for the detection of bicinchoninic acid.^{69,70}

Laser Treatment - Dependent on the type of paper selected as silicone is used for parchment paper and wax is used for wax paper, but both block the pores in the paper and the channels are created through entire hydrophobization followed by selective dehydrophobization.⁷¹ This device successfully measured haemoglobin levels via a luminal reaction and chemiluminescence.⁷¹

1.3.2 Types of Paper

The type of paper used in these methods can vary depending on the application of which is required on the device. Whatman no.1 filter paper has a pore size of 11 μM and has most frequently been the paper platform of choice due to the medium retention and flow rate, thus it is therefore referred to as the standard grade filter paper.⁵³ Whatman no.4 filter paper has a larger pore size of 20 – 25 μM thereby increasing the surface area of the filter paper and will thus in comparison have a faster flow rate than the

Whatman no.1.⁵³ Flow rate is defined as the migration speed of a fluid along the length of a strip and is one of the main parameters to take into consideration when choosing a paper type, alongside pore size and distribution.⁷² It is the pore size of the paper which effects the retention time and the size of the particles which can be used on a particular paper platform.⁷²

In contrast, nitrocellulose paper provides a platform for detection methods such DNA detection as the paper has the ability to immobilise antibodies and enzymes.⁵³ The antibodies, which are made up from proteins and contain an amino group and a carboxyl group are able to bind to the nitrocellulose membrane due to the electrostatic attraction between the negative charge of the amino groups on the membrane and the positive charge of the antibodies carboxyl group.⁵³ In previous years the nitrocellulose paper devices were more delicate when compared to the filter paper devices, but recent advances have produced them more robust and readily available e.g. introduction of nylon into the membranes.⁵³

Another consideration when choosing a type of paper for a POC device is the colour.⁷² When performing image analysis, the ideal colour of the paper would be white, allowing for as little interference with the result as possible.⁷² However, the colour can be effected by the process the paper undertook to create channels, humidity and the age, as paper eventually turns yellow/brown.⁷²

Recently the most useful paper platform diagnosis device have been produced for the identification of the blood group for a patient.⁷³ This is a device much needed in emergency situations as a patient rapidly losing blood in the field will not have the time to wait until the matching blood group is identified before transfusion.⁷⁴ It is a simple and quick visual test which can be performed in the space of 5 min and is a perfect example of how paper microfluidic devices are shaping the future of modern medicine.^{73,74} Paper previously spotted with the antibodies for specific blood groups e.g. A, B, AB, O and including the Rhesus factor.^{73,74} The blood upon application from a small sample or finger prick will agglutinate when the corresponding blood is mixed on the paper with the matching antibodies, whilst incorrect blood groups do not react.^{73,74}

One of the issues that has created problems for microfluidics from the beginning when using serum or plasma samples in medical devices is the amount of pre-treatment a sample has to undergo to be prepared for application into the microfluidic device.⁷⁵⁻⁷⁷ The main problem has been, the removal of red blood cells (RBCs) from the serum sample which can cause interference with assays which is usually performed by the centrifugation of a sample, as the larger cells such as RBCs are spun down whilst the smaller cells found in serum remain at the top of the sample.⁷⁸ To run a serum sample on a microfluidic device is not ideal as centrifugation would be required and increases the pre-treatment required for use in the device.⁷⁸ Research by Henry *et al.*⁷⁸ has produced membranes in which larger molecules or cells such as white blood cells (WBCs) and RBCs are trapped within the membranes network whilst plasma flows out from the front,

separating the whole blood (LF1, MF1, VF1 and VF2).⁷⁸ The membranes do not interfere with the products in human blood and do not interfere with the analysis of the sample, allowing for less pre-treatment to be performed before the sample can be used in a microfluidic device.⁷⁸

1.3.3 Physical Properties of Paper

The main advantage of using a paper platform as a microfluidic device is the ability for liquids to travel through the paper matrix without further pumping methods.^{79,80} This is due to water being a polar molecule, i.e. there is an uneven distribution of electrons.⁸¹ Water contains one oxygen atom and two hydrogen atoms, thus there are four pairs of electrons surrounding the oxygen atom, and two electrons are covalently bonded with the hydrogen atoms leaving two unshared electrons.⁸¹ Water has a partial positive charge near the hydrogen atoms and a partial negative charge near the oxygen atom creating an electrostatic attraction between oxygen and the hydrogen's and allowing water to form hydrogen bonds with surrounding water molecules.⁸¹ Paper is made of cellulose fibres which contain many positively charged hydrogen atoms thereby allowing the oxygen atom of the water molecule to interact with the cellulose as opposed to each other.⁸¹

Another benefit of using microfluidics is the fluid flow as according to the Reynolds number (Re).⁸² The Re number is described as a measure of the inertial forces e.g. density (ρ) and viscosity of fluid (η), diameter of a channel (d) and the flow rate (v)⁸² (equation 1.1). If the calculated Re value is less than 10, the flow is described as laminar flow, where fluid flows in parallel with no disruption between the layers. If Re is calculated $>2,000$ then fluid

movement is described as turbulent with high and chaotic diffusion between the layers.⁸²

$$\text{Re} = \frac{\rho v d}{\eta}$$

Equation 1. 1: The Reynolds number.

1.3.3.1 The Washburn Equation

The Washburn equation describes the flow of a liquid under its own capillary force in a horizontal tube which can be characterised for the movement of fluid in a porous substrate, e.g. paper.^{83,84} As a paper network provides a low cost and “pump-less” alternative to other microfluidics devices much work has been completed in understanding the movement of fluid through porous membranes.⁷⁹ The Washburn equation describes that a volume of fluid (L) moves through a paper matrix according to the surface tension (γ), pulling the fluid into the paper determined by pore size (D), however opposed to this is a viscous resistance (η) which increases as the fluid travels over time (t) along a length eventually decreasing the flow of the fluid penetrating the paper, equation 1.2.^{83,85}

$$L = \frac{yDt}{4\eta}$$

Equation 1. 2 The Washburn Equation.⁷⁹

This equation can be applied to paper microfluidics and in determining the correct channel length and time taken for the sample to reach a particular area.^{79,83,85} According to the Washburn equation to slow the fluid movement a channel can be widened and therefore increase the viscous resistance, slowing down the fluid movement.^{79,83,85} However if a channel of a constant width is used for transport of fluid then the flow of fluid is better described by Darcy's Law.^{79,86}

1.3.3.2 Darcy's Law

In a paper matrix, laminar flow occurs due to the low Re number which commonly occurs in dimensions less than 1 mm.⁸² However, as described by Yager's group it is Darcy's law (equation 1.3) which best describes fluid behaviour in paper due to the porous nature of the cellulose matrix, explaining that the resistance to flow is proportional to the length of the channel in the paper.⁸⁶ The volumetric flow rate (Q) is determined by the permeability of the paper (k), the length of the paper network (L) and the cross sectional area of paper (width, w and height, h) whilst taking into account the dynamic viscosity (μ) of the fluid and the pressure drop as fluid travels away from initial application (ΔP).

$$Q = \frac{kwh}{\mu L} \Delta P$$

Equation 1. 3: Darcy's law, describing fluid behaviour in paper networks.⁸⁶

As described in work by Yager *et al.* it has been demonstrated that the paper network can effectively replace the conventional “Y microfluidic device” fabricated from glass as long as there is a sufficient source of fluid and an unfilled absorbance capacity of the paper to maintain the flow of fluid.⁸⁶

1.3.3.1 Young's Relation Equation

In using a paper microfluidic device it is common practise to measure the angle at which a device is described as hydrophilic (water loving) or hydrophobic (water hating) using a water droplet.^{84,87} As most methods of creating channels in paper is to change the physical properties of the paper to hydrophobic whilst keeping areas as hydrophilic, this thereby creates a “channel” and gives liquid a path to follow.^{84,87} The angle at which a liquid interface meets a solid surface, the shape of the droplet on the flat surface is determined by the Young's Relation (the ability of a liquid to maintain contact with a solid surface, resulting from intermolecular interactions when the two are brought together)^{84,87} as shown in the equation 1.4 and discussed later in chapter 2.2. The Youngs Relation equation calculates the contact angle (θ) from the solid surface free energy (γ_{SV}), liquid surface free energy (γ_{LV}) and the liquid/solid interface (γ_{SL}).

$$\gamma_{SV} = \gamma_{SL} + \gamma_{LV} \cos \theta$$

Equation 1. 4: The Youngs Relation Equation to describe the hydrophobic and hydrophilic angle of a platform.

If the fluid is strongly attached to the surface (hydrophilic solid) the droplet will spread out and have an angle less than 90°, if the droplet is larger than 90° then the surface is hydrophobic.

1.3.4 Analysis with Paper

There are three main areas of detection which are best suited for paper microfluidic devices which is constantly been upgraded, renewed and re-tested to allow for the most accurate method to be utilised.^{53,54} This allows for both quantitative analysis (data which can be measured numerically) and qualitative analysis (data which relies on observation and interpretation) to be performed.⁵³ The use of digital result taken from many paper microfluidic devices already available allows a numerical value to be calculated from the result e.g. ImageJ provides a numerical measurement according to the density of a colour change thereby allowing for a quantitative result to be measured which is more accurate than qualitative measurements.^{53,54}

1.3.4.1 Colourimetric Analysis

The most widely used analytical analysis performed on paper devices is the simple, yet effective colourimetric assay. The change in colour can be observed by the users eye, or be measured via an image using computer software i.e. Adobe photoshop, ImageJ. However, these assays are subject to; varying light conditions, the user's interpretation and contamination from the environment, but can be controlled by ensuring identical parameters for

each device and assay performed. These assays can be simple, based on a reaction between the reduction of iron(III) and 1,10-phenanthroline⁶⁵ or be slightly more complex and based on the interaction of antibodies to detect a toxin.⁸⁸ For example, aflatoxin M1 (AFM1) in milk was detected as an immunochromatographic assays for a direct detection of the target toxin. This was obtained by acquiring images of the strips and correlating intensities of the coloured lines in proportion to the analyte concentrations.⁸⁸

1.3.4.2 Electrochemical detection

Electrochemical detection requires three electrodes, a reference, a counter and a working which can be incorporated into a paper platform. Through the addition of a conductive ink (graphite) connecting the circuit and a portable a potentiostat, the paper device can then perform voltammetric experiments (information about an analyte is obtained by measuring the current as the potential is varied).⁵³ An example of this was the electrochemical analysis of glucose, uric acid and lactate in by Dungchai et al.⁵⁶ In this work, electrodes were screen printed onto filter paper and the detection of glucose, uric acid and lactase demonstrated in biological samples using the reactions glucose oxidase, uricase and lactate oxidase respectively.⁵⁶

1.3.4.3 Chemiluminescence

Chemiluminescence (CL) can be performed on a paper device as first described by Yu *et al.*⁸⁹ who detected glucose and uric acid simultaneously through glucose oxidase reactions and urate oxidase reactions. Whilst this method remains an effective method for analysis in paper microfluidic devices it can however be improved by the addition of an electrochemical

detection alongside as used by Delaney *et al.*⁹⁰ This device was based upon Inkjet printing to create a paper microfluidic channel, which was combined with screen-printed electrodes to create a disposable sensors which can be used and read without a traditional photo-detector. The sensing mechanism was based on the orange luminescence due to the reaction of tris(2,2'-bipyridyl)ruthenium(II) (Ru(bpy)₃²⁺) with certain analytes.⁹⁰

1.3.5 Three Dimensional Paper Devices

Another advantage that has been reported widely in the literature is the ability to produce two dimensional (2D) and three dimensional (3D) paper devices using common household products such as sellotape.⁴⁴ The use of a 3D paper device allows the user to have more control over the fluid flow rate and fluid direction in the device as it can be used to generate multiple patterns of flow, which can be completed by pressing together and closing the gap between two vertically aligned channels allowing fluid to wick from one to the other.⁴⁴ This work has been demonstrated by various groups including Whiteside's and illustrates that more than one analyte can be measured at a time.⁹¹

The art of origami has also been used to create three dimensional paper devices as the folding of the paper creates layers and channels within the paper network.^{2,92-95} In one such example which origami was used to create a novel 3D microfluidic paper-based immuno-device by Ge *et al.*⁹² This group, integrated into one device, blood plasma separation from whole blood samples, automation of rinse steps, and multiplexed CL detections which was fabricated using wax printing before been folded into shape.⁹² Another

example of origami was fabricated on a single sheet of flat paper using photolithography.⁹³ This device could be unfolded to reveal each layer after analysis and was proven to accurately work by demonstrating colourimetric and fluorescence assays.⁹³

1.3.6 Advantages of Paper Microfluidics

The various aspects of paper microfluidics show a great potential to LOC technology and is becoming a more recognised substrate material, figure 1.5. The natural ability of paper to flow fluids has shown its versatility in various fabrication methods and in the various detection methods previously described. This aspect of paper has influenced researchers into producing similar platforms shown in work by Bhandari *et al.*⁹⁶ who published research using silk yarn.⁹⁶ Silk yarn was produced as a similar platform to paper, with the natural ability to wick fluids through the created weaves on a loom and by dipping the produced weave (as a channel) into a blocking solution of bovine serum albumin (BSA), phosphate buffered saline and a detergent Tween-20.⁹⁶ This made the silk yarn hydrophilic by creating an unequal sharing of electrons (electronegative charge).⁹⁶ The benefit from using this method as opposed to paper is the ability to fold and manipulate the platform without causing any damage to channels or areas with pre dried reagents as paper is slightly less flexible, however, this method has a more expensive fabrication from the cost of the specialised hand loom and would require a trained user to produce.

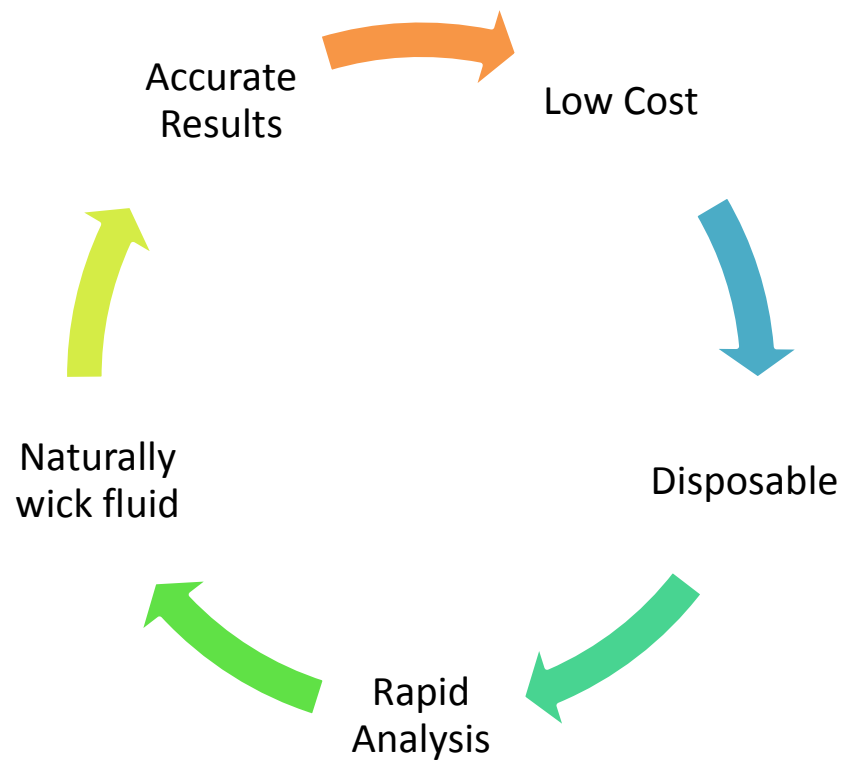


Figure 1. 5: Advantages of using paper microfluidics as opposed to conventional microfluidic devices already available.

1.4 Photolithography

Photolithography, as first mentioned in chapter 1.3.1 was a method initially used in the manufacturing of circuit boards used in electronic devices in the 1920s, then later in the 1950s for semiconductor use.⁹⁷⁻⁹⁹ The expansion in the field of microfluidics has since seen the photolithography method used in the development of channels in glass, and most recently in the production of channels in filter paper.^{57,58,100} In 1935 the first negative photoresist was developed by Louis Minsk of Eastman Kodak from poly(vinyl cinnamate) and in 1940 Otto Suess of Kalle Division developed the diazonaphthaquione-based positive photoresist.^{98,101}

In photolithography, a pattern is transferred onto a surface through exposing a surface to an ultraviolet (UV) light through a pre-designed mask.^{102,103} Upon exposure to the UV light (10 - 350 nm), the photoresist will become more or less soluble, depending on the chemical properties of the photoresist used, (more commonly referred to as a positive or negative photoresist).^{103,104} The exposed surface is then washed or soaked in a developer to remove the solubilised areas which have either been exposed or not exposed to the UV light depending on which photoresist has been used in the process. If the UV exposed areas of the photoresist have become more soluble then it is referred to as a positive photoresist and if the areas which have not been UV exposed become more soluble then it is referred to as a negative photoresist, shown in figure 1.6.¹⁰⁵

There are three main components of a negative and positive photoresist; they are the solvent, the polymer and the sensitizers.¹⁰⁵ Solvent is required in both positive and negative photoresists as it permits the photoresist to remain as a liquid to spin-coat onto a surface. The polymer will either polymerise through cross linking, or photo-solubilise by breaking down into the monomers depending whether it be positive or negative photoresist. Finally, the sensitizer stimulates the photochemical reaction either by cross linking or breaking down when exposed to a UV light source.¹⁰⁴

The process of photolithography involves spin coating the surface, pre bake (soft bake) of the photoresist, alignment of a photo-mask, exposure to UV light, development and a post bake (hard bake), figure 1.6.¹⁰⁶ As illustrated in figure 1.6, the process of photolithography requires the photoresist to be spin coated onto a surface held in place on the spinner through a vacuum and is

typically spin at 3000 – 6000 rpm for 30 s to ensure an even thickness across the surface (as the excess is thrown off), which is usually 1 – 2 μM thick.¹⁰⁶ The pre bake (soft bake) is used to evaporate the coating solvent in the photoresist and to densify the photoresist after spin coating. It is usually heated at 90 – 100°C for 20 min in a convection oven or on a hot plate or something similar with a smooth surface to allow good thermal contact.¹⁰⁶ The alignment of the photo-mask is required to ensure removal of the correct areas in the development stage. The mask will be specifically designed for either a negative or positive photoresist.¹⁰⁶ The photoresist resist is exposed to a UV light through the photo-mask which will either polymerise or breakdown dependent of the nature of the photoresist (negative or positive).¹⁰⁶ The developing stage will remove the areas which have broken down in the photoresist either through exposure (positive) or not due to exposure (negative).¹⁰⁶ The post-bake (hard bake) is used to harden and stabilise the photoresist whilst removing any traces of the developer which may have been left behind.¹⁰⁶

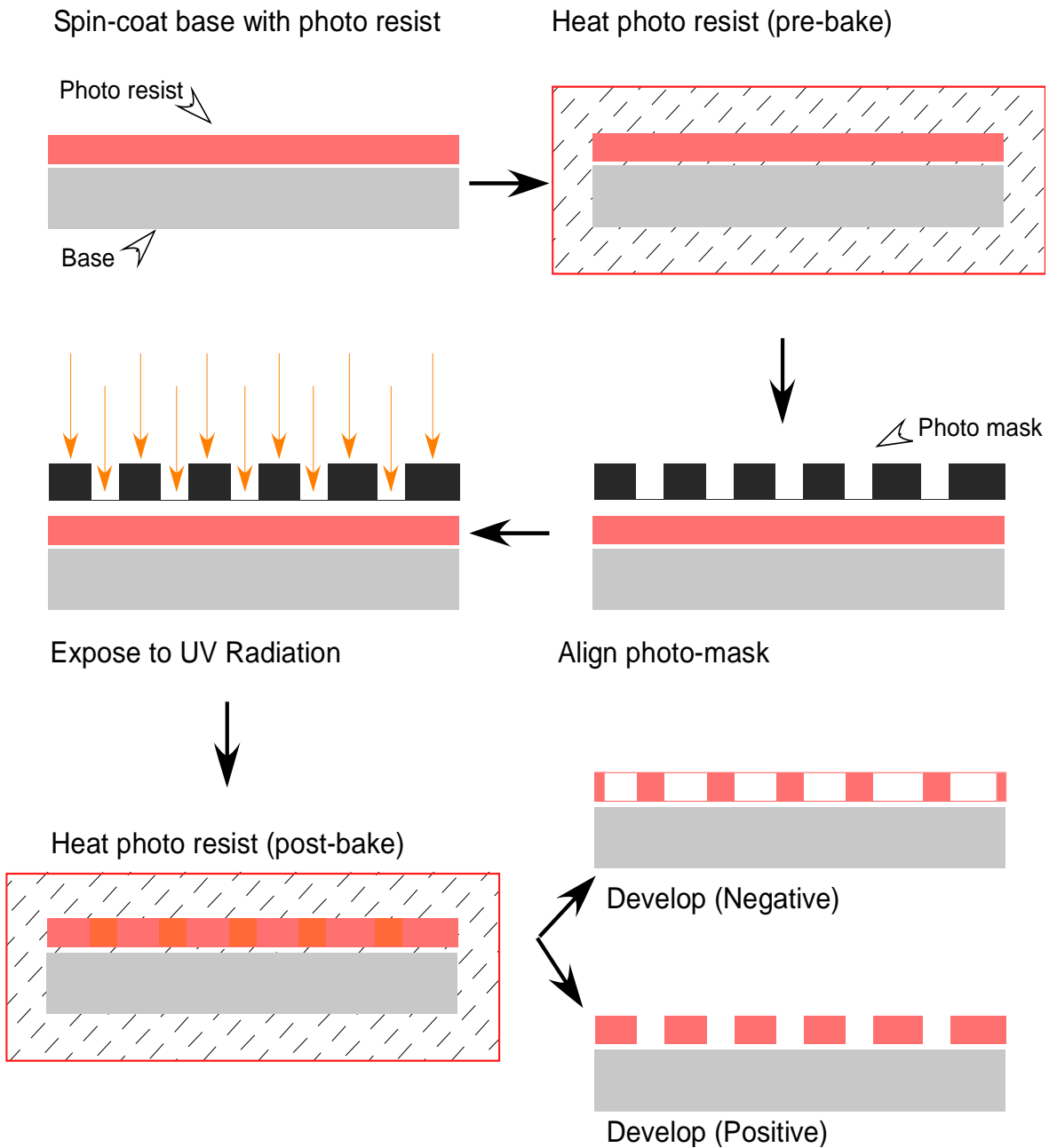


Figure 1. 6: Traditional photolithography method for both a negative and positive photoresists.

1.4.1 Negative Photoresist

The polymer mostly used in negative photoresists is a natural latex rubber, poly (cis-isoprene) produced from the spontaneous polymerisation of 2-methyl-1,3-butadiene.¹⁰⁴ It is the only known polymer which is simultaneously

elastic, air tight, water resistant, long wearing and adheres well to surfaces.¹⁰⁴ Two protons are added to further saturate the polymer and induce curling into a cyclicized polymer, with the added benefit of allowing a greater solid content in coating solutions and decreasing the thermal cross linking.^{107,108} Thus negative photoresist the polymer, cyclicized poly (cis-isoprene) is not chemically bonded, however upon exposure to UV light, the polymer cross links and polymerises, figure 1.7.^{104,107,108} The result is cyclicized poly (cis-isoprene), extremely soluble in non-polar, organic solvents such as toluene and xylene.^{104,107,108}

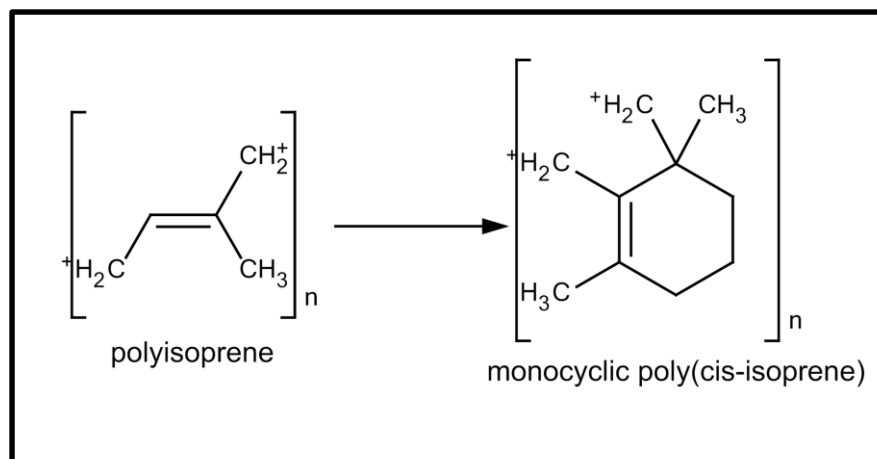


Figure 1. 7: Cyclised poly(cis-isoprene) polymer used in negative photoresists.

All negative photoresists work by cross linking a chemically reactive polymer via a photosensitive agent (usually bis-azide) which initiates the chemical cross linking reaction upon exposure to UV light.⁵⁹ In the bis-azide-cyclised polyisoprene photoresists, upon exposure to light the bis-azide decomposes into nitrogen and nitrenes, which produce polymer linkages that are not soluble in a developer solution.^{59,101} The unexposed areas of the negative photoresist (not to be cross linked) when the surface was exposed to UV

light through a photo-mask will be dissolved in the development stage.^{59,105} The developer, usually an ethyl lactate solvent, swells the photoresist allowing the uncrossed polymer chains to untangle and be washed away when applied. However, this swelling is one of the major drawbacks to using a negative photoresist as it can contribute to a loss of features and limit line width for the final product.^{59,101,105}

1.4.2 Positive Photoresists

A positive photoresist has been mainly used in the integrated circuit (IC) industry due to the fact that they do not swell during the development stage unlike the negative photoresists, thereby allowing a finer resolution for the final product.^{98,99,109}

The polymer used in positive photoresists is most commonly a phenolic resin, (a condensation polymer of aromatic alcohols and formaldehyde) such as the Novolac resin, (figure 1.8).⁹⁹ The Novolac resin (due to the OH group making the molecule hydrophilic) is soluble in common aqueous alkaline solutions such as sodium hydroxide, potassium hydroxide and ammonium hydroxide.⁹⁹ However, attached to the Novolac resin is a photo-sensitizer, diazonaphthaquione, this sensitizer is a hydrophobic and non-ionisable compound thereby making the resin also hydrophobic, figure 1.9. Upon exposure to UV light and the absorption of a photon, the diazonaphthaquione decomposes via the Wolff rearrangement (generation of ketenes), into an indene carboxylic acid (benzene ring fused with a cyclopentene ring) which is hydrophilic and produces gaseous nitrogen as a by-product, figure 1.10.

Novolac resins which contain indene carboxylic acid are readily dissolved by aqueous alkaline developers.

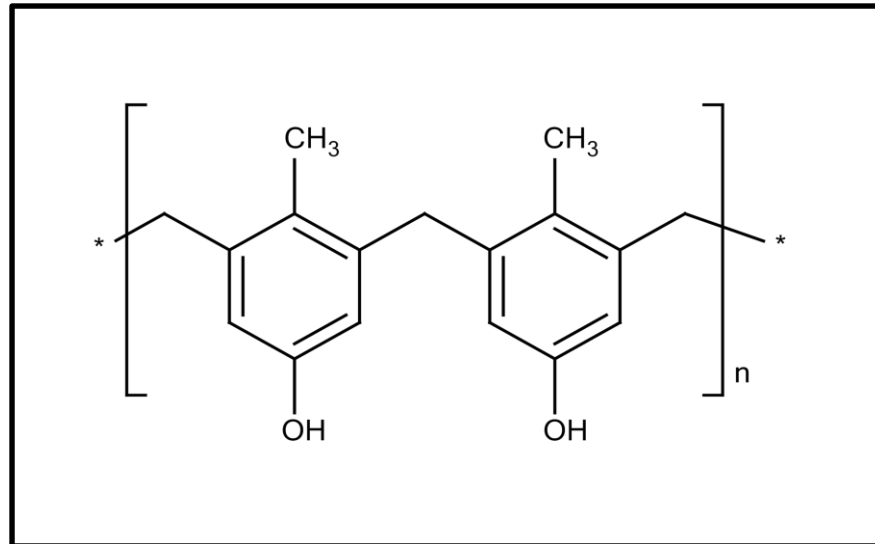


Figure 1. 8: The polymer of the Novolac resin.
Adapted from reference ¹¹⁰

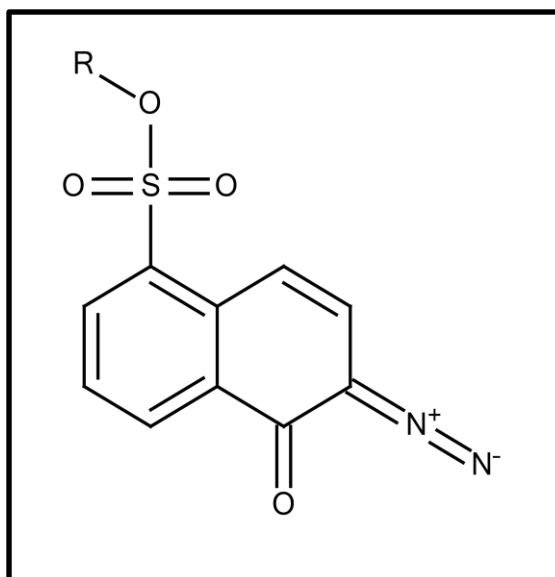


Figure 1. 9: The diazonaphthaquione structure.
Adapted from reference¹¹⁰

When light is absorbed in the presence of water, the diazonaphthaquione undergoes the 1-2 rearrangement in the Wolff rearrangement, shown in figure 1.10, whereby carbon six (labelled in parts two and three of figure 1.14) is moved along one molecule and pushed out of the carbon ring. This forms an intermediate carbene (part two) and a ketene (part three) before forming an indene carboxylic acid (part four) which is hydrophilic.

The Wolff rearrangement is the conversion of α diazoketene into a ketene, which was first reported in investigations completed in 1902 by Ludwig Wolff.^{110,111} In this case, the positive photoresist uses a Novalac resin and diazonaphthaquione.

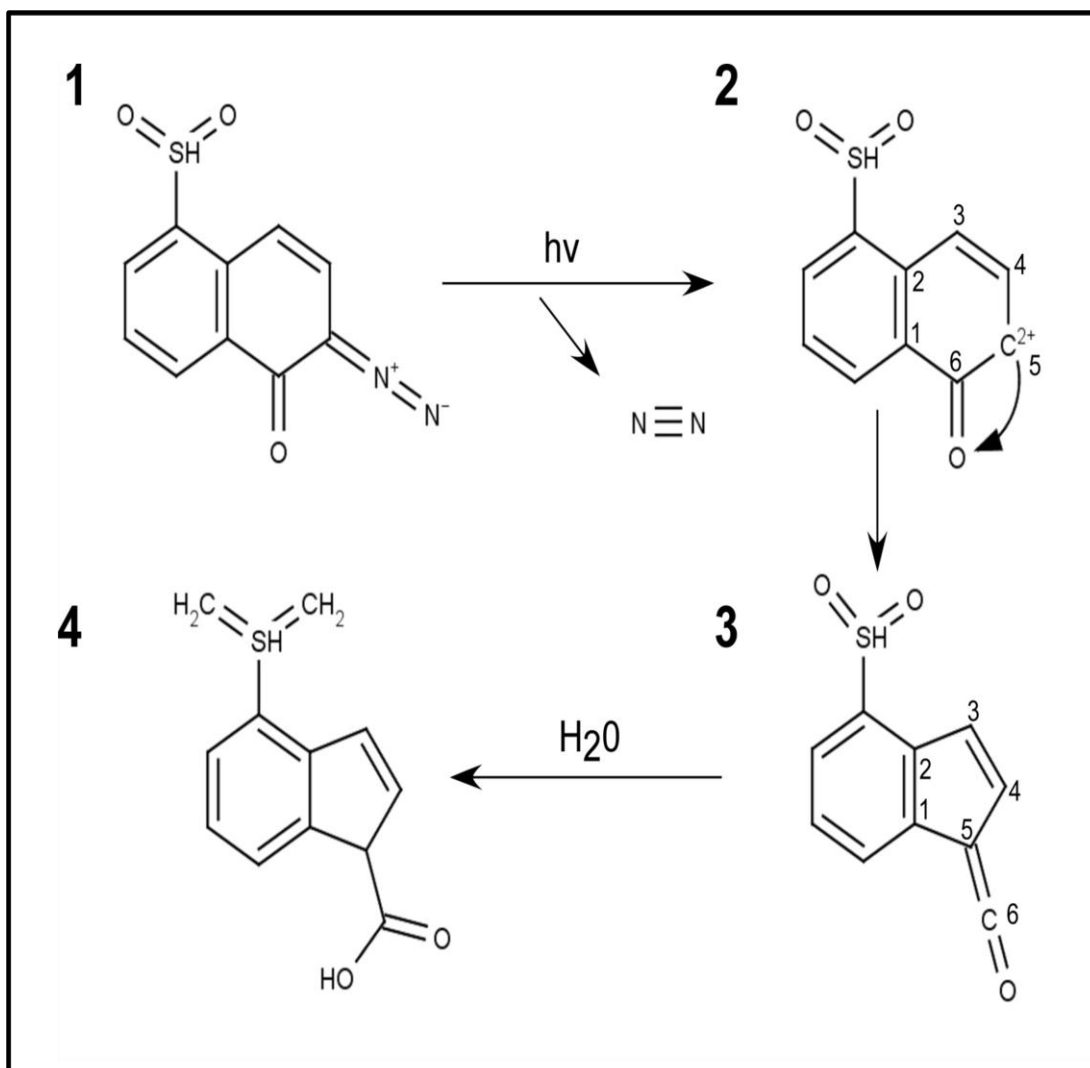


Figure 1. 10: The Wolff rearrangement .

Adapted from reference¹¹⁰

Panel 1: Shows diazonaphthaquinone molecule, **Panel 2:** The 1,2-rearrangement of carbon 6 to form a carbene, **Panel 3:** A ketene intermediate, **Panel 4:** Indene carboxylic acid (hydrophilic).

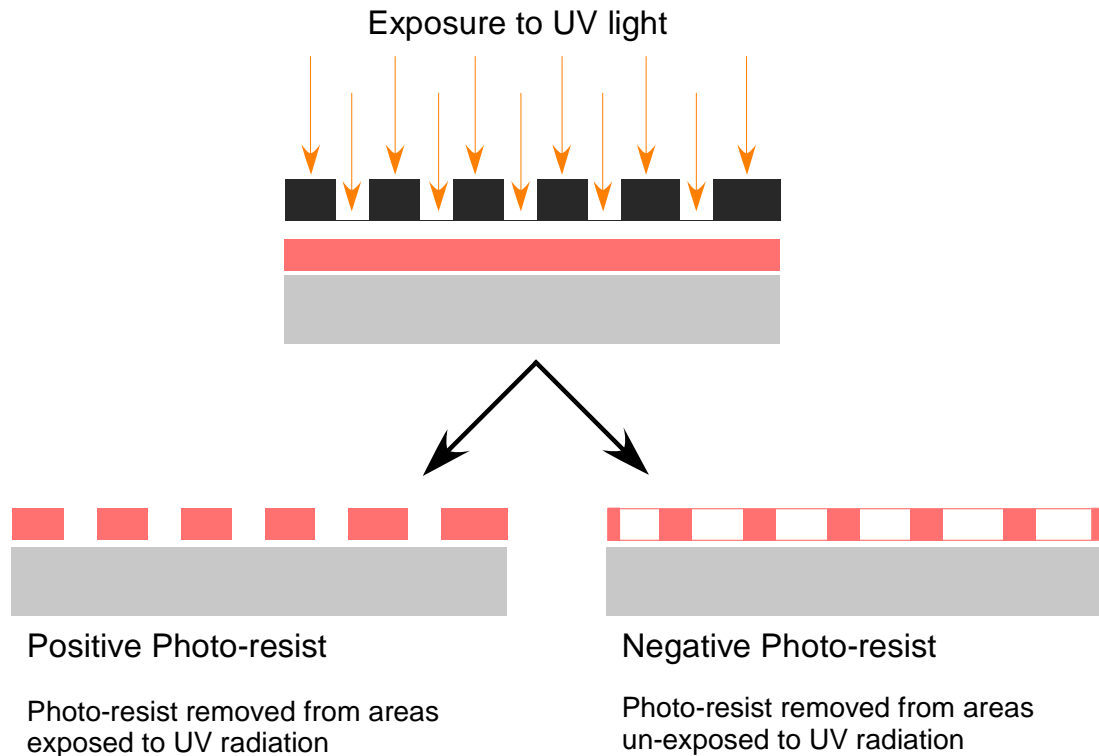


Figure 1. 11: A comparison between the two methods of using a positive or negative photoresist.

1.5 Colourimetric Assays

The development of modern science has been able to manipulate the electronic properties and specific wavelengths of chromophores through the use of spectroscopy. Initially this technique began by measuring the concentration of coloured compounds in a solution via colorimetry.^{112,113} This later was further advanced into the most commonly used analytical technique, spectroscopy and the development of the Beer-Lambert law.¹¹² Isaac Newton originally made the first key contribution to spectrophotometry and colorimetry in 1704 with his attempts to split white light into spectral

colours, it was Thomas Young who first described the effect of colour on the human eye and how it was perceived a hundred years later.¹¹²

When a coloured compound is dissolved in a solvent or solution, the intensity is dependent upon the concentration of the solution but the colour is dependent on the wavelength of visible light absorbed by the sample.¹¹² If a solution containing a coloured compound absorbs within the visible region of light then the transmitted light will; be coloured but the observed colour will be dependent on the “missing” wavelengths e.g if a compound absorbs orange light then blue light will be observed according to the colour wheel representation, figure 1.12.¹¹⁴

Colourimetric assays can be used to help us in many ways, e.g. they are able to distinguish a particular enzyme from another, to quantitatively measure catalytic activity, as well as inhibition of this activity, to generate proliferative and toxicity profiles, and even to determine the concentration of proteins in solution. They are a simple and convenient way to visualize biological processes.¹¹⁵ Even more appealing, many colourimetric assays are commercially available as kits, usually with a detailed protocol.

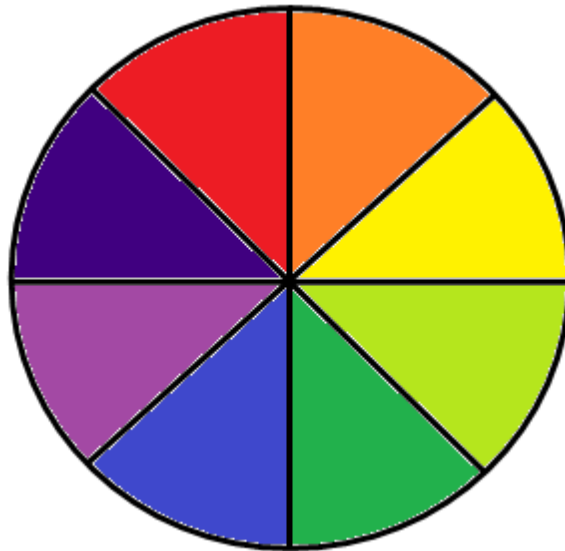


Figure 1. 12: Colour wheel of absorption within the visible region of light
Adapted from reference¹¹⁵

In microfluidics an assay which is simple to use at the same time as been cost effective can be an effective aid when it comes to measuring and monitoring cells or tissue inside a microfluidic chamber, mimicking the *in vivo* environment of the human body.¹¹⁶

In many recent studies, microfluidics has maintained the “simple to use” persona from the offset which has been achieved through the use of colourimetric assays and measuring an analyte via the colour concentration observed.¹¹⁷⁻¹²⁴ Computer software such as ImageJ, Adobe Photoshop have been used to aid in the analysis of such results.

One such example of using a colourimetric assay to aid in microfluidics as reviewed by Vega-Avila *et al.*¹²⁵ can aid in tissue viability. A media containing the required nutrients maintains the tissue or cells in a functional state for various drug treatments on the tissue which lowers the use of animal studies required whilst simultaneously creating more personal patient plans for people suffering from chronic diseases such as cancer, inflammatory bowel

disease and kidney failure. Thereby allowing various drugs to be tested on a patient's biopsy and allowing the best course of treatment to be decided. The use of a colourimetric assay allows the cell death rate or cell functionality to be continuously monitored e.g. the 3-(4,5-Dimethylthiazol-2-Yl)-2,5-Diphenyltetrazolium Bromide (MTT assay) first described by Mosmann.¹²⁶ The development and optimization of *in vitro* colourimetric assays provides for a simple, reliable, sensitive, reproducible, inexpensive and high-throughput method with which to assess the efficacy of novel chemotherapeutic pharmaceuticals on cell survival or proliferation early in the discovery process of drug development.¹²⁵

A more recent use of colourimetric assays in the field of microfluidics is the development of using paper as a platform which naturally wicks fluids along, as described in chapter 1.3.⁵³ This area of microfluidics was mainly headed by Whitesides group at Harvard University who have measured many analytes on paper using this idea such as glucose, uric acid, protein, cholesterol, BSA in a variety of fluids such as blood, urine and saliva.^{5,6,9,20,59,64,127} The main advantage of using colourimetric assays compared with other analytical techniques is the ability to complete the assay in a short time frame (> 30 min) and provide easy interpretable results as the colour can be read without sophisticated equipment unlike other methods such as enzyme-linked immunosorbent assay (ELISA), polymerase chain reaction (PCR) and electrochemical methods, figure 1.13.¹²⁸

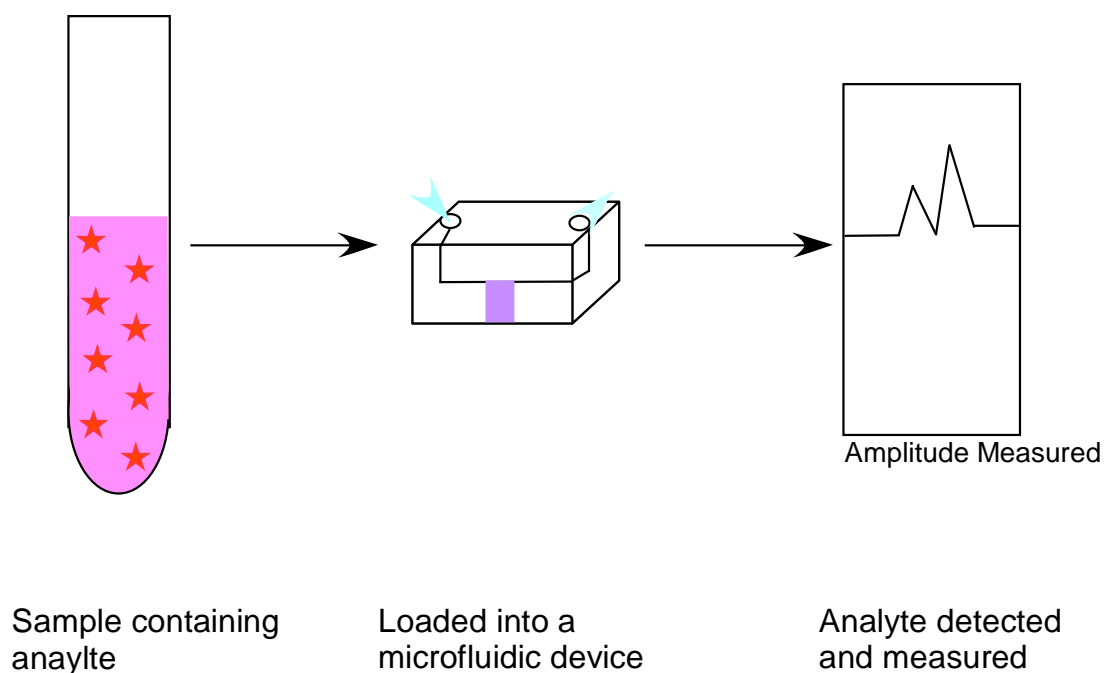


Figure 1. 13: Schematic illustration of a typical colourimetric assay performed using a conventional microfluidic device

1.5.1 Transition Metals in Coloured Complexes

Many common colourimetric assays rely upon the ability of the transition metals to form a coloured complex. Iron is an element classed as a transition metal, due to not having a complete d sub-shell, allowing the element to have more than one oxidation state, e.g. iron(II) and iron(III) and it is this property which allows iron(II) to form to a coloured complex.¹²⁹ As the d sub-shell is incomplete it is possible to promote an electron from a lower orbital by the absorption of a photon.¹²⁹ When light is passed through the solution containing transition metal complexes such as iron(II) with bathophenanthroline the energy of the light absorbed stimulates the transitions between electronic states within the molecule.¹²⁹ This creates the co-ordination bonds between the iron(II) molecule and the N atoms on the

bathophenanthroline molecule.¹²⁹ This transmitted light can be measured via UV/Vis spectroscopy within the visible region (380 – 780 nm) of the electromagnetic spectrum as the intensity of the absorption and its concentration are linearly related to according to the Beer Lambert Law.¹³⁰

1.5.1.1 Beer Lambert Law

The Beer Lambert Law states there is a dependence between the transmission of light through a substance (c) and the product of the absorption coefficient (ϵ) of a substance and the distance the light travels through the material, the path length (cm).^{130,131}

$$A = \epsilon bc$$

Equation 1. 5: The Beer Lambert Law to measure the transmission of light.

The proportion of the light absorbed is dependent on the number of molecules it interacts with, i.e. strongly coloured solution with a high concentration will be high absorbance due to a high number of molecules interacting with the light. If the solution is diluted, the absorbance will be low as there are less molecules reacting with the light (equation 1.5).^{130,131}

1.5.2 Condensation Reactions

A condensation reaction is the chemical reaction between two molecules or functional groups which combine to form a larger molecule. An example of this reaction has been used for the benefit of a colourimetric assay for the measurement of urea.¹³² Urea condenses with *o*-phthalaldehyde and

naphthylethylenediamine (NED) to form a coloured complex, and by following the Beer Lambert Law the colour intensity is directly proportional to urea concentration, which can be monitored using a spectrophotometer at 505 nm, figure 1.14.¹³²

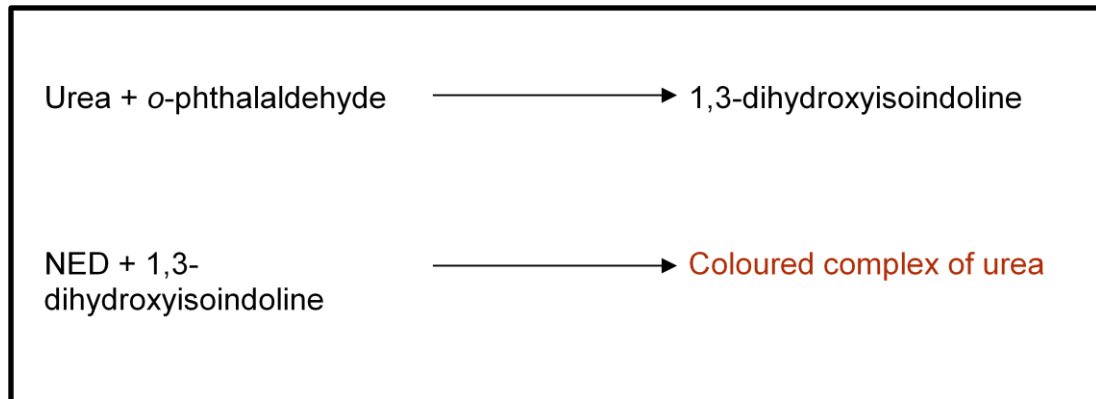


Figure 1. 14: Condensation reaction for a colourimetric assay for the detection of urea.

Adapted from reference¹³²

1.5.3 The Jaffe Reaction

As the colourimetric assay methods are still a large part in modern science, some of the principles were discovered many years ago.¹³³ One such example of this is the Jaffe reaction, discovered by Max Jaffe in 1886, where he first described the principles of creatinine with picric acid in an alkaline environment.¹³⁴ The creatinine molecule can form a red tautomer (also referred to as a Janovski complex, a reactive intermediate) with picric acid when in an alkaline solution by the shifting of hydrogen atoms, figure 1.15.¹³⁵

This method is still employed widely today as a measurement for creatinine concentrations in human serum and urine samples to determine renal

function. However, the reaction is known for its non-specificity by the presence of protein, glucose, ketone bodies and acetone.¹³⁶ Regardless of this factor it is still a highly used method as other methods such enzymatic methods and isotope dilution liquid chromatography mass spectrometry are highly expensive and cannot be used in routine analysis in the NHS.¹³⁶

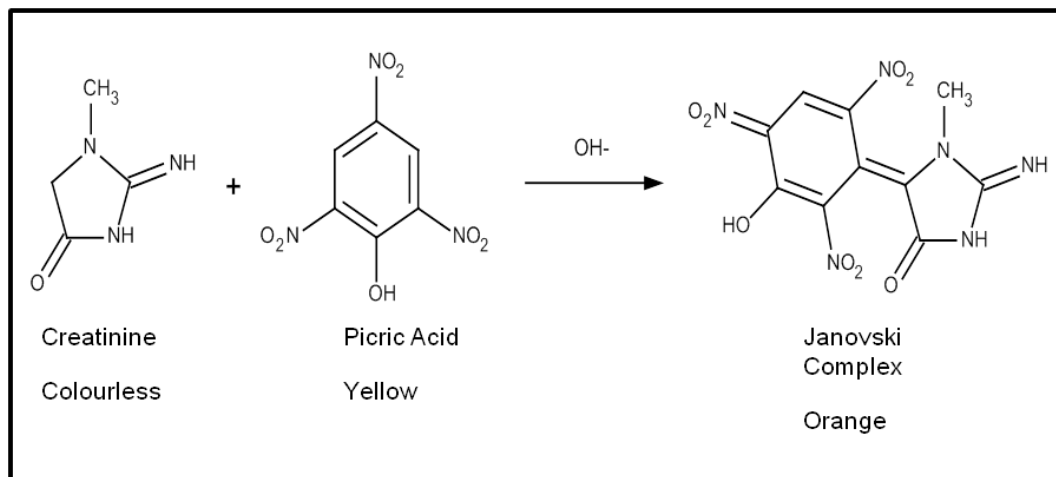


Figure 1. 15: The colourimetric assay of creatinine measurements in human samples.
Adapted from reference¹³⁶

Colourimetric assays in modern day science are a proof of principle that they remain an easily interpretable, reliable method for the detection and measurement of analytes within solutions. They can be used as an assay for biological, chemical and environmental applications.^{122,137,138}

1.6 Iron and Anaemia

Iron is an essential element for humans that is not produced by the body but absorbed via the diet.¹³⁹

Iron(II) has a strong ability to donate and accept electrons, so if any iron(II) was unbound within a cell it can catalyse the conversion of hydrogen peroxide into free radicals.¹⁴⁰ A free radical can cause damage to a wide variety of cellular structures and ultimately destroy the cell.¹⁴¹ This can contribute to the free radical of ageing theory (FRTA)¹⁴¹ initially published in 1956 by Denham Harman. As we age, free radicals (any atom or molecule that has an unpaired electron in its outer shell) accumulate in a cell causing incremental damage over time.¹⁴¹ However, there are several other contributing factors to the cause of increased free radicals, e.g. accumulation of iron(II)¹⁴², increased apoptosis,¹⁴³ and the more commonly known environmental factors such as smoking and diet, the reduction in metabolism through ageing and the body's reduced ability to metabolise fatty acids, lipid accumulation in arteries and organs such as atherosclerosis.

To prevent free radical damage, iron(II) is used in the body (70%) by the heme group proteins which all contain iron(II) at the centre where redox reactions and electron transport processes are carried out.¹⁴⁴ This binds haemoglobin in RBCs to oxygen (O₂) in the lungs where it is transported via the bloodstream to the organs and tissues around the body where it is replaced with carbon dioxide (CO₂) before being returned to the lungs for reversal. Therefore, restricting iron's ability to harm cells whilst providing the principle source of energy for cells in the body.¹⁴⁵

1.6.1 Transferrin

Transferrin is a glycoprotein, a protein which consists of oligosaccharide chains (simple sugars, monosaccharides) covalently attached to polypeptide side-chains (short chain amino acid monomers). Transferrin contains two active binding sites for iron(III) which involves the reduction of iron(II) from the enterocytes in the large intestine by the release of H^+ which is controlled via the pH. There are two halves to a transferrin protein (N lobe and C lobe) with each half consisting of two domains connected by a flexible hinge. In the iron-free form the two halves of the protein are well separated, by forming a water filled cleft allowing for easy access for iron(III).¹⁴⁶ Once iron(III) has been bound the protein will cleft together forming a strong bond which will only be triggered for release by a drop in pH, which results in protonation and dissociation of the iron(III).¹⁴⁶

Iron, insoluble as free iron(III) (also known as ferric iron) and toxic as free iron(II) (also known as ferrous iron), is distributed through the body as iron(III) bound to transferrin (80 kDa).¹⁴⁶ It is absorbed and oxidised to iron(III) via the duodenum in the large intestine by enterocytes before being transported via a transferrin protein (one transferrin protein can bind two iron(III) molecules) to the bone marrow where it is incorporated into the haemoglobin molecule or RBCs.¹⁴⁷ Iron can also be stored in the spleen as ferritin (450 kDa), which binds molecules of iron(III) and is released on a “need basis” where it would be transported via the transferrin protein to the bone marrow.¹⁴⁷ If a cell requires iron it will produce a transferrin receptor, where the transferrin protein incorporated with iron can bind and be

transferred inside the cell via endocytosis (production of a vesicle).¹⁴⁷ The transferrin protein has overcome two problems faced within the body and with iron transportation. One been, iron(III) is at a stable oxidation state which is insoluble and the second been iron(II) is toxic through the generation of OH radicals.

1.6.1.1 The Lauber Method

A method for measuring serum iron was described by Lauber *et al.*¹⁴⁸ in 1965 which allowed for the simultaneous protonation and dissociation of iron(III) into iron(II), quantifiable via a spectrophotometer. In the solution is a detergent (teepol) which lowers the pH to dissociate the iron(II), magnesium sulphate acts a salt as the sodium dithionite reduces the iron(III) into iron (II), (figure 1.16), allowing the iron(II) to form a complex with a coloured compound such bathophenanthroline or 1,10-phenanthroline.¹⁴⁸

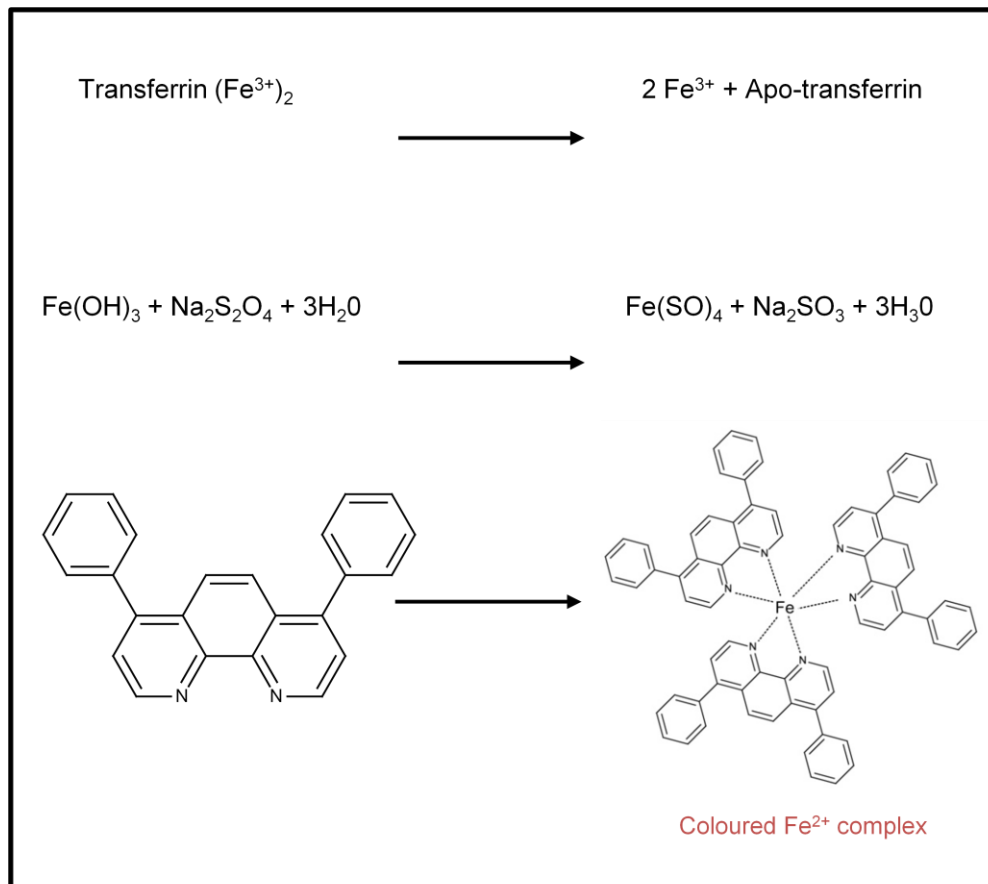


Figure 1. 16: The colourimetric detection using dissociation, reduction and reaction of iron(II) with bathophenanthroline in serum samples.

1.6.2 Haemoglobin

A Hb molecule is found in the RBCs and has two α chains and two β polypeptide chains, with each chain containing a heme molecule.¹⁴⁵ When the heme group is interacting with an O_2 molecule it is known as oxyhaemoglobin (HbO_2) and its association with oxygen is very weak so it can easily be dissociated.^{145,149} In the peripheral capillaries O_2 is very low, heme molecule releases the O_2 , (CO_2 levels will be very high in comparison) and the heme molecule will bind to the CO_2 forming carbaminohaemoglobin. In the lungs the O_2 levels will be very high so the CO_2 will be released and the O_2 attached to the heme molecule.¹⁴⁹

RBCs have a short lifespan and upon haemolysis (breakdown of haemoglobin) the heme is stripped of its iron where it can then be converted via three different pathways. One route excretes the iron by converting it into biliverdin, which is further converted into bilirubin and released into the bloodstream.¹⁵⁰ In the bloodstream bilirubin can bind to albumin where it is taken to the liver and converted into bile for excretion from the body.¹⁵⁰ The second route for iron can be recycled by binding to a plasma protein known as transferrin, where developing RBCs absorb the transferrin and iron complex and use it to synthesise new Hb molecules. Finally the third route removes iron from the bloodstream into the liver or spleen where it is stored as ferritin until it is needed.¹⁵⁰

1.6.3 Anaemia

Most well-nourished people have between 4 and 5 g of iron in their bodies, with over half this amount located bound to the haemoglobin.¹⁵¹ A lack of iron is more commonly referred to as anaemia and affects the oxygen transport around our body. A lack of oxygen to an organ can lead to severe complications and in extreme cases loss of life.¹⁵¹ Anaemia is defined as a reduction in blood haemoglobin concentration, reflected in a reduction in the oxygen carrying capacity of the blood.¹⁵² Symptoms of anaemia can vary from a feeling of fatigue, poor concentration, dyspnoea, angina, jaundice or pallor. Once a person is suspected of suffering from anaemia, the diagnosis is confirmed from a full blood count.¹⁵²

A full blood count is done on whole blood samples taken from the peripheral veins (not in the chest or abdomen) and the results received from the laboratory will include information on RBCs, WBCs and platelets.¹⁵³

RBCs will relate to information on the Hb concentration, the mean number of cells in the plasma and the RBCs width.¹⁵³ The normal concentration of Hb levels in children and adults is defined below in Table 1.1, anything below these values will suggest anaemia.¹⁵³

WBC information will relate to the type of WBC (this includes neutrophils, lymphocytes, monocytes, eosinophils and basophils) and if the level is normal or increased:¹⁵³

- Neutrophils are increased this suggests a bacterial infection, haemorrhage, inflammation, infarction or trauma
- Lymphocytes are increased this suggests a viral infection, TB, Syphilis or whooping cough.
- Eosinophils are increased this suggests asthma, allergy, parasitic infection, skin diseases such as eczema.
- Basophils are increased also in viral infections, Ulcerative colitis, malignancies and haemolysis.

Platelets are also counted as this will provide information on further diseases and infections.¹⁵³ If a low platelet count is found, this can suggest Leukaemia, viral infections, HIV and chemical toxicity.¹⁵³ If a high level of platelets is found this can suggest inflammatory disorders, acute infections, trauma and haemorrhage.¹⁵³

Table 1.1: WHO's threshold to define anaemia from haemoglobin blood concentrations.

Age and Sex	In blood /g/dL	In blood/mmol L⁻¹
Children 0-5 years	11	6.8
Children 5-12 years	11.5	7.1
Teens 12-15 years	12	7.4
Women, non pregnant	12	7.4
Women, pregnant	11	6.8
Men	13	8.1

The most severe consequence a person can suffer due to a lack of iron is known as iron deficiency anaemia (IDA), which is still considered the most common nutritional deficiency worldwide today, especially in developing countries.¹³⁹ Although the etiology of IDA is complicated, it generally results when the iron demands by the body are not met by iron absorption, regardless of the reason.¹³⁹ In developing countries the diagnosis of such nutritional deficiencies are required to be performed by a trained phlebotomist in poor working conditions and one of the main reasons behind the rationale of using microfluidics is due to a quicker assessment, using less reagents and using untrained personnel to perform the test or allowing the patients to test themselves.¹⁵⁴ “In particular, microfluidic diagnostic technologies are potentially applicable to global health applications, since

they are disposable, inexpensive, portable, and easy-to-use for detection of infectious diseases”.¹⁵⁵

Recent publications in microfluidics have focused on this area to try and impact in the diagnosis of disease and infection, once such study has miniaturised a POC device for the diagnosis in HIV and tropical diseases such as malaria.^{32,156} This device consisted of paper, plastic and glass fiber which performed isothermal, enzymatic amplification of HIV DNA.¹⁵⁶ The device can store lyophilized enzymes, facilitating the mixing of reaction components, and supports the recombinase polymerase amplification in five steps of operation with HIV DNA been detectable after 15 min.¹⁵⁶ Similar work has also been produced by Brynes *et al.*²³ who describe a portable system for centrifuge-free room temperature nucleic acid extraction from small volumes of whole blood for the PCR of HIV DNA.²³ The most commonly used HIV tests detect HIV RNA genome copies circulating in plasma through a reverse transcriptase-PCR based nucleic acid amplification test, typically requiring complex and time consuming sample preparation before analysis.²³ The work by Klapperich *et al.*²³ describes a portable device for nucleic acid extraction and storage using thermally stable reagents that do not require the use of electrical power and is capable of extracting HIV-1 viral RNA directly from whole blood in less than 35 minutes.²³

Another example of microfluidics been investigated into the use of diagnosing disease in the developing world is work described by Mudanyal *et al.*¹⁵⁷ who integrated microfluidics into the growing network of mobile phones to incorporate a reader platform to attach to a mobile phone and the camera

and to image a sample using a light-emitting diode (LED)-based illumination.¹⁵⁷ This can then be processed and transmit the resulting data, together with the RDT images and other related information (e.g., demographic data), to a central server.¹⁵⁷ This device was tested with samples of malaria, TB and HIV all which are major infections in the developing world.¹⁵⁷

1.6.4 1,10-Phenanthroline

1,10-phenanthroline (figure 1.17) is a heterocyclic organic compound used as a ligand in co-ordination chemistry, most commonly iron(II). The detection of iron via a colourimetric approach using 1,10-phenanthroline, measures the absorption of a colour change proportional to the amount of iron(II) present in the sample. The complexes of 1,10-phenanthroline with both metals and non-metals have been exploited since the 1930s.¹⁵⁸ 1,10-phenanthroline is a chromophore, soluble in aqueous solutions which reacts with iron(II), reduced from iron(III) to iron(II) by a reducing agent such as sodium dithionite or acetic acid. Upon this reduction the iron(II) can form a complex with three units of 1,10-phenanthroline by the nitrogen atoms which gives the complex its red colour.

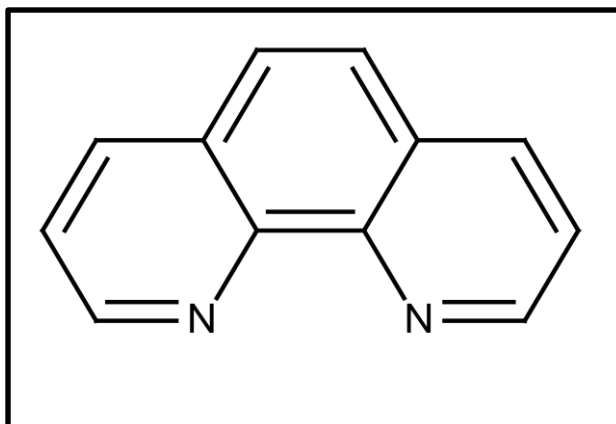


Figure 1. 17:1,10-Phenanthroline Molecule.

Figure 1.18 illustrates the 1,10-phenanthroline molecule in which the Fe(II) forms co-ordinate bonds with the two N atoms forming the coloured compound. The complex is then measured using a spectrophotometer at the wavelength 510 nm. ¹⁵⁸

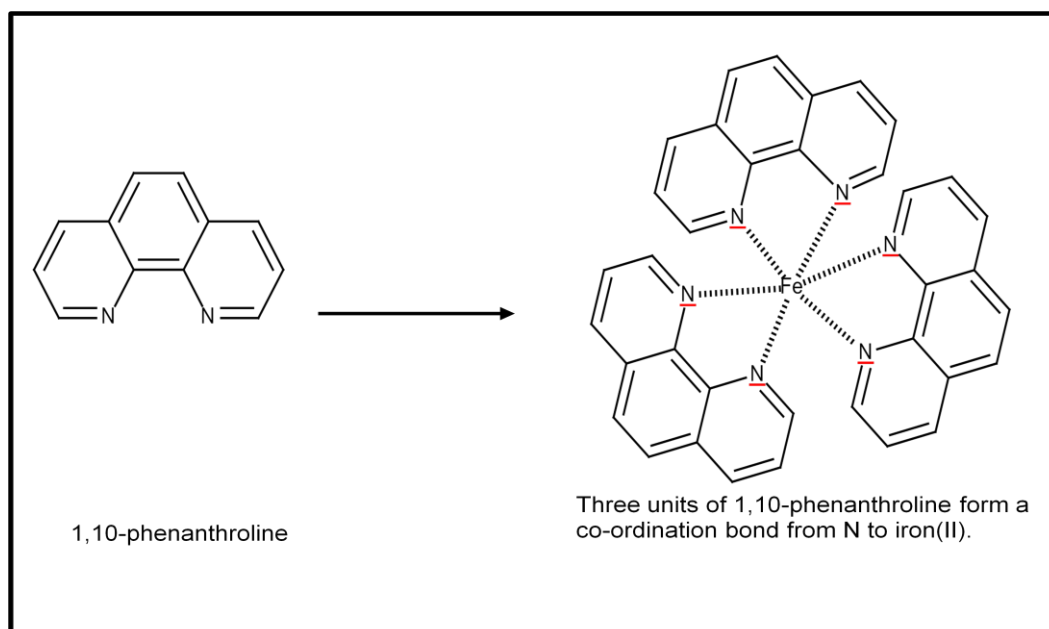


Figure 1. 18:1,10-phenanthroline reaction with iron(II).

1.6.5 Bathophenanthroline

An alternative to using 1,10-phenanthroline is a derivative of this molecule known as 4,7-diphenyl-1,10-phenanthroline (more commonly referred to as bathophenanthroline, see figure 1.19A).^{159,160} This organic reagent specific for iron(II), can detect iron(II) from 10 to 100 ng mL⁻¹ in a 100 mL sample, which is more sensitive than 1,10-phenanthroline.¹⁵⁹ It is only soluble in an alcohol solution with the reaction creating co-ordination bonds between the N atoms on three units of the bathophenanthroline, as the 1,10-phenanthroline molecule in figure 1.18.

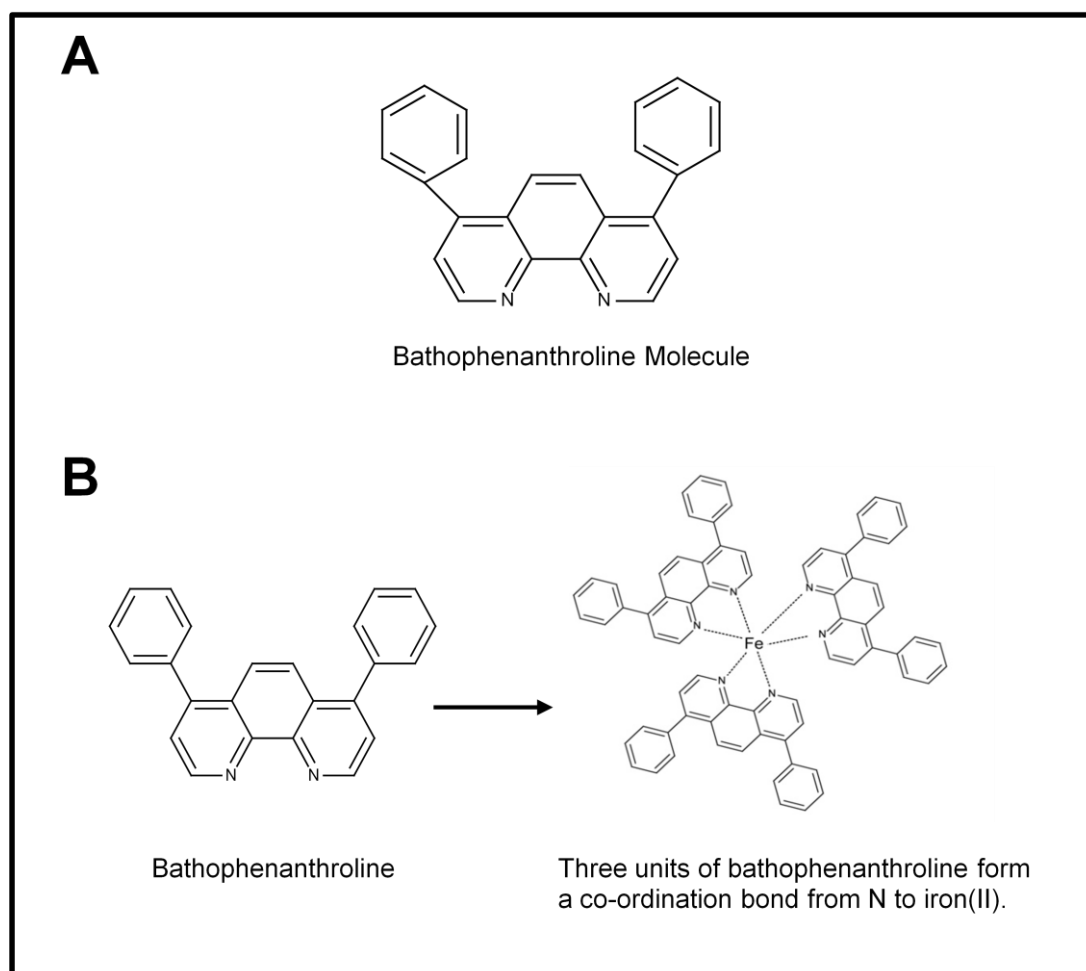


Figure 1. 19: Bathophenanthroline reaction with iron(II).

Panel A: Bathophenanthroline molecule, **Panel B:** Reaction of bathophenanthroline with iron(II) to create coloured product

Recent papers have been published which take advantage of the above reaction for iron(II) detection on a microfluidic scale using paper devices.⁶⁵ Total iron concentrations were detected in paper by spotting 1,10-phenanthroline into a channel created on paper via wax printing.⁶⁵ Human serum samples containing iron were wicked along the channel and the colour intensity was proportional to the iron present in that sample.⁶⁵ However, this study fails to mention how the iron concentration could be accurately measured as the iron solution suffers from a chromatographic effect, diluting the colour intensity when using 1,10-phenanthroline which could be overcome through the use of bathophenanthroline as an alternative.

Dungchai *et al.* stated “the use of multiple indicators for a single analyte allows for different indicator colours to be generated at different analyte concentration ranges, increasing the ability to visually discriminate colours.”¹⁶¹ Thereby meaning if bathophenanthroline and 1,10-phenanthroline were used simultaneously to detect iron(II) in a sample then the different indicator colours generated at different analyte concentration ranges increase the ability to better visually discriminate colours

1.7 The Kidneys and Renal Failure

In the mammal the kidneys are organs which filter all the waste products from the bloodstream and re-absorb any useful organic material, figure 1.20.¹⁶² However, the kidneys can function with as little as a 10% capacity before the patient will feel un-well, therefore been able to diagnose and treat

renal failure before reaching an end point is crucial for the prognosis of the patient.¹⁶²

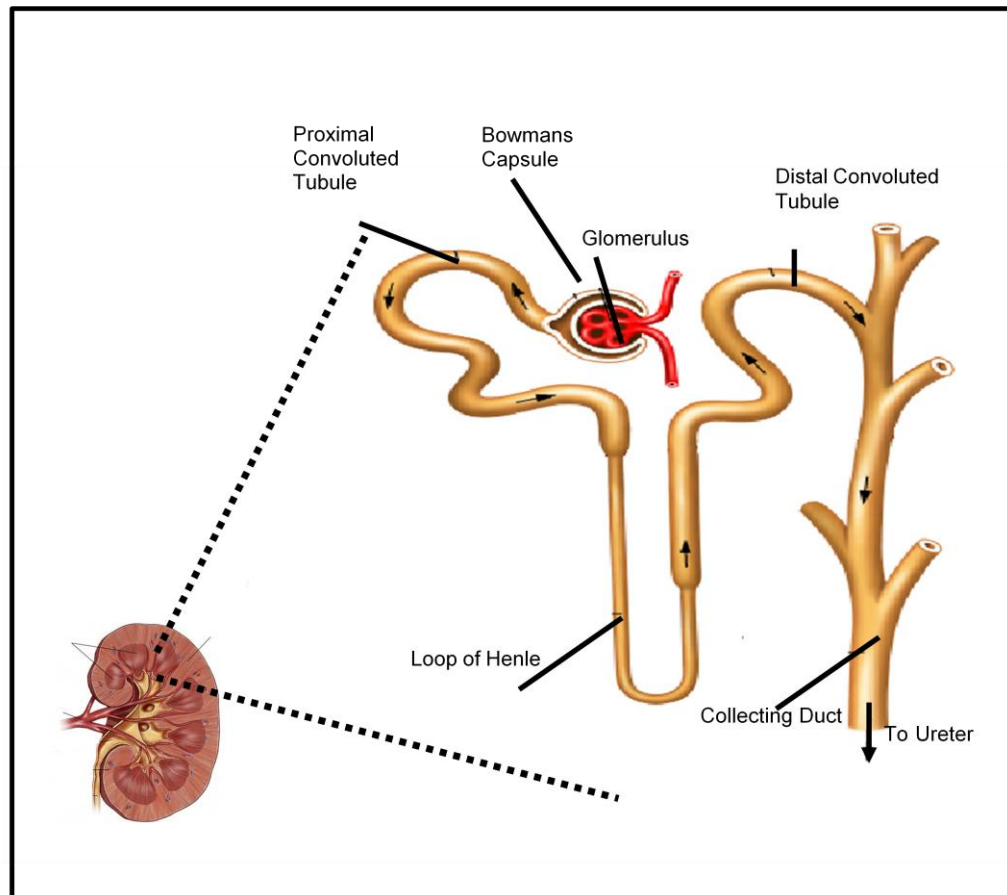


Figure 1. 20: The kidneys and the renal tubule for filtering waste products.
Adapted from reference¹⁶²

1.7.1 Renal Failure

Renal failure occurs when the kidneys no longer are able to maintain homeostasis and urine production declines.¹⁶³ This leads on to affect pH, ion concentrations, metabolic waste build-up which causes problems for muscle contraction, metabolism, and digestive functions etc.¹⁶⁴ If left alone the patient would progress from acute renal failure which can be reversible, to

chronic renal failure which cannot be reversed, its progression can just be slowed.¹⁶⁵ Most renal diseases attack the nephrons in both kidneys simultaneously causing them to lose their filtering capacity.¹⁶⁵ This damage to the nephrons can occur quickly, usually due to injury or poisoning, but most renal diseases destroy the nephrons slowly and silently.¹⁶⁵ It is only after years and sometimes decades that the damage becomes apparent.¹⁶⁵

The two most common causes of renal disease are due to diabetes and high blood pressure.¹⁶⁶ Certain drugs and poisons can stop the kidneys from working and these sudden drops in kidney function are known as acute kidney injury (AKI) or acute renal failure (ARF).¹⁶⁷ AKI or ARF can lead to the permanent loss in kidney function but if the kidneys are not severely damaged, acute kidney disease can be reversed.¹⁶⁷⁻¹⁷³ However, in comparison over half of the kidneys problems occur slowly, a person may have "silent" kidney disease for years and have not noticed the onset of the disease; this is the most striking and concerning feature of renal failure. Gradual loss of kidney function is called chronic kidney disease (CKD).^{168,174-177} People with CKD can go on to develop permanent kidney failure with an increased risk of a stroke or heart attack. Total or nearly total and permanent kidney failure is called end-stage renal disease (ESRD). People with ESRD must undergo dialysis or transplantation to stay alive.^{168,174-177}

Currently ESRD treatment consists of two options, dialysis or kidney transplant. Dialysis patients have to restrict their fluid intake and constantly be travelling to the hospital for dialysis to remove waste products from their blood, usually taking 4 h.¹⁷⁰ Unfortunately, this treatment can only prevail for

five to ten years for reasons currently with the only remaining option been a kidney transplant. This option is difficult as the chances of finding a donor match are slim and expensive as the patient will have to be on immunosuppressant drugs for the remainder of life to prevent the body from rejecting the organ.¹⁶⁸

Over 2 million people now require renal replacement therapy worldwide, In the developing world countries, access to the life-saving therapies has increased over recent years.^{174,178-181} Continued efforts to reduce the cost of renal dialysis, and to make transplantation more widely available but regardless renal replacement therapy remains unaffordable for the majority of those affected.^{174,178-181} Namely the immunosuppressant drugs required with an organ transplant remain un-affordable with nearly 600 million people not been able to afford renal replacement which results in the annual death of 1 million people from untreated kidney failure.^{174,178-181} Motivated by this dismal outcome the last two decades have resulted in an increase to the prevalence, prevention, and consequences of earlier and milder forms of renal impairment.^{174,178-181}

The symptoms of renal failure are highly variable but usually entail pressure or difficulty in urination, foamy or bubbly urine, an increased frequency in urination, blood in urine, weight loss, vomiting and diarrhoea.¹⁸⁰ CKD is usually gauged by calculating the glomerular filtration rate (GFR) by measuring serum creatinine level and is somewhere on a scale of one to five, figure 1.23.¹⁸⁰ Stage one is classed as a mild form of renal disease with slight diminished renal function with show little or no symptoms whereas

stage five is classed as a severe disease with the only option been to have dialysis or kidney transplant.¹⁸⁰

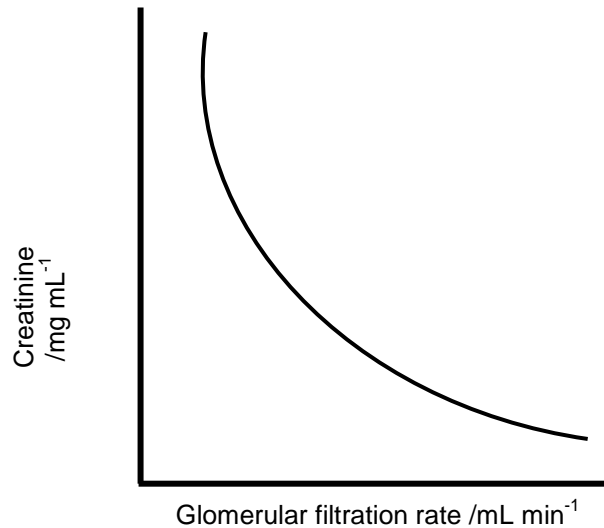


Figure 1. 21: The Glomerular filtration rate to measure kidney function.
Adapted from reference¹⁸⁰

The minimum amount of urine a person can excrete with 24 h is 500 – 600 mL and the simplest test to detect renal failure is a dipstick assay, where pre-prepared paper is dipped into a patient's urine sample to detect proteins, blood, glucose and bile.¹⁸² A pH test with litmus paper can also be performed to determine the acidity of the urine.¹⁸² However, these tests only detect a problem, they do not diagnose the cause.¹⁸²

As previously mentioned the kidneys have the ability to monitor the amount of body fluid and the concentrations of the filtered waste products of body metabolism, like urea from protein metabolism and uric acid from DNA

breakdown. These are two waste products in the blood can be measured; blood urea nitrogen (BUN) and creatinine.¹⁸² Both these waste products rise when the kidneys are unable to remove the waste products from the blood efficiently.¹⁸³ Much of the research done on these measurements of creatinine and urea are to gauge the seriousness of the kidneys problem¹⁸⁴.

However work completed by Belcher *et al.*¹⁸⁵ suggested that although creatinine does act as a marker for ARF, it is inhibited back by its non-specificity (Jaffe Reaction) as a marker for kidney injury alone but instead as a marker for changing kidney function. Creatinine level lacks sensitivity and specificity for the diagnosis of ARF and shows a significant delay time before increasing after the injury, therefore, the BUN test is performed alongside (measurement of blood urea nitrogen).¹⁸⁵

1.7.2 Urea

Urea is an organic compound (also known as carbamide) produced by the body as a way of excreting nitrogen containing compounds, therefore it is mainly found in urine, figure 1.27.¹⁸⁶ The process of deamination (breaking down of amino acids) occurs in the liver, where they are converted into ammonia, carbon and hydrogen.¹⁸⁶ However, ammonia is toxic to the human system so is further broken down by the addition of carbon dioxide into urea and uric acid, which can be safely filtered into the bloodstream, and then excreted by the kidneys.¹⁸⁷

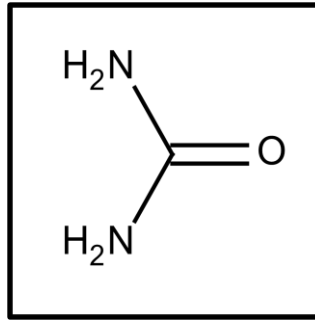


Figure 1. 22: The Urea molecule, produced as a waste product of human metabolism.

Normal levels in blood for urea are 6 - 20 mg dL⁻¹ and are usually measured through a BUN test, a high level of urea is indicative of acute or chronic renal failure and low levels of urea are indicative of liver failure or malnutrition.¹⁸⁸ As the kidney can function at 10% their normal capacity, they are not very demonstrative organs when they are in distress or failing, urea can be used as an early marker to gauge how badly damaged the kidneys are.¹⁸⁸

1.7.2.1 The Jung Method

The two commonly used methods for the detection of urea are the urease, phenol and hyochalite reaction and the diacetyl reaction.^{189,190} In the first detection method, a blue colour was observed when ammonia, phenol and hypochlorite were mixed, proportional to the amount of nitrogen in the solution, however, the reagents used in this reaction are unstable.¹⁸¹ The second reaction, the diacetyl reaction is another sensitive method for urea detection however the coloured product formed is unstable and only developed at 95°C.¹⁸⁹ The reaction relies on a diacetyl that yields a yellow colour with urea in presence of concentrated H₂SO₄.¹⁸⁹

In comparison with these methods, in 1975, Jung *et al.*¹³² described another method that was a colourimetric reaction measured spectrophotometrically for urea, *o*-phthalaldehyde and N-(1-naphthyl)ethylenediamine (NED).¹³² This reaction was based upon the condensation reaction between urea and an aldehyde (*o*-phthalaldehyde) in a strong acid solution (NED), figure 1.23.¹³² This reaction could be performed at 37°C with stable reagents to accurately measure urea concentrations in human serum samples, and became the preferred measurement of choice at that time.¹³²

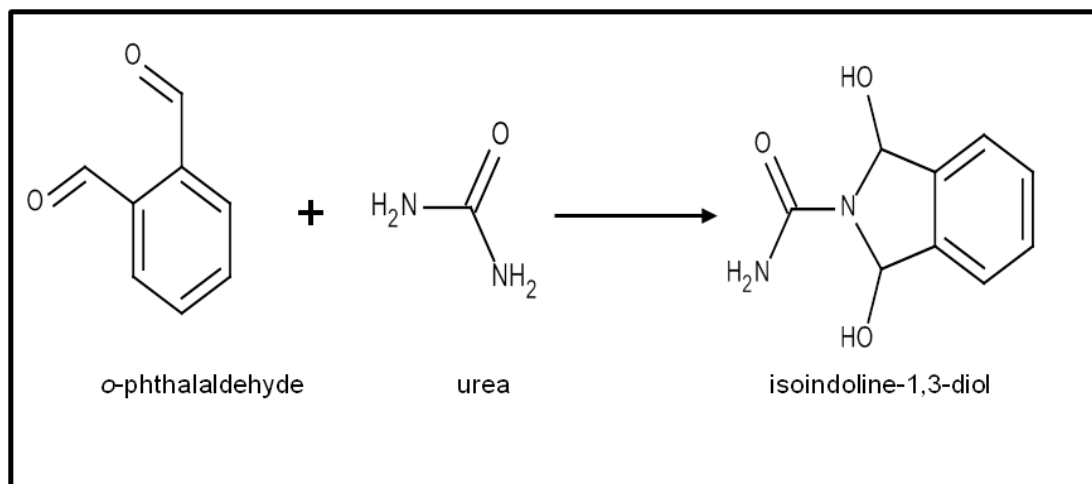


Figure 1. 23: The urea reaction for colourimetric detection spectrophotometrically.

1.7.3 Human Metabolism of Creatinine

In comparison with urea, creatinine is produced as a waste product by the muscles at a constant rate.^{123,191} As the muscle contracts, creatine phosphate is produced and broken down into creatinine which is released

into the bloodstream. ^{123,191} From here, it is excreted through the kidneys without any re-absorption back into blood stream. ^{123,191} Therefore, if the kidneys are unable to filter the blood of waste products a rise in creatinine levels is seen early, making creatinine a reliable marker for early stage renal disease and determining the glomerular filtration rate. ^{123,191}

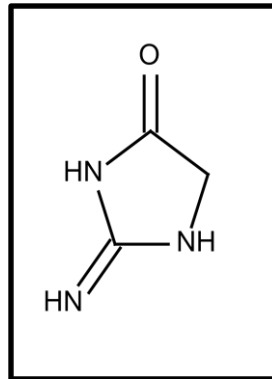


Figure 1. 24: A Creatinine molecule produced as waste from muscle activity.

1.7.3.1 The Jaffe Reaction

First discovered by Max Jaffe in 1886 and still used today the Jaffe Reaction has become a well known method to determine creatinine levels using picric acid in an alkaline environment as described in chapter 1.5.3.¹³³ However, it was Otto Folin who adopted this method for clinical use in the detection of creatinine in human serum samples.¹³⁴ He noted that there was interference in the results when measuring creatinine levels in serum causing falsely elevated results but in urine samples creatinine levels are much higher and it does not contain significant levels of interfering chromogens.¹³⁴

Due to this interference many researchers have attempted to develop an assay for creatinine which is as straight forward as the Jaffe Reaction.¹³⁶

Currently the methods of analysis are either, expensive and impractical such as the isotope dilution liquid chromatography-mass spectrometry or are affected by interfering compounds as the Jaffe Reaction, e.g. an enzymatic method which measures the production of hydrogen peroxide.¹³⁶

Regardless of the interference caused by the proteins and glucose in human serum samples, the Jaffe Reaction is still a widely used clinical test for renal diagnosis as counteracting this issue a BUN test would be measured alongside to ensure no false diagnosis is made.^{38,133,135,136,192-198}

1.8 Aims and Hypothesis

Taking into consideration that there is a major requirement to be able to perform routine medical tests in a resource limited area, microfluidics and paper based microfluidics is a technology to meet this need. The current issue for using many of the described miniaturised systems is they have to have a consistent power supply to supply flow of fluid through channels e.g. external pump. However, if paper were used as a platform then this problem would be overcome and the devices could be taken outside of the laboratory setting and into areas where power supply can be limited e.g. developing world countries. Therefore, the first aim was to design and fabricate a paper based device which can be used away from a laboratory setting by untrained personnel as a POC medical device.

The second aim was to create channels using photolithography as an inexpensive fabrication method and adapted for use within the paper structure to control the fluid movement towards a defined area and inhibiting

fluid from spreading outwards in every direction. Once established, the hydrophobic and hydrophilic areas will be compared ensuring they are strong enough to maintain the papers integrity.

The third aim was to use the paper platform for the detection of analytes in human samples in diseases and areas that are problematic within the developing world such as anaemia and kidney failure, which is also a major concern within the developed world and this device may have cross over.

Lastly, the fourth aim was to seek ethical approval for the use of various bodily fluids to determine which was best for the application on a paper microfluidic device. The results from the analysis taken from the paper device were compared to the results received from a hospital to ensure that the accuracy is maintained when using the paper device.

The hypothesis of this study is that a paper device will be used to establish routine diagnosis tests for urea, creatinine and iron(II), were results are not significantly different from those obtained from the hospital pathology laboratory.

Chapter 2: Experimental

This chapter aims to provide a general overview of the materials and methods employed along with detailed descriptions of the equipment used.

2.1 Fabrication of the Paper Device for Iron Analysis

2.1.1 Summary

To fabricate the paper devices photolithography was chosen as the method for patterning channels on to filter paper to control and direct fluid along a set course towards a “detection zone” as previously mentioned in chapter 1.11. Photolithography on paper was first described by Martinez *et al.*⁵⁸ however, the protocol described was adapted for use with a negative photoresist.

The method described here was adapted for suitable use with a positive photoresist in comparison with the negative photoresist used in the paper published.⁵⁸ The pre-bake time and temperature was optimised so that the polymer in the photoresist hardened and became hydrophobic, whilst not charring the filter paper or the photoresist. The exposure time of the photoresist to the UV light had to be evaluated to allow the light sensitive parts of the photoresist polymer to breakdown and become soluble to an alkaline solution. The development time was also assessed to evaluate how long the paper needed to be soaked in order to remove the exposed areas of the photoresist.

2.1.1 Materials

Whatman Number 1 chromatography paper was purchased from VWR (UK). The photo-masks used in all experiments were created in-house using an ink-jet printer (HP K5400 series) to print black ink patterned onto an inkjet printable acetate sheet and designed using Microsoft Word (2010). The hot plate (PC-420D) was purchased from Fisher Scientific (UK) and was used to bake the photoresist while the UV light source, a mega electronics small UV exposure unit (UV output 2 x 8 W) was obtained from Maplin Electronics (UK). The positive photoresist S1805-G2 and corresponding developer MF-319 was purchased from Chestech Ltd (UK).

2.1.1 Method

The filter paper was cut (with common household scissors and a ruler) into sizes 6 cm by 5 cm rectangular sheets and soaked for 5 min in the positive photoresist, the excess was removed by blotting onto tissue paper and subsequently left to air dry in a darkened fume cupboard in a covered container for 24 h. A photo-mask was designed using Microsoft word and once completed was printed on to an acetate sheet. Microsoft word was chosen as the computer software of choice as a high quality printer would allow a dense enough black photo mask to be used which would not let the UV light penetrate. Once cut to size the two masks were aligned and stuck in place with adhesive tape at three sides, figure 2.1. This allowed the photoresist coated paper to be slid in between the two photo-masks and be held in place when been exposed to UV light, which allowed the photoresist polymer to be broken down and removed by the developer solution.

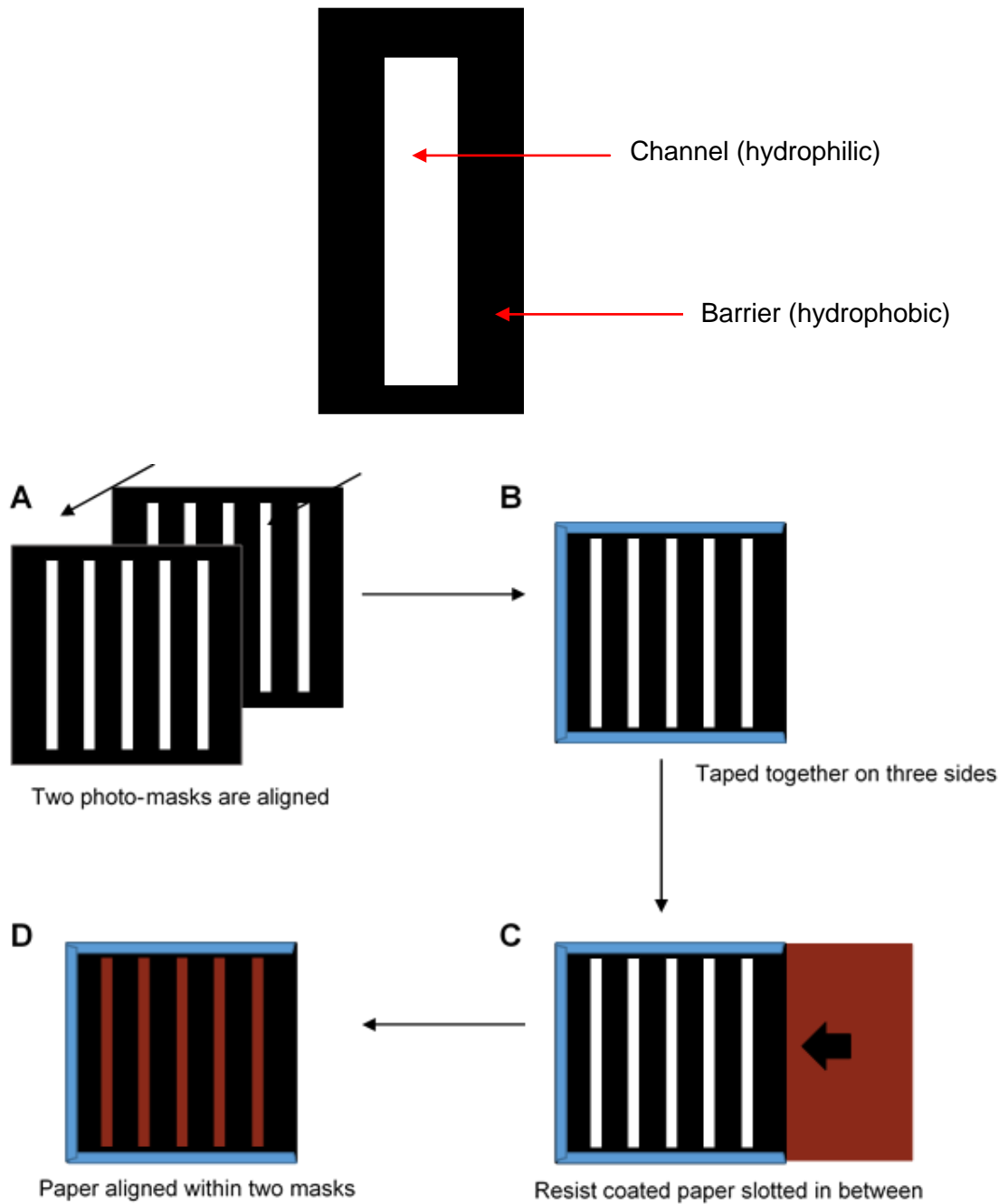


Figure 2.1: Schematic diagram of double-sided photo-mask.
Panel A: Alignment, **Panel B:** Adhesive tape used to fasten three sides of the two photomasks; **Panel C:** Photoresist coated filter paper slotted in between two photo-masks, **Panel D:** Device ready to be exposed to UV light

After the photoresist coated filter papers were completely dry, individual pieces of filter paper were heated at 90°C on the hotplate for 4 min. A copper plate was placed on top of the filter paper to ensure all areas of the paper were heated equally and to avoid the filter paper from curling. The filter paper was slid between the two identical copies of the photo-mask (figure 2.1C), which had previously been sandwiched on three sides and sealed with adhesive tape (figure 2.1B). The photo-mask and paper assembly was then placed into the UV light box and exposed for 5 min on each side (flipping the mask over after the first 5 min) allowing the UV light to penetrate fully through the filter paper permitting the channels to be well-defined throughout the entire thickness of the paper after development, figure 2.2.

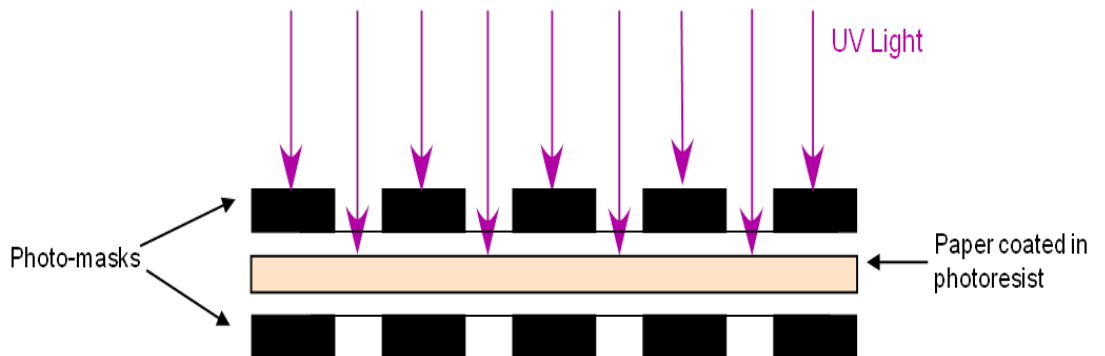


Figure 2.2: An illustration of the exposure of the photoresist-coated paper. *The UV light passed through the areas of the acetate film clear of black ink. The photo-mask is exactly positioned to allow identical patterned channels on both sides of the photoresist coated filter paper allowing the channel to be the entire thickness of the paper.*

The filter paper was developed in concentrated developer, due to a more efficient photoresist removal for 1 min and rinsed in purified water for 2 min whilst constantly gently agitated. The filter paper was then held for a further

30 s under a flowing cascade of purified water or until the water flowed clear. The completed paper devices were dried at room temperature for 1 h and stored in the dark in a sealed container at room temperature until use. If the devices were stored in the light, the photoresist would eventually degrade and become hydrophilic, by storing them in the dark the hydrophobic barrier remained intact.

2.2 Contact Angles

2.2.1 Summary

Contact angle measurements were used to determine how strongly water interacted with the surface of the photoresist coated filter paper. The shape of the droplet of liquid was measured according to the “Young’s Relation Equation” allowing the “wet ability” of the solids surface to be quantified.⁸⁷ Were the molecules of the liquid are attracted to the solid surface (hydrophilic), the drop will spread out and a contact angle of 0°- 30° will be measured, but if the surface is strongly hydrophobic then an angle larger than 90° will be measured⁸⁷.

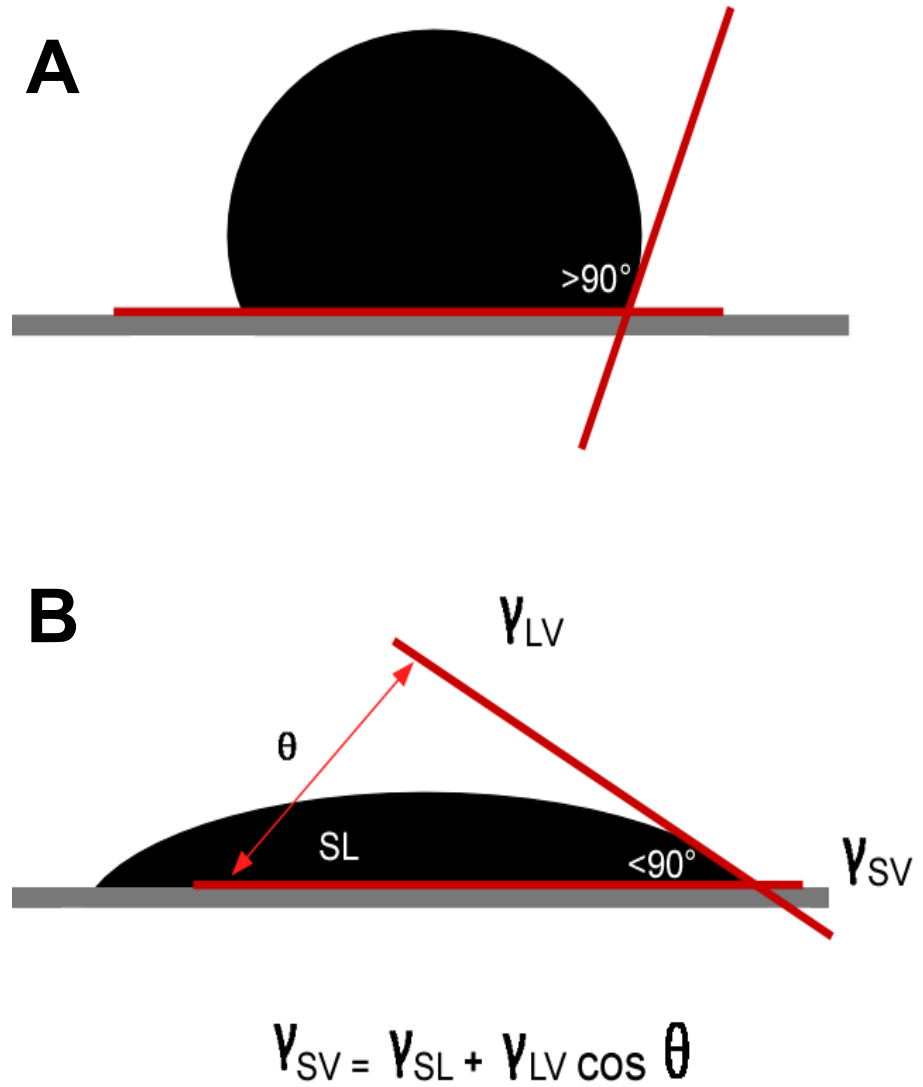


Figure 2.3: Contact angle measurements.
Panel A: Hydrophobic surface. **Panel B:** Hydrophilic surface

2.2.1 Materials

A 5 μL plastic syringe was purchased from Fisher Scientific (UK). The Krüss DSA10 goniometer was used to make the contact angle measurements (Research & Industrial Instrument Co, UK).

2.2.1 Method

Contact angles were measured on five paper devices both on the channel created via photolithography (which should be hydrophilic as the photoresist has been removed), and also to the side of the channel on an area which had not been exposed to UV light (which should be hydrophobic as the photoresist should have remained intact). This allowed for a comparison between the hydrophobic areas and the hydrophilic areas, thus determining how hydrophilic or hydrophobic the two areas were.

A paper device was attached via double sided tape (to ensure a flat surface throughout the experiment) to the platform of the goniometer. A 5 μL syringe was used to pipette purified water onto the paper device both on top of the channel and to the side of the channel and the contact angle measured using the goniometer. Five replicate measurements were made on each device.

2.3 Colourimetric Detection of Iron Spectrophotometrically

2.3.1 Summary

Iron was measured from human serum samples via a spectrophotometer due to the simultaneous reduction of iron(III) into iron(II) and the detachment of iron(III) from the transferrin protein to which it is bound in human serum, thereby allowing the concentration to be quantified as a coloured complex

which could be measured within the visible region (508 nm – 533 nm). The method adapted for use was from Lauber *et al.*¹⁴⁸

2.3.1 Materials

Fe₂O₃ (Iron(II)) and Fe₂SO₃ (iron(III)) sulphate hydrate puriss, meets analytical specification was used to create standard concentrations ranging from 0.1 M to 7.5 μM was purchased from Sigma Aldrich (UK) along with 1,10-phenanthroline and bathophenanthroline (titration by HClO₄, ≥99%). Sodium dithionite (technical grade 85%), magnesium sulphate (anhydrous, Reagent plus, ≥99.5%), teepol 610 S, sodium hydroxide (BioXtra pellets, ≥98%) purchased from Sigma Aldrich (UK). Eppendorfs and accumax variable and fixed volume pipettes used was purchased from VWR (UK) and Jencon (UK) respectively. Plastic, 1.5 mL cuvettes were purchased from Fisher Scientific (UK) and was used with a Perkin Elmer portable single beam spectrophotometer. Human whole blood, serum and plasma samples were used in accordance to the LREC ethical approval (CHEM/TMC/2011-1).

2.3.1 Method

The reducing agent, sodium dithionite (10 g) and magnesium sulphate (2 g) were dissolved in 160 mL of purified water and mixed with 240 mL of the detergent teepol using a magnetic stirrer. Added to this solution was 100 mL of sodium hydroxide (15 g sodium hydroxide per 500 mL of purified water) and the pH was altered to a pH between 5 - 6.2, to aid in the prevention of the 1,10-phenanthroline and the bathophenanthroline from creating a coloured complex with anything other than iron(II) . This stock solution was stored in a refrigerator for up to four months, after which it lost efficacy.

Fe_2O_3 standards were made to 0.1 M and 7.5 μM concentrations in purified water. Bathophenanthroline and 1,10-phenanthroline were at a concentration of 0.1 M.

In a cuvette, 1 mL of iron(III) solution or 1 mL human serum sample was mixed with 0.5mL of the teepol and sodium dithionite solution along with 0.1 mL of either bathophenanthroline or 1,10-phenanthroline. This was incubated at room temperature for 5 min which allowed the colour to develop. Once the reaction at 5 min had occurred, the sample was spun down using a centrifuge to remove the agglutinated teepol (which contained the larger molecules found in serum such as the transferrin protein). The sample was loaded into the spectrophotometer and the absorbance was measured at 508 nm for 1,10-phenanthroline reactions and 533 nm for bathophenanthroline reactions.

2.4 Colourimetric Detection of Iron on a Paper Device

Iron(II) was initially measured on a paper microfluidic device via colourimetric detection using 1,10-phenanthroline (508 nm) which in later experiments was colourimetrically detected using bathophenanthroline (533 nm). Both complexed with iron(II) to create coloured complexes which have been well-documented spectrophotometrically, however these methods were adapted for use on a paper platform.^{124,159,199-202}

2.4 .1 1,10-Phenanthroline Detection

2.4.1 Summary

1,10-phenanthroline measured iron(II) in aqueous solutions by creating a coloured complex with the iron(II) complex which could be quantified spectrophotometrically at 508 nm but adapted for use on a paper platform.^{124,199,203-205}

2.4.1 Materials

Fe₂SO₃ (Iron(III) sulphate meets analytical specification was used to create standard concentrations ranging from 0.1 M to 7.5 µM was purchased from Sigma Aldrich (UK) along with 1,10-phenanthroline (titration by HClO₄, ≥99%). Eppendorfs and pipettes used were purchased from VWR (UK) and Jencon (UK) respectively.

2.4.1 Method

The paper device designed for use with 1,10-phenanthroline had a total of five channels which were each 1 mm x 4 cm and allowed a total solution volume of 40 µL into the channel. This device would allow the measurement of five separate standard concentrations of iron to be calculated of a known volume.

1,10-phenanthroline was made to a concentration of 0.1 M and dissolved into 50 mL of purified water at room temperature and sonicated for 10 min to allow the crystals to fully dissolve. From that, 10 µL was spotted on to each

channel 0.5 cm from the top of the paper device and allowed to dry at room temperature for 15 – 20 min. When dried, 20 μL of each of the standard iron solutions was pipetted into the bottom corner of each individual channel and allowed to wick up the channels, merging into the dried 1,10-phenanthroline area and further along the channel until reaching the top. This was then left for 15 – 20 min and completely dried before analysis by using ImageJ (chapter 2.7).

2.4.2 Bathophenanthroline Detection

2.4.2 Summary

Bathophenanthroline is a derivative of 1,10-phenanthroline that is not soluble in aqueous solutions but in alcohol solutions. It was used in the second generation design of paper device for the detection of iron(II) in human serum samples. A chemical reaction containing bathophenanthroline was used to measure iron(II) in solution by creating a coloured complex with the iron(II) complex which could be quantified spectrophotometrically at 533 nm but adapted for use on a paper platform.

2.4.2 Materials

Bathophenanthroline (Bathophenanthroline disulfonic acid disodium salt trihydrate puriss. Pa, for the determination of Fe, $\geq 99\%$ UV) purchased from Sigma Aldrich (UK). Fe_2O_3 (Iron(III) sulphate meets analytical specification was used to create standard concentrations ranging from 0.1 M to 7.5 μM was purchased from Sigma Aldrich (UK) along with 100% ethanol.

2.4.2 Method

The paper device designed for use with bathophenanthroline possessed eight channels in the bottom layer which were 3 mm x 50 mm and allowed a total solution volume of 150 μ L. This device would allow for five standard known concentrations of iron with a known volume, two serum samples of iron taken from a patient and a channel left blank which was used for reference. On the top layer of the device was untreated filter paper which had been soaked in the bathophenanthroline reagent and cut to size (2 mm x 12 mm). These were taped along the top with adhesive tape and delicately placed directly over a channel from the bottom layer, thereby connecting the two layers when solution moved through the bottom channel and wicking through into the top layer, see figure 2.4.

Bathophenanthroline was made to a concentration of 0.1 M and dissolved in 50 mL of 100 % ethanol, then spotted onto untreated white filter paper and dried for 20 min at room temperature. Cut into small rectangles (2 mm x 12 mm), the filter paper was stuck in place at the top of the channel design using common adhesive tape. The iron standard solutions were pipetted (20 μ L) into the bottom corner of each channel in descending concentration, then wicked up the channel and were absorbed into the detection zone on the above filter paper shown in figure 2.4. The device was allowed to dry at room temperature for 15 – 20 min and analysed as described in chapter 2.7.

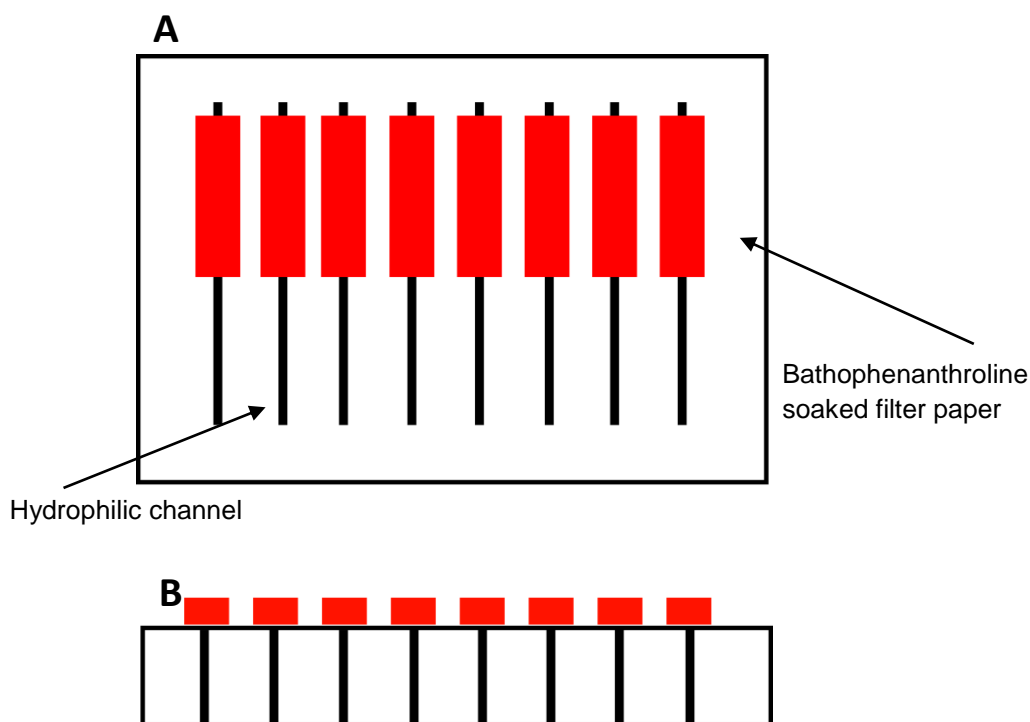


Figure 2.4: Schematic diagram of 2nd generation paper device design
Panel A: Plan view, **Panel B:** Side view of three dimensional paper device for iron detection using bathophenanthroline.

2.4.3 Reduction of Iron in Human Serum Samples on Paper

2.5.3 Summary

By using a method known as “The Lauber Method”¹⁴⁸ the transferrin protein can be detached and the reduction of the iron from iron(III) to iron(II) is achieved in the addition of a teepol (detergent) solution containing sodium dithionite (reducing agent). This method was previously developed for use for measuring serum spectrophotometrically but was adapted for use on paper microfluidic devices.

2.4.3 Materials

Sodium dithionite (technical grade 85%), magnesium sulphate (anhydrous, Reagent plus, $\geq 99.5\%$), teepol 610 S, sodium hydroxide (BioXtra pellets, $\geq 98\%$) were all purchased from Sigma Aldrich (UK). Eppendorfs were purchased from VWR (UK). Human serum and plasma samples were used in accordance to the LREC ethical approval (CHEM/TMC/2011-1).

2.4.3 Method

The reducing agent sodium dithionite (10 g) and magnesium sulphate (2 g) was dissolved in 160 mL of purified water and mixed with 240 mL of the detergent teepol. Added to this was 100 mL of sodium hydroxide (15 g sodium hydroxide per 500 mL of purified water) and the pH was altered to a pH between 5 - 6.2 to aid in the prevention of the bathophenanthroline from creating a coloured complex with any else other than iron(II).

Once the solution had been made, 200 μL of solution was added to an eppendorf and mixed with 50 μL of human serum sample or plasma sample. This formed a cloudy and agglutinated solution due to the removal of the transferrin protein, which when measured spectrophotometrically would have to be removed through centrifugation to avoid inhibiting the result measured. However, the use of the paper device allowed the larger proteins (such as transferrin) to become trapped or become limited in their movement and the smaller molecules to wick faster within the matrix of the cellulose fibres in paper ensuring no interferences with the bathophenanthroline reaction.

Using the second generation paper device previously described in chapter 2.4.2 (bathophenanthroline would be dried in the top layer of the device), 50 μL of the sample was pipetted onto the bottom of the channel and was wicked towards the detection zone in the top layer of the paper device. The sample would react colourimetrically with the bathophenanthroline and allowed to dry at room temperature for 15 – 20 min. Once dried, this would be photographed and analysed as described in chapter 2.7.

2.4.4 Iron(II) Detection via a Hospital Pathology Laboratory

The results measured from the paper devices were compared with the results received from the hospital pathology laboratory at Castlehill Hospital. The analysis of iron(II) levels in human serum samples were based on the same principles of the reduction of iron(III) to iron(II) and the removal of the transferrin protein before been measured spectrophotometrically 600 nm - 800 nm.²⁰⁶ However, in figure 4.8, hydrochloric acid removes the iron(III) from the transferrin protein in figure 4.8, step 1 and in figure 4.8, step 2 ascorbic acid reduces the iron(III) into iron(II) before been detected colourimetrically in figure 4.8, step 3 by TPTZ, a chromogen which forms a blue coloured complex by creating co-ordination bonds with the iron(II).²⁰⁶

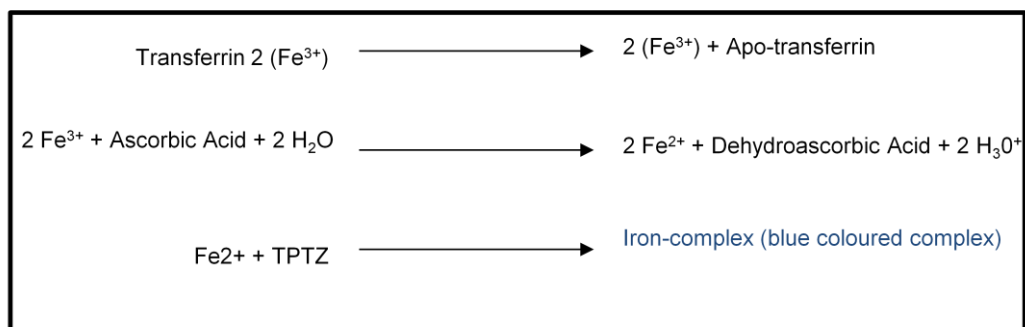


Figure 2.5: Pathology laboratory method for iron(II) detection in human serum samples.²⁰⁶

2.5 Colourimetric Detection of Urea using a Spectrophotometer.

6.5.1 Summary

The method for the detection of urea on filter paper was adapted from Jung *et al.*¹³² who developed a method for measuring urea spectrophotometrically in human serum samples. Results from the technique of using a spectrophotometer was compared with results from the paper devices, and reliability of the adapted technique were in turn compared with the results received from the hospital laboratory.

2.5.1 Materials

The *o*-phthalaldehyde (HPLC $\geq 99\%$), *N*-(1-Naphthyl)ethylenediamine (ACS reagent $\geq 98\%$), boric acid (Bioreagent $\geq 99.5\%$), urea (Bioreagent powder) and 30% (w/v) Brij L23 were all purchased from Sigma Aldrich (UK), along with concentrated sulphuric acid (AC grade). Plastic, 1.5 mL cuvettes were purchased from Fisher Scientific (UK) and was used with a Perkin Elmer portable single beam spectrophotometer. Human serum and plasma

samples were taken in accordance to LREC ethical approval (CHEM/TMC/2012-2).

2.5.1 Method

Reagent 1: The *o*-phthalaldehyde (200 mg L^{-1}) was mixed with 800 mL of purified water (fluorescent reagent for assaying amines) and 74 mL of concentrated sulphuric added. Once cooled 1 mL of 30% Brij solution (detergent) was added and the volume made up to 1 L with purified water.

Reagent 2: 431 mg L^{-1} of *N*-(1-Naphthyl)ethylenediamine (NED reagent), (widely used in the quantitative analysis of nitrate and nitrite) was added to 5 g boric acid (increases sensitivity of method) in 600 mL of purified water. To this, 222 mL of concentrated sulphuric acid was added and then 1 mL of 30% Brij solution when the sulphuric acid had cooled, this was made up to a final volume of 1 L with purified water.

A stock solution of urea contained 10 g of urea nitrogen per litre (21.433 g) for use as standard solutions containing 150 mg, 100 mg, 70 mg, 50 mg, 30 mg and 10 mg of urea with 5 mmol sulphuric acid.

To measure reaction spectrophotometrically 2.5 mL of each reagent one and two were mixed with 50 μL of each urea concentration. After incubation for 30 min at 37°C the absorbance was measured and recorded at 505 nm.

2.5.2 Colourimetric Detection of Urea on Paper

2.5.2 Summary

The method described here was first described by Jung *et al.* in 1975 and has been adapted for use on a paper microfluidic device.¹³²

2.5.2 Materials

The *o*-phthalaldehyde (HPLC $\geq 99\%$), *N*-(1-Naphthyl)ethylenediamine (ACS reagent $\geq 98\%$), boric acid (Bioreagent $\geq 99.5\%$), urea (Bioreagent powder) and 30% (w/v) Brij L23 were all purchased from Sigma Aldrich (UK), along with concentrated sulphuric acid (AC grade). Human serum and plasma samples were taken in accordance to LREC ethical approval (CHEM/TMC/2012-2).

2.5.2 Method

Reagent 1: The *o*-phthalaldehyde (200 mg L^{-1}) was mixed with 800 mL of purified water and 74 mL of concentrated sulphuric added. Once cooled 1 mL of 30% Brij solution was added and the final volume made up to 1 L with purified water.

Reagent 2: 431 mg L^{-1} of *N*-(1-Naphthyl)ethylenediamine (NED reagent) was added to 5 g boric acid in 600 mL of purified water. To this, 222 mL of concentrated sulphuric acid was added and then 1 mL of 30% Brij solution when the sulphuric acid had cooled, finally the overall volume was made up to 1 L with purified water.

A stock solution of urea contained 10 g of urea nitrogen per litre (21.433 g) for use as standard solutions containing 150 mg, 100 mg, 70 mg, 50 mg, 30 mg and 10 mg of urea with 5 mmol sulphuric acid.

Strips of untreated white filter paper were cut to size (10 mm x 50 mm) and soaked in 2.5 mL of reagents one and 2.5 mL of reagent two independently, then allowed to air dry at room temperature for 30 min. Once dried, the urea solutions were pipetted onto the bottom of each strip and the subsequent colour was allowed to develop for 10 min. If no colour change was observed within that time frame it would be classed as a negative result and assumed the urea concentration was within the normal clinical range for urea concentration in serum. If a colour change occurred a pink colour would be observed by eye on the filter strip, the user could assume the urea concentration was $\geq 150 \text{ mg mL}^{-1}$ and would be classed as a positive result thereby advising that patient to seek further medical assistance to determine the reason of an increased urea concentration within their serum.

2.5.3 Urea Detection via a Hospital Pathology Laboratory

The results received from the paper device were compared with the results received from the hospital pathology laboratory at Castlehill hospital. The analysis of urea levels in human serum, plasma and urine samples is based upon enzymatic principles compared with the colourimetric method adapted for use on a paper device. The measurement of urea is based upon the enzymatic conductivity rate method of urea converted to ammonia via the enzyme urease.^{207,208} A sample containing an unknown concentration of urea (10 μL) is mixed with a urease solution (in the ratio 1:76), were the reaction

converts the non-ionic species (urea) to one which is ionic ammonium ion and bicarbonate).^{207,208} During the reaction, the timed rate of increase of solution conductivity is directly proportional to the concentration of urea present in the sample, figure 2.6.^{207,208}

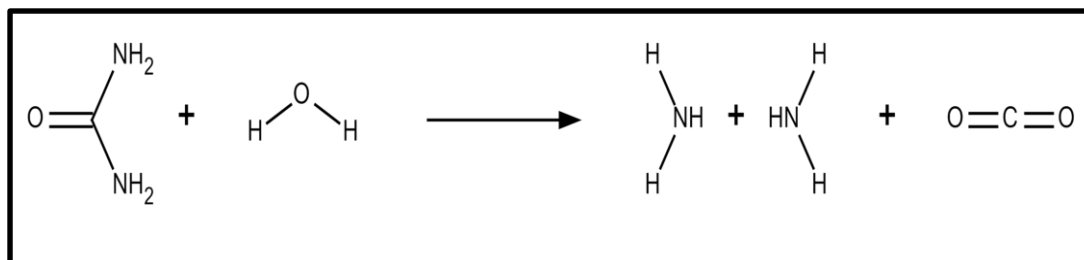


Figure 2.1: Pathology laboratory method for urea detection in human serum/plasma or urine samples.²⁰⁷

2.6 Colourimetric Detection of Creatinine using a Spectrophotometer

2.6.1 Summary

Developed from Liu *et al.*¹³⁶ the Jaffe reaction is considered a “gold standard” test for measuring creatinine concentration in human serum and urine samples. It was originally developed for use with a spectrophotometer at 520 nm as the creatinine reacts proportionally with the picric acid to create a coloured complex in the presence of an alkaline solution.¹³³⁻¹³⁵

2.7.1 Materials

Picric acid (13 % in purified water), ≥ 98% and sodium hydroxide BioXtra, ≥ 98% (acidimetric), pellets (anhydrous), creatinine anhydrous, ≥ 98% were all purchased from Sigma Aldrich (UK). Plastic, 1.5 mL cuvettes were purchased from Fisher Scientific (UK) and was used with a Perkin Elmer portable single beam spectrophotometer. Human serum and plasma

samples were taken in accordance to LREC ethical approval (CHEM/TMC/2012-3)

2.6.1 Method

Picric acid (20 mmol L^{-1}) was mixed in the ratio 1:4 with sodium hydroxide (0.2 mol L^{-1}) and stored as a “monoreagent”. To measure this reaction spectrophotometrically 1.5 mL of the monoreagent was mixed with 10 μL of standard creatinine concentration or human serum sample in a cuvette. This was allowed to sit for 5 min at room temperature, after which the absorbance was measured and recorded at 520 nm.

2.6.2 Colourimetric Detection of Creatinine using Paper

The method described for the colourimetric detection of creatinine was taken from Liu *et al.*¹³⁶ as a spectrophotometric method using the Jaffe reaction principle. This method was adapted as a paper dip stick assay for the detection of creatinine in human serum samples.¹³⁵ To determine the reliability of this method it was compared with the spectrophotometer analysis of human serum samples and a set of standard concentrations.

2.6.2 Materials

Picric acid (13 % in purified water), $\geq 98\%$ and sodium hydroxide BioXtra, $\geq 98\%$ (acidimetric), pellets (anhydrous), creatinine anhydrous, $\geq 98\%$ were all purchased from Sigma Aldrich (UK). Human serum and plasma samples were taken in accordance to LREC ethical approval (CHEM/TMC/2012-3)

2.6.2 Method

Picric acid (20 mmol L^{-1}) was mixed in the ratio 1:4 with sodium hydroxide (0.2 mol L^{-1}) and stored as a “monoreagent”. White filter paper was cut into strips of $20 \text{ mm} \times 10 \text{ mm}$ and dipped into the monoreagent solution. Whilst the paper strips remained wet they were dipped individually into the solution of a known creatinine concentration and repeated for standard concentrations within the clinical range ($5 \text{ mg mL}^{-1} - 25 \text{ mg mL}^{-1}$), as seen in figure 2.7. Once completed, another paper strip would be dipped into the unknown creatinine concentration in a human serum sample and all aligned onto a white background. The highest concentration on the right in descending order until a blank paper strip and the unknown sample strip. This would be imaged and analysed using ImageJ as described in chapter 2.7.

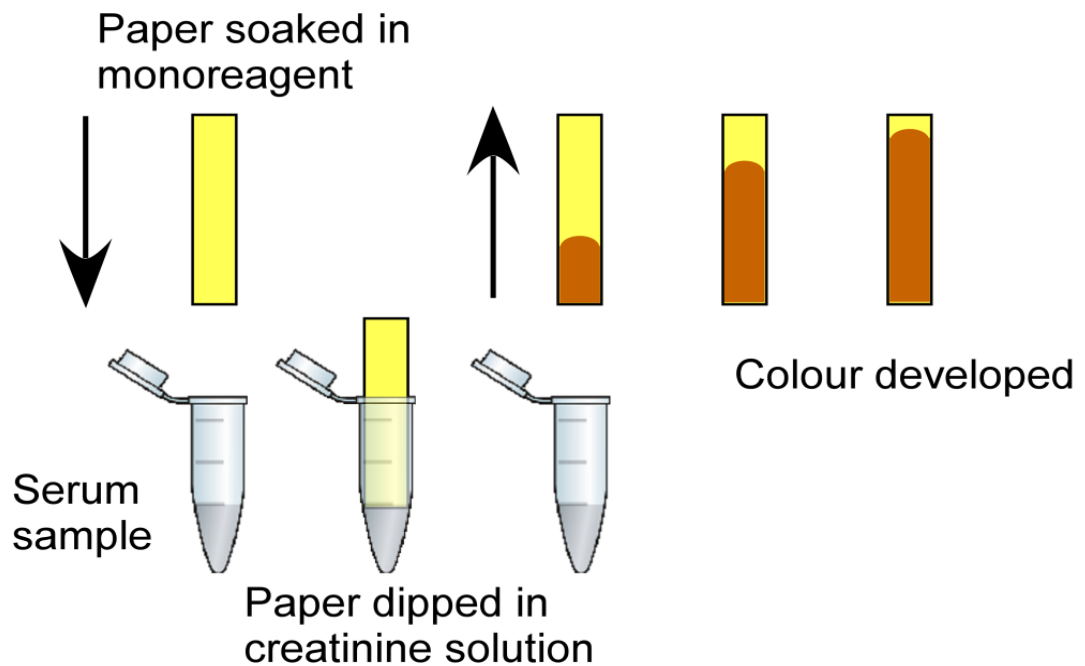


Figure 2.7: Schematic of creatinine dipstick assay.

2.6.3 Creatinine Detection via a Hospital Pathology Laboratory

Creatinine detection in the hospital was the same method as outlined in chapter 2.6.1 using a spectrophotometer and measuring the reaction product from picric acid and creatinine in an alkaline solution.

2.7 Analysis of Paper Device Images

2.7.1 Summary

Unless otherwise stated, the analysis of each photograph taken for the colourimetric detection of iron, urea and creatinine used identical parameters for each individual device to minimise the level of error associated with each device. The analysis and results of each paper device which uses a human

serum/plasma or whole blood sample will be compared to the pathology laboratory results at Castlehill Hospital, Cottingham, East Yorkshire, HU16 5JQ.

2.7.1 Materials

The cameras used, Samsung ES65 camera and the iPhone4s (iron(II) only) were used to photograph the paper devices. The analysis of each paper device was performed using the software, NIH freeware ImageJ (version 1.47).

2.7.1 Method

A digital image was taken with no flash on the camera and held within 15 cm (measured via a ruler) of the device on a white background then transferred to a computer for analysis. The paper device images were loaded individually into the ImageJ program and converted to a 32bit greyscale. A box was drawn around an individual detection zone of the standard concentrations and the integrated density or signal intensity (number of pixels) measured for red, blue and green light. This box was re-used on the subsequent channels of the paper device (without the area size been altered) and measured. ImageJ calculated the mean pixel intensity measured for each standard concentration, a channel was left blank and was used to calculate the background (as reference) and was normalised, as shown in figure 2.8.

Data was transferred to Microsoft Excel and a linear regression fitted to the standard concentrations. The background was subtracted from each result to normalise each sample.

The unknown concentration of a sample (iron(II), urea or creatinine) would be calculated using the line equation from the linear regression. The result from the device was compared with the result received from the hospitals pathology laboratory and in some cases (creatinine) from a spectrophotometer.

This was deemed as the most accurate analysis for each paper device for use as a single use device when compared to work described by Whitesides *et al.*⁴⁴, Henry *et al.*¹⁶¹ and Yager *et al.*⁸⁰ who have also used this same method with ImageJ or similar methods with Adobe photoshop.

Figure 2.8 illustrates a step by step process of how to complete the analysis using the ImageJ software.

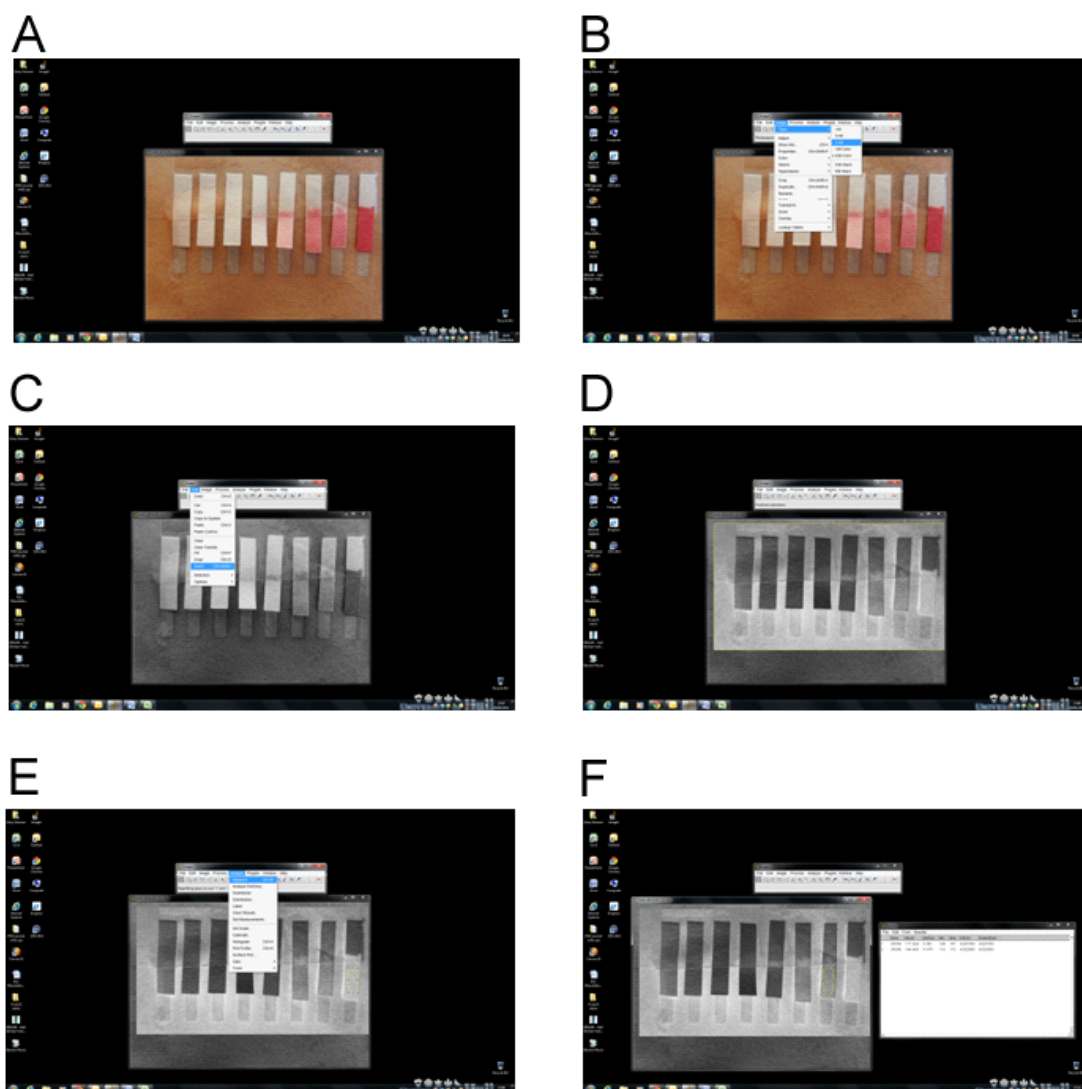


Figure 2. 8: ImageJ analysis of iron paper devices.

Panel A: Through ImageJ open the image for analysis. **Panel B:** Convert file in 32bit image. **Panel C:** Invert Image. **Panel D:** Select area for measurement by drawing a box around the detection zone of the device. **Panel E/F:** Measure the area, mean number of pixels and integrated density (area x mean grey value)

2.8 Mask Designs

The photo-mask designs used in this project are detailed below in figure 2.7 with the contact angles measured and correct fabrication procedure followed as detailed in chapter 3.

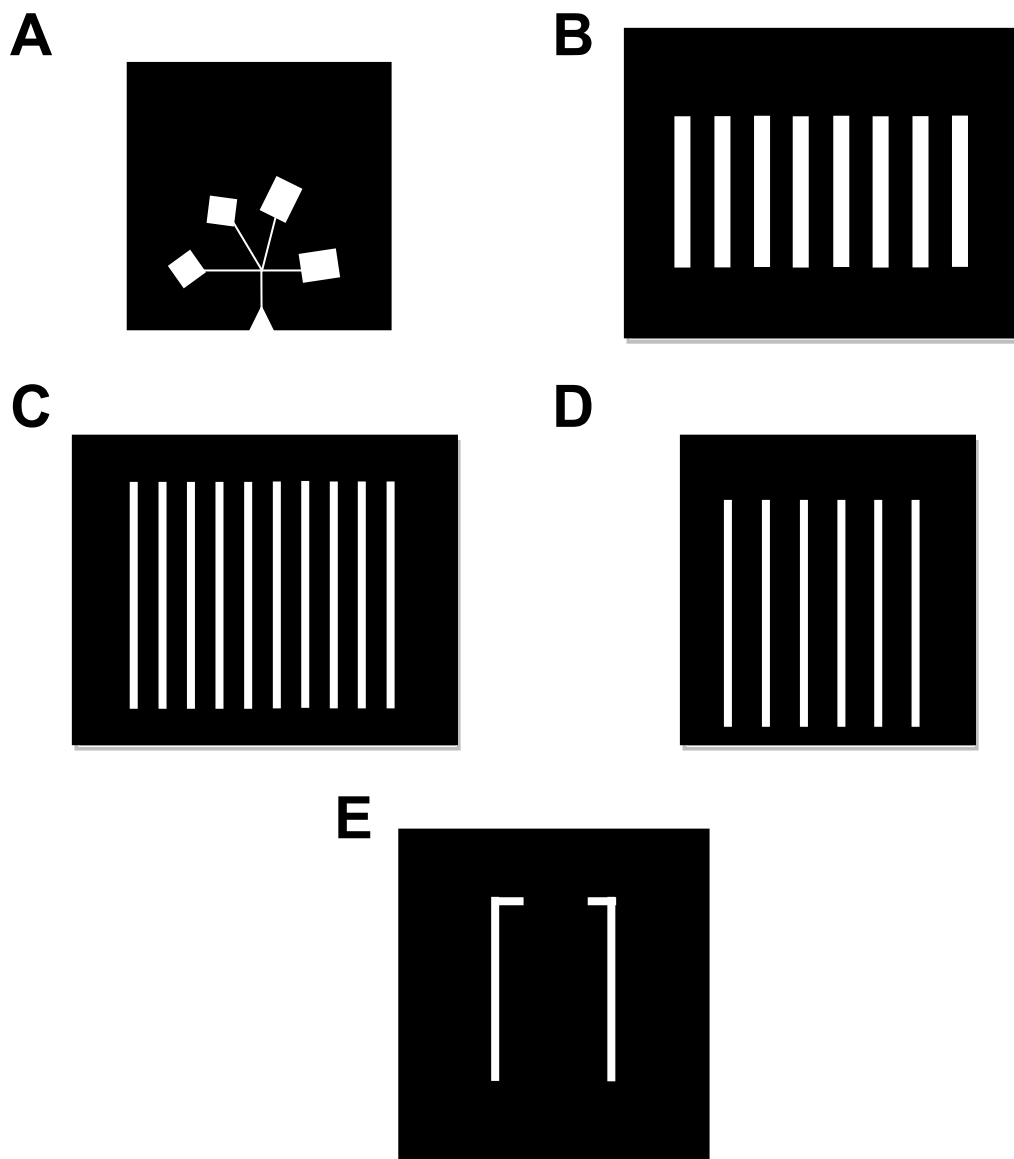


Figure 2. 9: Mask designs created with Microsoft word and used throughout this project to fabricate paper microfluidic devices from photolithography.

A: (Double Assay) mask design used as a complicated mask design from Whitesides group⁴³. **B:** (8 lane, 2nd generation) mask design for iron(II) analysis with bathophenanthroline. **C:** (10 lane) mask design for iron(II) analysis with 1,10-phenanthroline. **D:** (5 lane) mask design for iron(II) detection with 1,10-phenanthroline. **E:** (Initial design) used for the optimisation of fabrication of paper microfluidic devices using photolithography.

2.9 Statistical Analysis of Data

All results are depicted as a mean \pm the standard error of the mean (SEM) as a percentage and the “n” number of the experiments completed shown alongside each experiment. If the experiment could only be completed once this was due to either lack of sample or most commonly due to the use of the paper microfluidic devices as a single use device.

Group means were compared using statistical models published in other paper microfluidic devices ^{45,55,64,79,209-212}.

A paired student’s T-test, used to compare two sets of data which share a relationship,²¹³ using Microsoft Excel, data analysis.

The Analysis of Variance (ANOVA) testing was used to compare the variance amongst the group of data as each data set had differing mean values as different patient samples were used,²¹³ using Microsoft Excel, data analysis.

An F-test was used to compare the statistical models used in the data,²¹³ using Microsoft Excel, data analysis.

A P value of < 0.05 was considered as significantly different, a P value > 0.05 was not considered as significantly different.

Chapter 3: Fabrication

This chapter will discuss the optimisation process for the fabrication of the paper devices using the photolithography technique with a positive photoresist. The use of photolithography was initially described by Martinez *et al.*⁵⁸ who used a negative photoresist (SU-8). In contrast the photolithography method described in chapter 2.1 was optimised for use on filter paper when using a positive photoresist, which is more readily available and is a cheaper alternative to the negative photoresist, SU-8.

Photolithography was used to create hydrophilic channels in filter paper surrounded by a hydrophobic barrier, allowing the direction of fluid flow to be controlled and directed as illustrated in figure 3.1 and 3.2.

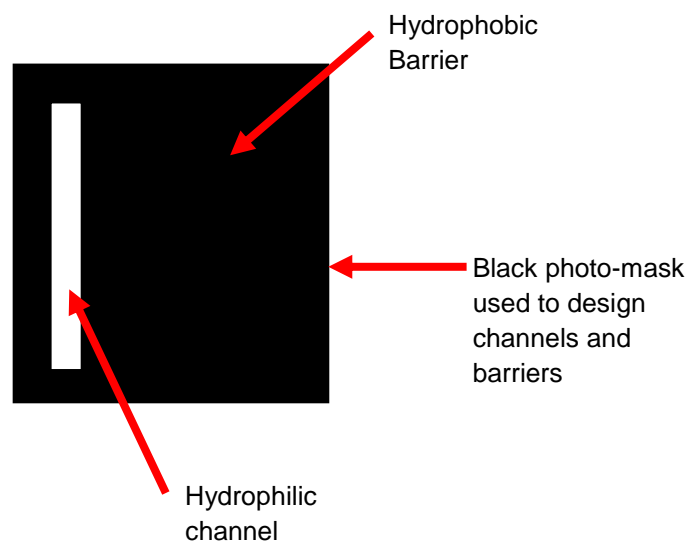


Figure 3. 1: Concept of barriers and channels in a piece of filter paper.

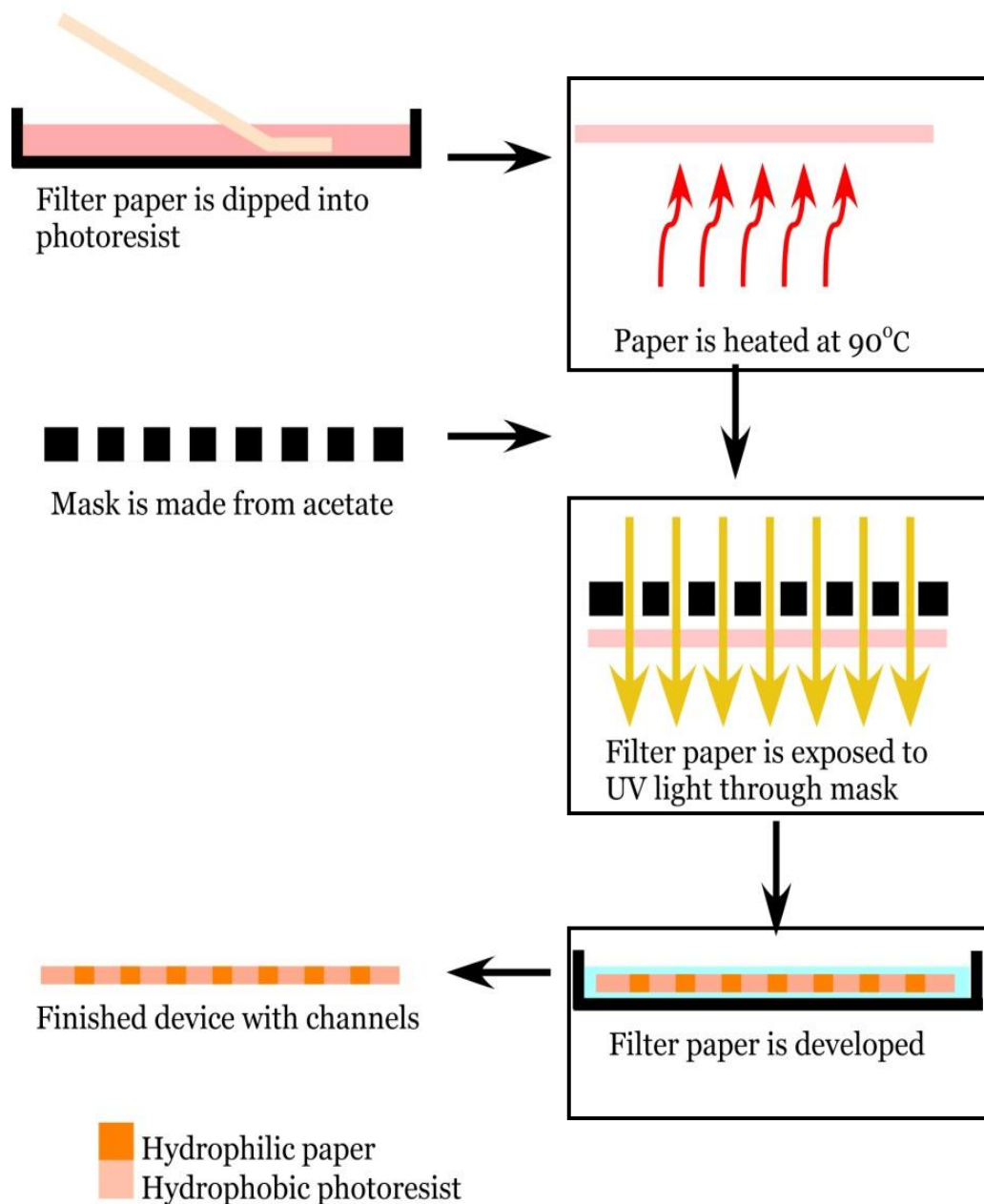


Figure 3.2: Photolithography in filter paper, highlighting areas requiring optimisation.
The boxes illustrate areas within photolithography which needed to be optimised to be able to apply this method onto a piece of filter paper.

Photolithography is a method originally intended for use on the production of integrated circuit boards rather than creating channels in filter paper.²¹⁴ This process has also been developed in the fabrication of glass microfluidic

devices,²¹⁵ however as paper is not as resilient as these materials specific steps had to be optimised before its use on filter paper. These optimised steps included; the pre-bake temperature, duration of the bake, the time for exposure to UV light and the length of time taken for the exposed photoresist to be removed by the developer.

3.1 Optimisation Results

3.1.1 Temperature

Initially experiments were carried out to determine the correct duration and temperature for the pre-bake which would harden the photoresist once it had been dried onto the filter paper. The purpose for the pre-bake was to ensure the photoresist was hydrophobic before progressing onto the following stages such as the exposure and development. Hydrophobicity was created through hardening the photoresist into the paper matrix which was caused by the heat, evaporating the solvent (allows the photoresist to be liquid) from the photoresist.

The optimum time and temperature was found to be 90°C for 4 min, if it was any cooler (< 80°C) in temperature the photoresist did not harden and become completely hydrophobic and if the temperature was any hotter (> 110°C) the filter paper began to burn and flake away at the edges. This was determined by placing a beaker of water containing a thermometer to ensure the correct temperature was achieved. It was also noted that if the photoresist had not been completely dried on the filter paper, then the photoresist would “shrink” on the paper and large areas of white would appear in spots on the device. The “white spots” was thought to be caused

by the evaporation of the solvent before the photoresist had completely saturated the filter paper as the white spots would be as hydrophilic as untreated filter paper.

As this was a satisfactory duration and temperature to evaporate the solvent from the photoresist, it was assumed this would remain the same for the post-bake process of the method as the aim of the step was the same, removing any remaining developing solution from the device in the final stage of the process.

3.1.2 Exposure

Once the correct temperature had been determined for the pre-bake process of the method, the filter paper would be exposed to a UV light through the photo-mask to remove certain areas (designed via a photo-mask) of the photoresist through breaking down as the photoresist polymer contains a light sensitive molecule. The area to be removed is pre-determined through the design of a photo-mask which can be produced using Microsoft word. Areas to be removed are put in white (which will be clear on an acetate sheet) against a black background and then printed out onto an acetate sheet.

The first attempt at fabricating a device was unsuccessful as shown in figure 3.2. The filter paper was coated in the photoresist and air dried for one day, then pre-baked at 90°C for 4 min. The filter paper was exposed for 50 s to the UV light. Initially 50 s was used for the exposure time as it was thought

that as paper is more fragile than surfaces this method was established for, less time would be required to break down the photoresist.

The filter paper was exposed to the UV light on one side of the paper, through the photo-mask “initial design” (figure 2.7E) which was held in place using adhesive tape. The device was developed for 10 min in the developing solution before post-baked at 90°C for 4 min. Once dried, a 10 μ L drop of purified water was pipetted onto several positions of the paper device to test for any differences in hydrophobicity across the paper device.

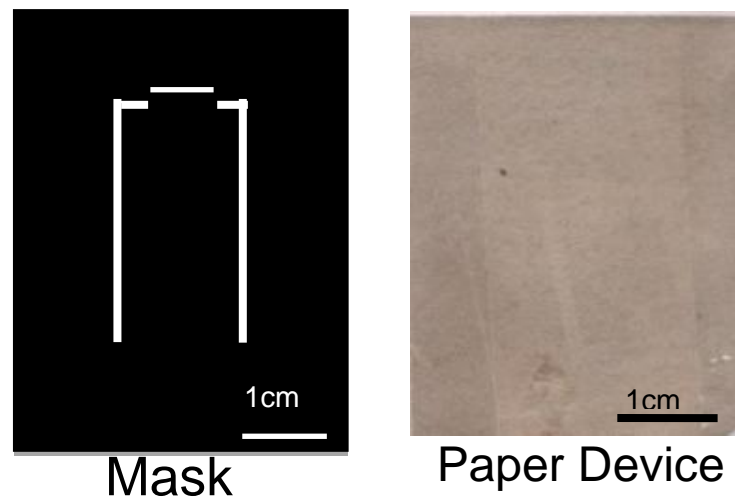


Figure 3.3: First attempt of fabricating a paper device with a simple photo-mask design for fabricating paper microfluidic devices using photolithography.

The first attempt revealed that the fabrication method was flawed as the purified water proved that the entire device was hydrophilic regardless of the photoresist, as the water was not absorbed into the device as would be expected in the hydrophilic regions of the device. Instead, the water would sit on top of the device as it would a hydrophobic surface. This allowed the

assumption to be made that the photoresist had been completely removed from the paper, either due to a too short period of time of exposure to the UV light or a too long time period in the developer. In brief this could be due to paper not been as resilient as the materials for which this process was intended for use and that not only was the solubilised photoresist (areas exposed to UV light) been removed, but also the photoresist which was not exposed.

To overcome the identified problem, the exposure of the paper device to UV light was increased to 5 min. This was based on when photolithography is performed on a glass microfluidic device, it is a thin layer on top of the glass similar to using filter paper the photoresist has been incorporated into the cellulose matrix of the paper infrastructure. This suggests, it may take longer for the UV light to penetrate and solubilise the photoresist polymer on paper. Whilst this step of the process was altered, the development step was maintained at 10 min, as this was used in the original photolithography method.⁵⁸ This aided to pin-point any variations in the method that could be identified when using filter paper. The concluding paper devices had no clearly defined channels, and when purified water was pipetted onto various areas of the device, in contrast to figure 3.2 the devices were hydrophilic, regardless of the photo-mask design as the water was fully absorbed into the paper (devices not shown).

To counteract the issue, paper devices were subjected to a 4 min pre-bake at 90°C, a 5 min exposure period to UV light through a photo-mask as before. However, in this instance the developing period was decreased to 5

min. It was assumed because filter paper is not as resilient as glass and the developer would remove the photoresist a lot easier and quicker as previously thought. It was from this process that the development period was deemed to be removing not only the exposed photoresist but also the unexposed photoresist. It was thought that it could be due to the photo-mask not been dense enough in colour to prevent light scattering from the UV bulb (block out the light). Therefore, the method was not defining the channels strongly enough thereby it allowed the barriers to leak into the hydrophobic areas on one side of the filter paper as the photo-mask was allowing light to penetrate through to areas of the filter paper which should be hydrophobic and not creating a high resolution which can be achieved in glass.

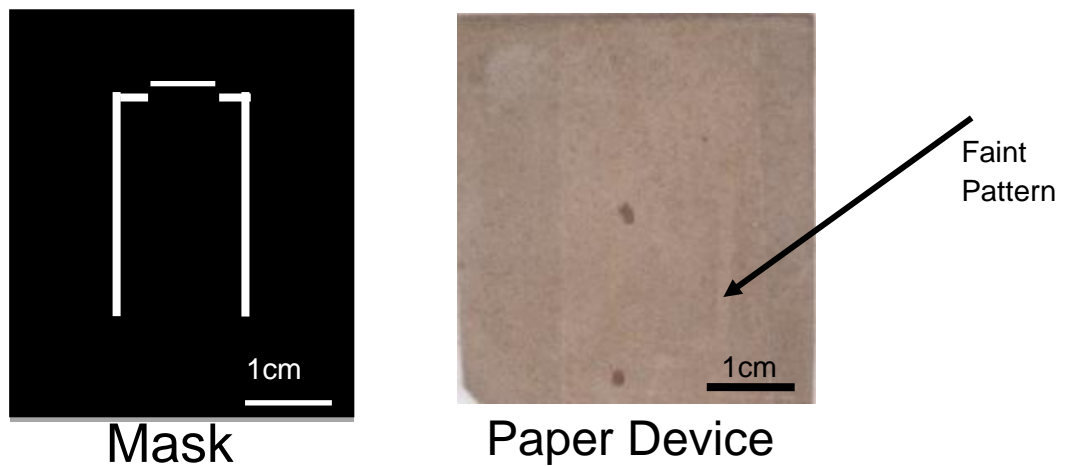


Figure 3.4: Second attempt of fabricating a paper device with a simple photo-mask design for fabricating paper microfluidic devices using photolithography.

It can be noted that the pattern from the mask can be slightly seen in figure 3.4, however it is incomplete, nevertheless illustrating these are minor improvements in the fabrication of paper devices.

Therefore, to strengthen the channels defined in the filter paper a double sided photo-mask was designed to allow the photoresist coated filter paper to be slipped in between two identically positioned and taped into place photo-masks (this would ensure the filter paper would be held in place during the exposure of both sides of the device), figure 3.5. The use of the double sided mask allowed channels to be created through the entire thickness of the paper, fabricating a stronger and more resilient channel to the developer.

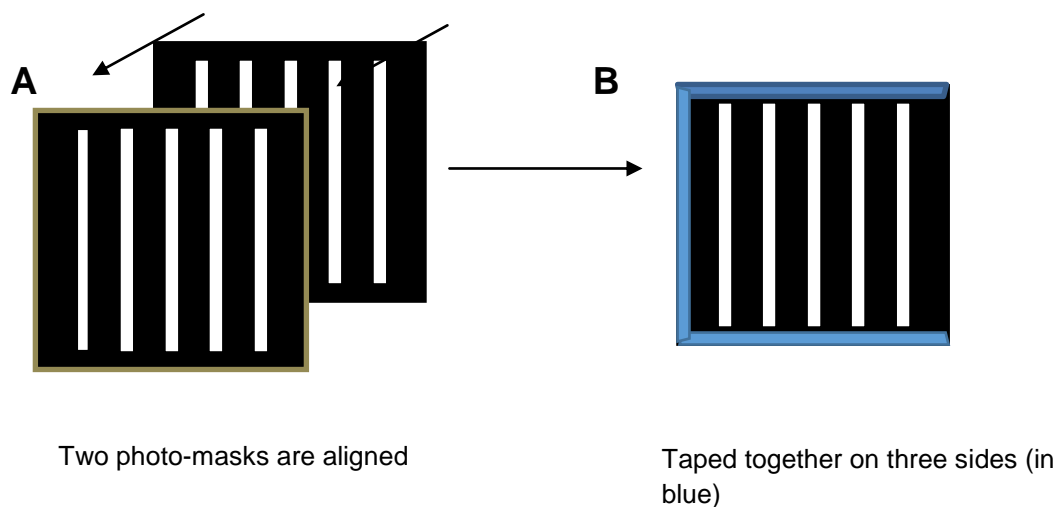


Figure 3.5: Schematic diagram illustrating the use of a double sided photo-mask. **Panel A:** illustrate the alignment of the two photo-masks, **Panel B:** illustrates the three sides of the photo-mask taped down to restrict the movement of the filter paper when it is in place.

3.1.3 Development

Through using the double sided photo-mask the UV light exposure time was increased to 6 min on each side of the filter paper, whilst the development period was steadily reduced from 10 min by 30 s every experiment per paper device. This successfully demonstrated that the optimum development time frame was between 30 s and 2 min, by the production of a clear and concise channel that could be seen in all of the paper devices fabricated, figure 3.5.

However, as the time decreased that the filter paper spent in the developer solution the paper devices become redder in colour when compared with the 2 min development period devices. This could be due to less photoresist been removed by the developer as the photoresist itself is a dark red solution, figure 3.6.

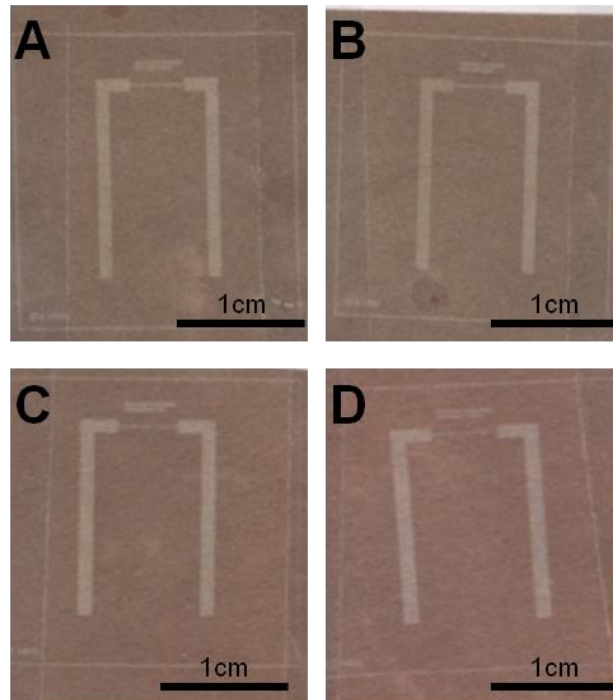


Figure 3.6: Determining optimum development time. Development by exposure to UV light was tested at the time intervals of 2 min (**Panel A**), 1.5 min (**Panel B**), 1 min (**Panel C**) and 30 s (**Panel D**).

To determine the channel and hydrophobic barrier, purified water was pipetted onto the channels bottom corner to see how “wick-able” the channels were at both 30 s and at 1 min. At both 30 s and 1 min development time’s purified water would wick along both channels, however at 30 s the fluid flow was slower when compared with purified water wicking through the channels in the 1 min channel. In comparison, at 1.5 min and 2 min the paper devices that had visible channels the water was not contained in the channels and fluid spilled out onto the photoresist uninhibited. It was thought that it could be possibly due to the increasing time in the developer that the paper spent, whereby the developer began to remove the

unexposed photoresist along with the exposed photoresist, therefore returning the paper back to its natural hydrophilic state.

3.2 Determination of Development by Contact Angle Analysis

Once established there was a clear and defined channel in the filter paper created by the photolithography technique, a more concise time frame had to be determined. This was when only the exposed areas of photoresist were removed by the developer, leaving the unexposed areas intact. The use of measuring the contact angle would determine how hydrophobic and hydrophilic the paper had become after the photolithography process and thus determining the hydrophobic difference between areas on the paper device i.e. areas which had been removed should be hydrophilic or areas which had not been removed through exposure to UV light should be hydrophobic in the photoresist coated filter paper.

For an area to be described as hydrophobic (no affinity for water) its contact angle should be measured over 90° and for an area to be described as hydrophilic (strong affinity for water), then a contact angle should be measured as small as possible ($< 90^\circ$) which can be seen in figure 3.7. This was measured by pipetting 5 μL of purified water onto the device and measuring the corresponding contact angle with a goniometer, as described in chapter 2.2.

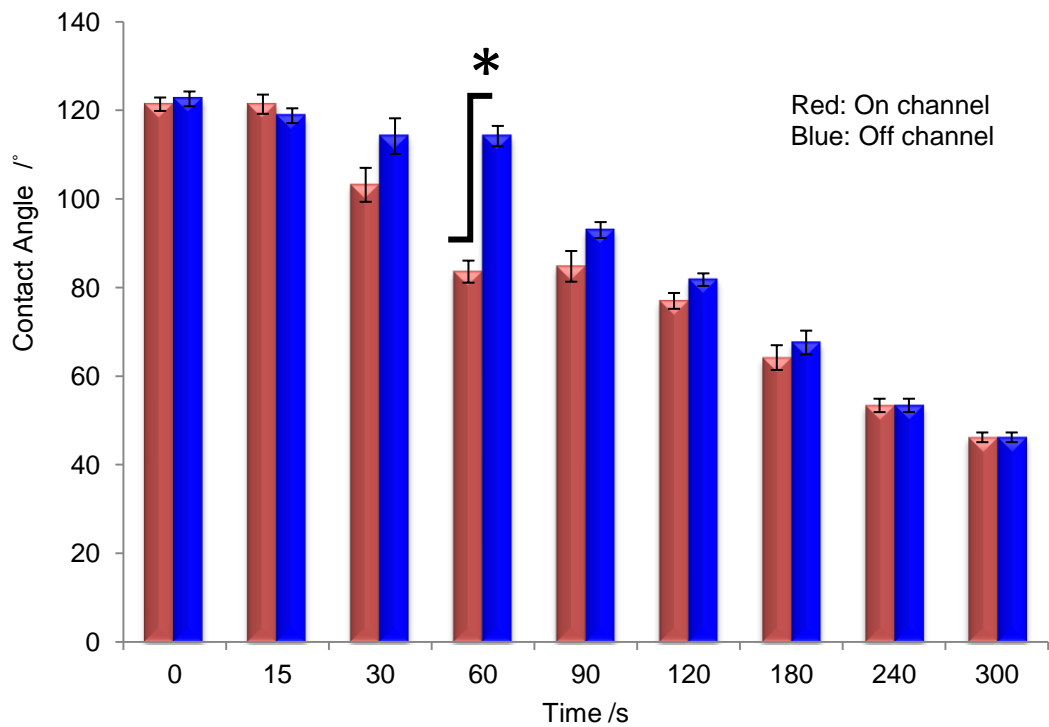


Figure 3.7: Contact angle results using the “initial device” design. This graph illustrates the greatest significant difference within results ($P < 0.05$) depicted as * as the optimum time period for paper device fabrication, ($n=10$).

The contact angle results show the optimum development time-frame to produce hydrophilic channels surrounded by a hydrophobic barrier was 1 min (60 s in figure 3.6). A paired Students t-test showed this was the greatest significant difference between the measurements ($P= 0.01$) when compared with the other results.

The fabrication method was further tested to ensure reproducibility with various other designs which in some cases were more complicated whilst in others remained simple, figure 3.8. The device designed by Martinez *et al.*⁴³ using a negative photoresist was described as a complex design for the measurement of two analytes created using photoresist. Figure 3.8 illustrates

this complex design is reproducible when using a positive photoresist as an alternative, thereby illustrating how the photolithography method outlined is successful in creating hydrophobic barriers in paper regardless of the patterns complexity e.g. for a double assay (taken from figure 2.7A).

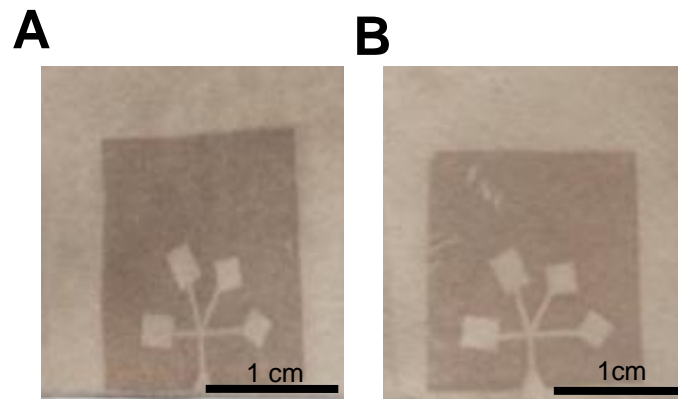


Figure 3.8: Complicated designs of channels that can be fabricated into a paper device.⁴³

However, it was noted that due to the different patterns the development period was dependent on how much photoresist had to be removed e.g. in a device where only a small channel was been created a shorter time frame would be required when compared with a device which had a larger channel. This observation affected every design encountered therefore, to ensure the optimum development time for each device design the contact angle was measured for each design. Table 3.1 illustrates each optimum development time frame and the measured contact angle for the different designs used in this project, (n=5).

Table 3. 1: Adjusted development time for contact angles.

Paper Device Design	Development Period Time /s	Contact Angle on channel (n=5)	Standard Deviation	Contact Angle off channel (n=5)	Standard Deviation
Initial Design	60	65.1°	1.7	98.9°	2.5
5 lane design	60	64.9°	1.8	100.8°	1.5
10 lane design	80	65.4°	2.4	93.3°	2.8
8 lane, 2 nd generation design	80	62.5°	1.4	99.7°	1.2

This data enabled the reproducibility of paper devices with various patterns used to create the channels (figure 3.9). Each device was designed for the number of measurements required to incorporate the measurement of a number of standard concentrations of samples alongside an unknown concentration and a blank to be used as a reference in the analysis, as described in chapter 2.7.

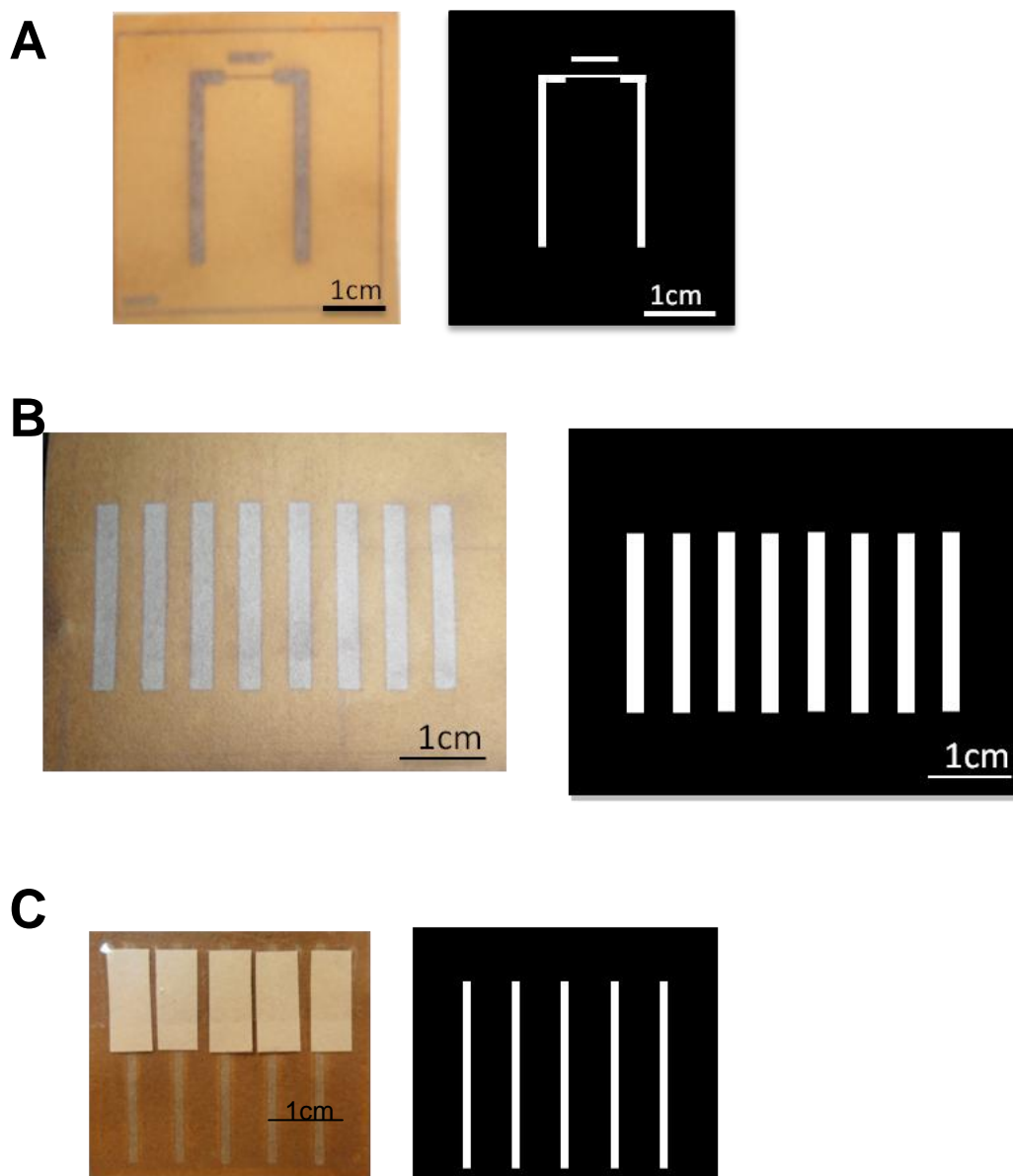


Figure 3.9: Channel designs used for various measurements of analytes. **Panel A:** Initial design of a two lane paper device and mask. **Panel B:** Eight lane 2nd generation paper device and mask. **Panel C:** Five lane paper device and mask.

The devices, once fabricated had to be stored at room temperature in the dark to maintain the hydrophobic barrier created within the device. The devices stored in the dark were usable for an unknown period of time after fabrication. It is assumed that as long as the devices were stored in the dark

the photoresist would not breakdown and they would not become hydrophilic therefore the hydrophobic barrier would remain intact for indefinite amount of time, however this theory was not tested. It was thought if the devices were stored in a warm and moist environment they barrier would be broken down as the paper would age faster e.g. lose colour and become brown and mouldy, however this theory was tested but a cool, dry environment was preferred for storage.

3.3. Cost of Fabrication

The main focus in developing many of the POC devices today is to allow the fabrication process to be more cost effective than already available but remaining as accurate as the current methods. The cost of fabricating these devices is broken down in table 3.2, explaining how cost effective these devices could be when compared to glass or polymer microfluidic devices. This was completed by example for manufacturing 100,000 devices using the method outlined once optimised using the positive photoresist.

Table 3. 2: Cost of consumables for fabricating 100,000 paper devices using the photolithography method when optimised.

Equipment Required	Total Cost	Cost per device (100,000 devices)
Filter Paper	£20 (500 pieces)	4p
UV Light Source	£139.00	1.39p
Photoresist	£123.00 (1 L)	1.23p
Acetate	£13.70 (50 sheets)	1.37p
Printer	£79	0.8p
Hot Plate	£245	2.45p
Syringe	£35.97 (pack of 100)	3.6p
Total Cost	£655.67	14.84p

3.4 Discussion

In the area of developing medical devices, there remains a growing requirement that the devices be of single use to prevent cross contamination yet remain cost effective.⁵³ Paper microfluidics is slowly bridging this ideal through the development of creating channels in the paper matrix which allow fluid to flow without any external force, an ideal source for use in the developing world.^{53,72} The ideal of been cost effective as outlined in table 3.2 is comparable with the cost of manufacturing polymer or glass devices which have been produced for as little as 5 - 14 cents²¹⁶, however this is not as cost effective as the paper devices which can be produced for as little as 15p.

The fabrication of such devices that had previously been established was through the creation of etching channels into a solid support,^{3,30} however these methods use costly materials, such as glass and silicon which for use as a one-time device is not cost effective.^{53,72} Adaptations of methods for use with an alternative and less expensive approach by using cheaper materials, such as paper, have received much interest within research groups in recent years.^{45,64,65,217-219} The process illustrated within this chapter highlights an approach such as photolithography can be altered and optimised for use on a paper platform, creating the desirable medical device much needed in the developing world.^{2,32,43,45,58}

The use of the positive photoresist in comparison with the negative photoresist further highlights this approach of maintaining low cost yet creating a very usable device in the medical community. The positive photoresist can produce high resolution channels and sharp borders which can sometimes be lost in other methods such as wax printing.^{98,99} For the positive photoresist to be correctly utilised in a paper platform the optimisation of this method included the pre and post bake time and temperature, the exposure time and development time.

The pre-bake time and temperature was established at 90°C for 4 min as at a higher temperature the paper would begin to burn and flake rendering the paper unusable, additionally for any duration of time longer than 4 min a similar problem was encountered. If the time and temperature were any lower the positive photoresist would not harden, so when exposed to UV light

would not become hydrophobic, therefore removed by the developer in the last step of the method.

The exposure time was determined to be 6 min on each side of the paper. Initial experiments used a shorter exposure time frame and showed that the UV light had fully saturated the exposed areas, but were not fully removed by the developer. The breakthrough was establishing the use of a double sided photo-mask, allowing the channels to be fabricated through the entire thickness of the filter paper, strengthening the hydrophobic barrier. Before this realisation, fluid was slow at moving through the channels but when the first paper device was exposed on both sides the UV light was able to fully penetrate the paper and the fluid moved along the paper faster and completely filled the channel.

It was also noted that during the exposure of the filter paper to the UV light through the double-sided photo-mask could heat up. The bulb used in the UV light box was an 8 W bulb thereby creating 8 W of heat in an enclosed space. This heating would cause the ink on the acetate sheet to melt and when removing the paper, the paper would be covered in the acetate ink. Therefore, to prevent this from happening the photo-mask would have a layer of clear acetate on the surface touching the filter paper and then the photo-mask with the design of channels on which would be sellotaped together as shown in figure 3.4.

The developing stage was a crucial stage in completely removing the exposed areas of the photoresist and not eroding the unexposed areas at the

same time. This was achieved through measuring the contact angles at varying development time frames and establishing that this process was specific to each design and device used. The developer was initially diluted to varying concentrations but all the experiments failed to remove the photoresist in a satisfactory manner therefore it was decided to use the developer as a 100 % solution. The time frame had to be precise within 10 s of the allotted time frame determined by the measurement of the contact angles because if the paper device was taken out early or after that allotted time the device would be unusable and either the fluid would wick everywhere regardless of the hydrophobic barrier or would sit on the device as it would be too hydrophobic to absorb any of the liquid.

It was deemed that the post bake process was not required as the post bake was used to evaporate any remaining developer and to adhere the photoresist to the surface. As the photoresist was incorporated fully into the papers cellulose matrix it did not require any further adhering. The drying of the devices at room temperature was sufficient to remove the developer solution and as the devices sufficiently allowed fluids to wick along the channels it did not require further investigation.

Each device (from chapter 2, figure 2.7) were fabricated and dried, were tested with 5 - 10 μL of purified water to detect any inaccuracies in the fabrication. The devices could be made four at a time by aligning them on the hot plate on the UV light box and from this 75% of the devices would be fully hydrophobic with the channels been hydrophilic from the quality control checks put in place. The first check was to place 5 - 10 μL of purified water

onto the channel and time the distance travelled from one end to the other. According to Darcy's law this was 12 s per channel.⁸⁶ The second control check was to measure the contact angles of the channels and ensure they were fully hydrophilic ($< 90^\circ$). If any of the devices which were incorrect by leaking or if they were too hydrophobic i.e. they would not wick fluid they were immediately disposed. The devices which passed the quality control and had been fabricated correctly were stored in the dark at room temperature until use. If they were not stored in the dark the light would eventually break down the photoresist and the entire device would return to its natural hydrophilic state. These devices that were stored in the dark could be used after an indefinite amount of time without any leakages.

To the best of our knowledge this is the first method which has used a positive photoresist for a photolithography technique when using paper as a platform. The novelty in using a positive photoresist for paper microfluidics has the additional benefit of providing a cheaper alternative to the negative photoresist (SU-8).

This paper platform can now be used for detection of analytes in samples to diagnose infections or diseases, for this project anaemia and kidney failure. Iron, urea and creatinine will be detected in human serum samples to determine a diagnosis for a patient as a POC device that can be performed away from a laboratory setting by untrained personnel, allowing for a fast diagnosis which leads to a better prognosis for the patient.

Chapter 4: Colourimetric Detection of Iron

Iron is an essential nutrient required by the body absorbed via the diet and is a leading nutrition deficiency worldwide. There is a huge need to be able to assess iron levels quickly and efficiently in patients thought to be suffering from anaemia as a lack of iron in the human body can lead to further complications and in worst case scenarios, multiple organ failure as described in chapter 1.6.¹⁶² This is most commonly measured in human serum samples (where RBCs and WBCs have been removed through centrifugation) and using a spectrophotometer the reduction of iron(III) into iron(II) and resulting coloured complex measured.^{147,220} Although this is a simple method, it can still take up to 5 days in the developed world for patients to receive a result from the hospital pathology laboratory and in the developing can prove impossible as the equipment required (centrifuge and spectrophotometer) are expensive pieces of equipment. The main purpose in the production of POC device is to minimise this delay and to aid in the diagnosis of diseases and infections.

Initially iron(II) was measured on a paper device within the clinical range of 5 μM and 75 μM and compared to the conventional method using a spectrophotometer by using 1,10-phenanthroline, a common complexing reagent which forms a red coloured complex with iron(II) proportional to the iron(II) concentration.¹⁹⁹

In later experiments, iron(II) was measured using a derivative of 1,10-phenanthroline, bathophenanthroline, a complexing reagent which forms a

red coloured complex proportional to the concentration of iron(II) however, the complex is soluble only in alcohol solutions, allowing the detection zone of the iron(II) to remain stationary preventing any inaccuracies caused through a chromatography effect in the paper channel.^{200,201,221}

The paper devices were analysed using the software ImageJ and statistically measured as outlined in chapter 2.7. The performance of the system was assessed by comparison with standard methods performed at a clinical level, determining any statistical differences within the results achieved on the paper devices.

4.1: 1-10-Phenanthroline Results on Paper

To measure the iron concentration on a paper device, channels were created via photolithography as outlined in chapter 2.1. The devices were designed to have a total of six channels, which allowed for the measurement of five concentrations of iron(II) from 0.1 M to 0.001 M that were run simultaneously onto a single device, using the individual channels. This maintained in every device a constant concentration and volume of 1,10 -phenanthroline throughout, 5 μL of 0.1 M pipetted into each channel before being dried at room temperature for 30 min and the same amount of each standard concentration of iron(II) sample pipetted (15 μL) into each channel, which wicked up the channel into the detection zone of 1,10-phenanthroline. The natural matrix of the paper cellulose fibres would allow the samples to mix and a red/pink coloured complex formed as a result.

Firstly, 5 μL of 1,10-phenanthroline was pipetted into the devices channels (photo-mask design “5 lane”, figure 2.7) in the top half of the channel and allowed to dry at room temperature for thirty 30 min before the addition of the iron(II) samples at the opposite end of the channel. This was to allow the iron sample to wick through the detection zone and mix well with the 1,10-phenanthroline before drying into the channel, figure 4.1.

Secondly, the iron sample would be pipetted into the bottom of each channel, wick along the channel into the detection zone and the sequential addition of reagent and sample was designed to trap any debris in samples used on the device, such as in human whole blood sample. Debris would be any large cells (such as RBCs and WBCs) in the whole blood which would travel at a slower rate through the paper matrix when compared with the smaller molecules (such as iron(II)). This would prevent any contamination of the detection zone in the paper matrix and prevent any hindrances in the development of a colour change from the mixing of iron(II) and 1,10-phenanthroline. Once the red/pink colour change had fully developed and dried 10 min at room temperature, a digital photograph would be taken and analysed via ImageJ. A standard concentration curve of iron(II) was constructed to show linear regression thus allowing an unknown concentration to be calculated.

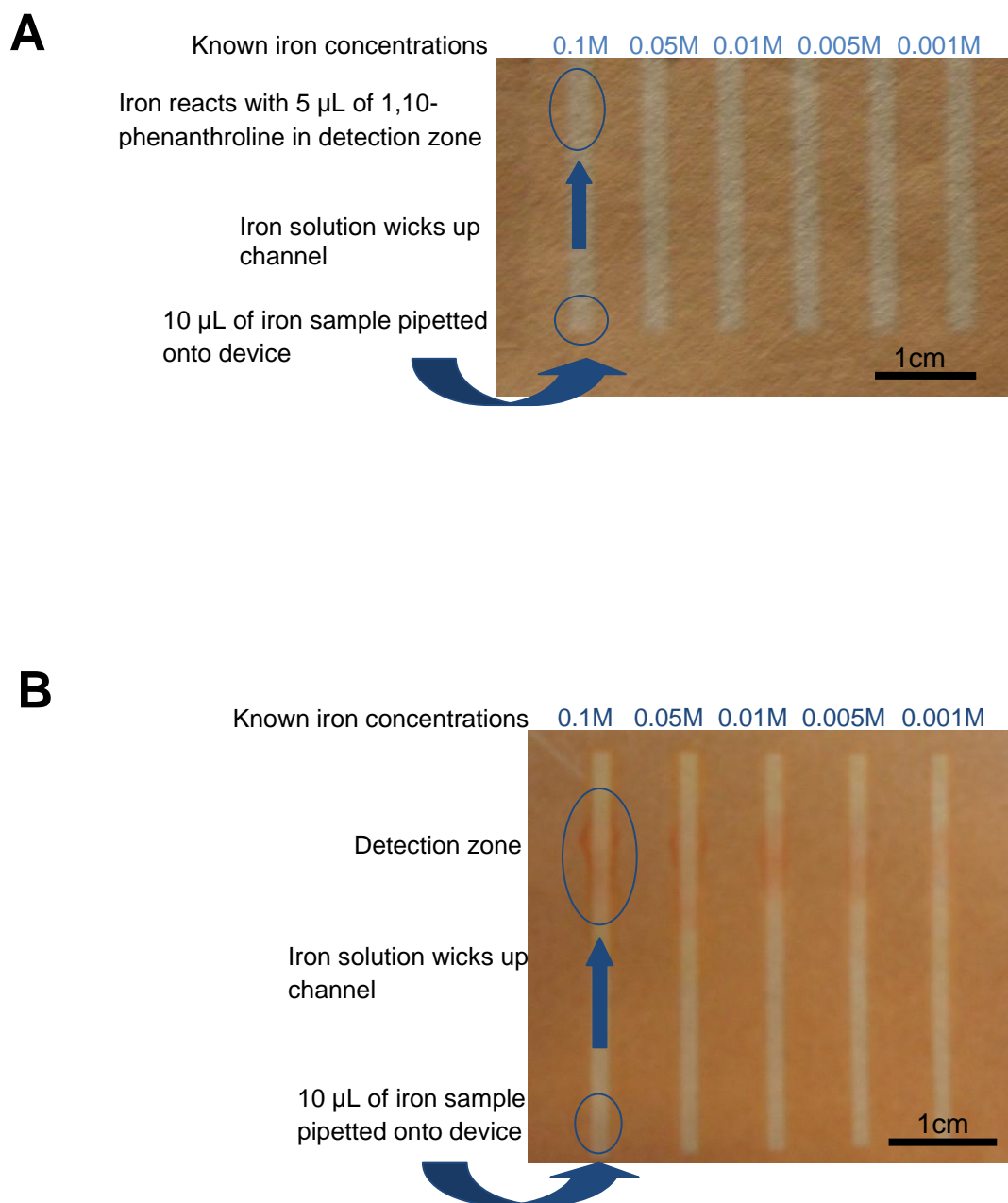


Figure 4.1: Coloured reaction of 1,10-phenanthroline with iron(II) on a paper device. **Panel A:** Process of introduction of samples onto the paper device. **Panel B:** Iron(II) reacting with 1,10-phenanthroline to form a pink coloured product.

Iron(II) and 1,10-phenanthroline was pipetted onto a paper microfluidic device and the resulting analysis completed, (figure 4.2) that deposits varying iron concentrations from 0.1 M to 0.001 M. The paper device was photographed as a whole, but each individual detection region was analysed individually. This was performed in ImageJ and an area square drawn around the largest detection zone (area in which 1,10-phenanthroline had been deposited) visible and then dragged across into each subsequent detection zone for each subsequent concentration of iron(II), as described in chapter 2.2.

However, problems were encountered in this experiment, the main issue been with the reactant 1,10-phenanthroline and the corresponding colour change to pink/red when reacting with iron(II). This was due to difficulty when trying to measure the colour change in the channel of the paper device as 1,10-phenanthroline is soluble in aqueous solutions. This experiment required aqueous solutions for the iron(II) samples, as the solution would transport (wick) the iron(II) into the detection zone, however the detection zone (1,10-phenanthroline) did not remain stationary within the channel. Therefore, the iron(II) solution had a “chromatographic effect” whereby the liquid would not remain stationary in the channel as according to Darcy’s Law⁸⁶ fluid would continue to wick if there is a sufficient source of fluid and an unfilled absorbance capacity of the paper to maintain the flow of fluid.⁸⁶ Thereby, spreading the detection zone along the channel and inhibiting a correctly calculated colour intensity when analysing with ImageJ (as the colour would appear less concentrated as it was spread over a large area).

This was most clearly seen in the channel containing the highest concentration of iron(II) (0.1 M) outlined in figure 4.2A.

It was also noted in the analysis of the initial iron(II) measurements that the trend of the graph decreased as the concentration of iron(II) increased. It was at this point that it was discovered that the image when analysing in ImageJ has to be inverted to allow the darker colours to be recorded as the higher density values rather than vice versa.

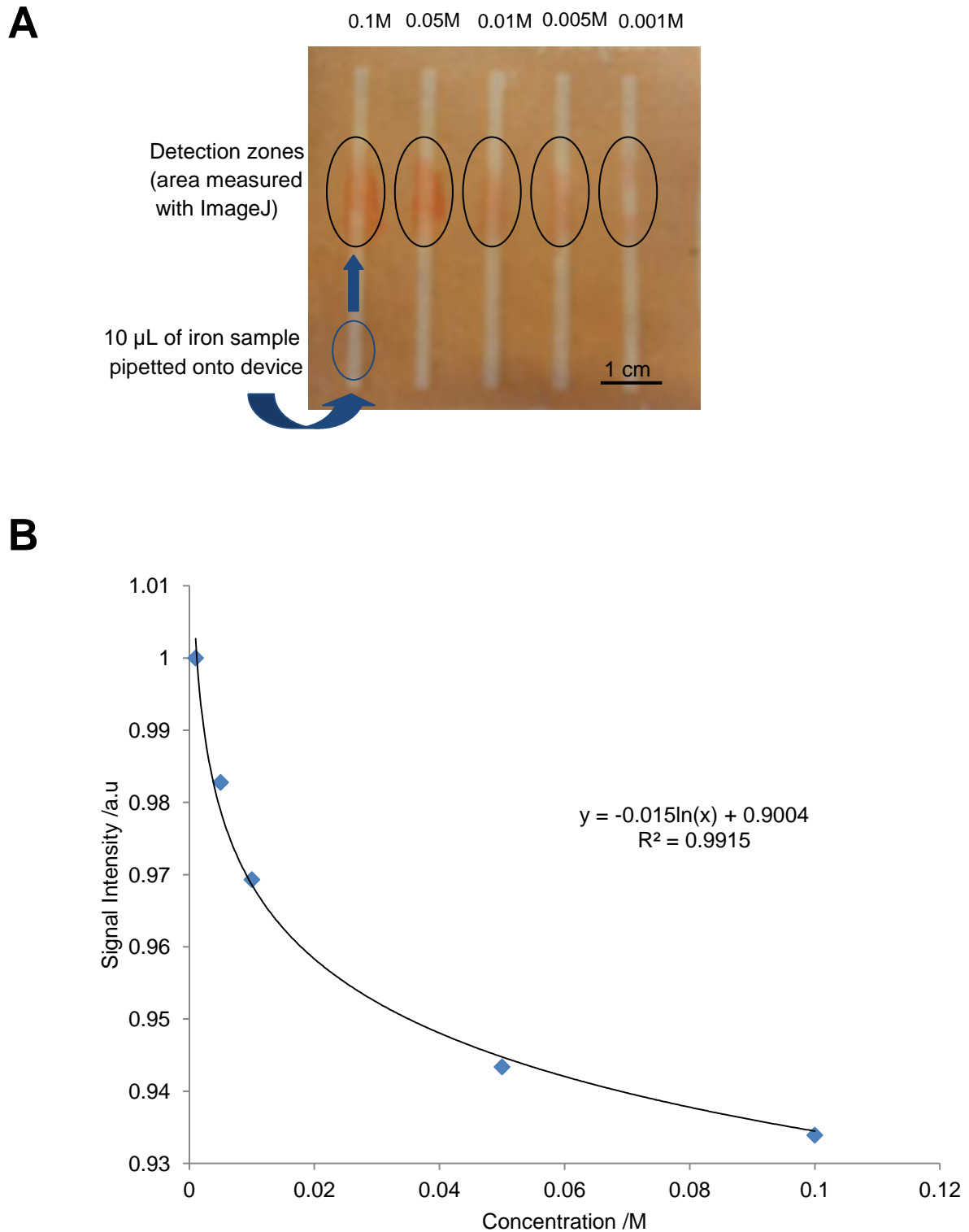


Figure 4.2: Preliminary results of iron(II) detection on paper microfluidic device using 1,10-phenanthroline ($R^2=0.9915$), $n=1$.

Panel A: illustrates the introduction of samples onto the paper device and the area measured in analysis. **Panel B:** resulting analysis of paper device.

The results measured for the varying iron(II) concentrations between 0.1 M and 0.001 M were initially used to determine if the results recorded on the paper device were comparable when using 1,10-phenanthroline to measure iron(II) concentrations with the conventional, spectrophotometer method at 510 nm as described in chapter 2.4.

The paper device data was compared with data obtained using a spectrophotometer (figure 4.3). A solution of 1.5 mL of iron(II) was mixed with 0.75 mL of 1,10-phenanthroline and measured at 510 nm after 2 min. The corresponding data from the spectrophotometer readings show a linear increase of iron(II) concentration which was the expected result, figure 4.3. However, in comparison the paper device showed a curved line of signal intensity which decreased as the iron concentration increased, figure 4.2B.

From this, the assumption was made that the “chromatographic effect” of the 1,10-phenanthroline and iron(II) coloured complex was providing an inaccurate result for analysis, caused by leakage into the photoresist. The dried 1,10-phenanthroline was wicked along through the channel by the iron(II) solution, before being carried over the channel and into the hydrophobic barrier of the photoresist coated paper, giving the appearance of being a brighter pink/red colour. It was thought this may be due to the N-bonds in the 1,10-phenanthroline reacting with the polymer of the photoresist rather than the iron(II) alone. The loss of 1,10-phenanthroline reagent into the photoresist would cause inaccurate results and measure a higher result than expected.

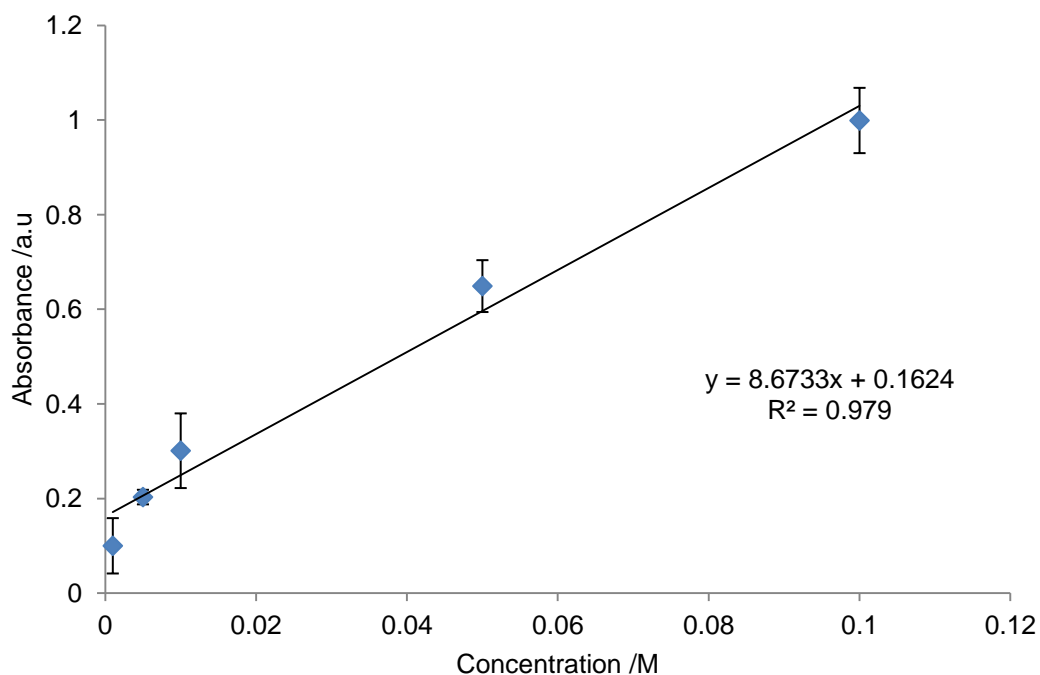


Figure 4.3: Spectrophotometer analysis of iron concentrations, ($R^2 = 0.979$), $n=5$.

4.2: Bathophenanthroline Detection

To prevent the chromatography effect reported in chapter 4.1, an alternative reagent for the detection of iron(II) was investigated that was not soluble in water. Bathophenanthroline is a derivative of 1,10-phenanthroline which is only dissolvable in alcohol, such as ethanol compared to 1,10-phenanthroline which was soluble in aqueous solutions. Thereby, the iron(II) aqueous solution for standard concentrations or human samples containing iron(II) would not move the bathophenanthroline (previously dried in the channel as the 1,10-phenanthroline) along the channel. Therefore, providing a solution to the chromatography effect caused by this movement when using 1,10-phenanthroline.

At this point, the channels were widened from 2 mm to 3.5 mm in the device design (photo-mask design8 lane, 2nd generation from figure 2.7B) allowing

the iron solution to wick along easier and faster than has been previously been recorded when using 1,10-phenanthroline. This was to improve the response time of the device from the addition of an iron(II) sample to result as if this was to be used for POC device, a fast yet accurate result is desirable. Applying Darcy's law⁸⁶ to the devices channels illustrated an increased volume of sample was required (15 μL as opposed to 10 μL) to allow diffusion through the channel to maintain velocity and reach the detection zone but, a better resolution was achieved in the channels from the photolithography method in fabricating the devices.

Originally, bathophenanthroline was pipetted onto the channel in the same manner as the 1,10-phenanthroline, but the ethanol easily dissolved and destroyed the photoresist created channels and the hydrophobic barrier. However, to compensate for this issue a three dimensional device was constructed preventing the bathophenanthroline from coming into contact with the photoresist coated paper, as outlined in chapter 2.5.2, figure 2.4.

The bathophenanthroline was soaked and dried onto untreated filter paper and cut to a size that would fit above one channel only on the device without entering in direct contact with neighbouring channels, thereby avoiding cross contamination of the samples. The iron(II) sample was added to the photoresist coated channel in the bottom layer as described in section 4.1 and wicked up the channel, upon reaching the top layer of untreated filter paper the iron(II) solution would then wick through and absorb through into the top layer of the device. This top layer contained the bathophenanthroline,

as shown in the schematic diagram of the layout of the device (chapter 2.5.2, figure 2.4).

Preliminary results for the iron concentrations measured using the 3D paper based device and bathophenanthroline are shown in figure 4.4A. The resulting analysis of the colour change from colourless to red/pink is shown in figure 4.4B. These graphs are not linear as a plateau can be seen at concentrations higher than 0.02 M, this is because the method has reached the limit of quantification (LOQ). However, at the lower concentrations between 1 mM and 10 mM a linear increase can be seen, within the clinical range of serum iron(II) concentrations.

Results are shown with and without the two higher molarities (0.05 M and 0.1 M) in figure 4.5 thus now showing a linear relationship in figure 4.5B which is in agreement with the spectrophotometer results, figure 4.6B. There is an improvement in the accuracy in measuring the coloured detection zone using ImageJ as the white background of the untreated filter provides less background interference when compared to the devices previously measured in the channel using 1,10-phenanthroline, figure 4.2.

The result showed that iron(II) could be detected and measured successfully between 0.00075 M and 0.1 M and the coloured complex of red/pink clearly seen for every concentration with an accurate analysis showing an increasing linear relationship between the signal intensity and concentration of iron(II) as also seen in the spectrophotometer results.

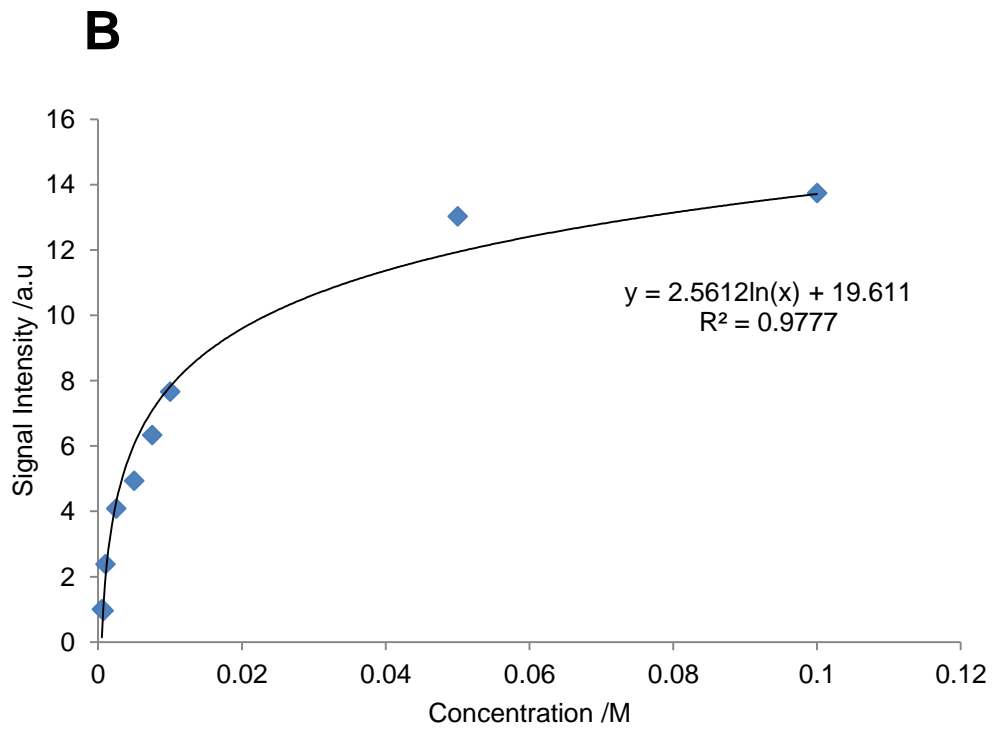
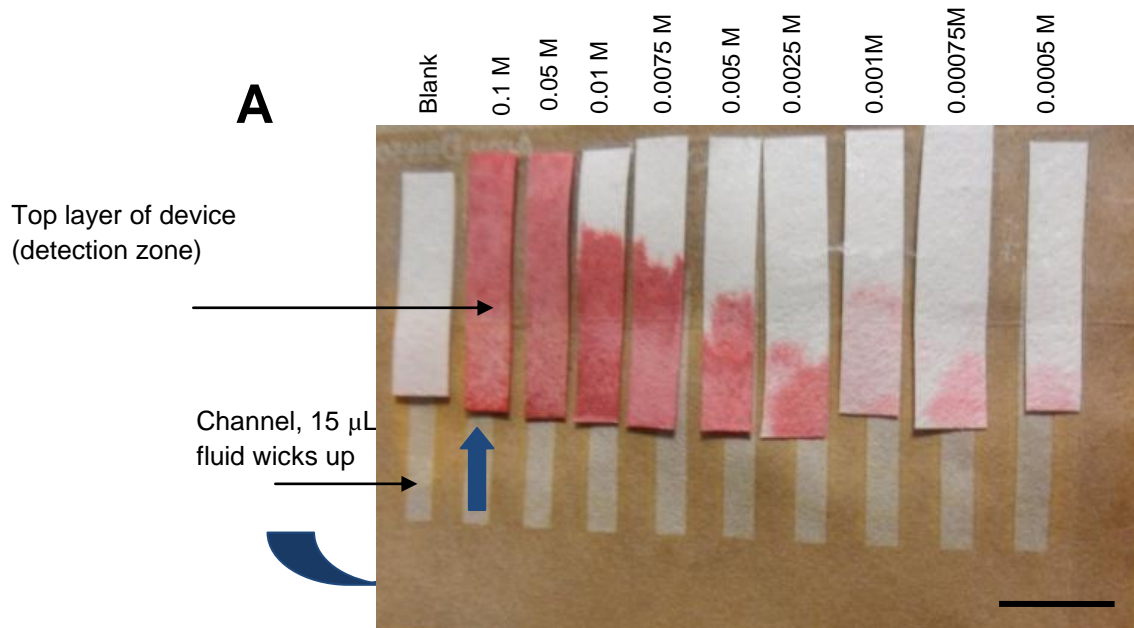


Figure 4. 4: Analysis of paper device using bathophenanthroline, $n=1$. ($R^2=0.9777$).
Panel A: 3D paper device with varying standard concentrations of iron(II). **Panel B:** Analysis of paper device.

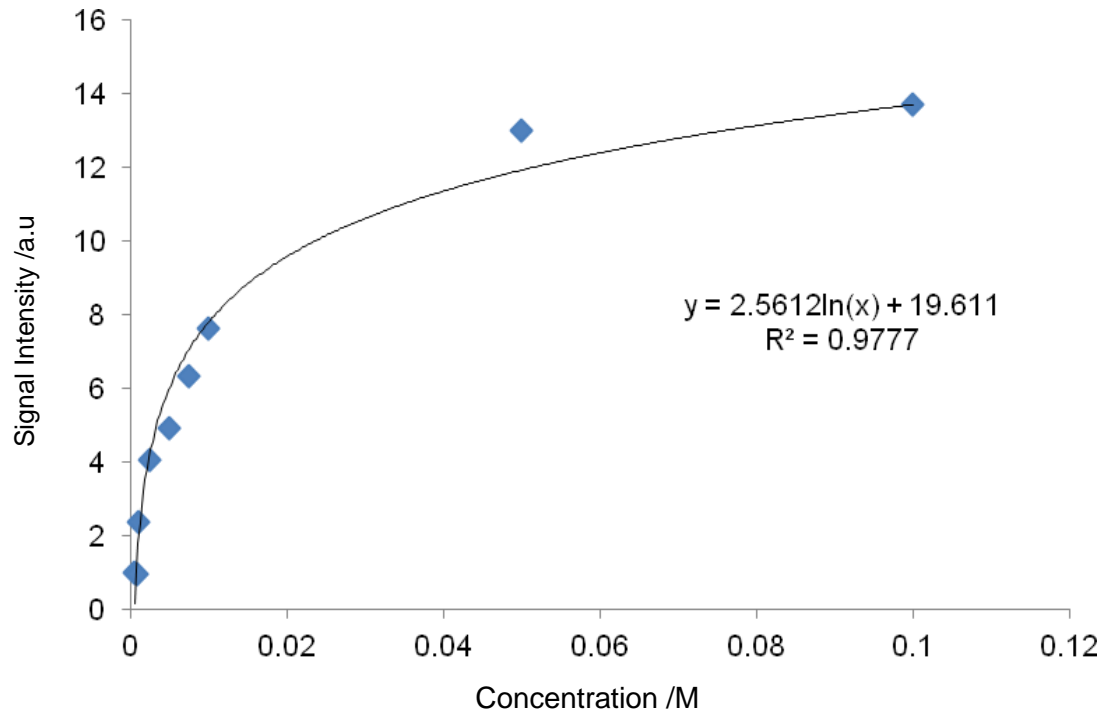
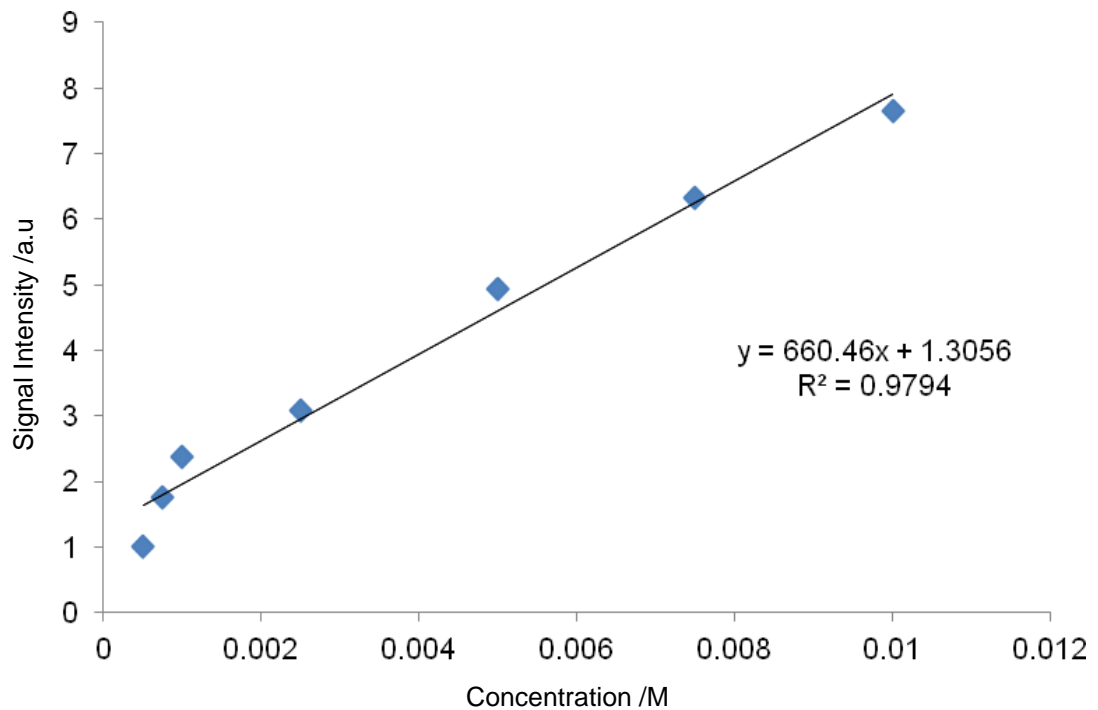
A**B**

Figure 4.5: Bathophenanthroline analysis on paper microfluidic device, $n=1$.

Panel A: Analysis including higher concentrations of iron(II) – 0.05 M and 0.1 M ($R^2=0.9777$). **Panel B:** Analysis not including higher concentrations of iron(II) – 0.05 M and 0.1 M, ($R^2=0.9794$).

For measurements in human serum samples or in whole blood samples the removal of the higher concentrations of iron(II) i.e. 0.05 M and 0.1 M was deemed acceptable as this is outside of the clinical range for both children and adults, male and females.^{205,222} The clinical range for iron(II) in human serum and plasma is between 7.5 μM and 75 μM ²²³ and between 0.006 M and 0.0007 M¹⁵⁰ in haemoglobin and the bathophenanthroline colourimetric method (figure 4.5) can be used in the range from 6.8 μM to 0.1 M.

Devices were measured as n=1 as they were to be presented as a POC device which would be a single use device and therefore as containing unknown biological hazards they would be destroyed after use. This would also be the same in regards to the analysis as differing light conditions could affect the digital images taken. Thus, in the case of each single use device the standard concentrations would be measured for that device only and the unknown sample of serum or whole blood would be calculated from the consequent analysis for that device only.

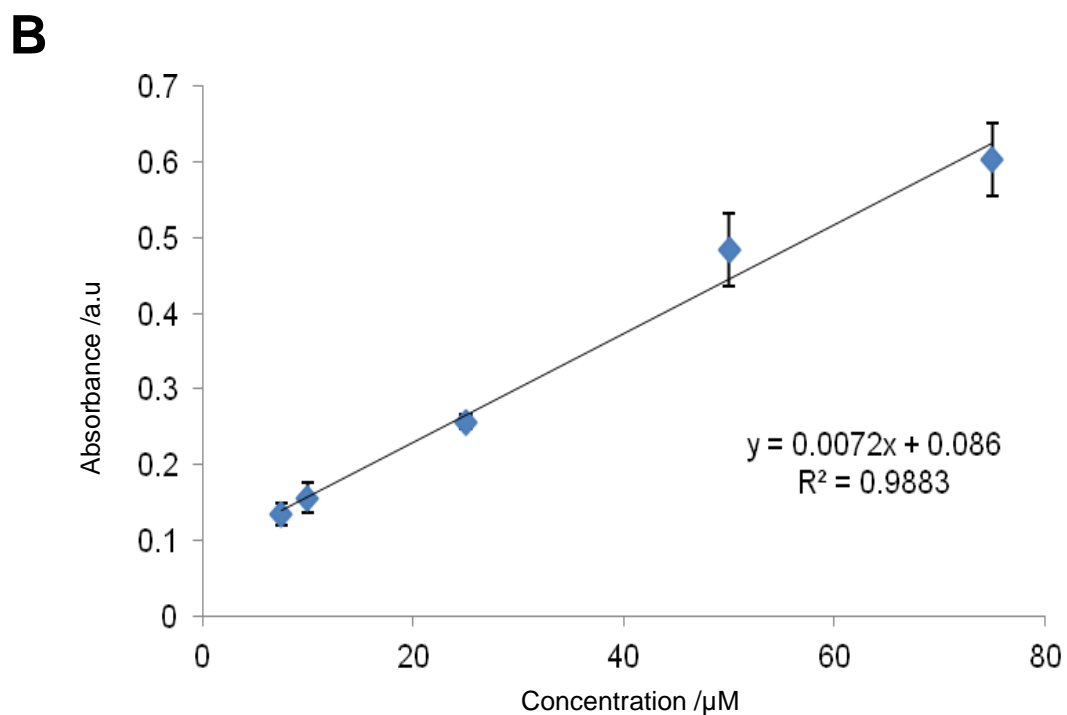
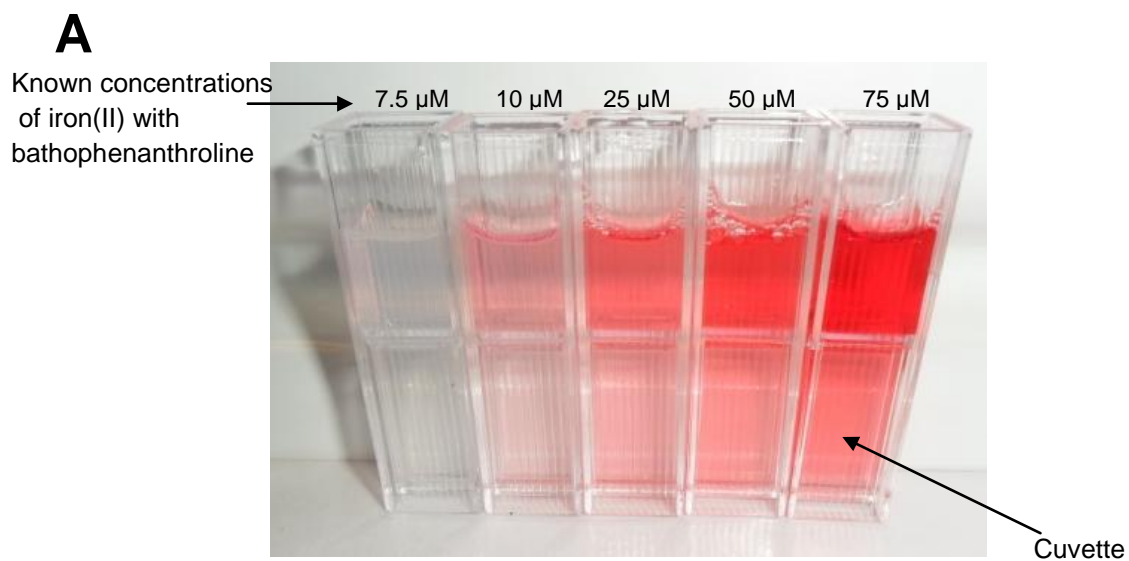


Figure 4.6: Spectrophotometric results using bathophenanthroline, $n=6$. ($R^2 = 0.9954$).

Panel A: Expected colour change observed in plastic cuvettes. **Panel B:** Analysis of iron(II) and bathophenanthroline spectrophotometrically.

4.3 Human Samples

4.3.1 Whole Blood Samples

Human whole blood samples were tested on the paper devices, initially without the addition of heparin however, the whole blood would clot and would not wick along the channel, becoming immobile in the channel. Heparin could not be added to the whole blood samples as it would cause interference in the reaction between iron(II) and bathophenanthroline.^{224,225}

To obviate to this problem, water was added to whole blood samples to allow the osmotic pressure to cause haemolysis in the RBCs, thus releasing the haemoglobin (containing iron(II)) that reacts with the bathophenanthroline complex in the top layer of the device. The addition of water into whole blood would also give the sample mobility, moving the whole blood along the channel and into the detection zone in the top layer, allow the concentration of iron(II) to be measured by the subsequent colour change, as explained in chapter 1.5. However, this would not work in the laboratory as the samples remained unusable as they did not wick along the channel, in addition, it was considered the red colour from RBCs in whole blood may interfere with the colour change and detection, thereby reducing analysis to be inaccurate and un-usable.

4.3.2 Serum and Plasma Samples

To devise a reliable and reproducible test, rather than whole blood, human serum and plasma samples with sample preparation could be used. Serum contains iron in the iron(III) form that is bound to a protein known as transferrin, for the purposes of the POC device to measure the iron, it would

need to be reduced to iron(II) to react with the bathophenanthroline whilst been removed from the transferrin protein.

Initial experiments focused on reducing the iron(III) into the iron(II) form by adding various reducing agents such as zinc powder or acetic acid to the serum sample. The addition of zinc or acetic acid into serum samples caused intense bubbling which rendered the serum sample un-usable, as the reaction would occur until the serum sample had fully evaporated.

It was then decided to investigate “The Lauber Method” to enable the simultaneous reduction of iron from iron(III) to iron(II) and release the iron from the transferrin protein, chapter 1.6.2.¹⁴⁸ The original method was created to spectrophotometrically measure iron(II) in serum samples but required the agglutinated proteins to be centrifuged to be removed before a measurement could be taken, however the use of a paper device allows the prepared sample to be pipetted straight onto the channel as the paper matrix traps the subsequent agglutinated proteins (such as transferrin), leaving the smaller molecules such as the reduced iron(II) to react with the bathophenanthroline complex further along the channel, in the top layer of the device. The method was completed for the paper device by adding the teepol and sodium dithionite solution to the serum sample before pipetting onto the channel as before, in chapter 4.1 and 4.2.

A new device was designed for the detection of iron(II) in human serum rather than in whole blood to allow for the incorporation of the Lauber method. The device was designed to have eight channels in total; five

channels (one for each iron standard concentrations ranging from 7.5 μM to 75 μM), one channel for a blank (used as a reference for background interference in the analysis) and two channels for the serum sample to be used in duplicate. The channels were fabricated to be wider (3.5 mm x 50 mm) than the device presented in sections 4.1 and 4.2 to incorporate the increase in volume from the addition of teepol and sodium dithionite to the serum sample.

Data analysis was performed as described in chapter 2.4. Preliminary results showed a strong correlation between results received via the spectrophotometer method and the paper device when compared using the standard iron(II) concentrations, figure 4.9. This was demonstrated by an ANOVA test, Students paired t-test and an f-test in all cases there was no significance difference, $P=0.235$ between the standard iron(II) concentrations. The linear regression trendline of both the paper device and the spectrophotometer method was compared and was shown to have no significance difference, $P=0.321$.

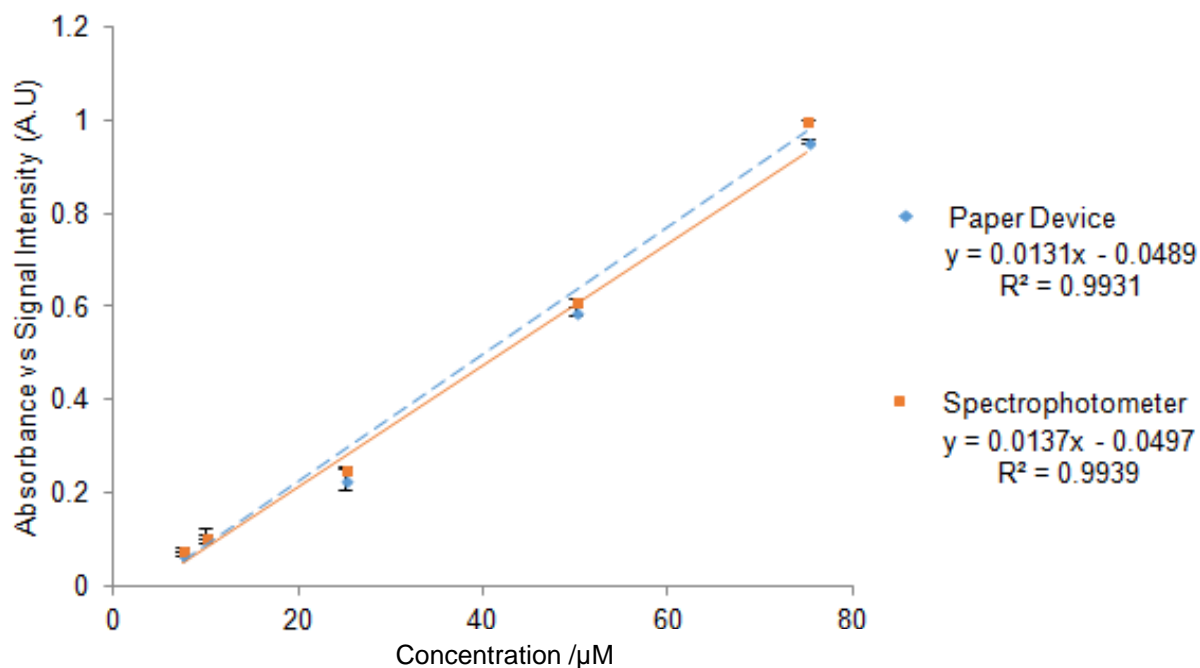


Figure 4.7: Comparison of methods using standard concentrations of iron(II), $n=6$. $R^2 = 0.9931 = \text{paper device}$, $R^2 = 0.9939 = \text{spectrophotometer}$.

4.3.3 Clinical Samples of Human Serum

Given the accurate results obtained when using the standard concentrations of iron(II), the bathophenanthroline method was further characterised for use with clinical samples using the Lauber method. The reduced volume in serum required for each assay (5 μL) enabled the sample to be repeated on ten paper devices for each serum sample measured, therefore validating the POC device.

Human serum sample analysis is shown in figure 4.9 using the modified Lauber method and bathophenanthroline detection on a paper device. The analysis of the results indicate that the patient's iron(II) level in serum was $13.6 \mu\text{M} \pm 1.3\% \text{ SEM}$ and this was within the normal range for sex and age

range of this specific patient, therefore it was concluded this patient was not suffering from anaemia.¹⁵¹ The data was in agreement with the findings from the hospitals pathology laboratory who measured an iron(II) level of $13 \mu\text{M} \pm 0.6\%$ SEM in that particular patient.

This method was used for various patients whose consent had been received (ethics appendix) and compared with results received from the hospital Table 4.1 shows a comparison between results from the hospital and the paper device, clearly illustrating no significant difference between the two methods in terms of accuracy and consistency. This was also confirmed at the statistical level by the F-test and a T-test presented in tables 4.2 and 4.3.

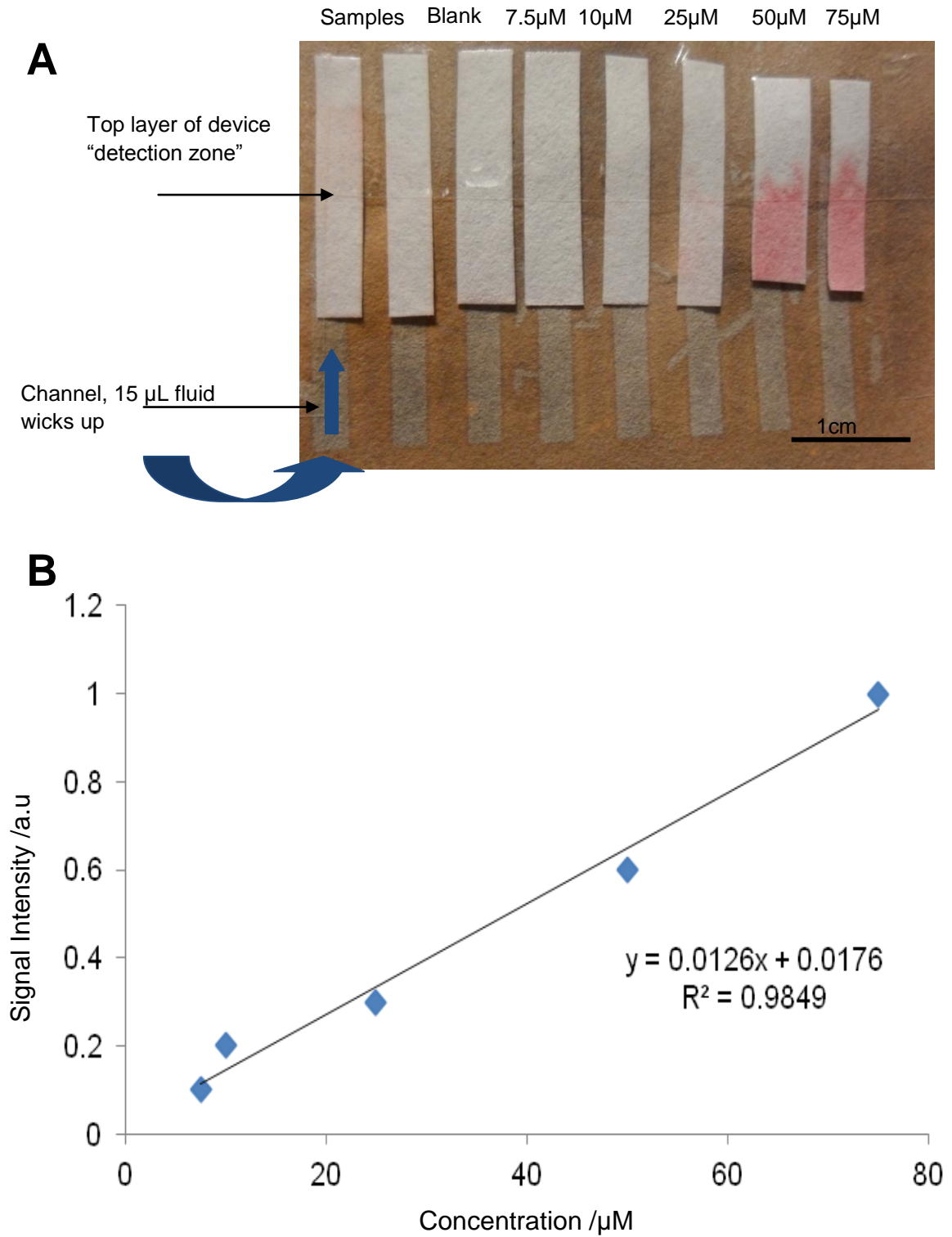


Figure 4.8: A paper device for iron(II) analysis in human serum, $n=2$, $R^2 = 0.9849$. **Panel A:** Paper device for analysis of known standard concentrations and unknown concentrations of iron(II), **Panel B:** Analysis of iron(II) in serum sample. Iron(II) = $13.6 \mu\text{M} \pm 1.3\% \text{ SEM}$.

Table 4.1: Comparison between results obtained from the paper device versus the clinical specified method, n=10.

Patient	Paper Device /μM	Pathology Results /μM
A	12 \pm 1.1%	11 \pm 0.6%
B	13 \pm 0.6%	13 \pm 0.6%
C	16 \pm 1.3%	15 \pm 0.6%
D	27 \pm 0.8%	26 \pm 0.6%
E	14 \pm 0.5%	15 \pm 0.6%
F	14 \pm 1.3%	14 \pm 0.6%
G	10 \pm 1.2%	9 \pm 0.6%
H	19 \pm 1.3%	19 \pm 0.6%
I	16 \pm 0.6%	16 \pm 0.6%
J	12 \pm 0.8%	12 \pm 0.6%
K	20 \pm 1.6%	21 \pm 0.6%
L	32 \pm 0.9%	30 \pm 0.6%
M	15 \pm 0.5%	14 \pm 0.6%
N	16 \pm 0.2%	16 \pm 0.6%
O	19 \pm 0.7%	17 \pm 0.6%
P	31 \pm 0.3%	30 \pm 0.6%
Q	15 \pm 0.5%	15 \pm 0.6%
R	26 \pm 0.7%	25 \pm 0.6%
S	11 \pm 0.6%	10 \pm 0.6%
T	9 \pm 0.7%	9 \pm 0.6%
U	15 \pm 0.4%	14 \pm 0.6%

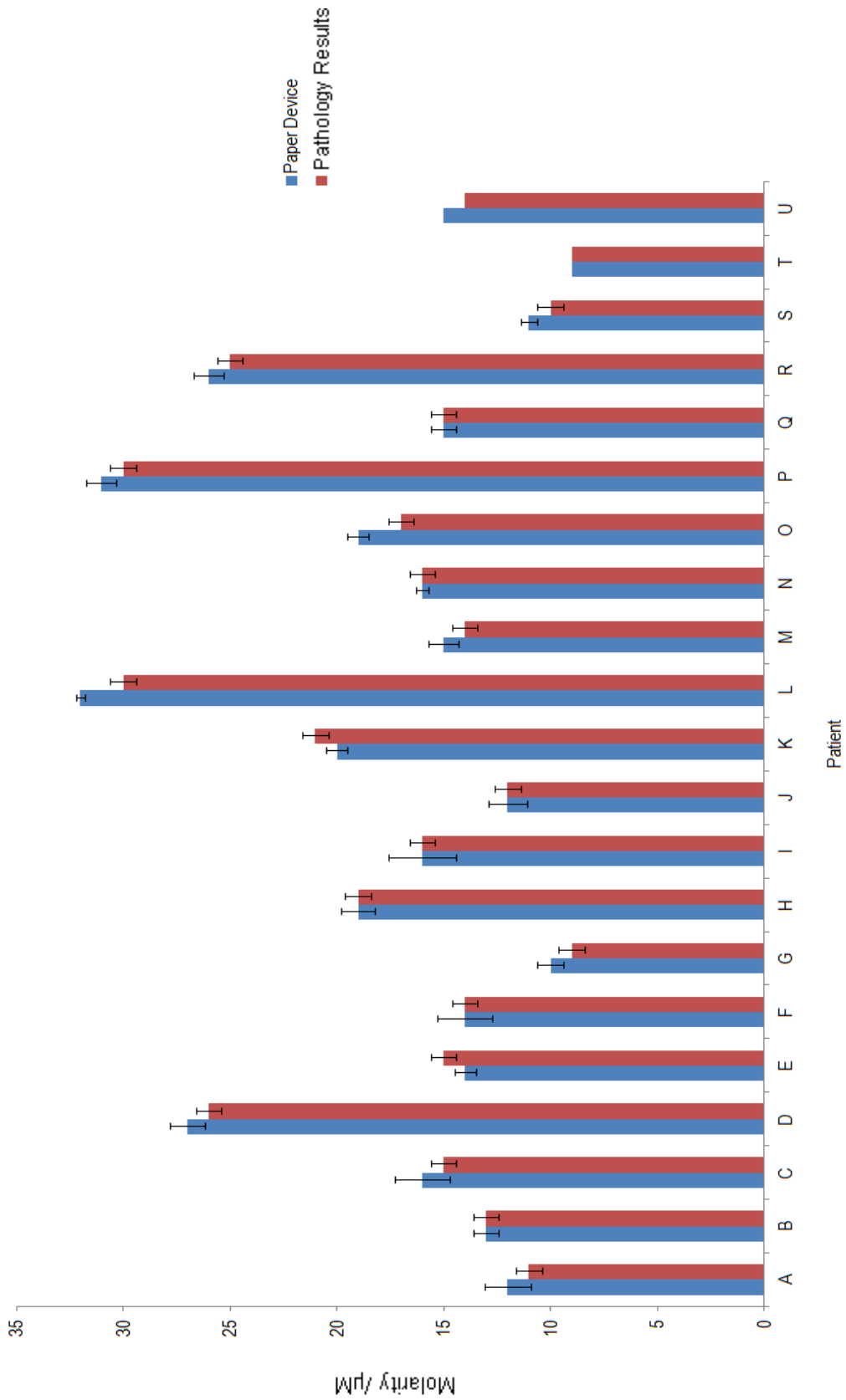


Figure 4. 9: Iron analysis for human serum samples using paper device versus hospital pathology laboratory method

The results from table 4.1 and figure 4.10 were statistically analysed to ensure there was no significant difference between the results from the paper device and results received from the hospital pathology laboratory. This was completed by using a paired student's t-test for each patient, which outlines there was no significant difference between any of the results for all patients, (P= 0.42, table 4.2).

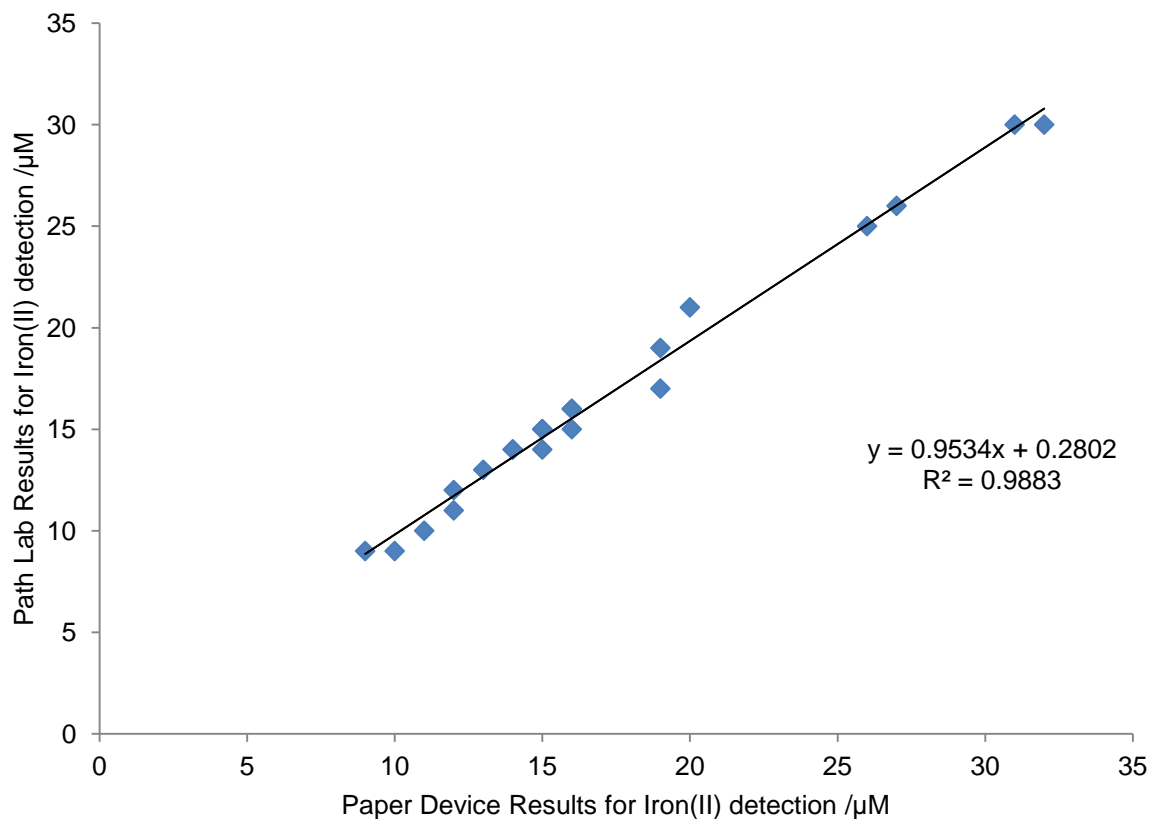


Figure 4. 10: Linear regression of results found using paper device vs. pathology results.

Taken from table 4.1 showing the correlation between the two methods for the measurement of iron(II) in serum samples.

The linear regression observed in figure 4.11 supports the paper device as an accurate method to measure iron(II) in human serum samples via a high correlation between the paper device results and the hospital pathology

results, $R^2=0.9883$. The intercept of figure 4.11 further illustrates no significance difference between the two methods, $P=0.89$.

The variance for the data was statistically analysed using an F-test which established there was no variances within the data when comparing the paper device results to the hospital pathology laboratory results, table 4.2.

Table 4.2: Statistical analysis of results from table 4.1, $P= 0.42$.

	Paper Device	Path Lab
Mean	17.5	17
Variance	44.05	40.10
Observations	20	20
df	19	19
F	1.09	
P(F<=f) one-tail	0.42	
F Critical one-tail	2.16	

Highlighted in bold illustrates no significant difference between results

4.4 Validation of Iron(II) Measurements using the Paper Device

The consistency of the paper device method was further established to ensure the method would also work for levels of iron(II) which would be outside the normal clinical range ($7.5 \mu\text{M}$ to $75 \mu\text{M}$) by measuring high and low levels of iron(II). This was completed for high levels of iron(II) by spiking a patients serum samples to have a total of $89 \mu\text{M}$ of iron(II) and been to the hospital pathology laboratory for testing.

Upon completing the analysis of the artificial serum sample, the results were compared with the standard colourimetric method using a

spectrophotometer, table 4.3. For low levels of iron(II) in serum, the consistency of the paper method was tested using samples from patients known to be suffering from anaemia, table 4.6. Statistics were used to ensure the reproducibility of this method to ensure the results from the paper device and the clinical method were not significantly different ($P > 0.05$) and the amount of variance within the results was not significantly different ($P > 0.05$).

The high levels of iron(II) in human serum samples maintained accuracy as the results were not significantly different from the pathology results received, $P > 0.05$ for both a paired Students T-test and F-test, table 4.4 and table 4.5.

The low levels of iron(II) in human serum samples maintained accuracy as the results were not significantly different from the pathology results received, $P > 0.05$ for both a paired Students T-test and F-test, table 4.7 and table 4.8.

Table 4.3: High levels of iron in serum samples to determine accuracy of method outside the clinical range, n=10.

Patient	Paper Device / μM	Pathology Results / μM
A	$87 \pm 0.7\%$	$88 \pm 0.2\%$
B	$85 \pm 0.4\%$	$87 \pm 0.3\%$
C	$89 \pm 0.6\%$	$89 \pm 0.4\%$
D	$86 \pm 0.5\%$	$85 \pm 0.3\%$
E	$91 \pm 0.3\%$	$86 \pm 0.6\%$
F	$87 \pm 0.9\%$	$89 \pm 0.4\%$
G	$89 \pm 1.2\%$	$89 \pm 0.4\%$

Table 4.4: Statistical analysis for high levels of iron(II) in serum (Paired T-test) P= 0.76.

	Paper Device	Path Lab
Mean	87.83	87.5
Variance	4.96	3.1
Observations	7	7
Pearson Correlation	0.17	
Hypothesized Mean Difference	0	
df	5	
t Stat	0.31	
P(T<=t) one-tail	0.38	
t Critical one-tail	2.01	
P(T<=t) two-tail	0.76	
t Critical two-tail	2.57	

Table 4.5: Statistical analysis for high levels of iron(II) in serum (F-test for Variance) P= 0.30.

	Paper Device	Path Lab
Mean	87.83	87.5
Variance	4.96	3.1
Observations	7	7
df	5	5
F	1.60	
P(F<=f) one-tail	0.30	
F Critical one-tail	5.05	

Table 4.6: Low levels of Iron in Serum Samples.

Patient	Paper Device (n=10) / μM	Pathology Results / μM
A	6 \pm 0.8%	6 \pm 0.6%
B	6 \pm 0.9%	7 \pm 0.6%
C	6 \pm 0.7%	6 \pm 0.6%
D	6 \pm 1.1%	6 \pm 0.6%

Table 4.7: Statistical analysis for low levels of iron(II) in serum (Paired T-test) P= 0.39.

	Paper Device	Path Lab
Mean	6	6.25
Variance	0	0.25
Observations	4	4
Pearson Correlation		
Hypothesized Mean Difference	0	
df	3	
t Stat	-1	
P(T<=t) one-tail	0.19	
t Critical one-tail	2.35	
P(T<=t) two-tail	0.39	
t Critical two-tail	3.18	

Table 4.8: Statistical analysis for low levels of iron(II) in serum (F-test for variance)
P= 0.32.

	Paper Device	Path Lab
Mean	6	6.33
Variance	0	0.33
Observations	4	4
df	2	2
F	0	
P(F<=f) one-tail	0.32	
F Critical one-tail	0.05	

4.3: Smartphone Analysis

In order to assess the possibility to use the device outside a laboratory setting, digital images of the paper devices were taken by using a mobile phone such as a Smartphone. This would allow the user to be less reliant on more equipment to complete the analysis. For example, to be able to use the paper device in the field the images of the paper devices could be sent via email to a central laboratory and analysed or the ImageJ software used to analyse the data from the paper device could be turned into an application (app) and analysed immediately using the mobile phone.

In this case, images once taken were transferred to a computer and analysed with ImageJ. An image of a paper device taken with a Smartphone camera and the results from the subsequent analysis is shown in figure 4.11. The results from the paper device indicate a serum iron(II) level of $13 \mu\text{M} \pm 0.8\%$ SEM with full results from patients presented in table 4.10. In the image taken with the Smartphone camera it was noted that there was more reflection in the image from the sellotape but this was deemed acceptable as this did not cause any interference in the area which was to be measured in ImageJ to calculate the signal intensity of each sample (standard concentrations and unknown samples).

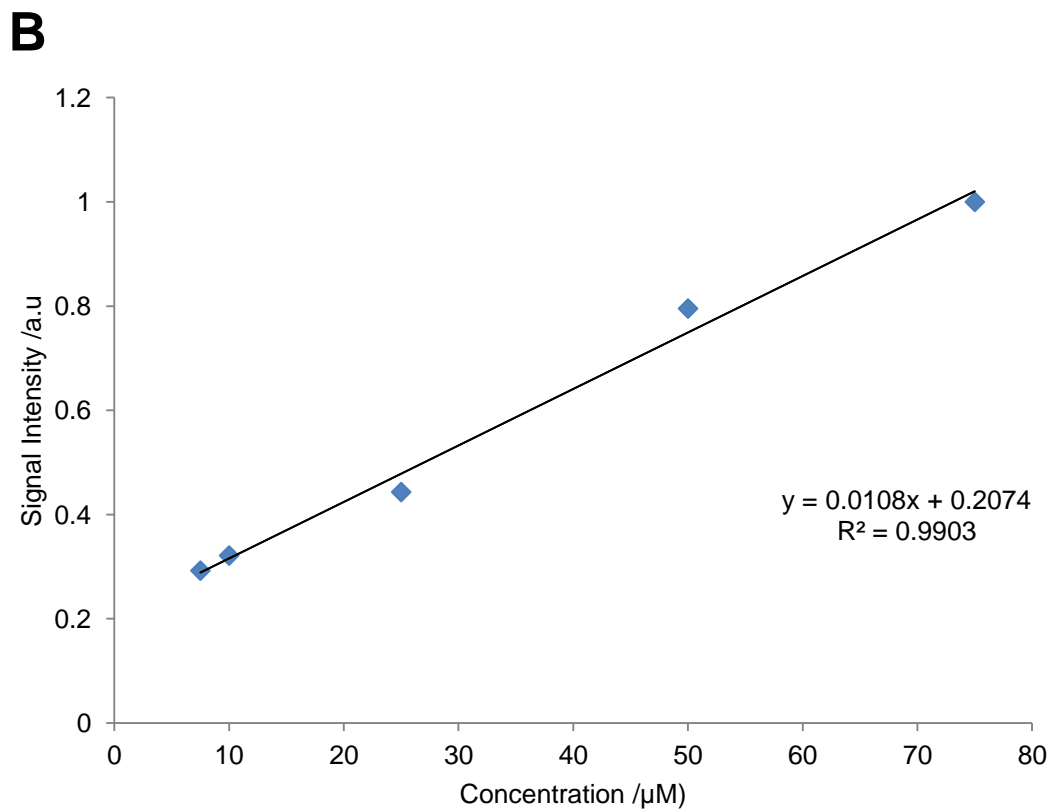
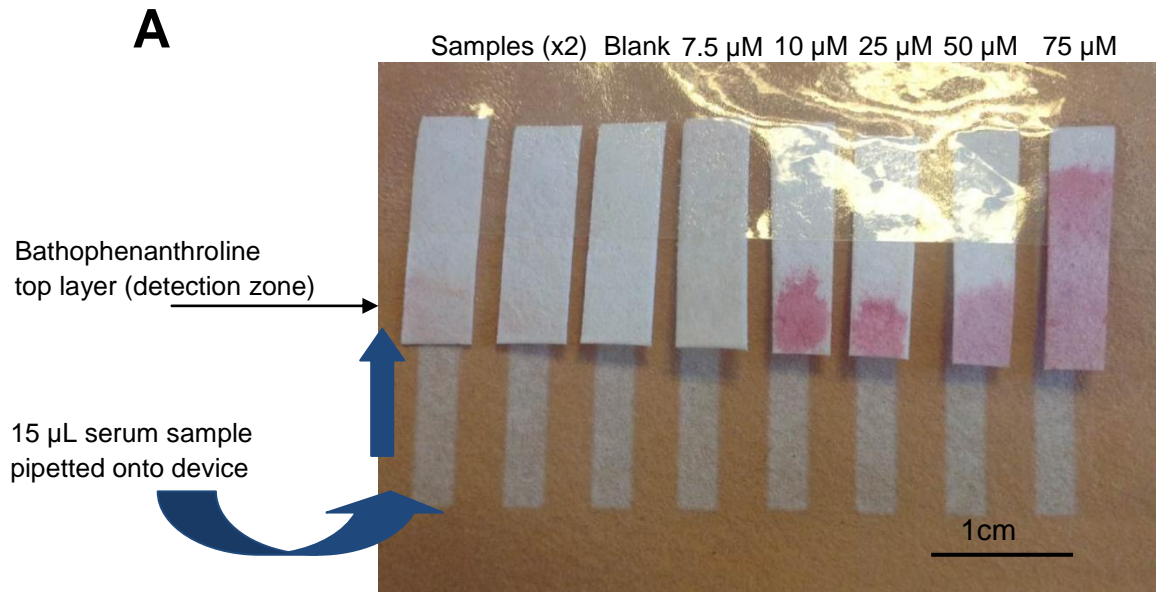


Figure 4.11: Paper device using human serum sample taken with a Smartphone camera (iPhone4s).

Panel A: Paper device with known and unknown concentrations of iron(II). **Panel B:** Analysis of paper device taken with Smartphone camera.

***note reflection in Panel A**

Table 4.9: Results from patients serum samples when using a Smartphone camera, n=10.

Patient	Paper Device with Smartphone camera / μM	Pathology Results / μM
A	$13 \pm 0.8\%$	$13 \pm 0.6\%$
B	$13 \pm 0.6\%$	$14 \pm 0.6\%$
C	$19 \pm 1.1\%$	$20 \pm 0.6\%$
D	$26 \pm 0.9\%$	$26 \pm 0.6\%$
E	$14 \pm 0.7\%$	$15 \pm 0.6\%$
F	$23 \pm 1.3\%$	$24 \pm 0.6\%$
G	$26 \pm 1.4\%$	$26 \pm 0.6\%$
H	$11 \pm 0.7\%$	$11 \pm 0.6\%$
I	$28 \pm 0.6\%$	$29 \pm 0.6\%$

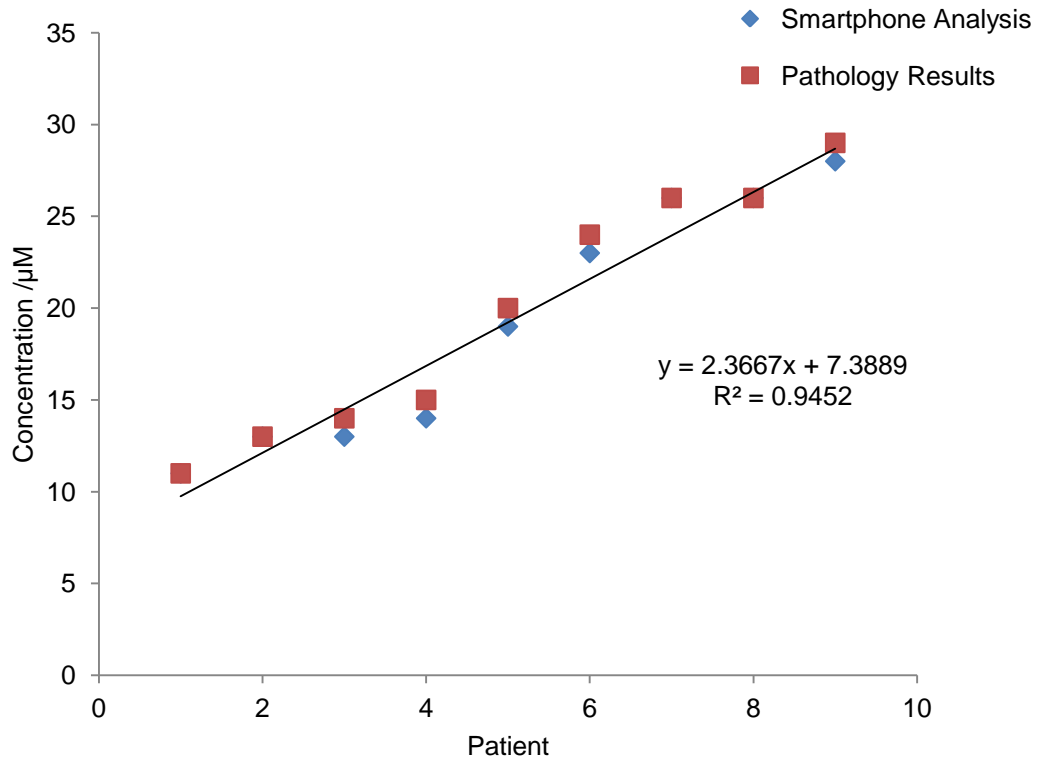


Figure 2. 13: Linear Regression of results found using the Smartphone camera vs. pathology results.

Taken from table 4.9 showing correlation between the two methods for the measurement of iron(II) in serum samples.

Statistical analysis of the results using a paired T-test and F-test showed there was no significant difference between the paper device and the standard method when using a Smartphone camera, ($P > 0.05$ in every patient result, $n=2$). Therefore demonstrating this device could be used away from the laboratory setting and the data collected emailed to a central server for computer analysis.

4.4: Whole Blood Analysis Revisited

The paper device presented in section 4.2 which was proven comparable to the conventional spectrophotometer method used in hospital pathology laboratories, still lacked the ability to detect iron(II) directly from unprocessed blood. For the paper device to be considered as a useful POC system usable by non-specialised personnel, the paper device has to incorporate a method to remove RBCs without having to centrifuge whole blood beforehand. Therefore, at present his paper device has limitations for its use e.g. in the developing world a centrifuge is an expensive piece of equipment which may not be available.

Charles Henry's group in the USA have utilised a paper membrane known as LF1 from Whatman syringe filters.⁷⁸ These plastic filters attach to plastic syringes and contain a porous membrane (1 mm) inside which is used to filter out impurities, such as in use with tissue culture.⁷⁸ Henry's group removed the paper membrane from inside the filters and incorporated the paper membrane into a 3D paper device to remove RBCs and WBCs by trapping the larger cells in the porous membrane (1 mm) through the cellulose matrix from whole blood and allow the smaller molecules contained in pure plasma to flow through the membrane uninhibited and into the paper device.⁷⁸

In figure 4.11A the paper device from chapter 4.2 can be seen with the incorporation of the LF1 membrane allowing 10 μ L of whole blood samples to be applied onto the paper device. This was completed by slotting the membrane in between the two layers of the device previously designed, as

this will allow the membrane to be in contact with the paper devices base (for support) and in contact with the top layer (detection zone) allowing the plasma and teepol etc. to wick through.

In figure 4.11B the addition of whole blood (mixed with 10 μ L of teepol solution and sodium dithionite as previously described, chapter 4.2) to the paper device can be seen to trap the RBCs at the bottom of the membrane within the porous matrix whilst allowing plasma to flow uninhibited into the detection zone were the free iron(II) would react with the bathophenanthroline.

However, the Lauber method developed for this paper device was designed for the detection of iron(II) in human serum samples and was shown to not contain any interfering agents through the alteration of the pH, whereas by incorporating the LF1 membrane which would allow human plasma into the paper device could contain a possible interfering agent e.g. fibrinogen. Fibrinogen is a plasma glycoprotein converted into fibrin by thrombin (an enzyme which cleaves peptide bonds in proteins) during the formation of a blood clot. Therefore, further experiments would have to determine whether interference from fibrinogen would cause any in-accuracies in the detection of iron(II) with bathophenanthroline.

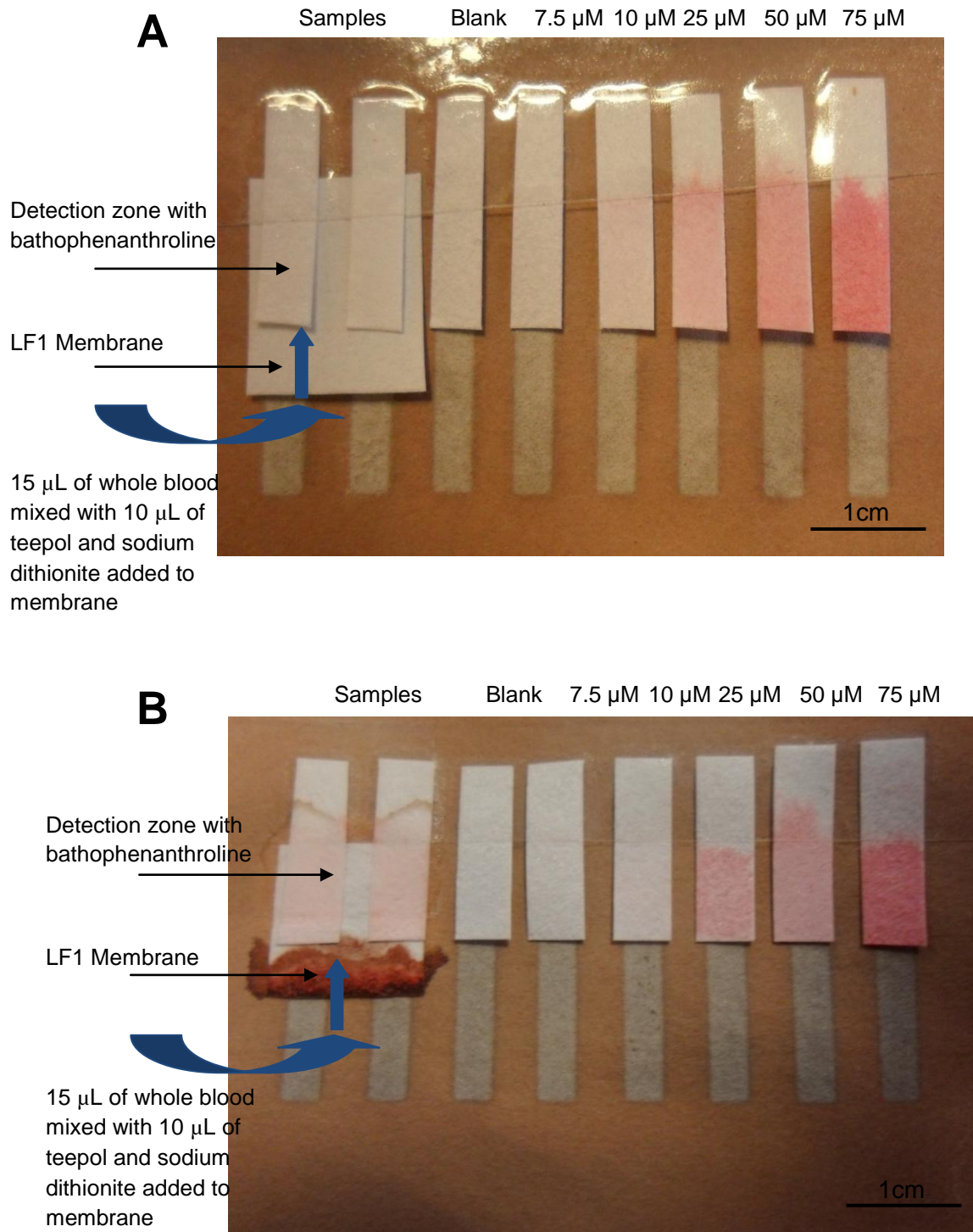


Figure 4.12: Blood separation using the LF1 membrane on the paper device. **Panel A:** Paper device with incorporation of LF1 membrane slotted under the top layer (detection zone) of the paper device. **Panel B:** Addition of whole blood onto the paper device.

The colourimetric reaction from colourless to pink for iron(II) with bathophenanthroline in figure 4.12B indicates that iron(II) is reacting correctly with the bathophenanthroline. The plasma samples were repeated ten times on ten devices in duplicate and presented in table 4.10. The statistical analysis including an ANOVA ($P= 0.37$), a paired Students T-test ($P= 0.35$) and an F-test for variability ($P= 0.37$) illustrates there was no significant difference between the results received from the paper device and the results received from the hospital pathology laboratory. Therefore, the paper devices reproducibility as a POC device from previous has been maintained. This would now be a more functional device in the developing world as a finger prick of whole blood would not require any pre-treatment (centrifugation) to remove WBCs and RBCs.

Table 4.10: Plasma Level of Iron from Whole Blood Samples.

Patient	Paper Device / μM	Pathology Results / μM
A	24 ± 0.8	$25 \pm 0.6\%$
A	23 ± 0.7	$25 \pm 0.6\%$
A	26 ± 0.8	$25 \pm 0.6\%$
A	25 ± 0.6	$25 \pm 0.6\%$
A	23 ± 0.5	$25 \pm 0.6\%$
A	25 ± 0.5	$25 \pm 0.6\%$
A	26 ± 0.8	$25 \pm 0.6\%$

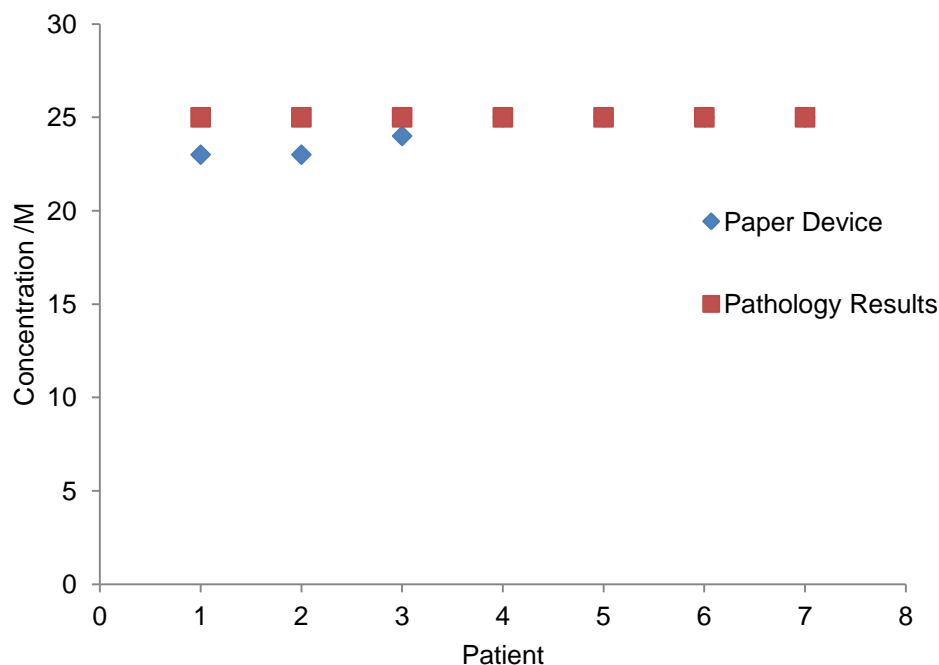


Figure 4.14: Linear Regression of results found using the whole blood vs. pathology results.

Taken from table 4.10 showing correlation between the two methods for the measurement of iron(II) in whole blood samples.

4.5: Discussion

In this chapter it was demonstrated that the paper device fabricated in chapter three can be successfully used as POC device outside of the laboratory setting by non specialised personnel. Its application would be suited for use in the developing world where anaemia is prevalent amongst the communities.²²⁶

The flow of these devices was determined as 12-15 s upon application of 10 μL of fluid, as according to Darcy's law⁸⁶ this allowed for sufficient fluid to

wick the fluid through the full length of the device.⁸⁶ This device was initially used to measure iron(II) using 1,10-phenanthroline. These initial experiments used 1,10-phenanthroline to detect iron(II) but the method suffered from inaccuracies as the aqueous solution of iron(II) and serum made this reagent un-practical by causing leakage and the detection zone needed to remain stationary for the analysis to be completed accurately. The dispersion of the 1,10-phenanthroline coloured complex made analysis difficult as this device had to remain simple, yet effective at measuring iron(II) content. The introduction of bathophenanthroline which was only soluble in alcohol (ethanol), meant the iron(II) in purified water would not have the same effect as the 1,10-phenanthroline. However, ethanol reacted and broke down the photoresist channel regardless of the hydrophobic barrier created. This led the development of a three dimensional device which used the photoresist created channels to control the fluid movement towards a detection zone at top of the channel, taking advantage of fluids natural ability to move through paper which was soaked in bathophenanthroline. The filter paper used on the top of the device was white in colour which allowed for no background interference which might have occurred had the colour change happened in the photoresist channel as the photoresist is also a red/pink colour as mentioned in the discussion of chapter 3.^{91,93,227} However, the second generation device required wider channels to allow the user to place with ease the top layer of the device which would be cut to size so there would be no cross contamination from channels on either side. According to Darcy's Law⁸⁶ the increase in width of channels would slow down the movement of the fluid and not fill the channel completely therefore the amount of fluid

added to the channel was increased to 15 μL which combated both issues and maintained the speed the fluid reached the detection zone in 12–15 s.⁸⁶

After successful analysis and measurement for concentrations of iron(II) in standard solutions within the normal clinical range (7.5 μM to 75 μM) on the paper devices when compared with the standard method using a spectrophotometer the first use of a human sample was to test human whole blood. However, this led to several problems for the detection iron(II), mainly that to measure iron(II) in serum. Firstly that iron(II) is complexed to the globular protein transferrin and secondly that it is in the iron(III) form in which bathophenanthroline would not react with as it can only form a coloured complex with the soluble iron(II) form. Initial experiments involved in the reduction of the iron(III) used various agents such as zinc, ascorbic acid and magnesium, but these reacted violently in the serum sample and rendered the sample useless. Purified water was tested for haemolysis the RBCs but the colour from RBCs affected analysis and visibility of the iron(II) reaction. The Lauber Method¹⁴⁸ was finally tried as it simultaneously reduces iron(III) and removes the globular protein, transferrin allowing a quantified measurement of iron(II) content in human serum samples.

To remove any potential error introduced by photography of the paper device the same conditions and at relatively the same distance through the use of measured side markers, erased such possible errors. Once the digital image had been transferred to a computer, the software ImageJ allowed a signal intensity to be measured from a specified area (chapter 2.2).

Once analysis had been determined, serum samples collected would be put onto the paper device and analysed within 20 min of collection they could be photographed. The use of a digital camera or a Smartphone camera showed no significant difference in the data obtained ($P < 0.05$). However, it was noted that there was more glare from the sellotape in the Smartphone camera pictures, this did not interfere with the analysis as this was above the detection zone and the area measured calculating the signal intensity. The use of the Smartphone camera allowed the image to be taken and either emailed to a computer for analysis or through the use of the dropbox application they were automatically uploaded to any computer which had the connection set up. This would provide a useful POC device for the developing world as one person could be in the field completing the tests on patients with the images been sent to central computer and another person performing the analysis and sending the results back to the person in the field.

The revisited whole blood analysis used iron(II) measurements taken from plasma samples (rather than serum samples) which had been separated out from whole blood via an LF1 membrane which trapped RBCs in the porous network. This development would allow a simple finger prick from a patient to be taken and smeared onto the device; the teepol and sodium dithionite solution could be added to the whole blood sample before been pipetted on the LF1 membrane thereby allowing the iron(II) to react with the bathophenanthroline solution as before when using serum samples.

The area of POC devices has seen a huge input of research in recent years⁸⁰, not only for the developing world but also for ease of use in the developed world.^{2,3,36,228-230} If patients could buy over the counter tests to use at home this would create a more beneficial financial role for the NHS as routine tests for patients, who suffer chronic illnesses do not have to travel to hospital or GP surgery every few weeks or days and results could be electronically sent to their doctors.^{41,42} If anything untoward was noticed by the doctor, then that patient could see a doctor for further tests.^{41,42}

Current methods for the detection of iron(II) in human samples and diagnosis of anaemia require skilled professionals and expensive equipment e.g. centrifuge to spin down red and white blood cells. A recent publication by Bond *et al.*⁴⁶ diagnosed anaemia in patients from haemoglobin levels of iron(II) using chromatography and a hand held reader which measured the intensity of the colour change once the RBCs had been lysed open from the addition of sodium deoxycholate.⁴⁶ However, this method although a simple POC device is not the most efficient diagnosis for anaemia due to haemoglobin levels of iron(II) been the last to be effected i.e. the iron(II) stores in the liver are depleted first then transported iron(II) is depleted before haemoglobin iron(II) is affected. Therefore, the best prognosis for an anaemia patient is to detect iron(II) depletion at the serum/plasma level before haemoglobin can be effected as this can lead to multiple organ failure in the most severe of cases. This POC device for haemoglobin level iron(II) detection could be further improved by improving the sensitivity of the device to allow for accurately detecting lower levels of iron(II) at the serum/plasma level which could be used for patients who are only just developing anaemia

rather than patients who are been severely affected and have been for a longer period of time.

Further work will be required if this device was to be used with plasma samples (to ensure there is or is not any interference from fibrinogen) but would overcome a major issue of having to centrifuge blood before use to separate out the serum layer from the whole blood. This was proven when work was completed into the use of the LF1 membrane that was able to trap RBCs allowing plasma to flow out into the section containing bathophenanthroline and successfully measure iron whilst maintaining accuracy. However, adding whole blood would still enable fibrinogen, a clotting agent present in blood, to filter through the analytical section. Since fibrinogen is not known if it interferes with the reaction of iron(II) with bathophenanthroline this would have to be discovered. On the other hand, it has been demonstrated by Lauber *et al.* that the altered pH of both the teepol solution and the bathophenanthroline allows specificity towards iron (II).²²¹

Chapter 5: Colourimetric Detection of Urea

This chapter will explain the process involved with the development of a colourimetric assay for determining renal failure in patients by the detection of urea in serum samples. Kidney failure is a chronic or acute disease most prevalent in the developed world. A POC device for the diagnosis of renal failure would aid in the prognosis before reaching end stage renal failure. Currently, methods involved in the diagnosis of renal failure measure waste products in blood samples such as creatinine and urea as these analytes rise when the kidneys are mis-functioning. The results gained from the paper device for measuring urea concentration in human serum samples were compared with the conventional method using a spectrophotometer to prove accuracy and consistency were maintained when using a paper device.

The paper device method was adapted for use on un-treated filter paper from Jung *et al.* which was initially used for measuring urea concentration in human serum samples spectrophotometrically within the clinical range of 10 mg mL⁻¹ and 150 mg mL⁻¹.¹³² To be developed for use on a paper device for the semi quantitative analysis of urea in human serum samples; the incubation time, the concentrations of the solutions used such as (o-phthalaldehyde, NED reagent and standard urea concentrations) and the colour development time had to be optimised.¹³²

5.1 Conventional Measurement of Urea

5.1.1 Optimisation

Urea concentrations were initially measured using the conventional laboratory method via a spectrophotometer at 505 nm, which turned red/orange from colourless when reacting with NED reagent and o-phthalaldehyde proportional to the amount of urea present in the sample. The conventional method was used to determine how accurate the results gained from the paper device were in comparison. Urea concentrations were initially measured within the normal clinical range between 10 mg mL^{-1} and 150 mg mL^{-1} to establish a standard linear regression from which unknown samples could be calculated.

The spectrophotometer method was initially completed from following and developing the reaction and method described by Jung *et al.*¹³² which created a linear increase proportional to the increasing concentration of urea, (figure 5.1) which clearly showed there were small errors associated with this method, $R^2 = 0.9903$. Figure 5.1 was constructed using all steps outlined steps within the method, including the incubation period of 30 min at 37°C prior to reading any measurements.¹³²

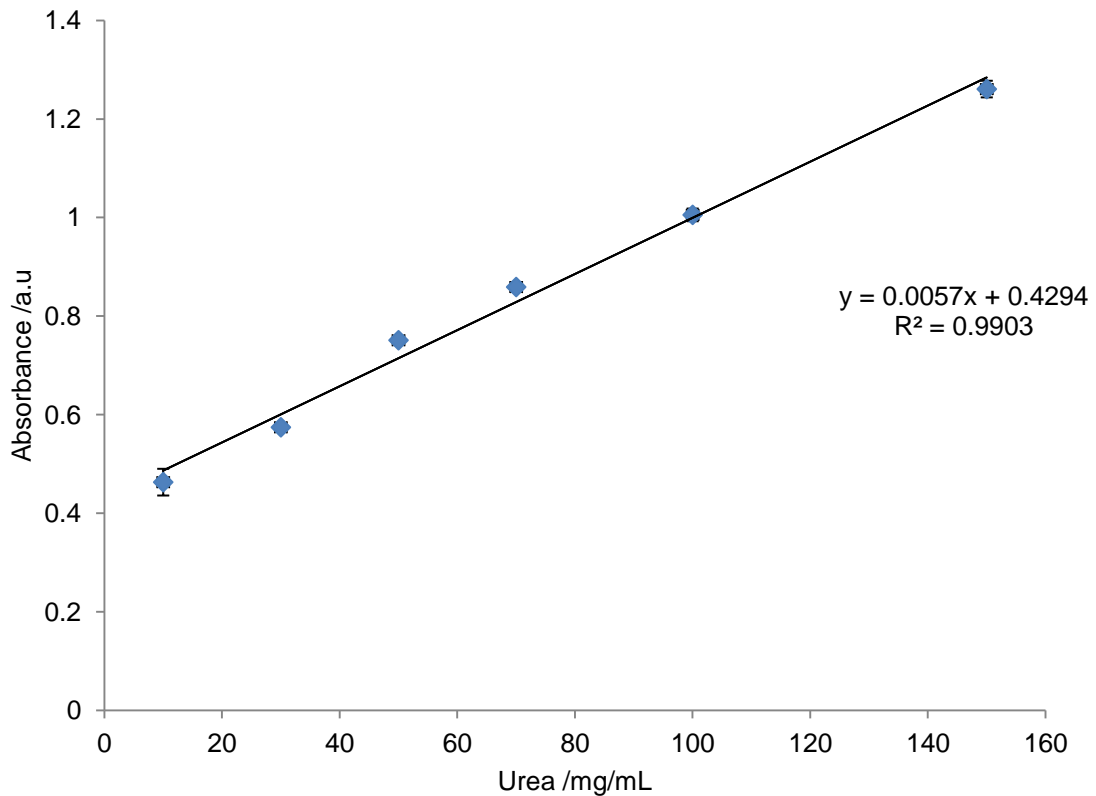


Figure 5.2: Standard concentrations for urea detection, n=10. Urea was measured spectrophotometrically at 505 nm at concentrations within the clinical range (10 and 150 mg). $R=0.9903$.

However, the incubation period of 30 min at 37°C outlined in the original method prior to reading any measurements could prove to be problematic when adapting this method for use on a paper based platform for a possible POC device. This is due to the requirement of sample preparation and more specifically the length of the incubation period required before a sample can be applied on to a possible POC device, inhibiting the overall desire for a fast result on a POC device.

Experiments were completed to understand if the incubation period time frame was a requirement or if the incubation period time frame could be reduced or removed from the method. It was also deduced if the method had to be completed at 37°C or if room temperature would suffice.

Figure 5.2A shows the method completed with 30 min incubation at 37°C versus figure 5.2B of 30 min incubation period at room temperature, (21 - 24°C). Statistical analysis of the linear gradient in both graphs shows no significant difference, $P= 0.135$ therefore allowing future experiments to use an incubation period at room temperature and thereby eliminating the requirement of a water bath or heater. However, it was noted that the absorption of urea spectrophotometrically is decreased when the samples are not incubated at 37°C but the linearity of increasing concentrations is maintained, e.g. $150 \text{ mg mL}^{-1} = 0.9 \text{ au}$ versus 0.5 au .

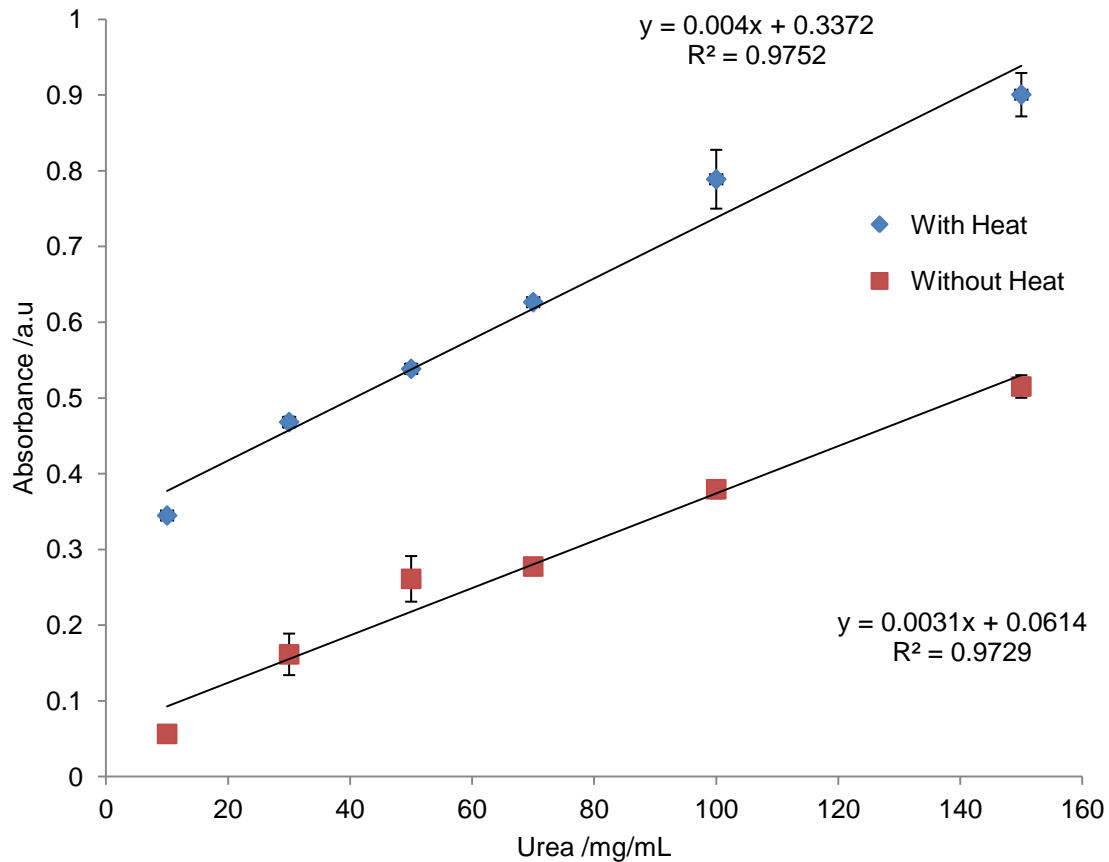


Figure 5.3: Absorption of urea when incubated at room temperature versus 37°C, n=10.

With Heat: Incubated at 37°C for 30 min ($R^2 = 0.9752$). **Without Heat:** Incubated at room temperature for 30 min, ($R^2 = 0.9729$).

Once determined the reaction of urea with NED and *o*-phthalaldehyde still occurred at room temperature, it was investigated to determine if the incubation period length could be shortened, (table 5.1) making this adapted method more suited as a POC test through a more instantaneous result. The incubation time was reduced by 5 min before reading the results spectrophotometrically and the R^2 value of each completed analysis compared via a paired Students t-test to establish any statistical differences in the data.

Table 5.1: Reduction of incubation time frame at room temperature, n=10

Time (min)	Linear Curve /R² value	P value (Paired Students T-test)
30	0.9981	0.236
25	0.9973	0.195
20	0.9939	0.102
15	0.9929	0.099
10	0.9443	0.068
5	0.9328	0.048

The colour change which occurred with the reduction of incubation period was observable with increasing concentrations from colourless to red/orange until 5 min were the colour change did not occur. Therefore, the optimum time frame incubation period at room temperature was at 15 min when the colour change was obvious and the R² value was not significantly different from the 30 min value as this would maintain an easy identification marker of the test for the user/patient to see were their urea levels when compared to the known standard concentrations, (figure 5.3).

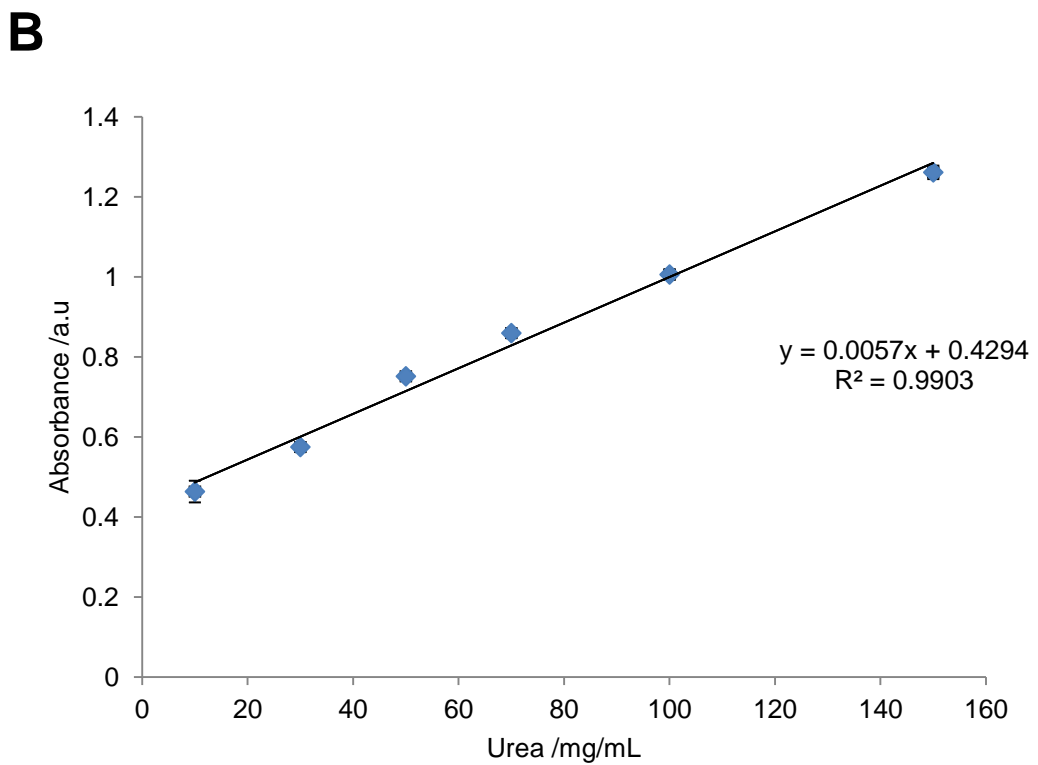
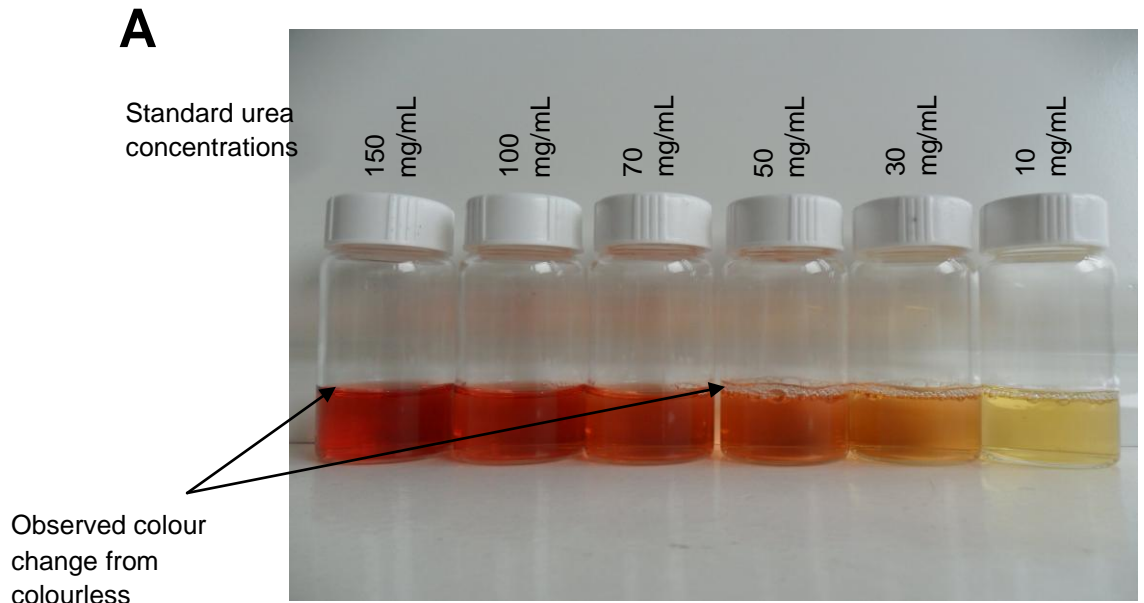


Figure 5.4: Standard urea concentrations of adapted method, n=10.

Panel A: Observed colour change of urea at the standard concentrations (10 mg-150 mg). **Panel B:** Analysis of standard urea concentrations, $R^2 = 0.9903$.

5.2 Measuring Urea using a paper device

5.2.1 Optimisation

Once it was established within the laboratory that accurate results could be achieved through the developed method spectrophotometrically, investigations began into whether the same reproducible results could be achieved using a paper device. The initial concept was to create channels into filter paper via photolithography (as in the previous chapters three and four for iron detection), but it was quickly established that the chemicals used in this colourimetric assay were not compatible with the photoresist. The sulphuric acid used in the NED reagent and *o*-phthalaldehyde quickly dissolved the hydrophobic barrier and spread through the entire paper regardless of any channel construction or hydrophobic barriers.

To prevent this, untreated filter paper was cut to size in thin strips (1 cm x 6 cm) and used as a dip stick assay instead. Aliquots of known urea samples could be prepared and the reagents required for the reaction to detect urea concentrations (via a colour change from colourless to orange/red through the NED reagent and *o*-phthalaldehyde) could be dried onto the paper device before application of the urea sample. If successful, to use this paper device as a POC device, it could be protected by an outer casing of plastic in much the same way as a home pregnancy kit, so the user/patient does not come into physical contact with the chemicals, figure 5.4.

Initial experiments used a three dimensional paper device constructed from filter paper, with a bottom layer cut into long thin strips (1 cm x 6 cm) and a top layer (detection zone) cut into a small rectangle (1 cm x 2 cm) which was

placed half way along. The top layer would contain the dried reagents (NED and o-phthalaldehyde) with the bottom layer providing a mode of transport for the urea sample to wick along to the detection zone. This would also prevent any contamination of the device and to ensure the area of the colour measured via ImageJ was consistently the same and to allow for a white background for analysis.

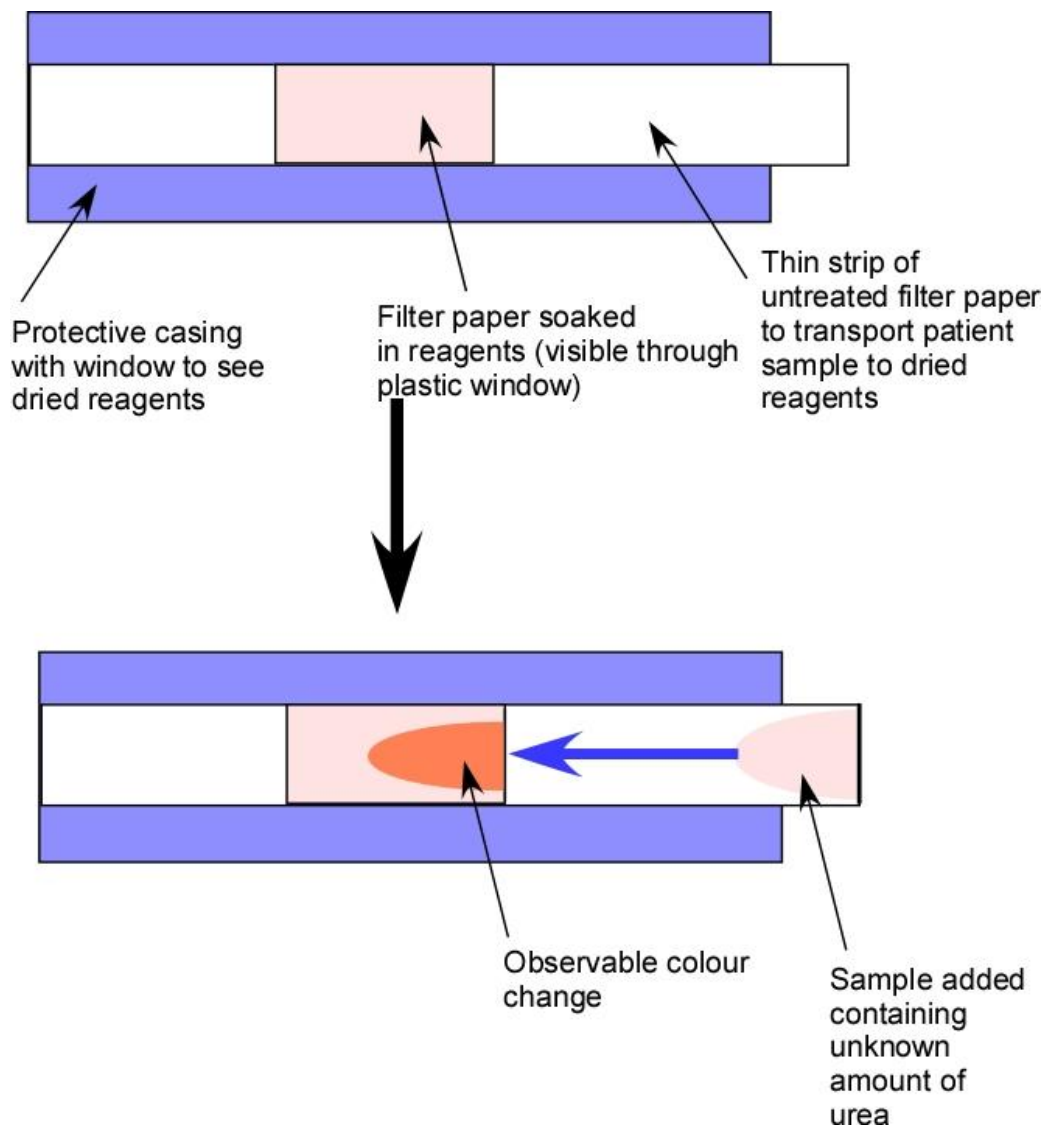


Figure 5.5: Schematic diagram illustrating paper device for urea detection. *First generation design of urea device which would protect user from contact with any chemicals.*

However, the resulting colour change which was easy to see in figure 5.3A was difficult to visualise regardless of concentration of chemicals, in what order the chemicals were applied to paper and how much of the chemicals were added to the paper device. Images taken of the paper devices and analysed via ImageJ could detect no differences in the signal intensities or integrated densities (red, green and blue light) for the varying concentrations of urea.

Experiments further investigated using the reagents when still wet on the paper device immediately after application and once the chemicals had been dried to establish if any colour change could be observed, table 5.2. ImageJ analysis could not detect any differences in the signal intensities of the paper devices from dry filter paper which had not been treated with chemicals from those which had.

Results concluded that the colour change from colourless to red/orange which is seen clearly in figure 5.3A is lost on the paper device or is very faint and not very clear for the user as shown in figure 5.5. The apparent reason for this remains unclear, but it is thought the paper matrix inhibits the condensation reaction between *o*-phthalaldehyde and urea in the presence of NED reagent.

Table 5.2: Varying chemical applications tested for urea detection on the paper device.

Applied 1st	Applied 2nd	Applied 3rd
1 mL <i>o</i> -phthalaldehyde (200 mg L ⁻¹)	1 mL NED reagent (431 mg L ⁻¹)	1 mL Urea (Standard Concentration)
1 mL <i>o</i> -phthalaldehyde (200 mg L ⁻¹)	1 mL Urea (Standard Concentration)	1 mL NED reagent (431 mg L ⁻¹)
1 mL NED reagent (431 mg L ⁻¹)	1 mL <i>o</i> -phthalaldehyde (200 mg L ⁻¹)	1 mL Urea (Standard Concentration)
1 mL NED reagent (431 mg L ⁻¹)	1 mL Urea (Standard Concentration)	1 mL <i>o</i> -phthalaldehyde (200 mg L ⁻¹)
1 mL Urea (Standard Concentration)	1 mL <i>o</i> -phthalaldehyde (200 mg L ⁻¹)	1 mL NED reagent (431 mg L ⁻¹)
1 mL Urea (Standard Concentration)	1 mL <i>o</i> -phthalaldehyde (200 mg L ⁻¹)	1 mL <i>o</i> -phthalaldehyde (200 mg L ⁻¹)

Standard concentrations of urea included 150, 100, 70, 50, 30 and 10 mg mL⁻¹

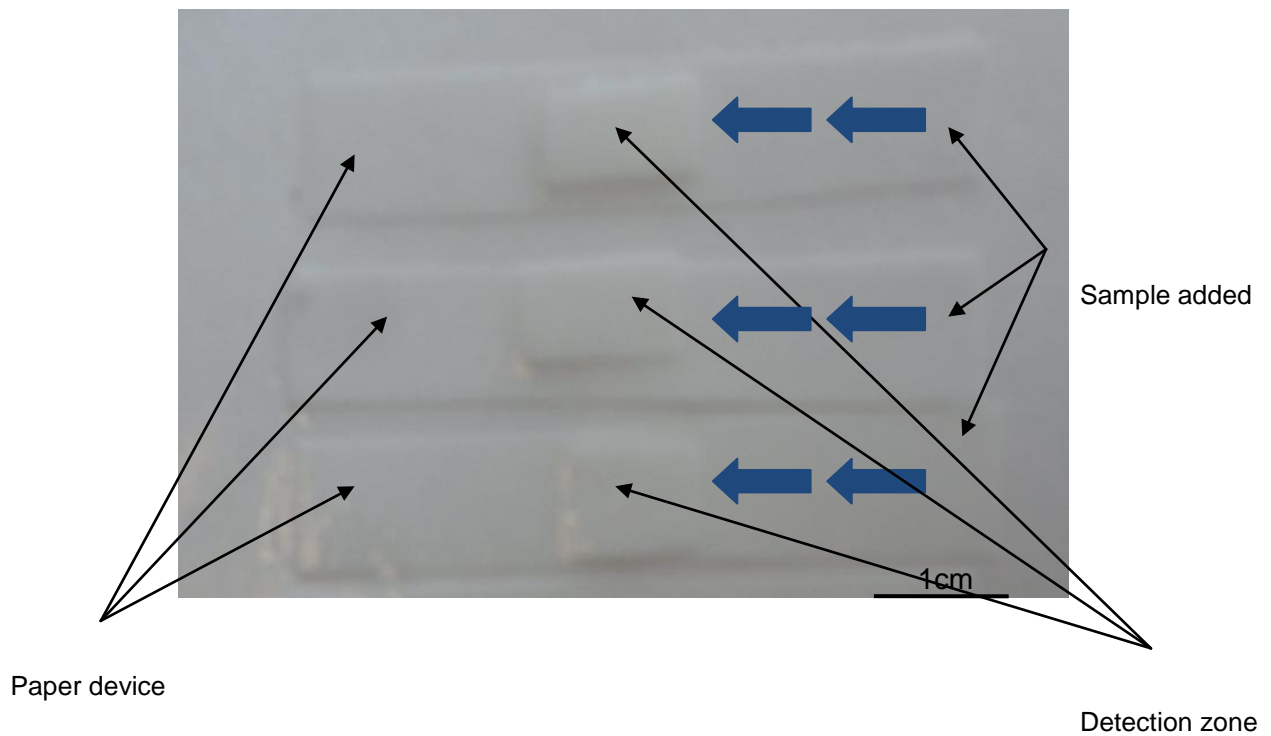


Figure 5.6: Urea concentrations on filter paper previously soaked in the reagents. *No colour change was observed on the paper device regardless of concentrations or order of application.*

Repeated experiments on paper devices failed to develop a colour, therefore it could not be quantified using ImageJ. However, in the higher ranges of the clinical samples, (150 mg mL^{-1}) a faint pink colour was observed, (figure 5.7). This enabled the experiments to be focused on using the paper device as a simple yes/no answer. If a sample contained $\geq 150 \text{ mg mL}^{-1}$ of urea a colour change was observed, if the sample contained $< 150 \text{ mg mL}^{-1}$ no colour change was seen. Thereby the user could make the assumption that if no colour change was observed on the paper device then the urea concentration was within the normal clinical range, the urea value was $< 150 \text{ mg mL}^{-1}$, and if a colour change was observed then the patient's urea levels

were in the higher ranges of the clinical norm ($> 150 \text{ mg mL}^{-1}$), further diagnostic tests would be required.

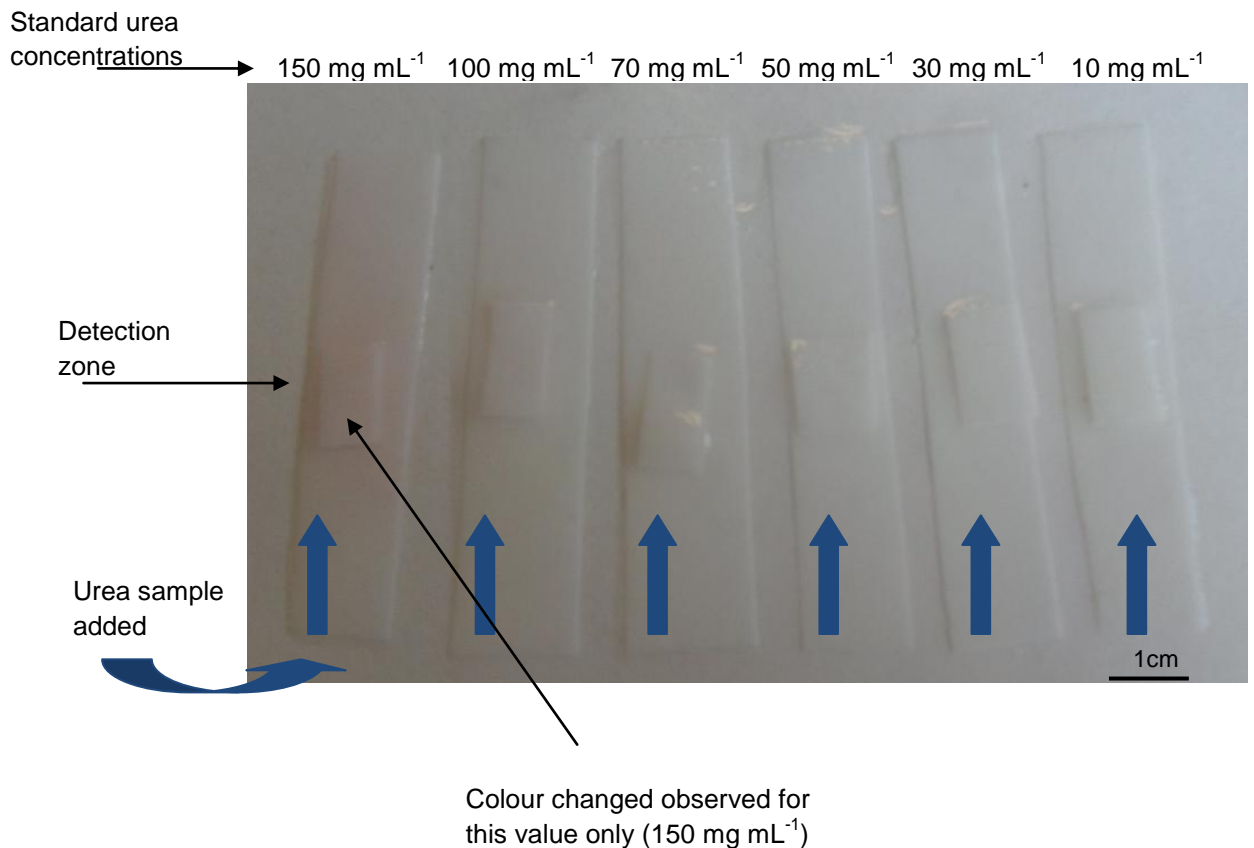


Figure 5.7: Urea detection on a paper device.
The red/orange colour change from colourless is observed only in the 150 mg mL⁻¹ concentration of the urea standards within the normal clinical range.

Once it was established that the colour change only occurred at the concentration of 150 mg mL^{-1} of urea or greater and that this was a repeatable observation using the standard urea concentrations, then reproducibility was required when using patient serum samples, table 5.3. The signal could be improved in future research by decreasing the reagent detection zone and concentrate the sample into a smaller area and thereby increasing the concentration of the sample.

Table 5.3: Comparison of patient results.

Patient	Paper Device (mg mL ⁻¹)	Pathology Results (mg mL ⁻¹)	Agreement
A	> 150	169 ± 0.6%	YES
B	< 150	55 ± 0.6%	YES
C	< 150	29 ± 0.6%	YES
D	< 150	48 ± 0.6%	YES
E	> 150	156 ± 0.6%	YES
F	> 150	170 ± 0.6%	YES
G	< 150	36 ± 0.6%	YES
H	< 150	51 ± 0.6%	YES
I	> 150	159 ± 0.6%	YES
J	> 150	157 ± 0.6%	YES
K	> 150	161 ± 0.6%	YES
J	< 150	167 ± 0.6%	YES
L	> 150	180 ± 0.6%	YES
M	> 150	171 ± 0.6%	YES

Hospital results compared to paper device results (n=10) Agreement states YES = colour observed for samples > 150 mg mL⁻¹ and no colour observed in samples < 150 mg mL⁻¹.

A paired Students t-test and f-test (table 5.4) showed there was no statistical variance or difference, ($P=0.24$) within the results received from the hospital pathology laboratory and the results observed on the paper device. Thereby providing evidence that the paper device can be used to determine whether a patient has an increased urea concentration in serum samples with a positive or negative result.

Table 5.4: Statistical analysis of results from table 5.3, $n=11$, $P= 0.24$.

	Paper Device	Path Lab
Mean	108.3	81.8
Variance	3876.2	6136.4
Observations	11	11
df	10	10
F	0.6	
P(F<=f) one-tail	0.2	
F Critical one-tail	0.3	

Highlighted in bold illustrates no significant difference between results

5.3 Discussion

The development of this assay was to allow patients to monitor or determine the level of urea present in their serum sample away from the laboratory setting without the requirement of a trained user for the device. However, it was established that the colour change required from this method was not sensitive to detect the lower levels of urea within the clinical range as the colour change could not be observed in the filter paper. Therefore this assay was developed for patients to determine semi-quantitatively if their urea concentration within serum was within the normal clinical range.

The initial method was taken from Jung *et al.*¹³² and developed for use on filter paper to measure the colour change of this reaction in concentrations $\geq 150 \text{ mg mL}^{-1}$. The removal of the incubation step from the process at 37°C for 30 min to incubating the samples for 15 min at room temperature for both the conventional spectrophotometer assay and the paper device assay allowed for less preparation work to be completed to the sample before application onto the paper device and before any measurements were made using the device. Thereby allowing for a faster result which is ideal for a POC device whilst simultaneously scaling down the method into a microfluidic application.

Current methods available for the detection of urea are mainly dominated by the urease-catalysed hydrolysis, colourimetric methods or electrochemical detection methods, all of which require analytical instrumentation and trained users, which are not desirable for a POC device.^{231,232} A publication by Hu *et al.*²³¹ Detected urea in urine samples via chemiluminescence and has been

suggested that the light producing pathway is selective to urea but the mechanism behind this has not yet been found.²³¹ Further improvements could be made to his method as whilst the method could be scaled down into a possible POC device, chemiluminescence is not always desirable as the method would still require an external reader or black box to omit sunlight. Therefore the aim of this project was to create a user friendly POC device.

A dipstick assay was originally proposed for the urea colourimetric assay, similar to the concept used for the home testing pregnancy kit.²³³ The paper device would use filter paper cut to size as a thin strip, providing mobility to a serum sample (applied at the end of the strip) which would wick along to a small square of filter paper cut and placed on top of the bottom layer, which would contain the previously dried reagents (NED reagent and o-phthalaldehyde) to react with urea to form a coloured product which would be visualised in the top layer (detection zone) of the paper device.

This would also allow the device to be protected by a plastic casing with a window (surrounding the detection zone) for the patient to see the resulting colour change from colourless to red/orange. However, when trying to put this method on to the filter paper device the colour was lost and after 1 h the solutions would turn the filter paper a yellow/brown colour and start to disintegrate due to the sulphuric acid in the NED reagent corroding the filter paper, regardless of order the solutions were applied to the filter paper, concentration or whether the solutions were allowed to react with urea whilst still wet on the paper device or had been allowed to air dry.

Experiments failed to establish a method of applying the solutions to the filter paper and to detect urea within the clinical range in either standard solutions of urea or human serum samples. Further investigations revealed that only concentrations of urea $\geq 150 \text{ mg mL}^{-1}$ would react with the NED reagent and *o*-phthalaldehyde to produce a coloured complex, independent of which order the solutions were applied to the paper device. The urea sample containing $\geq 150 \text{ mg mL}^{-1}$ would always react with the NED reagent and *o*-phthalaldehyde whilst still wet on the paper or had been allowed to air dry and no matter what order they had been applied to the paper device. From this point, experiments were concentrated on developing the assay as a simple semi-quantitative method to allow the user a simple yes/no answer in regards to urea concentration.

When compared with hospital pathology laboratory results the repeated results seen from the paper devices were accurate in their confirmation on the visualisation of a red/orange coloured product, only seen when the serum sample contained $\geq 150 \text{ mg mL}^{-1}$ of urea. If the urea concentration was below the threshold of 150 mg mL^{-1} no coloured complex could be visualised. Although ImageJ was attempted to analyse the devices to provide a more accurate concentration value, this proved an inaccurate representation of the results visualised on the paper device because the coloured complex could only be seen at $\geq 150 \text{ mg mL}^{-1}$ it was deemed that this test would be more useful for POC visual eye test device.

This test would provide an accurate result to a patient of their urea content in their serum samples through a simple yes or no result which is easily

observable by eye, providing a POC device that could be used in the developed world, where kidney failure is most problematic. This POC device would be used in a field setting away from the laboratory as an aid in helping to find a diagnosis for renal function on a faster time scale than current analysis of urea levels.^{170,183,188}

The device requires no computer for analysis and maintains a cheap and easy to use design with a yes or no result. If a “no” result is seen then the patient need take no further action and if a “yes” result is observed then a doctor could be contacted for further follow up. When compared to current methods of diagnosis in renal function, a patient has to see a doctor first and then be seen by a specialist, with current waiting lists on the NHS been from anywhere of three to four weeks²³⁴ this POC device would provide a solution in reducing these waiting times, and a faster prognosis makes a better diagnosis.^{166-168,183}

Chapter 6: Colourimetric Detection of Creatinine

This chapter will aim to show the results and discuss a POC device developed using the Jaffe reaction on Whatman no.1 filter paper as a dipstick assay to detect creatinine levels in human serum samples. Creatinine is a marker for determining renal function in a patient as an early diagnosis marker, it is a waste product produced by muscles and removed from the bloodstream via the kidneys.^{185,235,236} If the kidneys are malfunctioning creatinine levels elevate, alongside urea levels.^{208,235} Therefore, making this analyte an accurate and early marker for kidney function tests.²⁰⁸

There is a much needed requirement to able to assess renal function and status in patients before ESRD is reached, as for many patients there is no cure, only lifelong treatment via dialysis or organ transplant.^{174,237} This is due to the kidneys not been a responsive organ, capable of functioning at 10% however unable to regenerate past this point.²³⁸ To approach this area, a POC device would aid patients who suffer from chronic kidney failure to monitor their renal function without having to travel or been seen by a doctor/specialist every few weeks, allowing the patient to be more independent and lead a better quality of life.^{41,42}

The paper device was designed to incorporate creatinine standard samples of a known concentration within the clinical normal range of 5 mg mL⁻¹ and 25 mg mL⁻¹²³⁹ and an unknown sample run alongside, quantified using ImageJ

and determining the presence or absence of renal failure in a patient. The performance of the system was then assessed by comparison with standard methods performed both at the internal and clinical level.

6.1 Conventional Measurement of Creatinine

The gold standard method for the measurement of creatinine in human serum samples is the Jaffe reaction where picric acid reacts and forms a tautomer with a creatinine molecule in an alkaline solution to produce an orange coloured complex, (Janovski complex).^{133,134} The conventional method uses a spectrophotometer at 520 nm to measure the coloured Janovski complex which is proportional to the amount of creatinine present in the sample. Creatinine was initially measured through following the reaction and method outlined by Liu *et al.*¹³⁶ thereby, creating a linear increase of increasing concentrations of creatinine, (of which was expected), and detecting creatinine in the clinical range via a spectrophotometer, figure 6.1. In figure 6.1 it is clearly seen there are small error margins (SEM between 0.009 and 0.124 mg mL⁻¹) for a linear increase of absorption for increasing concentrations of creatinine at 520 nm, which would allow unknown concentrations of creatinine within the clinical range (5 – 25 mg mL⁻¹) to be accurately determined from the linear regression as was used for the iron(II) determination in human serum samples, chapter 4.

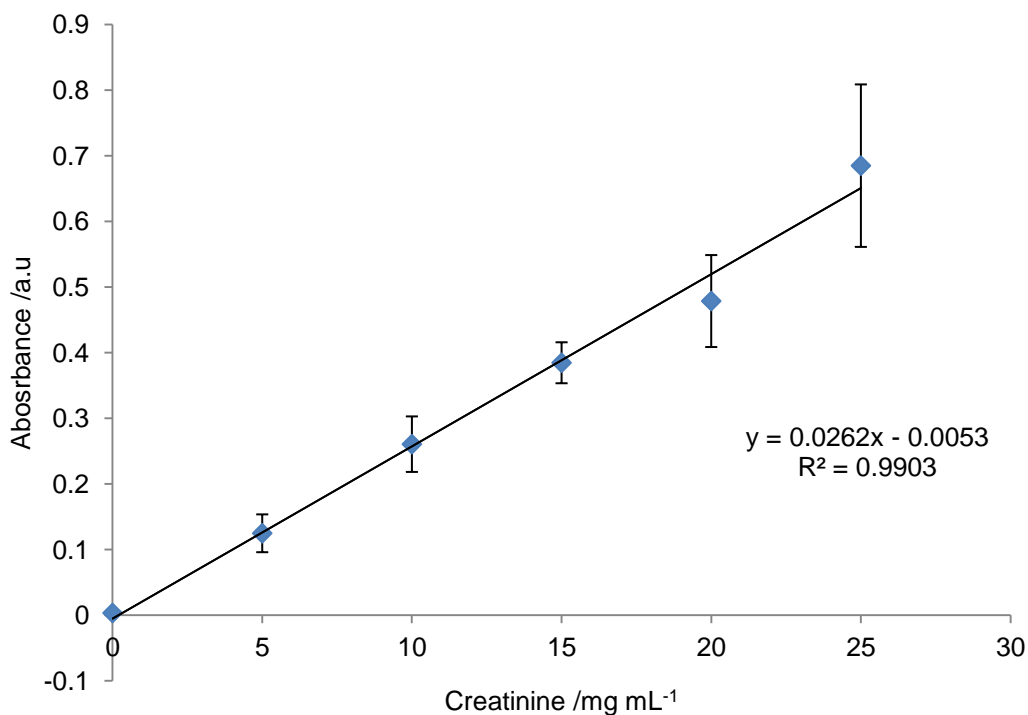


Figure 6.1: Creatinine concentration within the clinical range, $n=10$. Clinical range = $5 - 25 \text{ mg mL}^{-1}$, measured via a spectrophotometer at 520 nm , ($R^2=0.9903$).

6.2 Creatinine Detection using a Paper Based Method

As the gold standard method and corresponding results for creatinine detection within the normal clinical range using standard solutions was determined an accurate representation of measurement, it was investigated whether this experiment could be reliably reproduced using a paper format.

Initial experiments investigated the assay on squares of filter paper cut to size ($2 \text{ cm} \times 2 \text{ cm}$) and the picric acid in alkaline solution pipetted onto the square before the addition of the creatinine containing solution. However, similar to the initial iron(II) assay using 1,10-phenanthroline a chromatographic effect was visible and a “ring” around the edges of the solutions was visible as illustrated in figure 6.2. This was thought to be due to

the filter paper having a large surface area and not constricting the solutions applied to the filter paper to a channel or particular “detection zone” as in the previous two chapters.

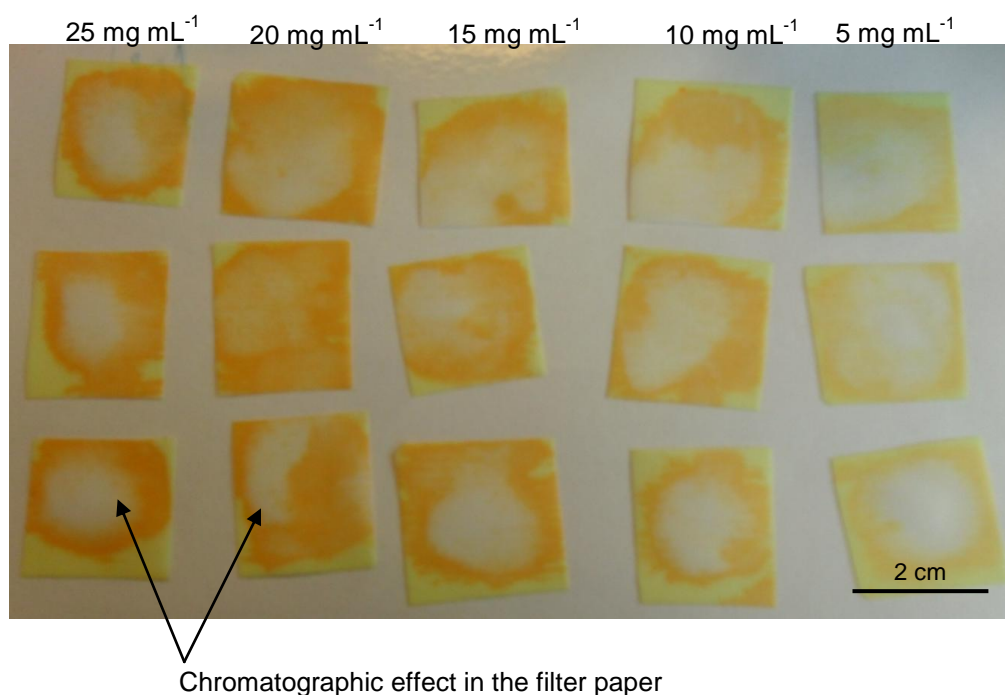
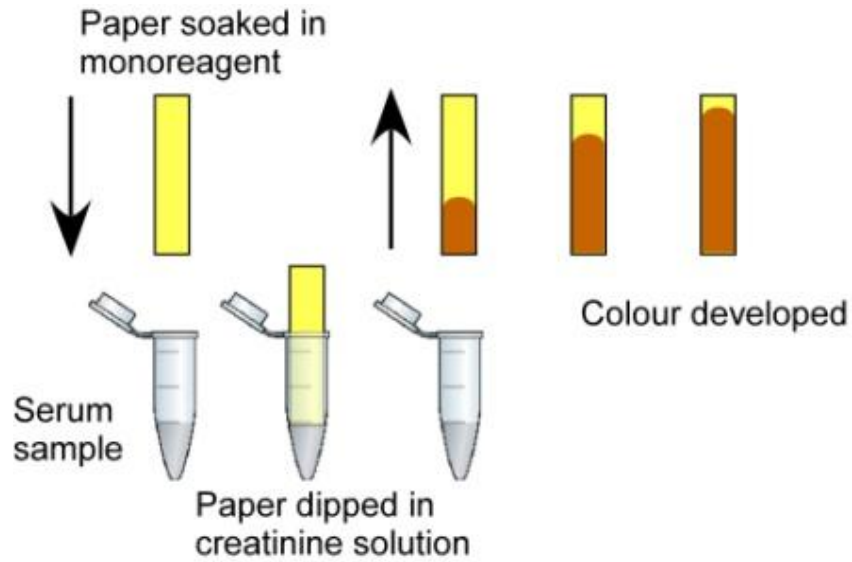


Figure 6.2: Jaffe Reaction on filter paper illustrating the chromatographic effect (n=3).

The paper device was further developed to a dip stick assay, which allowed the solutions to travel along a thin length of paper cut to size (1 cm x 5 cm) in a more constricted manner as the solutions would be wicking in one direction only, thereby giving a more accurate representation and analysis of the consequent colour change from yellow to orange. This was due to the colour change occurring from the bottom of the device upwards in one direction as opposed to in every direction when the solutions were applied centrally.

It was noted that the use of picric acid (20 mmol) could be mixed in the alkaline solution (NaOH, 0.2 mol L⁻¹) mixed in the ratio 1:4 for storage before application on to the filter paper, reducing the pre-treatment preparation (preparation of a sample before been applied onto the paper device, such as incubation or mixing of reagents etc). This is also because the picric acid is a derivative of trinitrotoluene (TNT) and by further dilution it is less explosive, (already diluted to 13% before use). The mixed solution could then be pipetted onto the bottom edge of the filter paper or held and dipped immediately into either the standard solutions or serum solutions and the colour change observed within 5 min. The solution would have to remain wet on the filter paper for the application of a serum sample due to the flammable risk associated with this picric acid and alkaline solution when it is allowed to dry.

Initial results in figure 6.3 demonstrate the Jaffe reaction method was feasible when constricting the solution to a smaller surface area, and allowing the solution to wick along a length of filter in one direction only as an orange colour was developed after 5 min of administration of the sample with no chromatography effect. Nevertheless, as the solutions dried on the filter paper the colour change was slowly lost, but this did not affect the results or the analysis as the image could be photographed and correctly analysed before this occurred. The resulting assay was photographed and analysed via ImageJ as previously described in chapter 2.2 as shown in figure 6.4.



Schematic diagram for use of dipstick assay

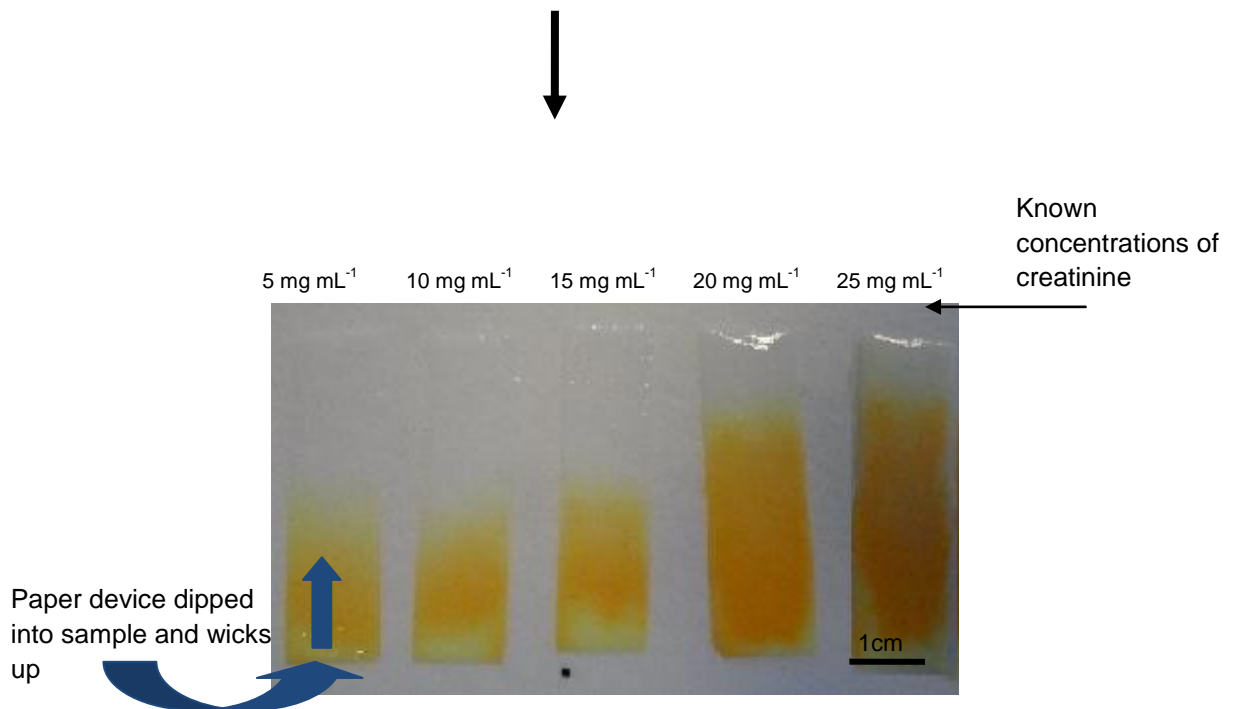


Figure 6.3: Preliminary creatinine assay using a paper device as a dipstick assay. Using standard concentrations within the clinical range (5–25 mg mL⁻¹), n=1.

However, the Jaffe reaction required an incubation period of 5 – 10 min to develop a colour change from yellow to orange when using the paper device as the colour change occurs more slowly when compared with the spectrophotometer method which is an immediate colour development. This was thought to be due to the solutions having to diffuse through the paper matrix, slowing down the reaction time between picric acid and creatinine as opposed to the solutions been in a cuvette or eppendorf where diffusion in liquid is faster. Therefore, the analysis in figure 6.4 was an inaccurate representation of creatinine level as the colour change continued to develop for 10 min after the image had been photographed. Further experiments would be required to determine an accurate time frame for this incubation period to allow for a more accurate analysis to be performed (this could also improve the R^2 value in the analysis of figure 6.4).

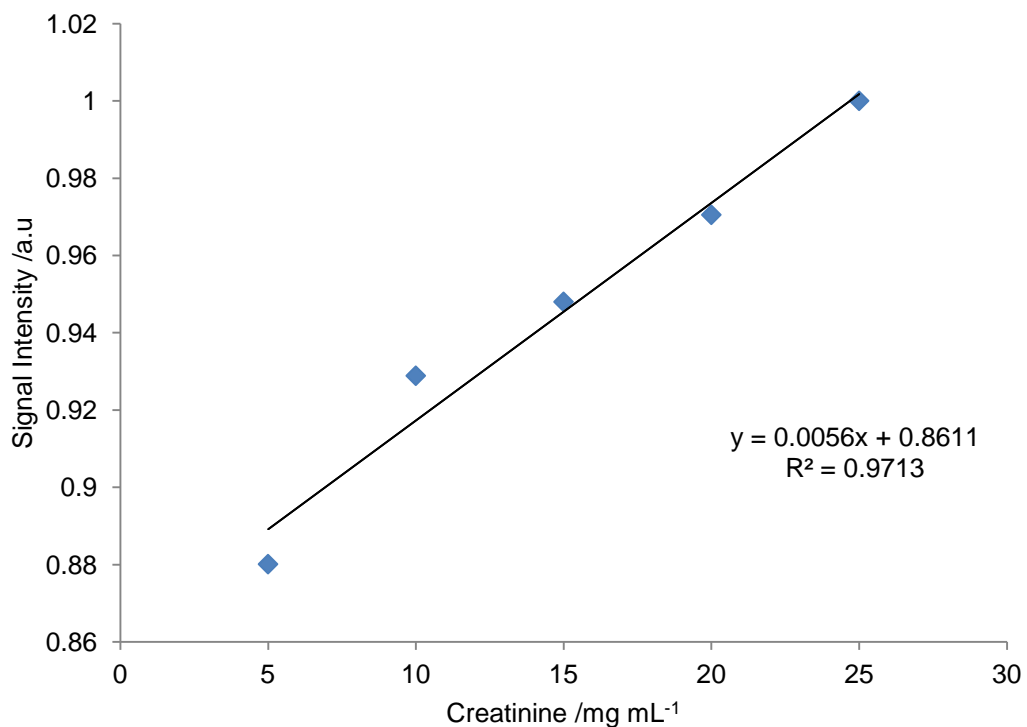


Figure 6.4: Analysis of paper based assay for creatinine standard concentrations, $n=1$, $R^2 = 0.9713$.

Experiments were carried out to detect the optimum time frame required for the correct analysis for the colour change observed in the Jaffe reaction when completed on filter paper. The method used for the spectrophotometer readings required a no incubation period at room temperature as the reaction of creatinine with picric acid to create a tautomer occurred immediately, but when adapting this method for use with filter paper, the paper matrix slowed this reaction down by inhibiting the mixing of the picric acid with the creatinine.

Therefore, the time was measured to determine how long the reaction would require to take place for the coloured tautomer between picric acid and creatinine to be fully developed and how long before the colour was lost which was caused by the drying out of the reagents. It was shown that the incubation period required was 10 min for the colour to fully develop in the paper device but after 25 min the colour began to degrade as the picric acid dried causing the reactivity to be lost. Thereby, the following analysis is an example of results received by a 10 min incubation period, figure 6.5. This was also adequate time left over for the analysis to be completed and repeated if necessary before the colour degradation occurred.

Once experiments had determined this method was feasible on a paper device, experiments into the use of artificial serum samples from Randox (supplier of artificial serum sample) were investigated for use on the paper device. The known amount of creatinine was supplied with the paperwork for each artificial serum sample along with the error associated with each sample, table 6.1. This would allow the determination of any interference

which could be caused by the presence of other analytes such as glucose and bilirubin when using the Jaffe reaction to determine creatinine level in serum samples.^{135,192}

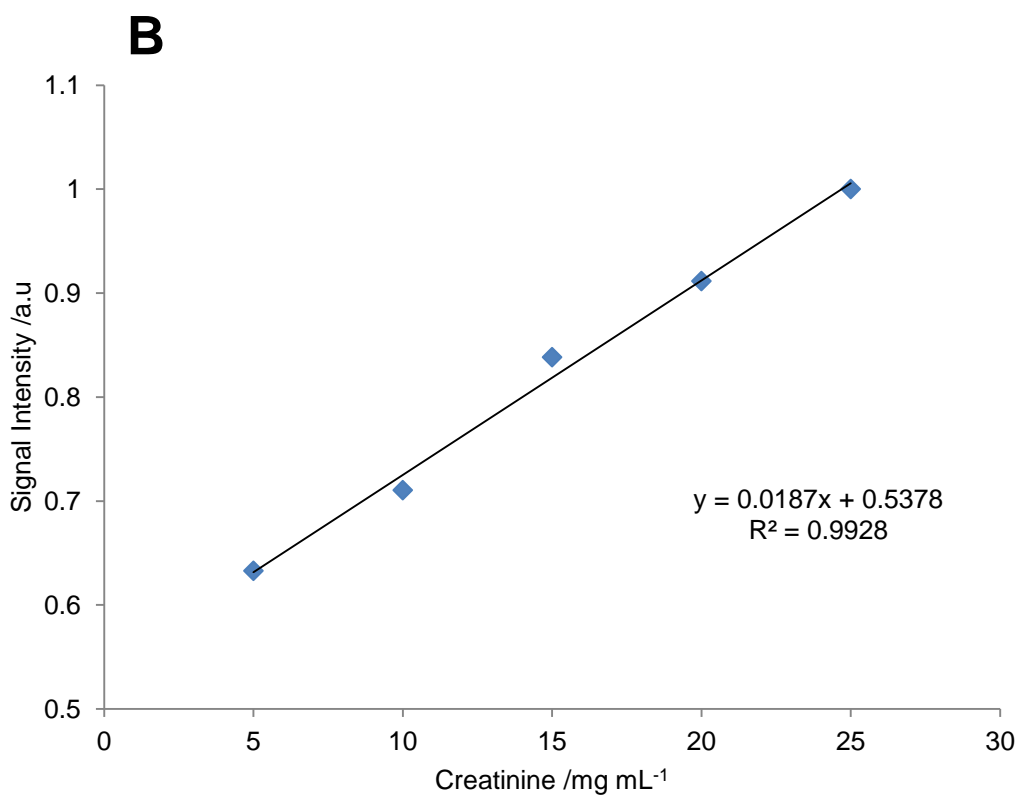
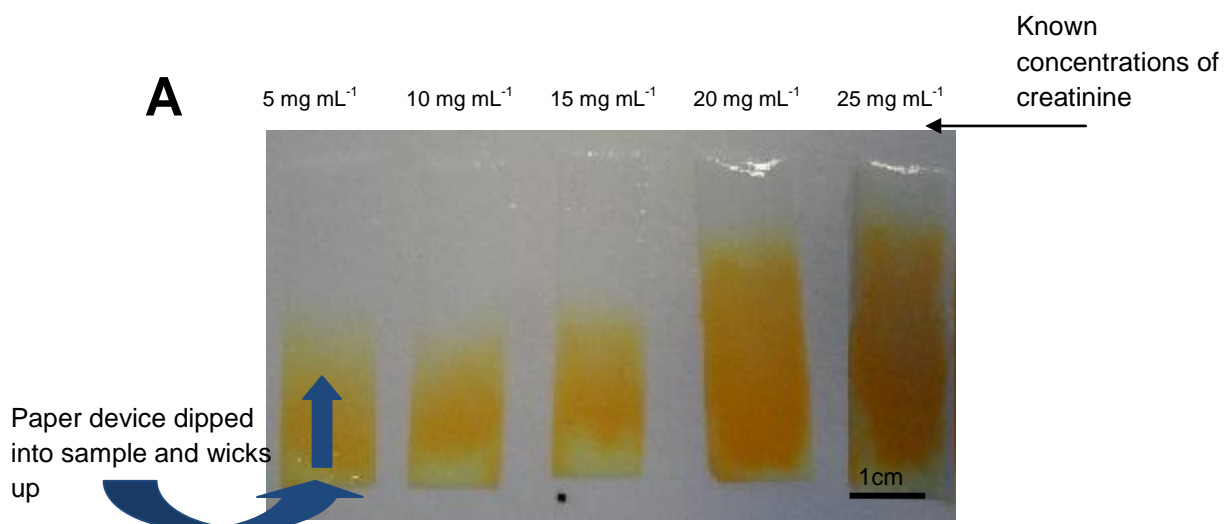


Figure 6.5: Analysis of creatinine standard concentrations using a paper device, n=1.

Panel A: Paper device with a constricted surface area (n=1), **Panel B:** Analysis of device, $R^2 = 0.9928$.

Table 6.1: Results of creatinine level when using the paper platform compared to artificial serum samples, n=10.

Sample	Paper Device (mg mL⁻¹)	Artificial Serum (mg mL⁻¹)
A	1.35 ± 1.8%	1.37 ± 0.6%
B	1.36 ± 1.1%	1.37 ± 0.6%
C	1.39 ± 1.5%	1.37 ± 0.6%
D	1.37 ± 1.9%	1.37 ± 0.6%
E	1.32 ± 1.5%	1.37 ± 0.6%
F	3.92 ± 1.1%	3.88 ± 1.1%
G	3.87 ± 1.2%	3.88 ± 1.1%
H	3.9 ± 1.3%	3.88 ± 1.1%
I	3.84 ± 1.8%	3.88 ± 1.1%
J	3.88 ± 1.7%	3.88 ± 1.1%

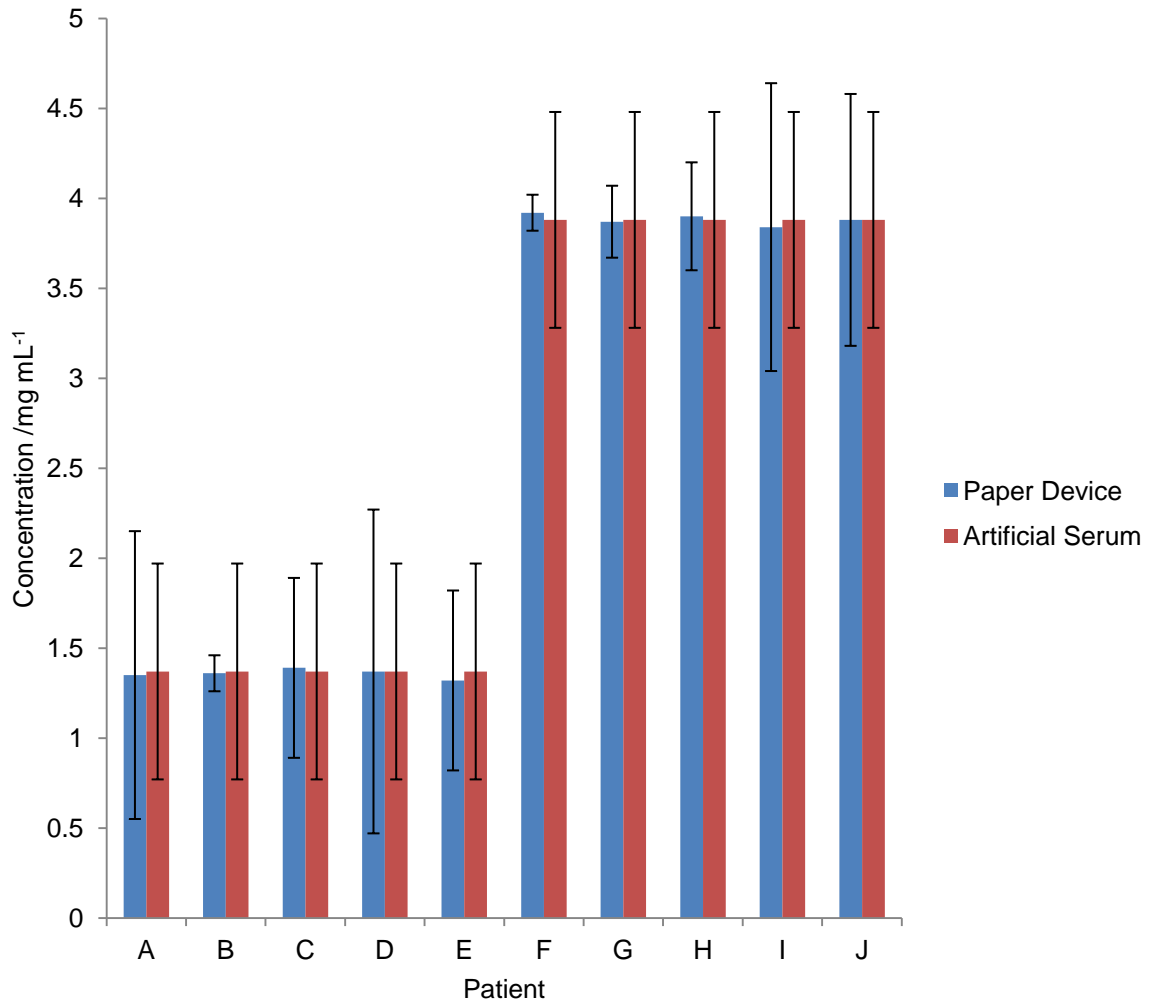


Figure 6.6: Comparison of results from paper platform and expected results in artificial serum, n=10 .
Results taken from table 6.1

Statistical analysis of the above results determined there were no significant difference ($P= 2.131$) between the results gained from the paper device when compared with the known amount of creatinine in the artificial serum sample. Tables 6.2 and 6.3 show the results received from a paired Students T-test and F-test respectively of the results for each sample, (n=10).

Table 6.2: Paired Students T-test illustrating no significant difference shown in table 6.1, $P = 2.131$.

A

	Paper	Artificial
Mean	3.9	3.9
Variance	0.00092	0
Observations	50	50
Pearson Correlation	-	
Hypothesized Mean Difference	0	
df	4	
t Stat	0.1	
P(T<=t) one-tail	0.4	
t Critical one-tail	2.1	
P(T<=t) two-tail	0.9	
t Critical two-tail	2.8	

B

	Paper	Artificial
Mean	1.4	1.37
Variance	0.00067	0
Observations	50	50
Pearson Correlation	-	
Hypothesized Mean Difference	0	
df	4	
t Stat	-1.036	
P(T<=t) one-tail	0.2	
t Critical one-tail	2.1	
P(T<=t) two-tail	0.4	
t Critical two-tail	2.8	

Highlighted in bold illustrates no significant difference within the results.

Panel A: Known artificial serum content of $1.37 \pm 0.6\%$, **Panel B:** Known artificial serum content of $3.88 \pm 0.6\%$.

Table 6.3: F-test illustrating no significant variances in the results shown in table 6.1.

A

	Paper	Artificial
Mean	1.358	1.37
Variance	0.00067	0
Observations	50	50
df	4	4
F	65535	
P(F<=f) one-tail	0.40	
F Critical one-tail	6.38	

B

	Paper	Artificial
Mean	3.882	3.88
Variance	0.00092	0
Observations	50	50
df	4	4
F	65535	
P(F<=f) one-tail	0.40	
F Critical one-tail	6.38	

Highlighted in bold illustrates no significant variances within the results.

Panel A: Known artificial serum content of $1.37 \pm 0.6\%$, **Panel B:** Known artificial serum content of $3.88 \pm 0.6\%$.

Investigations began into the use of human serum samples collected from the hospital. The results received from the paper device method were compared with the results read from the spectrophotometer as opposed to the hospital pathology laboratory, as they were unable to provide analysis for this set of data, table 6.4.

Table 6.4: Comparison of creatinine results from human serum samples using the paper device to the spectrophotometer method, n=10.

Patient	Paper Device (mg mL ⁻¹)	Spectrophotometer (mg mL ⁻¹)
A	10 ± 0.6%	11 ± 0.8%
B	18 ± 1.9%	18 ± 0.8%
C	15 ± 2%	15 ± 0.8%
D	23 ± 1.5%	23 ± 0.8%
E	9 ± 1.3%	9 ± 0.8%
F	20 ± 0.8%	20 ± 0.8%
G	15 ± 0.6%	16 ± 0.8%
H	18 ± 1.2%	18 ± 0.8%
I	17 ± 1.6%	18 ± 0.8%
J	16 ± 0.8%	16 ± 0.8%
K	6 ± 0.6%	6 ± 0.8%
L	10 ± 1.4%	11 ± 0.8%
M	14 ± 1.3%	14 ± 0.8%
N	17 ± 0.6%	18 ± 0.8%
O	23 ± 0.5%	24 ± 0.8%
P	20 ± 0.9%	20 ± 0.8%
Q	16 ± 1.8%	16 ± 0.8%
R	9 ± 1.6%	8 ± 0.8%
S	10 ± 1.2%	11 ± 0.8%
T	19 ± 2.1%	19 ± 0.8%

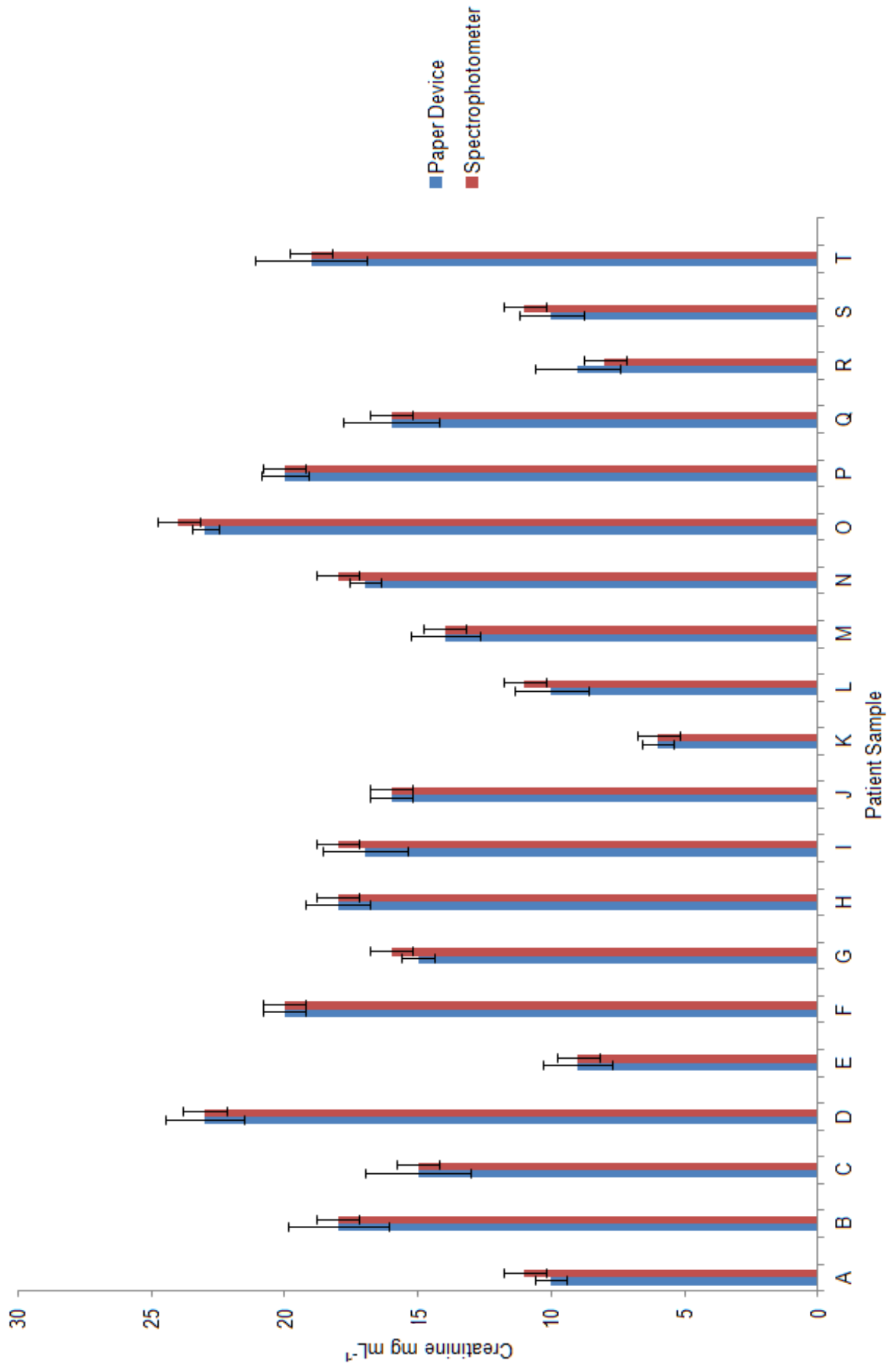


Figure 6. 6: Creatinine detection using paper device versus spectrophotometer

Table 6.5: Statistical analysis taken from figure 6.6 illustrating no significant differences within results.

	Paper Device	Spectrophotometer
Mean	15.25	15.55
Variance	23.67	24.15
Observations	20	20
df	19	19
F	0.98	
P(F<=f) one-tail	0.48	
F Critical one-tail	0.46	

Highlighted in bold illustrates no significant variance within the results

The statistical analysis supports the paper device as an alternative POC device for the measurement of creatinine in human serum samples when compared to the conventional method using a spectrophotometer (P=0.48). This successfully demonstrates the paper device as a dipstick assay when adapting the Jaffe reaction onto a paper matrix which can be used outside of the laboratory setting.

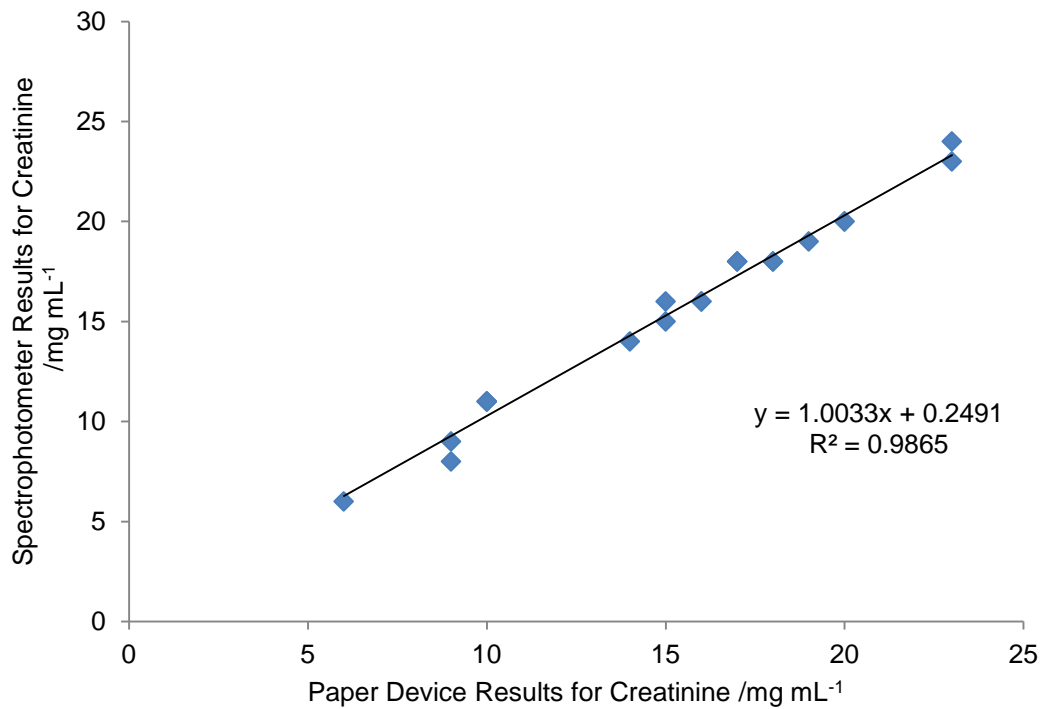


Figure 6. 7: Linear regression of results found using paper device vs. spectrophotometer.
Results taken from table 6.4 showing the correlation between the two methods for the measurement of creatinine in serum samples.

The linear regression observed in figure 6.7 supports the paper device as an accurate method to measure creatinine in human serum samples via a high correlation between the paper device results and the spectrophotometer results, $R^2=0.9865$. The intercept of figure 6.7 further illustrates no significance difference between the two methods, $P=0.83$.

6.3 Discussion

The initial creatinine assay used in this chapter was based on the principles of the Jaffe reaction, originally discovered and developed by Max Jaffe in 1886.^{38,133,135,240} However, this method has been adapted for use as a colourimetric assay on a paper platform, creating a simpler and more effective method for the diagnosis of renal function for patients. The dipstick assay can be performed by untrained personnel away from a clinical setting or laboratory. Optimally, this is a possible POC device which could be used worldwide as an aid to diagnosis renal failure in patients with suspected renal function problems and could be used alongside the urea assay on paper described in chapter 5. This device combines a much needed result within 5 min of receiving a serum sample whilst maintaining the accuracy associated with the Jaffe reaction and allowing for a correct analysis of that patients creatinine level in serum.

Unfortunately for this series of experiments hospital results were not available as this was not a test used on the patient samples we were able to attain from the hospital and therefore the serum samples received did not have a known amount of creatinine. Therefore, as the Jaffe reaction has been a well documented reaction in the literature and is known as a “gold standard” test for creatinine detection in serum when using a spectrophotometer, the serum samples analysed using the paper device could be compared with the analysis of the spectrophotometer.^{133,135,192,193} Repeated experiments (n=10) illustrated there was little error in the

spectrophotometer method data and it was deemed acceptable to use this as a comparison analysis for the paper device.

Once determined that the colour occurrence between picric acid and creatinine in an alkaline solution for this assay was measurable within the clinical range ($5 - 25 \text{ mg mL}^{-1}$) steps were taken to optimise the method for use on a paper device. Initially, the use of filter paper in this method increased the incubation period of 5 min (used in the spectrophotometer method) to 10 min on the paper device, which was due to the solutions having to travel through the cellulose matrix in the paper device which thereby caused the reaction between picric acid and creatinine to be slowed down. This also created issues with the application of solutions onto the paper device, initially the solutions were pipetted onto a square paper device however this created a chromatographic effect and the colour intensity was lost as the solutions were not confined by channels or in size. This led to the use of cutting the paper device into a long rectangle (1 cm x 5 cm) which decreased the surface area of the paper device and by dipping the paper device into the solutions (firstly into the picric acid and sodium hydroxide and then secondly into the standard solutions or serum sample) this confined the solutions to move in one direction only (up the device) and along the length of paper. Nevertheless, this theory decreased the chromatographic effect which was highly visible when the solutions were pipetted straight onto the paper which made analysis of the colour change highly difficult.

The picric acid is a derivative of Trinitrotoluene (TNT) had to be kept as a wet solution due to the high risk of an explosion when dry but this was a low risk

as the solution used was 13% before been further diluted when stored in an alkaline solution which created the reaction conditions required for the colourimetric detection of creatinine.

Experiments used artificial serum samples containing a pre-determined concentration of creatinine which were measured spectrophotometrically and when using the paper device. A paired student t-test and a variance f-test showed there was no significant difference ($P > 0.05$) within the results measured. This was also in agreement when using human serum samples on the paper device as the statistical analysis of the data showed there was no significant difference between the two methods (as shown through the use of a paired student t-test and f-test for variance, $P > 0.05$).

The problems which have been encountered in this chapter such as the chromatographic effect, incubation time and the application of samples onto the paper device have been eliminated or made to be manageable with the restrictions that this project aimed to achieve, such as a device been made portable and easy to use for on-trained personnel as current methods do not incorporate POC devices in the measurement of serum creatinine.

Current methods for the detection of creatinine have relied upon the Jaffe Reaction and a spectrophotometer, however attempts have been made to decrease the level of interference associated with this reaction. This has been through measuring the Jaffe reaction assay at both very alkaline pH, and after acidification to a more neutral pH as interfering substances react at neutral pH, and by difference a more accurate result could be obtained.²⁴¹

The most current research is focusing on establishing the glomerular filtration rate as a measurement of renal function and how efficiently waste products (such as urea and creatinine) are cleared.²⁴¹ This is completed by measuring exogenous products such as inulin but these methods are costly and require trained personnel. The clearance of endogenous substances, such as urea and creatinine, requires both serum and an accurately timed urine collection.²⁴¹ Therefore there is a large area of research in the measurement of creatinine and urea required for kidney failure to be diagnosed using a POC device.

Chapter 7: Discussion and Conclusion

Since microfluidics first came into existence, extensive research has been completed into the development of an alternative to the conventional laboratory methods of analysis and diagnosis that are currently employed.^{3,64,215,230,242} This is not only to be beneficial in the developed world but also for use in the developing world, where current diagnosis methods and medical treatments available are not good enough.^{2,31,58,154,243}

Encompassing the development of microfluidics are a few problems; the requirement to have a device deemed as easy to use and to be used “in the field,”²⁴⁴ which is a device cheap or at least cheaper to manufacture.^{56,64,65,75}

At the same time, this device has to be comparable to current methods which gives a result as accurate.^{230,245,246} Currently the technology is struggling to overcome these issues as outlined by Whitesides *et al.*⁶ who has stated that the technology remains in its infancy, and requires a great deal of work before it can become more active in the fields of academic research.⁶

The microfluidic devices that have been published have been manufactured mainly from glass, silicon, polymers and PDMS.^{3,230,242} However, the microfluidic platform receiving much interest in more recent years has been the adaptation of filter paper into a microfluidic device.^{9,56,75,90,116,154,161,245,247-}

²⁴⁹ Paper based microfluidics cover all these aspects which have proven to be problematic for other platforms as previously mentioned in chapter 1 e.g. no requirement for an external pumping force to transport reagents, inexpensive and easy to manufacture, easily disposable etc.^{22,45,64,250}

Conventional paper based tests have gained great success in POC diagnostics due to their simplicity, such as using simple methods and simple analysis techniques like in colourimetric assays and yes/no responses of detection. However, recent investigations have challenged to extend this theory and have started to use more elaborate and difficult techniques on paper, techniques which may require washing steps or antibody attachment i.e. PCR, CL, ELISA based assays, electrochemical detection or immunoassays to detect various analytes.^{9,23,90,100,247,248} An example of using electrochemical detection is described in the work by Carvalho *et al.*⁵⁴ where photolithography was used to make a gold electrochemical cell on a strip of polyester coupled to a strip of paper which chromatographically separated before quantifying uric acid and ascorbic acid.¹⁰⁰ Another example of electrochemical detection which incorporated paper into the device could make an accurate voltammetric measurement that was referenced by an electrode with a constant, well-defined potential.²⁵¹ The cost of the portable device was sufficiently low that it could be for single-use application, as the method of fabrication was wax printing.²⁵¹ However, drawbacks to both these methods are the voltammograms and electrochemical detection would require a trained user to be able to perform these methods.²⁵¹

Another example of creating more complex methods on a paper device was work published by Whitesides *et al.*⁹ who developed a paper based ELISA. A negative photoresist was used to create a layout similar to a 96 well plate, where antibodies were spotted onto the test zones and the colourimetric readout completed from the resulting image.⁹ However a drawback to this

method is the paper has to be suspended in air to prevent the samples in each test zone from mixing into each other.

Additionally, microfluidic devices have been developed to not only diagnose infections or diseases but to also aid in identification of various blood types.⁷³

This area is lacking in the ability to be able to identify blood groups quickly and accurately especially in low resource settings when a blood transfusion is required immediately for a patient whose blood group is unknown.²⁵²

Recent work has been published into this area using paper microfluidic devices which aims to identify which blood group a patient is by the agglutination or non-agglutination of samples dependent on which antigens are present in the sample (A, B, AB and O).^{73,253} This is a perfect example of a microfluidic device which encompasses the previous problems as it is quick, easy, and in-expensive which does not require any electrical power.^{73,74} This type of research is essential for use in the developing world and also in a military setting where blood typing is quick, simple and inexpensive.⁷³

There are many areas in which paper microfluidics could be used to allow medical tests to be carried out away from the laboratory setting in limited resource areas.^{2,32,45,58,154,210} Through aiming to encompass a similar approach as mentioned previously, where POC testing can be simplified and inexpensive but give the same consistent and reliable results as the conventional laboratory technique the work completed has been based around achieving this. The main niche that requires further research is to establish microfluidic devices that can incorporate a simple method and a

simple detection system to analyse analytes within a human sample giving an accurate diagnosis.^{32,45,58} The colourimetric assay method on a paper based microfluidic device is far easier to understand and analyse when optimising a device to be used away from a laboratory setting along with been inexpensive to use, which allows the idea of using the devices in the developing world as far more plausible.^{2,32,45,58} The aim of this project from the onset was to use the paper platform for a microfluidic device and to be able to measure analytes from the human body to make an accurate diagnosis of disease or infection within a patient.

The project has outlined colourimetric methods for the detection of iron(II), urea and creatinine in human serum samples using a paper based platform. The devices designed and used were inexpensive (< £1 per device) when compared with the conventional methods. They used fewer reagents (15 μ L), gave a fast result in every case (10 – 30 min maximum), which were easy to analyse (from a photograph and transferred to ImageJ) and gave results that were not significantly different from the conventional methods (largest SEM encountered was \pm 2%).

Initial paper fabrication used photolithography and a positive photoresist which created a novel fabrication method for paper microfluidics. This method was successful in creating hydrophilic channels within a hydrophobic surrounding (barrier) for naturally wicking fluids and solutions. Upon this fabrication, a colourimetric assay for iron(II) was developed which would be a useful device to be used in the developing world were untrained personal

could use this device to determine iron(II) levels in people who do not have access to modern day medicine.

A paper platform was simultaneously developed to detect creatinine and urea in human serum samples as simple dip stick assay, turning colour proportional to the amount present and analysis was via ImageJ software (or in the case for urea the visibility of a colour change by eye). These devices were designed as easy to use POC devices with a real-World application in determining renal function in patients in the developing world who do not have the healthcare available in the developed world.

The methods described are all methods that have been previously optimised as a conventional laboratory technique using a spectrophotometer^{132,136,148} but have been developed and miniaturised for the use on a paper microfluidic device. However, these devices maintained the accuracy for which they are known (chapter 4, table 4.1).^{132,136,148}

The main purpose drawn from this project was to be able to use paper to utilise a possible POC device made either entirely or partially from filter paper. The idea of creating hydrophilic channels within a hydrophobic setting, and using photolithography has proven to be a successful method for this.

Conclusion

In conclusion the findings in this research was to establish filter paper as an accurate (SEM <2%) and user friendly platform on which colourimetric tests can be performed. The successful creation of channels via photolithography or through the development of optimising dipstick assays detected three individual analytes in human serum samples within the expected clinical range. The aim of the project has been fulfilled by the development of colourimetric assays for iron(II), urea and creatinine which used a paper platform in each case which allowed for their accurate detection and measurement when compared to the conventional methods available.

7.1 Further Work

As the previous chapters have indicated, further work would be necessary to be able to produce these devices on a larger scale and further research would be required to attain a device user friendly.

Iron

The iron method currently showed that a finger prick could be used to detect iron(II) in human serum samples through the structuring and layering of a 3D paper device made entirely from paper and tape. However, the research into the Lauber Method used the pH to prevent any interferences with the coloured complex formed upon the reaction of bathophenanthroline and iron(II) but this research did not take into account the use of plasma as a

sample. Serum does not contain fibrinogen whereas plasma samples do, further work would have to be completed to ensure there are no interferences from this.

Urea

The urea method employed used a semi-quantitative result as either a positive or negative result; this allowed the assumption to be made that the patient whose sample had been tested would require further analysis to determine the reason behind an increased urea concentration. As a diagnostic test this could be further improved by finding a method in which a quantified result could be measured, giving the user an exact concentration of urea. This assay could be used in conjunction with the creatinine assay for further analysis and for a better diagnosis of the patient and the underlying cause. It could also be possible to run the sample on one device and detect both analytes simultaneously to diagnose kidney failure however experiments would have to be completed to ensure there are no interferences with both assays and the reagents required.

Another possible avenue would be to determine if this device could incorporate the plasma membrane to trap RBCs as the iron device in chapter 4. This would allow less pre-treatment of the sample before application on to the device as centrifugation to remove the RBCs from the sample away from a laboratory setting could prove a shortfall in this area.

Creatinine

The creatinine assay was based upon the same principles as the urea device as a dipstick assay, allowing a sample to wick along a length of paper until reaching a detection zone where the colour change would be observable to the user. These long strips of paper however, are prone to breaking and snapping as a result of incorrect storage and transportation. To overcome this problem, work could be carried out to incorporate a plastic casing over the paper giving the device a more rigid yet still easy to handle approach, keeping the detection zone visible to allow the user to read or image the result whilst having a more defined area for analysis, figure 7.1

Another possible avenue would be to determine if this device could incorporate the plasma membrane to trap RBCs as the iron device in chapter 4. This would allow less pre-treatment of the sample before application on to the device as centrifugation to remove the RBCs from the sample away from a laboratory setting could prove a shortfall in this area.

References

1. Carrilho, E., Phillips, S.T., Vella, S.J., Martinez, A.W. & Whitesides, G.M. Paper microzone plates. *Analytical Chemistry* **81**, 5990-5998 (2009).
2. Govindarajan, A.V., Ramachandran, S., Vigil, G.D., Yager, P. & Bohringer, K.F. A low cost point-of-care viscous sample preparation device for molecular diagnosis in the developing world; an example of microfluidic origami. *Lab on a Chip* **12**, 174-181 (2012).
3. Biehl, M. & Velten, T. Gaps and Challenges of Point-of-Care Technology. *Sensors Journal, IEEE* **8**, 593-600 (2008).
4. Christodoulides, N. Lab-on-a-Chip Methods for Point-of-Care Measurements of Salivary Biomarkers of Periodontitis. *Annals of the New York Academy of Sciences* **1098**, 411-428 (2007).
5. Bracher, P.J., Gupta, M. & Whitesides, G.M. Patterned paper as a template for the delivery of reactants in the fabrication of planar materials. *Soft Matter* **6**, 4303-4309 (2010).
6. Whitesides, G.M. The origins and the future of microfluidics. *Nature* **442**, 368-373 (2006).
7. Whitesides, G.M. What Comes Next? *Lab on a Chip* **11**, 191-193 (2011).
8. Weibel, D.B. & Whitesides, G.M. Applications of microfluidics in chemical biology. *Current Opinion in Chemical Biology* **10**, 584-591 (2006).
9. Cheng, C.M., Paper-based elisa. *Angewandte Chemie - International Edition* **49**, 4771-4774 (2010).
10. Brunner, G.A., Validation of Home Blood Glucose Meters With Respect to Clinical and Analytical Approaches. *Diabetes Care* **21**, 585-590 (1998).
11. Clarke, W.L., Cox, D., Gonder-Frederick, L.A., Carter, W. & Pohl, S.L. Evaluating Clinical Accuracy of Systems for Self-Monitoring of Blood Glucose. *Diabetes Care* **10**, 622-628 (1987).
12. Farmer, A., Impact of self monitoring of blood glucose in the management of patients with non-insulin treated diabetes: open parallel group randomised trial. *BMJ* **335**, 132 (2007).
13. Parvin, C.A. Impact of point-of-care testing on patients' length of stay in a large emergency department. *Clinical Chemistry* **42**, 711-717 (1996).
14. Pickup, J., McCartney, L., Rolinski, O. & Birch, D. In vivo glucose sensing for diabetes management: progress towards non-invasive monitoring. *BMJ* **319**, 1289 (1999).

15. Sönksen, P.H., Judd, S.L. & Lowy, C. HOME MONITORING OF BLOOD-GLUCOSE: Method for Improving Diabetic Control. *The Lancet* **311**, 729-732 (1978).
16. Webster, A., Dyer, C.E., Haswell, S.J. & Greenman, J. A microfluidic device for tissue biopsy culture and interrogation. *Analytical Methods* **2**, 1005-1007 (2010).
17. Woods, J., Docker, P.T., Dyer, C.E., Haswell, S.J. & Greenman, J. On-chip integrated labelling, transport and detection of tumour cells. *ELECTROPHORESIS* **32**, 3188-3195 (2011).
18. Zhang, X., Jones, P. & Haswell, S.J. Attachment and detachment of living cells on modified microchannel surfaces in a microfluidic-based lab-on-a-chip system. *Chemical Engineering Journal* **135**, Supplement 1, S82-S88 (2008).
19. Tanweer, F., Louise Green, V., David Stafford, N. & Greenman, J. Application of microfluidic systems in management of head and neck squamous cell carcinoma. *Head & Neck* **35**, 756-763 (2013).
20. Bracher, P.J., Gupta, M. & Whitesides, G.M. Patterning precipitates of reactions in paper. *Journal of Materials Chemistry* **20**, 5117-5122 (2010).
21. Ellerbee, A.K., *et al.* Quantifying Colourimetric Assays in Paper-Based Microfluidic Devices by Measuring the Transmission of Light through Paper. *Analytical Chemistry* **81**, 8447-8452 (2009).
22. Chin, C.D., Linder, V. & Sia, S.K. Commercialization of microfluidic point-of-care diagnostic devices. *Lab on a Chip* **12**, 2118-2134 (2012).
23. Byrnes, S. A portable, pressure driven, room temperature nucleic acid extraction and storage system for point of care molecular diagnostics. *Analytical Methods* **5**, 3177-3184 (2013).
24. Gallegos, D. Label-free biodetection using a smartphone. *Lab on a Chip* **13**, 2124-2132 (2013).
25. He, M. & Liu, Z. Paper-Based Microfluidic Device with Upconversion Fluorescence Assay. *Analytical Chemistry* **85**, 11691-11694 (2013).
26. Hibbard, T. Point of Care Monitoring of Hemodialysis Patients with a Breath Ammonia Measurement Device Based on Printed Polyaniline Nanoparticle Sensors. *Analytical Chemistry* **85**, 12158-12165 (2013).
27. Rivet, C., Lee, H., Hirsch, A., Hamilton, S. & Lu, H. Microfluidics for medical diagnostics and biosensors. *Chemical Engineering Science* **In Press, Corrected Proof**(2010).
28. Mark, D., Haeberle, S., Roth, G., von Stetten, F. & Zengerle, R. Microfluidic lab-on-a-chip platforms: requirements, characteristics and applications. *Chemical Society Reviews* **39**, 1153-1182 (2010).

29. Klasner, S. Paper-based microfluidic devices for analysis of clinically relevant analytes present in urine and saliva. *Analytical and Bioanalytical Chemistry* **397**, 1821-1829 (2010).
30. Proliferation of microfluidics in literature and intellectual property. *Lab on a Chip* **4**, 16N-20N (2004).
31. Chin, C.D., Linder, V. & Sia, S.K. Lab-on-a-chip devices for global health: Past studies and future opportunities. *Lab on a Chip* **7**, 41-57 (2007).
32. Mabey, D., Peeling, R.W., Ustianowski, A. & Perkins, M.D. Tropical infectious diseases: Diagnostics for the developing world. *Nat Rev Micro* **2**, 231-240 (2004).
33. Molyneux, D.H., Hotez, P.J. & Fenwick, A. "Rapid-Impact Interventions": How a Policy of Integrated Control for Africa's Neglected Tropical Diseases Could Benefit the Poor. *PLoS Med* **2**, e336 (2005).
34. Zhao, W., Ali, M.M., Aguirre, S.D., Brook, M.A. & Li, Y. Paper-Based Bioassays Using Gold Nanoparticle Colourimetric Probes. *Analytical Chemistry* **80**, 8431-8437 (2008).
35. Ohman, E.M. Risk stratification with a point-of-care cardiac troponin T test in acute myocardial infarction. *The American Journal of Cardiology* **84**, 1281-1286 (1999).
36. Apple, F.S., Ler, R., Chung, A.Y., Berger, M.J. & Murakami, M.M. Point-of-Care i-STAT Cardiac Troponin I for Assessment of Patients with Symptoms Suggestive of Acute Coronary Syndrome. *Clin Chem* **52**, 322-325 (2006).
37. Floriano, P.N. Use of Saliva-Based Nano-Biochip Tests for Acute Myocardial Infarction at the Point of Care: A Feasibility Study. *Clin Chem* **55**, 1530-1538 (2009).
38. Apple, F.S. Future Biomarkers for Detection of Ischemia and Risk Stratification in Acute Coronary Syndrome. *Clin Chem* **51**, 810-824 (2005).
39. Cramer, G.E. Lack of concordance between a rapid bedside and conventional laboratory method of cardiac troponin testing: Impact on risk stratification of patients suspected of acute coronary syndrome. *Clinica Chimica Acta* **381**, 164-166 (2007).
40. Chin, C.D., Linder, V. & Sia, S.K. Commercialization of microfluidic point-of-care diagnostic devices. *Lab on a Chip* (2012).
41. Koch, S. Home telehealth—Current state and future trends. *International Journal of Medical Informatics* **75**, 565-576 (2006).
42. Nickelson, D.W. Telehealth and the evolving health care system: Strategic opportunities for professional psychology. Vol. 29 527-535 (American Psychological Association, US, 1998).
43. Martinez, A.W., Phillips, S.T., Whitesides, G.M. & Carrilho, E. Diagnostics for the Developing World: Microfluidic Paper-Based Analytical Devices. *Analytical Chemistry* **82**, 3-10 (2009).

44. Martinez, A.W., Phillips S.T. Programmable diagnostic devices made from paper and tape. *Lab Chip* **10**, 2499-2504 (2010).
45. Li, X., Ballerini, D.R. & Shen, W. A perspective on paper-based microfluidics: Current status and future trends. *Biomicrofluidics* **6**(2012).
46. Bond, M.M. Chromatography Paper as a Low-Cost Medium for Accurate Spectrophotometric Assessment of Blood Hemoglobin Concentration. *Lab on a Chip* (2013).
47. Comer, J.P. Semiquantitative Specific Test Paper for Glucose in Urine. *Analytical Chemistry* **28**, 1748-1750 (1956).
48. Jung, W. An innovative sample-to-answer polymer lab-on-a-chip with on-chip reservoirs for the point-of-care testing of thyroid stimulating hormone. *Lab on a Chip* (2013).
49. Kiilerich-Pedersen, K., Daprà, J., Cherré, S. & Rozlosnik, N. High sensitivity point-of-care device for direct virus diagnostics. *Biosensors and Bioelectronics* **49**, 374-379 (2013).
50. Lillehoj, P.B., Huang, M.-C., Truong, N. & Ho, C.-M. Rapid electrochemical detection on a mobile phone. *Lab on a Chip* (2013).
51. Liu, C. Membrane-Based, Sedimentation-Assisted Plasma Separator for Point-of-Care Applications. *Analytical Chemistry* **85**, 10463-10470 (2013).
52. Von Lode, P. Point-of-care immunotesting: Approaching the analytical performance of central laboratory methods. *Clinical Biochemistry* **38**, 591-606 (2005).
53. Liana, D.D., Raguse, B., Gooding, J.J. & Chow, E. Recent Advances in Paper-Based Sensors. *Sensors* **12**, 11505-11526 (2012).
54. Carvalhal, R.F., Carrilho, E. & Kubota, L.T. The potential and application of microfluidic paper-based separation devices. *Bioanalysis* **2**, 1663-1665 (2010).
55. Li, X., Tian, J. & Shen, W. Progress in patterned paper sizing for fabrication of paper-based microfluidic sensors. *Cellulose* **17**, 649-659 (2010).
56. Dungchai, W., Chailapakul, O. & Henry, C.S. Electrochemical Detection for Paper-Based Microfluidics. *Analytical Chemistry* **81**, 5821-5826 (2009).
57. Ma, J. A simple photolithography method for microfluidic device fabrication using sunlight as UV source. *Microfluidics and Nanofluidics* **9**, 1247-1252 (2010).
58. Martinez, A.W., Phillips S.T. Simple Telemedicine for Developing Regions: Camera Phones and Paper-Based Microfluidic Devices for Real-Time, Off-Site Diagnosis. *Analytical Chemistry* **80**, 3699-3707 (2008).

59. Bruzewicz, D.A., Reches, M. & Whitesides, G.M. Low-Cost Printing of Poly(dimethylsiloxane) Barriers To Define Microchannels in Paper. *Analytical Chemistry* **80**, 3387-3392 (2008).
60. Lu, Y., Lin, B. & Qin, J. Patterned Paper as a Low-Cost, Flexible Substrate for Rapid Prototyping of PDMS Microdevices via "Liquid Molding". *Analytical Chemistry* **83**, 1830-1835 (2011).
61. Abe, K., Kotera, K., Suzuki, K. & Citterio, D. Inkjet-printed paperfluidic immuno-chemical sensing device. *Analytical and Bioanalytical Chemistry* **398**, 885-893 (2010).
62. Abe, K., Suzuki, K. & Citterio, D. Inkjet-Printed Microfluidic Multianalyte Chemical Sensing Paper. *Analytical Chemistry* **80**, 6928-6934 (2008).
63. Li, X., Tian, J., Nguyen, T. & Shen, W. Paper-Based Microfluidic Devices by Plasma Treatment. *Analytical Chemistry* **80**, 9131-9134 (2008).
64. Carrilho, E., Martinez, A.W. & Whitesides, G.M. Understanding Wax Printing: A Simple Micropatterning Process for Paper-Based Microfluidics. *Analytical Chemistry* **81**, 7091-7095 (2009).
65. Dungchai, W., Chailapakul, O. & Henry, C.S. A low-cost, simple, and rapid fabrication method for paper-based microfluidics using wax screen-printing. *Analyst* **136**, 77-82 (2011).
66. Xiao, L. A rapid, straightforward, and print house compatible mass fabrication method for integrating 3D paper-based microfluidics. *ELECTROPHORESIS* **34**, 3003-3007 (2013).
67. Zhong, Z.W., Wang, Z.P. & Huang, G.X.D. Investigation of wax and paper materials for the fabrication of paper-based microfluidic devices. *Microsyst Technol* **18**, 649-659 (2012).
68. Olkkonen, J., Lehtinen, K. & Erho, T. Flexographically Printed Fluidic Structures in Paper. *Analytical Chemistry* **82**, 10246-10250 (2010).
69. Metters, J.P., Houssein, S.M., Kampouris, D.K. & Banks, C.E. Paper-based electroanalytical sensing platforms. *Analytical Methods* **5**, 103-110 (2013).
70. Nie, Z., *et al.* Electrochemical sensing in paper-based microfluidic devices. *Lab on a Chip* **10**, 477-483 (2010).
71. Chitnis, G., Ding, Z., Chang, C.-L., Savran, C.A. & Ziaie, B. Laser-treated hydrophobic paper: an inexpensive microfluidic platform. *Lab on a Chip* **11**, 1161-1165 (2011).
72. Yetisen, A.K., Akram, M.S. & Lowe, C.R. Paper-based microfluidic point-of-care diagnostic devices. *Lab on a Chip* (2013).
73. Al-Tamimi, M., Shen, W., Zeineddine, R., Tran, H. & Garnier, G. Validation of Paper-Based Assay for Rapid Blood Typing. *Analytical Chemistry* **84**, 1661-1668 (2011).

74. Khan, M.S., Thouas, G., Shen, W., Whyte, G. & Garnier, G. Paper Diagnostic for Instantaneous Blood Typing. *Analytical Chemistry* **82**, 4158-4164 (2010).
75. Cate, D.M., Dungchai, W., Cunningham, J.C., Volckens, J. & Henry, C.S. Simple, distance-based measurement for paper analytical devices. *Lab on a Chip* (2013).
76. Jokerst, J.C., Emory, J.M. & Henry, C.S. Advances in microfluidics for environmental analysis. *Analyst* **137**, 24-34 (2012).
77. Liu, Y., Garcia, C.D. & Henry, C.S. Recent progress in the development of [small mu]TAS for clinical analysis. *Analyst* **128**, 1002-1008 (2003).
78. Songjaroen, T., Dungchai, W., Chailapakul, O., Henry, C.S. & Laiwattanapaisal, W. Blood separation on microfluidic paper-based analytical devices. *Lab on a Chip* (2012).
79. Fu, E., Ramsey, S., Kauffman, P., Lutz, B. & Yager, P. Transport in two-dimensional paper networks. *Microfluidics and Nanofluidics* **10**, 29-35 (2011).
80. Yager, P., *et al.* Microfluidic diagnostic technologies for global public health. *Nature* **442**, 412-418 (2006).
81. Constable, C.E.H.a.E.C. *Chemistry*, (Pearson Education Limited, Essex, 2006).
82. Colin, M., Colin, T. & Dambrine, J. VALIDITY OF THE REYNOLDS EQUATION FOR MISCIBLE FLUIDS IN MICROCHANNELS. *Discrete and Continuous Dynamical Systems-Series B* **17**, 801-834 (2012).
83. Fisher, L.R. & Lark, P.D. An experimental study of the washburn equation for liquid flow in very fine capillaries. *Journal of Colloid and Interface Science* **69**, 486-492 (1979).
84. Giovambattista, N., Debenedetti, P.G. & Rossky, P.J. Effect of Surface Polarity on Water Contact Angle and Interfacial Hydration Structure. *The Journal of Physical Chemistry B* **111**, 9581-9587 (2007).
85. Hamraoui, A. & Nylander, T. Analytical Approach for the Lucas–Washburn Equation. *Journal of Colloid and Interface Science* **250**, 415-421 (2002).
86. Osborn, J.L., *et al.* Microfluidics without pumps: reinventing the T-sensor and H-filter in paper networks. *Lab on a Chip* **10**, 2659-2665 (2010).
87. Liukkonen, A. Contact angle of water on paper components: Sessile drops versus environmental scanning electron microscope measurements. *Scanning* **19**, 411-415 (1997).
88. Anfossi, L., *et al.* Optimization of a lateral flow immunoassay for the ultrasensitive detection of aflatoxin M1 in milk. *Analytica Chimica Acta* **772**, 75-80 (2013).

89. Yu, J., Ge, L., Huang, J., Wang, S. & Ge, S. Microfluidic paper-based chemiluminescence biosensor for simultaneous determination of glucose and uric acid. *Lab on a Chip* (2011).
90. Delaney, J.L., Hogan, C.F., Tian, J. & Shen, W. Electrogenerated Chemiluminescence Detection in Paper-Based Microfluidic Sensors. *Analytical Chemistry* **83**, 1300-1306 (2011).
91. Martinez, A.W., Phillips, S.T. & Whitesides, G.M. Three-dimensional microfluidic devices fabricated in layered paper and tape. *Proceedings of the National Academy of Sciences of the United States of America* **105**, 19606-19611 (2008).
92. Ge, L., Wang, S., Song, X., Ge, S. & Yu, J. 3D Origami-based multifunction-integrated immunodevice: low-cost and multiplexed sandwich chemiluminescence immunoassay on microfluidic paper-based analytical device. *Lab on a Chip* **12**, 3150-3158 (2012).
93. Liu, H. & Crooks, R.M. Three-Dimensional Paper Microfluidic Devices Assembled Using the Principles of Origami. *Journal of the American Chemical Society* **133**, 17564-17566 (2011).
94. Liu, H., Xiang, Y., Lu, Y. & Crooks, R.M. Aptamer-Based Origami Paper Analytical Device for Electrochemical Detection of Adenosine. *Angewandte Chemie International Edition* **51**, 6925-6928 (2012).
95. Scida, K., Li, B., Ellington, A.D. & Crooks, R.M. DNA Detection Using Origami Paper Analytical Devices. *Analytical Chemistry* **85**, 9713-9720 (2013).
96. Bhandari, P., Narahari, T. & Dendukuri, D. 'Fab-Chips': a versatile, fabric-based platform for low-cost, rapid and multiplexed diagnostics. *Lab on a Chip* (2011).
97. Willson, C.G. & Bowden Murrae, J. Organic Resist Materials. in *Electronic and Photonic Applications of Polymers*, Vol. 218 75-108 (American Chemical Society, 1988).
98. Dill, F.H., Hornberger, W.P., Hauge, P.S. & Shaw, J.M. Characterization of positive photoresist. *Electron Devices, IEEE Transactions on* **22**, 445-452 (1975).
99. Mack, C.A. Development of Positive Photoresists. *Journal of The Electrochemical Society* **134**, 148-152 (1987).
100. Carvalhal, R.F., Simão Kfour, M., de Oliveira Piazzetta, M.H., Gobbi, A.L. & Kubota, L.T. Electrochemical Detection in a Paper-Based Separation Device. *Analytical Chemistry* **82**, 1162-1165 (2010).
101. Shaw, J.M., Gelorme, J.D., LaBianca, N.C., Conley, W.E. & Holmes, S.J. Negative photoresists for optical lithography. *IBM Journal of Research and Development* **41**, 81-94 (1997).
102. DeVore, T.C., Augustine, B.H., Christenson, A.M. & Corder, G.W. A Photolithography Laboratory Experiment for General Chemistry Students. *Journal of Chemical Education* **80**, 183-null (2003).

103. *Introduction to Microlithography*, (AMERICAN CHEMICAL SOCIETY, 1983).
104. Reichmanis, E. & Thompson Larry, F. Polymers in Microlithography. in *Polymers in Microlithography*, Vol. 412 1-24 (American Chemical Society, 1989).
105. O'Brien Michael, J. & Soane David, S. Resists in Microlithography. in *Microelectronics Processing*, Vol. 221 325-376 (American Chemical Society, 1989).
106. Hung-Pin, C., *et al.* Design and process considerations for fabricating RF MEMS switches on printed circuit boards. *Microelectromechanical Systems, Journal of* **14**, 1311-1322 (2005).
107. Reichmanis, E. & Thompson, L.F. Polymer materials for microlithography. *Chemical Reviews* **89**, 1273-1289 (1989).
108. Reichmanis, E., Frank Curtis, W., O'Donnell James, H. & Hill David, J.T. Radiation Effects on Polymeric Materials. in *Irradiation of Polymeric Materials*, Vol. 527 1-8 (American Chemical Society, 1993).
109. *Polymers in Microlithography*, (American Chemical Society, 1989).
110. Kirmse, W. 100 Years of the Wolff Rearrangement. *European Journal of Organic Chemistry* **2002**, 2193-2256 (2002).
111. Meier, H. & Zeller, K.-P. The Wolff Rearrangement of α -Diazo Carbonyl Compounds. *Angewandte Chemie International Edition in English* **14**, 32-43 (1975).
112. Berns, R.S., Motta, R.J. & Gorzynski, M.E. CRT colorimetry. part I: Theory and practice. *Color Research & Application* **18**, 299-314 (1993).
113. Koenderink, J.J. Color atlas theory. *J. Opt. Soc. Am. A* **4**, 1314-1321 (1987).
114. Turner, R.S. The Origins of Colorimetry: What did Helmholtz and Maxwell Learn from Grassmann? in *Hermann Günther Graßmann (1809–1877): Visionary Mathematician, Scientist and Neohumanist Scholar*, Vol. 187 (ed. Schubring, G.) 71-86 (Springer Netherlands, 1996).
115. Johnston, W.M. & Kao, E.C. Assessment of Appearance Match by Visual Observation and Clinical Colorimetry. *Journal of Dental Research* **68**, 819-822 (1989).
116. Chen, X., *et al.* Determination of glucose and uric acid with bienzyme colorimetry on microfluidic paper-based analysis devices. *Biosensors and Bioelectronics* **35**, 363-368 (2012).
117. Abe, A., Yamashita, S. & Noma, A. Sensitive, direct colourimetric assay for copper in serum. *Clinical Chemistry* **35**, 552-554 (1989).

118. Apilux, A., *et al.* Lab-on-Paper with Dual Electrochemical/Colourimetric Detection for Simultaneous Determination of Gold and Iron. *Analytical Chemistry* **82**, 1727-1732 (2010).
119. Blicharz, T.M., *et al.* Use of Colourimetric Test Strips for Monitoring the Effect of Hemodialysis on Salivary Nitrite and Uric Acid in Patients with End-Stage Renal Disease: A Proof of Principle. *Clinical Chemistry* **54**, 1473-1480 (2008).
120. Butler, A.R. & Walsh, D. Colourimetric non-enzymic methods for the determination of urea. Consideration of the chemical principles upon which an analytical method is based is an essential step in the optimization of that method. It can also contribute to the simplification of procedures used and hence cut the costs of many routine analyses. *Trends in Analytical Chemistry* **1**, 120-124 (1982).
121. Cretich, M., *et al.* Coating of nitrocellulose for colourimetric DNA microarrays. *Analytical Biochemistry* **397**, 84-88 (2010).
122. Oncescu, V., O'Dell, D. & Erickson, D. Smartphone based health accessory for colourimetric detection of biomarkers in sweat and saliva. *Lab on a Chip* (2013).
123. Sergeeva, T.A., *et al.* Colourimetric test-systems for creatinine detection based on composite molecularly imprinted polymer membranes. *Analytica Chimica Acta* **770**, 161-168 (2013).
124. Somidevamma, G. & Rao, G.G. Colourimetric determination of iron (III) with 1,10-phenanthroline. *Fresenius' Journal of Analytical Chemistry* **187**, 183-187 (1962).
125. Vega-Avila, E. & Pugsley, M.K. An overview of colourimetric assay methods used to assess survival or proliferation of mammalian cells. *Proceedings of the Western Pharmacology Society* **54**, 10-14 (2011).
126. Mosmann, T. Rapid colourimetric assay for cellular growth and survival: Application to proliferation and cytotoxicity assays. *Journal of Immunological Methods* **65**, 55-63 (1983).
127. Whitesides, G.M. Viewpoint on "Dissolvable fluidic time delays for programming multi-step assays in instrument-free paper diagnostics". *Lab on a Chip* (2013).
128. Vella, S.J., *et al.* Measuring Markers of Liver Function Using a Micropatterned Paper Device Designed for Blood from a Fingerstick. *Analytical Chemistry* **84**, 2883-2891 (2012).
129. Burgess, J. & Twigg, M.V. Iron: Inorganic & Coordination Chemistry. in *Encyclopedia of Inorganic Chemistry* (John Wiley & Sons, Ltd, 2006).
130. Kocsis, L., Herman, P. & Eke, A. The modified Beer–Lambert law revisited. *Physics in Medicine and Biology* **51**, N91 (2006).
131. Fuwa, K. & Valle, B.L. The Physical Basis of Analytical Atomic Absorption Spectrometry. The Pertinence of the Beer-Lambert Law. *Analytical Chemistry* **35**, 942-946 (1963).

132. Jung, D., Biggs, H., Erikson, J. & Ledyard, P.U. New Colourimetric Reaction for End-Point, Continuous-Flow, and Kinetic Measurement of Urea. *Clinical Chemistry* **21**, 1136-1140 (1975).
133. Greenwald, I. THE CHEMISTRY OF JAFFE'S REACTION FOR CREATININE II. THE EFFECT OF SUBSTITUTION IN THE CREATININE MOLECULE AND A POSSIBLE FORMULA FOR THE RED TAUTOMER1. *Journal of the American Chemical Society* **47**, 1443-1448 (1925).
134. Delanghe, J.R. & Speeckaert, M.M. Creatinine determination according to Jaffe—what does it stand for? *NDT Plus* **4**, 83-86 (2011).
135. Husdan, H. & Rapoport, A. Estimation of Creatinine by the Jaffe Reaction. *Clinical Chemistry* **14**, 222-238 (1968).
136. Liu, W.-S., *et al.* Serum Creatinine Determined by Jaffe, Enzymatic Method, and Isotope Dilution-Liquid Chromatography-Mass Spectrometry in Patients Under Hemodialysis. *Journal of Clinical Laboratory Analysis* **26**, 206-214 (2012).
137. Safavieh, M., *et al.* A simple cassette as point-of-care diagnostic device for naked-eye colourimetric bacteria detection. *Analyst* **139**, 482-487 (2014).
138. Sechi, D., Greer, B., Johnson, J. & Hashemi, N. Three-Dimensional Paper-Based Microfluidic Device for Assays of Protein and Glucose in Urine. *Analytical Chemistry* **85**, 10733-10737 (2013).
139. Clark, S.F. Iron Deficiency Anemia. *Nutrition in Clinical Practice* **23**, 128-141 (2008).
140. Pirzio-Biroli, G. & Finch, C.A. Treatment of iron deficiency anemia in the adult. *Journal of Chronic Diseases* **6**, 302-306 (1957).
141. Harman, D. Aging: A Theory Based on Free Radical and Radiation Chemistry. *Journal of Gerontology* **11**, 298-300 (1956).
142. Zecca, L., Youdim, M.B.H., Riederer, P., Connor, J.R. & Crichton, R.R. Iron, brain ageing and neurodegenerative disorders. *Nat Rev Neurosci* **5**, 863-873 (2004).
143. Higami, Y. & Shimokawa, I. Apoptosis in the aging process. *Cell and Tissue Research* **301**, 125-132 (2000).
144. Dzik, W. Three respiratory gases and the red cell: oxygen, carbon dioxide and nitric oxide. in *State of the Art Presentations*, Vol. 5 (ed. Mayr, W.R.) 234-238 (Blackwell Publishing, Oxford, 2010).
145. Adair, G.S., Bock, W.t.c.o.A.V. & H. Field, J. THE HEMOGLOBIN SYSTEM. *Journal of Biological Chemistry* **63**, 529-545 (1925).

146. Cheng, Y., Zak, O., Aisen, P., Harrison, S.C. & Walz, T. Structure of the Human Transferrin Receptor-Transferrin Complex. *Cell* **116**, 565-576 (2004).
147. Bainton, D.F. & Finch, C.A. The diagnosis of iron deficiency anemia. *The American Journal of Medicine* **37**, 62-70 (1964).
148. Lauber, K. Determination of serum iron and iron-binding capacity without deproteinization. *Zeitschrift für klinische Chemie und klinische Biochemie* **3**, 96-99 (1965).
149. Sakai, H., *et al.* Metabolism of hemoglobin-vesicles (artificial oxygen carriers) and their influence on organ functions in a rat model. *Biomaterials* **25**, 4317-4325 (2004).
150. Gordon, S. Homeostasis: A scavenger receptor for haemoglobin. *Current Biology* **11**, R399-R401 (2001).
151. Wood, M.M. & Elwood, P.C. Symptoms of iron deficiency anaemia. A community survey. *British journal of preventive & social medicine* **20**, 117-121 (1966).
152. Kwiatkowski, J.L., West, T.B., Heidary, N., Smith-Whitley, K. & Cohen, A.R. Severe iron deficiency anemia in young children. *The Journal of Pediatrics* **135**, 514-516 (1999).
153. Dillon, R. & Harrison, C. Full blood count. *British Journal of Hospital Medicine* **70**, M38-M41 (2009).
154. Foudeh, A.M., Fatanat Didar, T., Veres, T. & Tabrizian, M. Microfluidic designs and techniques using lab-on-a-chip devices for pathogen detection for point-of-care diagnostics. *Lab on a Chip* (2012).
155. Lee, W.G., Kim, Y.-G., Chung, B.G., Demirci, U. & Khademhosseini, A. Nano/Microfluidics for diagnosis of infectious diseases in developing countries. *Advanced Drug Delivery Reviews* **62**, 449-457 (2010).
156. Rohrman, B.A. & Richards-Kortum, R.R. A paper and plastic device for performing recombinase polymerase amplification of HIV DNA. *Lab on a Chip* **12**, 3082-3088 (2012).
157. Mudanyali, O., *et al.* Integrated rapid-diagnostic-test reader platform on a cellphone. *Lab on a Chip* **12**, 2678-2686 (2012).
158. Schoffers, E. Reinventing Phenanthroline Ligands – Chiral Derivatives for Asymmetric Catalysis? *European Journal of Organic Chemistry* **2003**, 1145-1152 (2003).
159. Smith, G.F., McCurdy, W.H. & Diehl, H. The colourimetric determination of iron in raw and treated municipal water supplies by use of 4:7-diphenyl-1:10-phenanthroline. *Analyst* **77**, 418-422 (1952).
160. Quinteros, A., Farré, R. & Lagarda, M.J. Optimization of iron speciation (soluble, ferrous and ferric) in beans, chickpeas and lentils. *Food Chemistry* **75**, 365-370 (2001).

161. Dungchai, W., Chailapakul, O. & Henry, C.S. Use of multiple colourimetric indicators for paper-based microfluidic devices. *Analytica Chimica Acta* **674**, 227-233 (2010).
162. Martini, F.H. Fundamentals of Anatomy and Physiology. **International Edition**, 687-698 (2006).
163. Zawada, R.J.X., Kwan, P., Olszewski, K.L., Llinas, M. & Huang, S.-G. Quantitative determination of urea concentrations in cell culture medium. *Biochemistry and Cell Biology* **87**, 541-544 (2009).
164. Mouton, R. & Holder, K. Laboratory tests of renal function. *Anaesthesia & Intensive Care Medicine* **7**, 240-243 (2006).
165. Pépin, M.-N., Bouchard, J., Legault, L. & Éthier, J. Diagnostic Performance of Fractional Excretion of Urea and Fractional Excretion of Sodium in the Evaluations of Patients With Acute Kidney Injury With or Without Diuretic Treatment. *American Journal of Kidney Diseases* **50**, 566-573 (2007).
166. Anderson, R.J. Chapter 56 - Acute Renal Failure. in *Critical Care Medicine (Third Edition)* (eds. Joseph, E.P., Md & R. Phillip Dellinger, M.D.) 1165-1187 (Mosby, Philadelphia, 2008).
167. Bellomo, R., *et al.* Acute renal failure - definition, outcome measures, animal models, fluid therapy and information technology needs: the Second International Consensus Conference of the Acute Dialysis Quality Initiative (ADQI) Group. *Critical Care* **8**, R204 - R212 (2004).
168. Hudson, K.B. & Sinert, R. Renal Failure: Emergency Evaluation and Management. *Emergency Medicine Clinics of North America* **29**, 569-585 (2011).
169. Lameire, N., Van Biesen, W. & Vanholder, R. Acute renal failure. *The Lancet* **365**, 417-430 (2005).
170. Levy, E.M., Viscoli, C.M. & Horwitz, R.I. The effect of acute renal failure on mortality: A cohort analysis. *JAMA* **275**, 1489-1494 (1996).
171. Liaño, F. & Pascual, J. Epidemiology of acute renal failure: a prospective, multicenter, community-based study. Madrid Acute Renal Failure Study Group. *Kidney international* **50**, 811-818 (1996).
172. McBride, W.T. & Gilliland, H. Acute renal failure. *Surgery (Oxford)* **27**, 480-485 (2009).
173. McCullough Md, M.P.H.P.A., Wolyn Md, R., Rocher Md, L.L., Levin Md, R.N. & O'Neill Md, W.W. Acute Renal Failure After Coronary Intervention: Incidence, Risk Factors, and Relationship to Mortality. *The American Journal of Medicine* **103**, 368-375 (1997).
174. Barsoum, R.S. Overview: End-Stage Renal Disease in the Developing World. *Artificial Organs* **26**, 737-746 (2002).

175. McCarthy, J.T. A Practical Approach to the Management of Patients With Chronic Renal Failure. *Mayo Clinic Proceedings* **74**, 269-273 (1999).
176. Stafford-Smith, M., Patel, U.D., Phillips-Bute, B.G., Shaw, A.D. & Swaminathan, M. Acute Kidney Injury and Chronic Kidney Disease After Cardiac Surgery. *Advances in Chronic Kidney Disease* **15**, 257-277 (2008).
177. Zhang, Q.-L. & Rothenbacher, D. Prevalence of chronic kidney disease in population-based studies: Systematic review. *BMC Public Health* **8**, 117 (2008).
178. Part 3. Chronic kidney disease as a public health problem. *American journal of kidney diseases : the official journal of the National Kidney Foundation* **39**, S37-S45 (2002).
179. Part 7. Stratification of risk for progression of kidney disease and development of cardiovascular disease. *American journal of kidney diseases : the official journal of the National Kidney Foundation* **39**, S170-S212 (2002).
180. Part 4. Definition and classification of stages of chronic kidney disease. *American journal of kidney diseases : the official journal of the National Kidney Foundation* **39**, S46-S75 (2002).
181. Part 5. Evaluation of laboratory measurements for clinical assessment of kidney disease. *American journal of kidney diseases : the official journal of the National Kidney Foundation* **39**, S76-S110 (2002).
182. Aronson, D., Mittleman, M.A. & Burger, A.J. Elevated blood urea nitrogen level as a predictor of mortality in patients admitted for decompensated heart failure. *The American Journal of Medicine* **116**, 466-473 (2004).
183. Faisst, M., Wellner, U.F., Utzolino, S., Hopt, U.T. & Keck, T. Elevated blood urea nitrogen is an independent risk factor of prolonged intensive care unit stay due to acute necrotizing pancreatitis. *Journal of Critical Care* **25**, 105-111 (2010).
184. Pookaiyaudom, P., Seelanan, P., Lidgey, F.J., Hayatleh, K. & Toumazou, C. Measurement of urea, creatinine and urea to creatinine ratio using enzyme based chemical current conveyor (CCCII+). *Sensors and Actuators B: Chemical* **153**, 453-459 (2011).
185. Belcher, J.M., Edelstein, C.L. & Parikh, C.R. Clinical Applications of Biomarkers for Acute Kidney Injury. *American Journal of Kidney Diseases* **57**, 930-940 (2011).
186. Bonventre, J.V. & Sabbiseti, V. Chapter 48 - Acute Kidney Injury: Biomarkers from Bench to Bedside. in *Chronic Kidney Disease, Dialysis, and Transplantation (Third edition)* 668-676 (W.B. Saunders, Philadelphia, 2010).
187. Lespinas, F., Dupuy, G., Revol, F. & Aubry, C. Enzymic urea assay: a new colourimetric method based on hydrogen peroxide measurement. *Clin Chem* **35**, 654-658 (1989).

188. Kazory, A. Emergence of Blood Urea Nitrogen as a Biomarker of Neurohormonal Activation in Heart Failure. *The American Journal of Cardiology* **106**, 694-700 (2010).
189. Reynolds, R.D., Guanci, D.F., Neynaber, C.B. & Conboy, R.J. Base-catalyzed condensations of o-phthalaldehyde with urea and thiourea. *The Journal of Organic Chemistry* **43**, 3838-3840 (1978).
190. Weatherburn, M.W. Phenol-hypochlorite reaction for determination of ammonia. *Analytical Chemistry* **39**, 971-974 (1967).
191. Zava, T.T., Kapur, S. & Zava, D.T. Iodine and creatinine testing in urine dried on filter paper. *Analytica Chimica Acta* **764**, 64-69 (2013).
192. Kroll, M.H., Roach, N.A., Poe, B. & Elin, R.J. Mechanism of interference with the Jaffé reaction for creatinine. *Clinical Chemistry* **33**, 1129-1132 (1987).
193. Larsen, K. Creatinine assay by a reaction-kinetic principle. *Clinica Chimica Acta* **41**, 209-217 (1972).
194. Lolekha, P.H., Jaruthunyaluck, S. & Srisawasdi, P. Deproteinization of serum: Another best approach to eliminate all forms of bilirubin interference on serum creatinine by the kinetic Jaffe reaction. *Journal of Clinical Laboratory Analysis* **15**, 116-121 (2001).
195. Lolekha, P.H. & Sritong, N. Comparison of techniques for minimizing interference of bilirubin on serum creatinine determined by the kinetic Jaffé reaction. *Journal of Clinical Laboratory Analysis* **8**, 391-399 (1994).
196. Lustgarten, J.A. & Wenk, R.E. Simple, Rapid, Kinetic Method for Serum Creatinine Measurement. *Clinical Chemistry* **18**, 1419-1422 (1972).
197. Perakis, N. & Wolff, C.M. Kinetic approach for the enzymic determination of creatinine. *Clinical Chemistry* **30**, 1792-1796 (1984).
198. Songjaroen, T., Maturros, T., Sappat, A., Tuantranont, A. & Laiwattanapaisal, W. Portable microfluidic system for determination of urinary creatinine. *Analytica Chimica Acta* **647**, 78-83 (2009).
199. Brandt, W.W., Dwyer, F.P. & Gyarfas, E.D. Chelate Complexes of 1,10-Phenanthroline and Related Compounds. *Chemical Reviews* **54**, 959-1017 (1954).
200. McMahon, J.W. An acid-free bathophenanthroline method for measuring dissolved ferrous iron in lake water. *Water Research* **3**, 743-748 (1969).
201. Neevel, J.G. Application Issues of the Bathophenanthroline Test for Iron(II) Ions. *Restaurator* **30**, 3-15 (2009).

202. Perry, R.D. & Clemente, C.L.S. Determination of iron with bathophenanthroline following an improved procedure for reduction of iron(III) ions. *Analyst* **102**, 114-119 (1977).
203. Nakhleh, E.T., Samra, S.A. & Awdeh, Z.L. Isoelectric focusing of phenanthroline iron complexes and their possible use as pH markers. *Analytical Biochemistry* **49**, 218-224 (1972).
204. Rigas, P.G. & Pietrzyk, D.J. Liquid chromatographic separation and indirect detection of inorganic anions using iron(II) 1,10-phenanthroline as a mobile phase additive. *Analytical Chemistry* **58**, 2226-2233 (1986).
205. Xu, J., Che, P. & Ma, Y. More sensitive way to determine iron using an iron(II)-1, 10-phenanthroline complex and capillary electrophoresis. *Journal of Chromatography A* **749**, 287-294 (1996).
206. Diehl, H., . Smith, G.F.,. The Iron Reagents, Bathophenanthroline, 2,4,6-Tripyridyl-s-triazine, Phenyl-2-pyridyllocine. in *GF Smith Chem Co* (1960).
207. Paulson, G., Ray, R., Sternberg, J.,. A Rate-Sensing Approach to Urea Measurement. *Clin Chem* **17**(1971).
208. Horak, E., Sunderman, Jr, W.,. Measurment of Serum Urea Nitrogen Ion Conductivimetric Urease Assay. *Annals of Clinical Laboratory Science* **2**(1972).
209. Leung, V., Shehata, A.-A.M., Filipe, C.D.M. & Pelton, R. Streaming potential sensing in paper-based microfluidic channels. *Colloids and Surfaces A: Physicochemical and Engineering Aspects* **364**, 16-18 (2010).
210. Liu, X.Y., *et al.* A portable microfluidic paper-based device for elisa. 75-78 (Cancun, 2011).
211. Park, T.S., Li, W., McCracken, K.E. & Yoon, J.-Y. Smartphone quantifies Salmonella from paper microfluidics. *Lab on a Chip* (2013).
212. Phillips, S.T. & Lewis, G.G. The expanding role of paper in point-of-care diagnostics. *Expert review of molecular diagnostics* **14**, 123-125 (2014).
213. Bliss, C. Statistic in Biology. Vol. I. *IMcGraw-Hill, New York* (1967).
214. Sirringhaus, H., *et al.* High-Resolution Inkjet Printing of All-Polymer Transistor Circuits. *Science* **290**, 2123-2126 (2000).
215. Haeberle, S. & Zengerle, R. Microfluidic platforms for lab-on-a-chip applications. *Lab on a Chip* **7**, 1094-1110 (2007).
216. Becker, H. & Locascio, L.E. Polymer microfluidic devices. *Talanta* **56**, 267-287 (2002).
217. Kurra, N. & Kulkarni, G.U. Pencil-on-paper: electronic devices. *Lab on a Chip* (2013).

218. Mukhopadhyay, R. Microfluidics: On the Slope of Enlightenment. *Analytical Chemistry* **81**, 4169-4173 (2009).
219. Rivet, C., Lee, H., Hirsch, A., Hamilton, S. & Lu, H. Microfluidics for medical diagnostics and biosensors. *Chemical Engineering Science* **66**, 1490-1507 (2011).
220. Beard, J.L. Iron Biology in Immune Function, Muscle Metabolism and Neuronal Functioning. *The Journal of Nutrition* **131**, 568S-580S (2001).
221. Lauber, K. Determination of serum iron; a comparison of two methods: Teepol/dithionite/bathophenanthroline versus guanidine/ascorbic acid/Ferrozine (author's transl). *Journal of clinical chemistry and clinical biochemistry. Zeitschrift fur klinische Chemie und klinische Biochemie* **18**, 147-148 (1980).
222. Dill, K. Sensitive Analyte Detection and Quantitation Using the Threshold Immunoassay System. in *Environmental Immunochemical Methods*, Vol. 646 89-102 (American Chemical Society, 1996).
223. Burch, H.B., Lowry, O.H., Bessey, O.A. & Berson, B.Z. The Determination of Iron in Small Volumes of Blood Serum. *Journal of Biological Chemistry* **174**, 791-802 (1948).
224. Huisman, W. Interference of imferon in colourimetric assays for iron. *Clinical Chemistry* **26**, 635-637 (1980).
225. Jacobs, J.C. & Alexander, N.M. Colorimetry and constant-potential coulometry determinations of transferrin-bound iron, total iron-binding capacity, and total iron in serum containing iron-dextran, with use of sodium dithionite and alumina columns. *Clinical Chemistry* **36**, 1803-1807 (1990).
226. Montresor, A., *et al.* Field trial of a haemoglobin colour scale: an effective tool to detect anaemia in preschool children. *Tropical Medicine & International Health* **5**, 129-133 (2000).
227. Ge, L., *et al.* Three-dimensional paper-based electrochemiluminescence immunodevice for multiplexed measurement of biomarkers and point-of-care testing. *Biomaterials* **33**, 1024-1031 (2012).
228. Ahn, J.S., *et al.* Development of a point-of-care assay system for high-sensitivity C-reactive protein in whole blood. *Clinica Chimica Acta* **332**, 51-59 (2003).
229. Gardeniers, J.G.E. & Berg van den, A. Lab-on-a-Chip Systems for Biomedical and Environmental Monitoring. *International Journal of Computational Engineering Science* **4**, 157-161 (2003).
230. Gervais, L., de Rooij, N. & Delamarche, E. Microfluidic Chips for Point-of-Care Immunodiagnosics. *Advanced Materials* **23**, H151-H176 (2011).

231. Hu, X., *et al.* Determination of trace amounts of urea by using flow injection with chemiluminescence detection. *Analyst* **119**, 1829-1833 (1994).
232. Francis, P.S., Lewis, S.W. & Lim, K.F. Analytical methodology for the determination of urea: current practice and future trends. *TrAC Trends in Analytical Chemistry* **21**, 389-400 (2002).
233. Daviaud, J., *et al.* Reliability and feasibility of pregnancy home-use tests: laboratory validation and diagnostic evaluation by 638 volunteers. *Clinical Chemistry* **39**, 53-59 (1993).
234. Dimakou, S., Parkin, D., Devlin, N. & Appleby, J. Identifying the impact of government targets on waiting times in the NHS. *Health Care Manag Sci* **12**, 1-10 (2009).
235. Aronson, D., *et al.* Serum blood urea nitrogen and long-term mortality in acute ST-elevation myocardial infarction. *International Journal of Cardiology* **127**, 380-385 (2008).
236. Cockcroft, D.W. & Gault, M.H. Prediction of Creatinine Clearance from Serum Creatinine. *Nephron* **16**, 31-41 (1976).
237. Slocum, J.L., Heung, M. & Pennathur, S. Marking renal injury: can we move beyond serum creatinine? *Translational Research* **159**, 277-289 (2012).
238. Williamson, A., Singh, S., Fernekorn, U. & Schober, A. The future of the patient-specific Body-on-a-chip. *Lab on a Chip* **13**, 3471-3480 (2013).
239. Enzymatic assays for creatinine: Time for action. *Scandinavian Journal of Clinical & Laboratory Investigation* **68**, 84-88 (2008).
240. Fossati, P., Prencipe, L. & Berti, G. Enzymic creatinine assay: a new colourimetric method based on hydrogen peroxide measurement. *Clinical Chemistry* **29**, 1494-1496 (1983).
241. Peake M, W.M. Measurement of Serum Creatinine -Current Status and Future Trends. *Clinical Biochemistry* **27**, 173-184 (2006).
242. Andersson, H. & Berg, A.v.d. Microfabrication and microfluidics for tissue engineering: state of the art and future opportunities. *Lab on a Chip* **4**, 98-103 (2004).
243. Barsoum, R.S. Chronic Kidney Disease in the Developing World. *New England Journal of Medicine* **354**, 997-999 (2006).
244. Rolland, J.P. Paper microfluidics as an enabling platform for low-cost diagnostics. 1 (2012).
245. Cheng, C.-M., *et al.* Millimeter-scale contact printing of aqueous solutions using a stamp made out of paper and tape. *Lab on a Chip* **10**, 3201-3205 (2010).

246. Teles, F.S.R.R. Biosensors and rapid diagnostic tests on the frontier between analytical and clinical chemistry for biomolecular diagnosis of dengue disease: A review. *Anal. Chim. Acta* **687**, 28-42 (2011).
247. Delaney, J.L., Doeven, E.H., Harsant, A.J. & Hogan, C.F. Use of a mobile phone for potentiostatic control with low cost paper-based microfluidic sensors. *Analytica Chimica Acta* **790**, 56-60 (2013).
248. Delaney, J.L., Doeven, E.H., Harsant, A.J. & Hogan, C.F. Reprint of: Use of a mobile phone for potentiostatic control with low cost paper-based microfluidic sensors. *Analytica Chimica Acta* **803**, 123-127 (2013).
249. Fenton, E.M., Mascarenas, M.R., López, G.P. & Sibbett, S.S. Multiplex lateral-flow test strips fabricated by two-dimensional shaping. *ACS Appl Mater Interfaces* **1**, 124-129 (2009).
250. Jahanshahi-Anbuhi, S., *et al.* Paper-based microfluidics with erodible polymeric bridge giving controlled release and timed flow shutoff. *Lab on a Chip* (2013).
251. Lan, W.-J., *et al.* Paper-based electroanalytical devices with an integrated, stable reference electrode. *Lab on a Chip* **13**, 4103-4108 (2013).
252. Godino, N., Comaskey, E., Gorkin Iii, R. & Ducreé, J. Centrifugally enhanced paper microfluidics. 1017-1020 (Paris, 2012).
253. Zhu, H., *et al.* Cost-effective and Rapid Blood Analysis on a Cell-phone. *Lab on a Chip* (2013).

Appendix

- 1) Posters and presentations completed in the period of this research study.
- 2) Ethical approval required for the testing of human serum and plasma samples in this research study:

- i. Iron
- ii. Creatinine
- iii. Urea detection.

1) Posters and Presentations

DAWSON, A., Cleland, J., Jones, S. A., McCreedy, T. Paper Microfluidics for Clinical Diagnostics using Colourimetric Detection Methods. Oral Presentation at Analytical Research Forum, Stevenage GSK, (2013)

DAWSON, A., Cleland, J., Jones, S. A., McCreedy, T. Paper Microfluidics for Clinical Diagnostics. Oral Presentation at Departmental Colloquia, University of Hull, (2013)

DAWSON, A., Cleland, J., Jones, S. A., McCreedy, T. Paper Microfluidics in Point of Care Diagnostics. Oral Presentation at 3rd Microfluidic European Conference, Heidelberg (2012)

DAWSON, A., Cleland, J., Jones, S. A., McCreedy, T. Fabrication of Paper Microfluidics. Poster Presentation at Departmental Colloquia, University of Hull (2012)

DAWSON, A., Cleland, J., Jones, S. A., McCreedy, T. Measuring Health in the 21st Century. Poster Presentation at Analytical Research Forum, Manchester (2011)

2) Planned Publications

Iron(II) detection in human serum samples using a paper microfluidic device

Creatinine detection in human serum samples using the Jaffe Reaction on a paper platform

3) Ethical Approval